UNIVERSITY OF DEUSTO

DYNAMIC AND SCALABLE STRATEGIES TO LOWER THE IDENTIFICATION TIME AND ENERGY CONSUMPTION IN ALOHA-BASED RFID ANTI-COLLISION PROTOCOLS

Dissertation presented by Laura Arjona Aguilera

for the *Engineering for the Information Society and Sustainable Development* PhD program

Directed by Dr. Asier Perallos Ruiz and Dr. Hugo Landaluce Simon

UNIVERSITY OF DEUSTO

DYNAMIC AND SCALABLE STRATEGIES TO LOWER THE IDENTIFICATION TIME AND ENERGY CONSUMPTION IN ALOHA-BASED RFID ANTI-COLLISION PROTOCOLS

Dissertation presented by Laura Arjona Aguilera

for the *Engineering for the Information Society and Sustainable Development* PhD program

Directed by Dr. Asier Perallos Ruiz and Dr. Hugo Landaluce Simon

The PhD candidate The advisors

Bilbao, September 2018

Dynamic and Scalable Strategies to lower the Identification Time and Energy Consumption in Aloha-based RFID Anti-collision Protocols

Author: Laura Arjona Aguilera

Advisors: Dr. Asier Perallos Ruiz and Dr. Hugo Landaluce Simon

Text printed in Granada

First edition, September 2018.

Abstract

The fourth industrial revolution is coming, promising to bring together the worlds of production and network connectivity in an Internet of Things (IoT). One capable and feasible technology to build in intelligence to a product is Radio Frequency Identification (RFID) technology. This technology uses a spectrum of radio frequency to transfer the identification information between two communication devices: reader and tags. A remarkable characteristic of this technology is that it does not need a direct line of sight between the reader and the tags to establish communication. In addition, it is a low-intrusive technology, which can be easily adapted to the IoT paradigm. The core application of RFID technology is to read a code stored in the tags' internal memory, which uniquely identifies them. Thus, tags can be attached to a large number of different items for numerous applications, highlighting activity recognition, localization systems, tracking, and mobile sensing applications.

The coexistence of several tags in the same identification zone of the reader provides RFID technology with a great flexibility at the expense of the tag collision problem. Tags share the same communication channel (the air) and may respond simultaneously to the same reader command, interfering and garbling their waveforms. The reader then is unable to interpret the information received from the tags, requiring tags to re-transmit their messages. As a result, tags collisions extend the time employed by the reader to identify the tag set and also the energy consumed in the process. Anti-collision protocols are then proposed to arbitrate the tags' responses, with the main goal of maximizing the

number of tags identified by a time unit and minimizing the energy consumed by the reader during the identification process.

Most RFID manufacturers currently follow the EPCglobal Class 1 Generation 2 (EPC C1G2) standard. This standard employs the Slot Counter anti-collision protocol, which belongs to the Dynamic Frame Slotted Aloha (DFSA) category. DFSA protocols are characterized by providing tags a set of time slots where tags must randomly choose one time slot to transmit their message. The main challenge that DFSA protocols aim to solve is determining the number of time slots that are contained in one set. The Slot Counter protocol follows a set of recommendations from the current standard to face this challenge, but the exact values of some configuration parameters are not specified. Furthermore, the Slot Counter protocol does not scale efficiently to large tag set sizes, because it presents a smooth behaviour. This lack of definition provides large improvement possibilities in the field of DFSA protocols. Consequently, many DFSA algorithms have recently appeared in the literature to improve the performance of the Slot Counter protocol.

This dissertation provides a solution to the tag collision problem by proposing two dynamic and scalable strategies for DFSA protocols: fuzzy logic and tag estimation. These two strategies are then applied to a traditional DFSA protocol based on the current standard, resulting in four novel anti-collision protocols. The proposed protocols improve the performance of existing DFSA protocols, including the Slot Counter, in terms of the tags identification time and the energy efficiency in passive RFID systems. Finally, a physical RFID experimentation system is presented to implement and evaluate user-configurable DFSA protocols based on EPC C1G2.

To all those who trusted me from the beginning of this journey

Acknowledgements

This work is the product of many individuals. Thanks to my advisors, Prof. Asier Perallos and Dr. Hugo Landaluce, for their support on so many fronts and whose technical knowledge and creative insights have been invaluable.

A special thanks to Prof. Joshua Smith, for making possible my international stay at UW Sensors Systems Lab, which has been incredibly valuable for my personal and professional career.

A special thanks to all the UW Sensor Systems lab group members for being so helpful with me, and for such a warm welcome to their lab.

A special thanks to Dr. Pavel Nikitin, for his technical insights, and for helping me taking my research closer to the physical world.

Also, thanks to all the present and former Mobility research group members who have contributed to the projects I present here and without whom this wouldn't have been nearly as much fun.

Finally, thanks to my family, Maite, Manuel, Victor, Cintia, Yaki, and Terri, for keeping close despite great distances. And thanks to Gorka for his unconditional support, helping me to complete this hurdling journey.

Thanks a lot! ¡Muchas gracias!

Laura Arjona

September, 2018.

Contents

List of Figures

List of Tables

Glossary

E/n	Reader energy consumption per tag identified
ΔQ	Variation of the parameter Q
Δ	Limit of the slots occupancy at which the frame size should be increased
ϵ	Estimation error
$\hat{n}$	Estimated tag set size
BLF	Backscatter-link frequency
c_i	Number of idle slots in one frame
$c_i(n, L)$	Expected number of idle slots in one frame
c_k	Number of collision slots in one frame
$c_k(n, L)$	Expected number of collision slots in one frame
c_s	Number of single slots in one frame
$c_s(n, L)$	Expected number of single slots in one frame
col_rate	Tag collision rate
E_r	Energy of the reader received signal
E_{th}	Threshold energy value for the energy of the received signal to detect an idle response

ET Time required by the reader to estimate a tag set size

IT Time required by the reader to identify one tag

k Length in bits of tags' EPC

L Frame size

n Tag set size

p Pointer slot. It refers to the slot where the frame size is examined

P_{tx} Reader receiving power

P_{tx} Reader transmitting power

$RTcal$ Duration of the reader-to-tag calibration period

SW Idle or collision response rate

T_1 Time needed for the tags to generate their responses after every reader command

T_2 Time needed for the reader to receive all the tag transmissions

T_3 Maximum period of time that the reader waits for a tag's response before considering the slot as idle

T_{EPC} Duration of a tag EPC

$t_{IT}(n, L)$ Expected time to identify one tag in a frame

T_i Duration of an idle slot

T_k Duration of a collision slot

T_{QA} Duration of the reader command QA

T_{Qc} Duration of the reader command Qc

T_{QR} Duration of the reader command QR

T_{RR} Frame size increase factor

T_s Duration of a single slot

$Tari$ Reference time interval for a reader $data$-0 transmission

TIR Tag identification rate. Number of tags identified per time unit

$TRcal$ Duration of the tag-to-reader calibration period

The road to success is always under construction

Lily Tomlin

CHAPTER

1

Introduction

THE fourth industrial revolution is coming, promising to bring together the worlds of production and network connectivity in an Internet of Things (IoT). One capable and feasible technology to build in intelligence to a product is Radio Frequency Identification (RFID) technology [Murofushi 17]. This technology is currently the most popular system for item identification and tracking, and thus the main enabler for the IoT vision. The huge improvement in Ultra High Frequency (UHF) RFID is leading to a widespread diffusion of several kinds of passive RFID tags in products. Current examples of RFID expansion can be found in activity recognition, localization and tracking systems, and mobile sensing [Yang 14, Pradhan 17, Hessar 13, Agrawal 17].

1.1 Radio Frequency Identification Technology

RFID is an automatic wireless data collection technology with a long history. First functional passive UHF RFID systems with a range of several meters appeared in early 1970s [Nikitin 06]. Since then, RFID has experienced a tremendous growth. At first glance, the concept of RFID and its application seems simple and straightforward. But in reality, RFID is a technology that spans systems engineering, software development, circuit theory, antenna theory, radio propagation, microwave techniques, receiver design, integrated circuit design, encryption, materials technology, mechanical design, and network engineering, to mention a few. The work of this thesis focuses on the network stack development, in particular, on the Medium Access Control (MAC) layer.

1.1.1 Operation principles

A typical RFID system consists of a reader, antennas, tags, and a control unit (often a computer). The reader uses connected antennas to wirelessly communicate with the tags inside the interrogation zone using radio waves. The traditional application of RFID technology is to read the Electronic Product Code EPC stored in the tags' internal memory, which uniquely identifies them. Tags are then attached to a wide variety of objects with the main purpose of unequivocally identify them.

1.1.2 Classification

RFID originated from RADAR technology, and it has greatly evolved since then. Traditionally, the main purpose of RFID tags was to track and identify objects. Currently, there are tags which are also capable of performing sensing and computational tasks [Sample 08, Zhao 15, Zhang 11]. RFID systems can be classified into three groups according to their form and functionality.

1. Active RFID.

   Includes tags with a battery which emit radio signals, acting as a classical transceiver. These can have a very long range and they do not require a complex or expensive interrogator. They can be based on protocols such as

ZigBee, Bluetooth / BLE, or LoRa. These are still considered RFID tags even though they do not use backscatter[1]

2. Semi-passive RFID.

   Includes tags which communicate with the reader using backscatter and which use a battery to power digital logic in the tag.

3. Passive RFID.

   Includes tags without batteries which use backscatter to communicate with the reader. Passive RFID tags can be classified into four main groups.

   (a) Chip-based ID tags.

   Tags with an integrated circuit containing digital logic. These tags are designed to operate in one of the three following frequency ranges:

   i. Low Frequency (LF) - NFC 125 kHz.
   ii. High Frequency (HF) - NFC 13.56 MHz.
   iii. Ultra High Frequency (UHF) - EPC C1G2 [EPCglobal 15] 860-960 MHz.

   (b) Chipless ID tags.

   Tags without an integrated circuit which still can backscatter their ID in some way. There are two main types of chipless ID tags.

   i. UHF Surface Acoustic Wave (SAW) tags. Their operation is based on micro-acoustics of piezoelectric crystals instead of semiconductor physics [Plessky 10].
   ii. Other chipless UHF/microwave band tags. Currently, these types of tags are only seen in research.

   (c) Computational RFID (CRFID) and RFID sensor tags.

   Currently there is a growing class of battery-free computational and sensing tags which go beyond simple barcodes replacement functionality. Two main groups of CRFIDs have been reported in the literature.

[1] Form of communication used by most commercial RFID tags. It consists of the variation of the amplitude of the incoming electromagnetic waves, which are reflected back in the tag antenna according to the digital data which is required to transmit [Finkenzeller 03].

i. UHF WISP, NFC-WISP, UMass Moo.
These are re-programmable and open source tags for rapid implementation of battery-free sensing or other applications [Sample 08, Zhao 15, Zhang 11].

ii. Digital UHF sensor and actuator tags such as Farsens products [Farsens].

(d) Chipless UHF sensor tags.

These tags are shown only in research, and they can do sensing tasks using chipless methods.

This dissertation focuses on passive RFID tags identification. Compared to active and semi-passive RFID, the main advantages of passive RFID tags are: smaller sticker form factor, lower cost, and longer lifetime. However, this is achieved at the expense of a smaller operation range.

1.2 Tag Anti-collision protocols in passive RFID systems

An RFID communication system typically needs at least one reader and one or more tags. All the participants must share a unique communication channel: the air. Given the boom in the use of High Frequency HF, Ultra High Frequency UHF, and microwaves frequency ranges for communications, the readers' detection range has been greatly increased. In this scenario, it is very common to find a large amount of tags powered and operating in the same frequency. Thus, there is a high probability that tags will transmit their messages simultaneously, leading to collisions.

1.2.1 The tag collision problem

Due to the shared nature of the communication channel, signals coming from different tags often collide, producing interferences and cancellations. The interferences produced between the messages transmitted by the tags are known as message collisions, and they cause illegible and lost data. In the field of RFID, this problem is known as the tag collision problem and it represents a focus of interest in current research. Collisions oblige the reader to retransmit commands asking for the tags' messages, wasting bandwidth and increasing the identification time and the energy consumption of the global system.

Due to the inherent restrictions in RFID, traditional multiple-access methods can not be applied to this technology to avoid the tags collisions. While classic multiple-access protocols chase a performance and stability improvement, as well as a reduction in the packets delay; collision-resolution protocols in RFID seek for a reduction in the total time and energy required to identify a set of tags. Due to their particular characteristics in addition to the different goals they chase, collision-resolution protocols in RFID are called anti-collision protocols.

In RFID, a collision occurs when two or more tags transmit their message simultaneously, as showed in Figure 1.1. In this figure, the reader schedules the tag's responses in time, so that tags must select a unique time slot to transmit their messages. In this example, tag A and tag B have selected the same time slot and a collision occurs between them. Consequently, both tags have to re-transmit their

$RN16$ message later in the identification process. The $RN16$ message will be explained in Section 2.1. Tag C is correctly identified in the second time slot, because it finds the channel idle and it does not interfere with any other tag in the area.

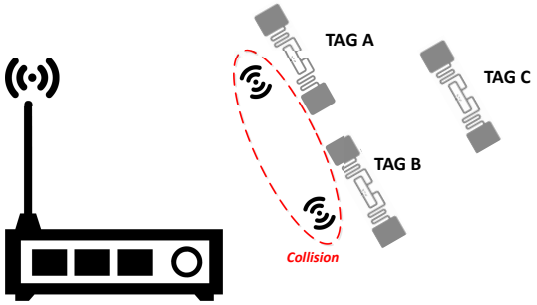

(a)

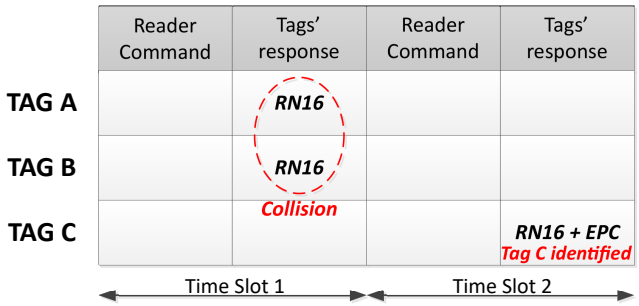

(b)

Figure 1.1: The tag collision problem in RFID: (a) general outline example, (b) its corresponding time domain.

The three main characteristics desired for an anti-collision protocol are:

- Fast identification: the time employed for identifying the tags located in the reader interrogation zone must be as low as possible, so that it results imperceptible. Therefore, the amount of information exchanged between the elements in the system should be reduced.

- Minimum reader energy consumption. The growing interest in mobile devices is making mobile and battery powered RFID readers, such as hand-readers and smart-phones with an attached reader, increasingly attractive. These RFID readers require energy-efficient anti-collision protocols to minimize the tags collisions and to expand the reader's battery life.

- Scalability. The number of passive tags can be very large due to their low cost, easy disposability, and powerless operation. In these scenarios, anti-collision schemes need to be scalable to large population sizes in order to maintain a positive performance for a wide range of tag set sizes.

1.2.2 Anti-collision protocols in the MAC layer

The existing anti-collision protocols in the MAC layer that can be found the literature are classified into three main groups: Aloha-based, tree-based, and hybrid protocols [Klair 10].

Tree-based protocols [Capetanakis 79], in essence, split colliding tags into subsets, and further split the subsets repeatedly up to the successful response of all the tags that are within the interrogation zone.

Aloha based present four main variants. In Pure Aloha (PA), a tag will respond to the reader commands randomly after being energized. Slotted Aloha (SA) divides time into slots and schedules tags to respond only at the boundary of the time slots. Frame Slotted Aloha (FSA) and Dynamic Frame Slotted Aloha (DFSA) divide time into frames, and frames into slots and mandate each tag to respond in only one slot per frame. An identification process consists of a set of frames, and the number of slots contained in one frame is named *frame size*. While in FSA the frame size is fixed during the identification process, in DFSA it is variable. The key feature which differentiates a DFSA protocol is the strategy it follows to update the frame size along the identification of a set of tags. The fact that EPCglobal Class-1 Generation-2 (EPC C1G2), the current standard in RFID, uses a DFSA structure to arbitrate collisions, highlights the relevance of this scheme.

Finally, hybrid protocols consist of a combination of Aloha and tree based protocols [Wu 13]. They are usually organized in more than one phase, and a different strategy (tree or Aloha) is applied in each phase.

Aloha based protocols are probabilistic, since the tag responses are organized randomly. These responses are distributed among various slots, and the more uniformly spaced are the transmissions, the higher is the probability of success. Tree based protocols are, on the other hand, deterministic: they identify the total number of tags in the interrogation zone. The total amount of information transmitted

between readers and tags is usually higher than in Aloha based protocols. However, the tags' cost is usually lower in tree based protocols.

A reduced number of hybrid protocols have been presented in the state-of-the-art of RFID anti-collision protocols, because their computational complexity is higher than Aloha and tree protocols.

This dissertation proposes a set of DFSA protocols which lower the tag identification time and the energy consumed by the reader of existing DFSA protocols.

1.3 Thesis Statement

Signals coming from different RFID tags often collide, producing interferences and cancellations, referred as tags collisions. Collisions oblige the reader and tags to retransmit their messages. This scenario results in a waste of bandwidth and a increase in the tags identification time and energy consumption of the global RFID system. Dynamic Frame Slotted Aloha (DFSA) protocols are currently the most popular strategies used to deal with tags collisions in RFID systems. The key feature which differentiates a DFSA protocol is the strategy employed by the reader to update the frame size along the identification of a set of tags.

This dissertation provides a solution to the tag collision problem by proposing two dynamic and scalable strategies to update the frame size in DFSA protocols: fuzzy logic and tag estimation. These two strategies are then applied to a traditional DFSA protocol based on EPC C1G2, resulting in four novel anti-collision protocols. Three research objectives are proposed to further bound the work developed.

1.3.1 Main research objectives

This dissertation addresses three main objectives to achieve the hypothesis presented in the previous section:

1. Apply fuzzy logic to dynamically adjust the transmission frame size of DFSA anti-collision protocols based on EPC C1G2. The resulting protocols will improve the performance of existing DFSA protocols in terms of the the tags identification time in passive RFID systems.

2. Design a fast and scalable procedure to estimate an RFID tag population. The proposed estimator will be then applied to a DFSA anti-collision protocol based on EPC C1G2 to improve the performance of existing protocols in terms of the tags identification time and energy efficiency in passive RFID systems.

3. Design a physical RFID experimentation system to implement and evaluate the performance of user-configurable DFSA anti-collision protocols based on EPC C1G2.

1.4 Structure and general methodology

This dissertation is comprised by seven publications, which are listed in Section 1.6. Its main goal is to minimize the tags identification time and the energy consumed by the reader in passive RFID systems by developing efficient DFSA anti-collision protocols. This is done in two different ways: i) applying fuzzy logic to select the frame size and to select the slot where this frame size is examined, and ii) developing an scalable and fast tag estimator to calculate the frame size according to the estimated tag set size. A chapter is dedicated to each of these aspects. Each of those chapters summarizes the publication or publications that are dedicated to that same aspect. Each publication is self-contained. Therefore, each of them includes its own state-of-the-art section, proposes its research questions, and describes the particular strategy that it applies, which is tailored to the main research questions. The full outline of the dissertation is described in section 1.7.

1.5 Contributions

This section summarizes the main contributions of this dissertation. Table 1.1 outlines the contributions, indicates their focus, and lists which research objective they are related to, in which chapter they are described, and in which publication they are included.

- **C1**. Study of the frame update policy of DFSA anti-collision protocols and classification of the main state-of-art protocols according to the policy they use.
- Contributions by using fuzzy logic:
  - **F1**. Fuzzy Rule Based System (FRBS) to examine L in a DFSA protocol
  - **F2**. Fuzzy Frame Slotted Aloha (FFSA) anti-collision protocol.
  - **F3**. Fuzzy Rule Based System (FRBS) to calculate L in a DFSA protocol.
  - **F4**. FuzzyQ anti-collision protocol.

Table 1.1: Summary of contributions.

	Focus	Research Objective	Chapter	Publication (Appendix)
C1	Survey	1,2	2	I (A)
F1	L examination	1	3	I (A)
F2	Anti-collision protocol FFSA	1	3	I (A)
F3	L calculation	1	3	II (B)
F4	Anti-collision protocol FuzzyQ	1	3	II (B)
E1	Tag estimator sMMSE	2	4	III (C)
E2	Tag estimator tMMSE	2	4	IV (D)
E3	Anti-collision protocol TAFSA	2	4	IV (D)
E4	Anti-collision protocol EASA	2	4	V (E)
P1	Experimentation with commercial tags	3	5	VI (F)
P2	Experimentation with sensor tags	3	5	VII (G)

- Contributions by estimating the tag population size:
  - **E1**. Scalable tag estimator sMMSE.
  - **E2**. Fast tag estimator tMMSE.
  - **E3**. Timing-Aware Frame Slotted Aloha (TAFSA) anti-collision protocol.
  - **E4**. Energy-Aware Slotted Aloha (EASA) anti-collision protocol.
- Contributions by using a physical RFID system:
  - **P1**. Commercial tags identification with Slot Counter protocol.
  - **P2**. Sensor tags identification with FuzzyQ protocol.

1.6 Publications

This thesis is a collection of seven publications. In this section, the publications are listed and briefly introduced.

1.6.1 Paper I

Paper I (Appendix A) is titled *"A Novel Frame Update Policy for RFID DFSA Tag Anti-Collision Protocols "*. It is under second review in a JCR journal. Using a fuzzy logic strategy for *L examination* in the frame update policy of DFSA protocols, it proposes the anti-collision protocol Fuzzy Frame Slotted Aloha (FFSA) for fast RFID tag identification.

This paper analyzes the frame size update policy of DFSA protocols in order to propose a novel policy based on fuzzy logic to lower the tags identification time of existing protocols. This policy is then applied to a DFSA protocol based on EPC C1G2, resulting in FFSA anti-collision protocol. Moreover, this paper surveys and classifies the most relevant DFSA state-of-the-art protocols according to their frame size update policy. Simulation results show that FFSA achieves a 10.71% improvement in the tag identification rate (tags/s) in relation to the Slot Counter protocol, employed in EPC C1G2. The complete reference of Paper I is listed next.

L. Arjona, H. Landaluce, A. Perallos, E. Onieva. "A Novel Frame Update Policy for RFID DFSA Tag Anti-Collision Protocols". Under review. Submitted on March 2018.

1.6.2 Paper II

Paper II (Appendix B) is titled *"Fast fuzzy anti-collision protocol for the RFID standard EPC Gen-2"*. It has been published in the journal IET Electronic Letters. Using a fuzzy logic strategy for *L calculation* in the frame update policy of DFSA protocols, it proposes the anti-collision protocol FuzzyQ for fast RFID tag identification.

The current standard in RFID employs the Slot-Counter Protocol to deal with tags collision, and it presents a lack of definition about the function to update the

frame size of the tags identification process. Most protocols in the literature propose solutions which are based on a smooth increase in the frame size L. Therefore, when the collision or idle rate is high, they must employ a relatively high number of slots and reader and tag bits to find an appropriate frame size.

The main goal of Paper II is to introduce an anti-collision protocol which lowers the tags identification time of the Slot Counter protocol employing the two following strategies: (i) to check whether the current frame size is appropriate at strategic slots and not at every slot. (ii) to achieve a more abrupt step size of the L parameter using a Fuzzy Rule Based System (FRBS). Simulated results show that FuzzyQ achieves a 7% average improvement in terms of tags identification time with respect to Slot Counter. The complete reference of this paper is listed next.

L. Arjona, H. Landaluce, A. Perallos, E. Onieva. "A fast Fuzzy anti-collision Protocol for the RFID Standard EPC Gen-2". *IET Electronic Letters*. Vol. 52, no. 8, pp. 663-665, April 2016.

IET Electronic Letters JCR IF (2016): 1.155.

Q3 in Engineering, Electrical & Electronic.

1.6.3 **Paper III**

Paper III (Appendix C) is titled *"Scalable RFID Tag Estimator with Enhanced Accuracy and Low Estimation Time"*. It has been published in the journal IEEE Signal Processing Letters. A tag estimator is presented to significantly decrease the normalized estimation error and to maintain a low estimation time compared to existing strategies.

The knowledge of the number of tags is critical in many RFID applications. Often, in such scenarios, it is desirable to simply estimate the number of tags without explicitly identifying individual tags, helping to reduce the processing time, and preserve people's privacy.

Paper III introduces the tag estimator sMMSE to provide an accurate and fast tag estimate under large-scaled tag environments. sMMSE updates the frame size by considering two key parameters: one determines the limit of the slots occupancy

at which the frame size should be increased, and the other one sets the frame size increase factor. Numerical results indicate that sMMSE significantly decreases the normalized estimation error and maintains a low estimation time compared to existing strategies in the literature. The complete reference of Paper III is listed next.

L. Arjona, H. Landaluce, A. Perallos, E. Onieva. "Scalable RFID Tag Estimator with Enhanced Accuracy and Low Estimation Time". *IEEE Signal Processing Letters*, vol. 24, no. 7, pp. 982-986. July 2017.

IEEE Signal Processing Letters JCR IF (2016): 2.528.

Q2 in Engineering, Electrical & Electronic.

1.6.4 **Paper IV**

Paper IV (Appendix D) is titled *"Timing-aware RFID anti-collision Protocol to increase the Tag Identification Rate"*. It has been published in the journal IEEE Access. Using a tag estimation strategy for *L calculation* in the frame update policy of DFSA protocols, it proposes the anti-collision protocol Timing-Aware Frame Slotted Aloha (TAFSA) to significantly increase the Tag Identification Rate (TIR) compared to existing strategies.

Currently, the number of tagged items sharing one reader interrogation area is growing, because almost anything can be tagged. Therefore, fast tag anti-collision protocols are required to minimize tags collisions. Paper IV first provides a thorough study of TIR in DFSA protocols, analyzing the main factor which affects this metric: the L *calculation* strategy of the frame update policy. Then, applying the conclusion of this analysis, the anti-collision protocol TAFSA is presented to increase TIR. Simulation results show that TAFSA, with an average of 56.7 tags identified per second, achieves a 10% average improvement in TIR in relation to the strategies of the comparison. The complete reference of Paper IV is listed next.

L. Arjona, H. Landaluce, A. Perallos, E. Onieva. "Timing-aware RFID anti-collision Protocol to increase the Tag Identification Rate". *IEEE Access*, vol. 6, pp. 33529-33541. June 2018.

IEEE ACCESS JCR IF (2017): 3.557.

Q1 in Computer Science, Information Systems.
Q1 in Engineering, Electrical & Electronic.
Q2 in Telecommunications.

1.6.5 **Paper V**

Paper V (Appendix E) is titled *"Energy-aware RFID anti-collision Protocol"*. It has been published in the journal MDPI Sensors. Using a tag estimation strategy for *L calculation* in the frame update policy of DFSA protocols, it proposes the anti-collision protocol Energy-Aware Slotted Aloha (EASA) to significantly decrease the energy consumed by the reader per tag identified compared to existing strategies.

Battery powered RFID readers require energy-efficient anti-collision protocols to expand the reader's battery life. The main goal of paper V is to present the anti-collision protocol EASA to decrease the reader energy consumption per tag. The frame size update strategy of EASA is configured to minimize the energy consumption per tag. As a result, EASA presents an energy-aware frame. The performance of EASA is evaluated and compared with several state of the art DFSA anti-collision protocols based on the current RFID standard. Simulation results show that EASA, with an average of 15 mJ consumed per tag identified, achieves a 6% average improvement in the energy consumed by the reader per tag in relation to the strategies of the comparison. The complete reference of Paper V is listed next.

L. Arjona, H. Landaluce, A. Perallos. "Energy-aware RFID anti-collision Protocol". *Sensors*, vol. 18, no. 6: 1904. June 2018.

SENSORS JCR IF (2017): 2.475.

Q1 in Instruments & Instrumentation.
Q2 in Chemistry, Analytical.
Q2 in Electrochemistry.

1.6.6 Paper VI

Paper VI (Appendix F) is a book chapter titled *"Survey and Analysis of RFID DFSA Anti-Collision Protocols and their physical implementation capabilities"*. It has been published in the book RFID Technology: Design Principles, Applications and Controversies. This chapter presents an analysis and classification of DFSA protocols in terms of their frame update policy and their physical implementation feasibilities, followed by the physical implementation of an Software Defined Radio (SDR) Ultra High Frequency (UHF) RFID reader to validate the performance of DFSA protocols based on the standard EPC C1G2.

Addressing the current interest in DFSA protocols which aim to improve the performance of the current standard, Paper VI first analyzes and classifies the most significant DFSA protocols. This analysis is followed by a discussion of the physical implementation capabilities of DFSA protocols in a real scenario. Then, an SDR RFID reader is presented to evaluate the performance of DFSA protocols following EPC C1G2 requirements in a real scenario. The proposed SDR reader is validated with an experimental implementation and evaluation of two DFSA anti-collision protocols using off-the-shelf RFID tags: the Slot Counter protocol and an ideal DFSA protocol. The experimental analysis of the two protocols performed in Paper VI demonstrate that their performance is strongly influenced by the frame size. Also, performance improvements are observed in the experimental results relation to the analytical values. The complete reference of Paper VI is listed next.

L. Arjona, H. Landaluce, A. Perallos, and A. Parks, "Survey and Analysis of RFID DFSA Anti-Collision Protocols and Their Physical Implementation Capabilities". RFID Technology: Design Principles, Applications and Controversies, Chapter 1, Ed. New York: Nova Science Publishers, March 2018.

1.6.7 Paper VII

Paper VII (Appendix G) is titled *"Experimental Validation of Anti-Collision Protocols for RFID Sensor Networks"*. It has been accepted for presentation at the workshop *"EURASIP RFID 2018"*. This paper evaluates the performance of FuzzyQ

and Slot Counter anti-collision protocols from a physical implementation perspective, and shows the relevance of the identification phase of an RFID sensor network with respect to the sensing time.

So far, significant effort has been invested in simulation-based analysis of the performance of anti-collision protocols regarding the tags identification time. However, no one has explored the experimental performance of anti-collision protocols in an RFID sensor network using CRFID. Paper VII: (i) demonstrates that the impact of one tag identification time over the total time required to read one sensor data from that same tag is very significant, and (ii) presents an Software Defined Radio (SDR) Ultra High Frequency (UHF) RFID system which validates the improvement of FuzzyQ (see Appendix B), a fast anti-collision protocol, in relation to the protocol used in the current RFID standard. This paper concludes that anti-collision protocols are an important and relevant part in the process of reading RFID sensors, because the identification time represents more than 59% of the sensing time. The complete reference of Paper VII is listed next.

L. Arjona, H. Landaluce, A. Perallos, and J.R. Smith, "Experimental Validation of Anti-Collision Protocols for RFID Sensor Networks". EURASIP RFID. Brno, Czech Republic. September 11-12, 2018.

1.7 Outline

This thesis is divided into 6 chapters and 7 appendixes. After this introduction (Chapter 1), four chapters summarize the seven publications that comprise this dissertation. Chapter 2 presents an analysis and classification of the main DFSA anti-collision protocols of the state-of-the-art. Chapter 3 focuses on improving the performance of existing DFSA anti-collision protocols by applying fuzzy logic to the frame update policy of DFSA protocols, and proposing two protocols for fast RFID tag identification. Chapter 4 focuses on improving the performance DFSA anti-collision protocols by applying a tag estimation algorithm to the frame update policy of DFSA protocols. Firstly, an accurate and scalable tag estimation algorithm is proposed. Then, two DFSA protocols which estimate the tag set size are presented, one which maximizes the tag identification rate, and the other one that

minimizes the energy per tag identified consumed by the reader. Chapter 5 presents an SDR-UHF-RFID reader to evaluate the performance of user-configurable anti-collision protocols. Chapter 6 summarizes the contributions of this thesis.

The papers that comprise this thesis (see Section 1.6) are appended. Appendix A and B contain **Paper I** and **Paper II**, both about the application of fuzzy logic to improve the performance of DFSA protocols. Appendix C contains **Paper III**, about an accurate and scalable tag estimation algorithm. Appendix D and E contain **Paper IV** and **Paper V**, both about the application of tag estimation algorithms to improve the performance of DFSA protocols. Appendix F and G contain **Paper VI** and **Paper VII**, both about the experimental validation of DFSA protocols in a physical RFID system.

CHAPTER

2

DFSA anti-collision protocols

MOST RFID manufacturers currently follow the EPCglobal Class 1 Generation 2 (EPC C1G2) standard [EPCglobal 15]. EPC C1G2 employs a DFSA protocol to arbitrate the tags collisions: the Slot Counter protocol. This protocol updates the frame size L with the parameters Q and C, so that $L{=}2^Q$ and $Q{=}Q{\pm}C$. EPC C1G2 does not specify the exact selection of the parameter C to update Q and L for the Slot Counter protocol. The standard only recommends using high C values if the previous Q value was low and vice versa. This lack of definition has led to many different alternatives, providing large improvement possibilities in the field of DFSA protocols. Furthermore, the Slot Counter protocol does not scale efficiently to increasing tag set sizes, because it performs smooth modifications of the frame size. Consequently, many DFSA algorithms have recently appeared in the literature to solve the RFID tag collision problem. They all share the dynamic nature of the frame size update along one inventory round. However, each of them applies a different strategy to give a particular value to the frame size with the aim of improving different metrics regarding the process of tag identification.

Some definitions are provided next to properly set the background of DFSA anti-collision protocols.

- *slot*: period of time that separates the tags' responses. Conventionally, three types of slots are considered, in terms of the tags' responses to the reader's commands: single (only one tag replies), collision (more than one tag replies in the same slot), and idle (none of the tags reply). In this context, the variables c_s, c_k, and c_i correspond to the number of single, collision, and idle slots in a frame, respectively.

- *frame*: sequence of L slots, where L represents the frame size. Tags can only transmit their response in one slot per frame.

- *command*: bit-string message transmitted by the reader to the tags.

- *inventory round*: period of time that begins when the reader transmits the initial command Qc and it ends when the reader interrupts the identification process and the tags loose their state. Ideally, an inventory round ends when all the tags inside the reader interrogation zone have been identified.

This chapter first introduces the Slot Counter protocol. Then, two main contributions of one of the works that forms this dissertation are summarized (see Appendix A). These contributions are (i) analysis of the frame size update policy of DFSA protocols, and (ii) classification of the main state-of-the-art DFSA anti-collision protocols.

2.1 Slot Counter protocol

EPC C1G2 employs the Slot Counter protocol to arbitrate the tags collisions. This protocol sets the transmission frame size L as a power of two, taking the value $L = 2^Q$, where $Q \in \mathbb{N}$ and $0 \leq Q \leq 15$. The parameter Q_{fp} is also defined to update the frame size, with $Q = round(Q_{fp})$. Figure 2.1 shows a flow chart of Slot Counter protocol.

Initially, the reader sets Q_{fp}=4, and Q=0. The inventory round is started when the reader transmits a Query command (Qc). Then, the reader alternates between QueryAdjust (QA) and QueryRep (QR) commands. QA starts a new frame with the updated L value and implies that tags must randomly select a slot in the frame (the initial value of their internal slot counter SC), while QR tells the tags to decrement

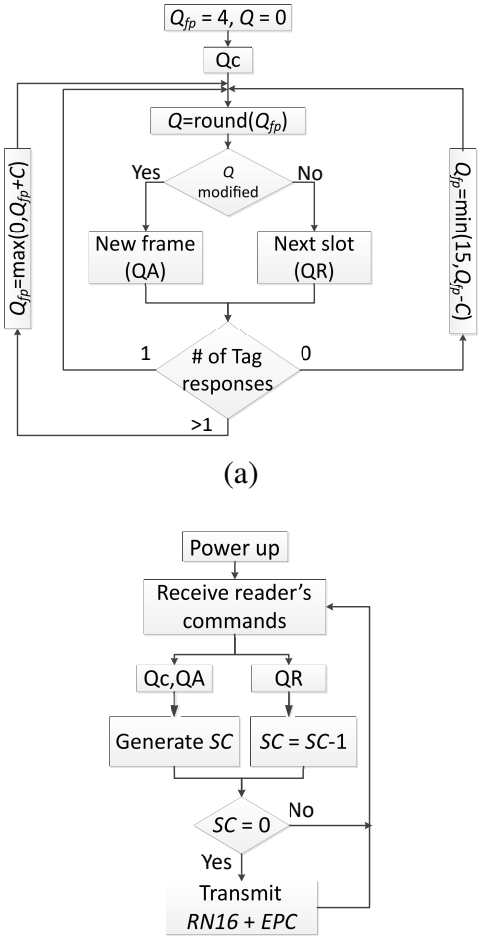

Figure 2.1: Flow diagram of Slot Counter anti-collision protocol: (a) for the reader, (b) for tags.

SC. Thus, when SC=0, the tag transmits a 16-bit random number $RN16$. Once the $RN16$ message is acknowledged (ACK), the tag transmits its EPC code of length k bits.

The frame size is set as $L=2^Q$, and its value is dynamically updated with the parameters Q and C, where Q=round(Q_{fp}). Regarding the time slot occupancy, there are three possible scenarios to update the value of Q_{fp} with C, as shown in Figure 2.1.

- Single slot: Q_{fp} remains unchanged. In this case, the reader replies to the tag with an ACK command followed by the same $RN16$ received by the tag.

When the tag correctly decodes the ACK command, it transmits its EPC

- Collision slot: Q_{fp}=Q_{fp}+C
- Idle slot: Q_{fp}=Q_{fp}−C

Next, the reader readjusts the frame size to $L = 2^Q$ where $Q = round(Q_{fp})$.

2.2 Analysis of the frame update mechanism for DFSA protocols

A wide variety of DFSA protocols can be found in the literature which update L with the aim of improving different metrics regarding the process of tag identification. The protocols proposed in the related publications (see Appendix A,B, D, and E) are compared with the main recent DFSA protocols, which are analyzed in the related publications.

The protocols analyzed in this dissertation are based on the RFID transmission model between the reader and the tags defined in Figure 2.2, meeting EPC C1G2 requirements.

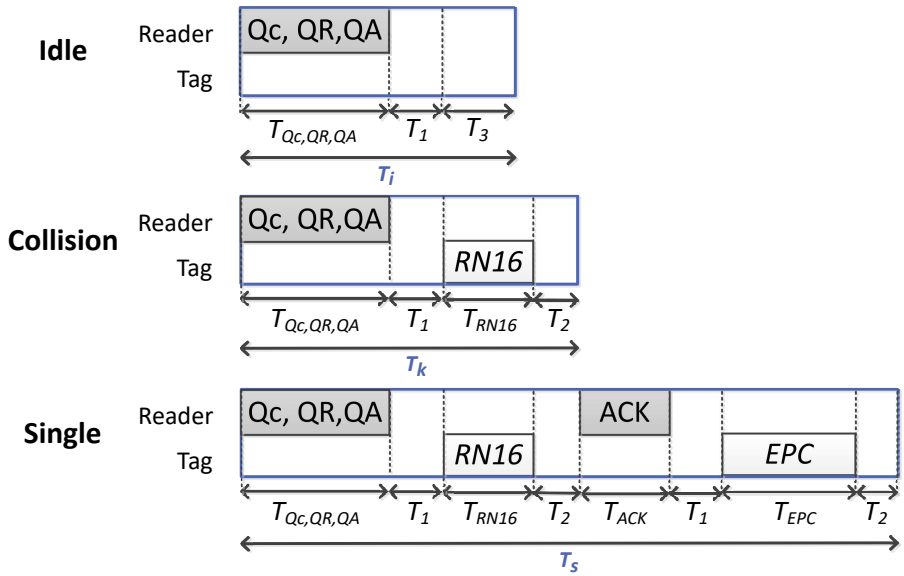

Figure 2.2: Link timing of EPC C1G2.

In this figure, three types of slots are represented: an idle slot, with no response, a collision slot, with more than one tag' simultaneous response, and a single slot, with only one tag response. According to this figure, a single slot has a duration T_s, and this slot involves two reader commands and two tag's responses. A collision slot has a duration T_k, and it involves one reader command and one tags' response. Finally, an idle slot has a duration T_i, and it only involves one reader command. The parameter T_1 refers to the time needed for the tags to generate their responses after every reader command. The parameter T_2 refers to the time needed for the reader to receive all the tag transmissions. Finally, a slot will be considered idle when the reader waits for the tags' responses for a time T_3. The duration of each reader command Qc, QA, and QR, is referred to as T_{Qc}, T_{QA}, and T_{QR}, respectively. T_{RN16} and T_{EPC} correspond to the duration of the tags' messages $RN16$ and EPC, respectively.

Establishing a clear classification of all DFSA protocols is not straightforward. A key feature which differentiates a DFSA protocol is the strategy it follows to update the frame size along the identification of a set of tags. To this end, this section establishes a classification of the main frame update policies employed by DFSA anti-collision protocols. The classification presented in this section considers three different perspectives to update L, which respond to the following three questions: how is L calculated? When is L examined? When a new frame must be started? Thus, the frame update policy of DFSA protocols is classified in the following three parts.

Frame size calculation. Two main strategies can be found in the literature to set a value for the frame size in DFSA protocols.

- Parameter Q: $f(Q)$. The value of L is set as a function of the parameter Q.
- Tag set size estimation. This strategy sets L as a function of the estimated number of tags $\hat{n}$. Two main strategies which set L as a function of $\hat{n}$ can be found in the literature: (i) L is set as a continuous function of $\hat{n}$: f($\hat{n}$); (ii) L is set as with a look-up table (LUT) according to $\hat{n}$: LUT($\hat{n}$).

Frame size examination. Four main strategies can be found in the literature to establish in which slot or slots within a frame the value of L must be examined.

The main goal if this examination is to decide if the current L value is appropriate or not during the identification process and decide if a new frame is needed.

- Frame by Frame (FbF). The simplest strategy is to calculate L only at the last slot of each frame.
- Pointer by Pointer (PbP). Some protocols define some particular slots within the frame, referred as the pointer p in this dissertation ($p<L$), where the value of L is examined to check its appropriateness.
- Slot by Slot (SbS). The third strategy is based on examining L at every slot of the frame.
- Hybrid. Some protocols present a two-phase tag identification process. To examine the frame size, they apply the strategy SbS in the first phase, and FbF in the second.

Frame break condition. Five main strategies can be found in the literature to decide, after calculating L, whether a new frame must be started, or on the contrary, if the reader must proceed with the next slot of the current frame.

- Different L. A new frame is started when the new value of L differs from the previous one.
- L fits $\hat{n}$ from an LUT: LUT($\hat{n}$). Some algorithms define an LUT based on $\hat{n}$ and L to check the appropriateness of L.
- Higher expected number of successful slots: $c_s(n, L)$. This policy breaks the current frame and starts a new one if the expected number of successful slots in the rest of the current frame is less than that expected in the new frame.
- Lower Identification Time: Lower IT. A new frame is started if the expected average time for one tag identification in the new frame is lower than the one in the current frame.
- End of Frame: EoF. In this case, a new frame is started when the current frame has finished.

A classification of the main up-to-date policies of DFSA protocols is summarized in Table 2.1. More details about the different frame update mechanisms of DFSA protocols can be found in the related work (see Appendix A).

Table 2.1: Classification of DFSA frame update policies.

	Operation
L calculation	f(Q)
	f($\hat{n}$)
	LUT($\hat{n}$)
L examination	FbF
	SbS
	PbP
	Hybrid
Frame break condition	Different L
	LUT($\hat{n}$)
	c_{s2}>c_{s1}
	Lower IT
	EoF

2.3 Classification of DFSA tag anti-collision protocols

This section presents some of the most important DFSA protocols in the literature, and classifies them according to their frame update policy. The classification is presented in Table 2.2. The protocols proposed in this dissertation (FFSA, FuzzyQ, TAFSA, and EASA), presented in the related publications (see Appendix A, B, D, and E), are shown in bold. From this table, it is clear that the most popular strategies to update the frame size are: tag estimation for *L calculation*, and Pointer by Pointer for *L examination*. In relation to the *frame break condition*, there is not a prevalent strategy, but a wide diversity of strategies are employed. A detailed description of the protocols included in Table 2.2 and their frame update policy is presented in the related publications (see Appendix A, B, D, and E).

Table 2.2: Classification of DFSA anti-collision protocols according to their frame update policy. The protocols proposed in this dissertation are shown in bold.

	L calculation	L examination	Frame break condition
Slot Counter[EPCglobal 15]	f(Q)	SbS	different L at $slot$ or EoF
Chen14[Chen 14]	LUT($\hat{n}$)	PbP	LUT($\hat{n}$) at p or EoF
ds-DFSA[Su 16]	LUT($\hat{n}$)	PbP+FbF	LUT($\hat{n}$) at p or EoF
DS-MAP[Chen 17]	LUT($\hat{n}$)	PbP+FbF	LUT($\hat{n}$) at p or EoF
Eom[Eom 10]	f($\hat{n}$)	FbF	EoF
ILCM-FbF[Solic 14]	f($\hat{n}$)	FbF	EoF
ILCM-SbS[Solic 16]	f($\hat{n}$)	SbS	Higher c_s at $slot$ or EoF
Chen16[Chen 16]	f($\hat{n}$)	PbP	different L at p or EoF
SSA[Duan 17]	LUT($\hat{n}$)	PbP	different L at p or EoF
DSSA[Duan 17]	LUT($\hat{n}$)	PbP	different L at p or EoF
FFSA (Appendix A)	f($\hat{n}$)	PbP with FRBS	Lower $t_{IT(n,L)}$ at p or EoF
FuzzyQ (Appendix B)	f(Q) with FRBS	PbP	different L at p or EoF
TAFSA (Appendix D)	f($\hat{n}$) with tMMSE	FbF	EoF
EASA (Appendix E)	f($\hat{n}$) with MMSE	FbF	EoF

The previous section indicated that the key feature which differentiates a DFSA protocol is the strategy it follows to update the frame size along the identification of a set of tags. This dissertation presents two different strategies to update the frame size of DFSA tag anti-collision protocols, with the aim of lowering the tags identification time and the energy consumed by the reader. The first one applies fuzzy logic to (i) select the value of Q for L *calculation*; and to (ii) obtain the value of the pointer slot p for L *examination*. The second one estimates the tag set size for L *calculation*. The proposed strategies share the following two characteristics:

- Dynamic: they are designed to adapt to the uncertain behaviour of an RFID tags identification process, where the number of active tags in each frame varies within an inventory round.

- Scalable: they maintain a positive performance for a wide range of tag set sizes.

Finally, each proposed strategy is applied to a typical DFSA anti-collision protocol based on EPC C1G2, resulting in four different DFSA protocols (two using the fuzzy logic strategy, and two using the tag estimation strategy). The proposed protocols perform a dynamic and scalable update of the frame size. Chapters 3 and 4 cover the two proposed strategies as well as the proposed anti-collision protocols.

CHAPTER

3

Fuzzy Logic in DFSA anti-collision protocols

THE arbitration of RFID communication is a stochastic process of unknown behaviour. However, a model based on fuzzy rules can be established to obtain a proper solution. Therefore, a general Fuzzy Rule Based System (FRBS) can be used to deal with this complex problem. The feedback of the tags' responses can be used to generate accurate outputs which will efficiently manage the transmission frame size of the resulting anti-collision protocol. In particular, a FRBS can be developed to improve the frame update policy of existing DFSA protocols. The proposed system must be dynamic, since the tag population varies (decreases as tags are identified by the reader), and scalable (maintaining a positive performance for a wide range of tag set sizes).

This chapter summarizes two of the works that form this dissertation (see Appendix A and B). The first one presents a FRBS for L examination, resulting in Fuzzy Frame Slotted Aloha (FFSA) protocol. The second one employs a FRBS for L calculation, resulting in FuzzyQ protocol.

3.1 Fuzzy logic for L examination: FFSA protocol

According to Table 2.1, three main strategies can be applied for L examination in a frame update policy of a typical DFSA protocol. The FbF strategy is not efficient in the case of large frames filled with many collisions, because the reader must wait until the frame has finished to update the frame size, increasing the identification time and the energy consumed by the reader. The SbS strategy might overload a reader that had only a limited capacity, because L is calculated at every slot. To mitigate the negative effects of FbF and SbS, the related work (see Appendix A) proposes a PbP strategy where the value of the pointer slot is dynamically updated using fuzzy logic. The PbP strategy provides the flexibility of breaking the current frame before it ends, maintaining a low computational complexity in the reader.

The proposed strategy applies a FRBS to adjust the value of the pointer for L *examination* in DFSA anti-collision protocols based on EPC C1G2. For this purpose, the current Q and the tag collision rate col_rate are modelled as fuzzy sets to adaptively update the value of the pointer. A zeroth-order Takagi Sugeno-Kang fuzzy system with a complete AND-composed rule is proposed. As shown in Fig. 3.1, the two input variables Q and col_rate are codified with three initial trapezoids.

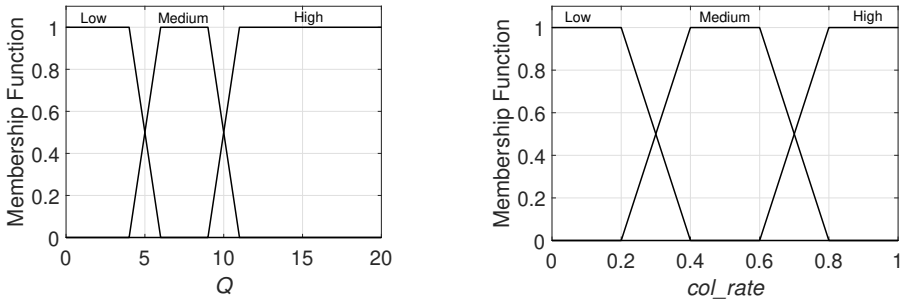

(a) (b)

Figure 3.1: Input membership functions: (a) Q, (b) col_rate.

The output p represents the slot where L must be examined. The rule set of the FRBS is composed by the following nine rules:

- Rule 1: IF (Q is Low) AND (col_rate is Low) THEN $p{=}L/2$.

- Rule 2: IF (Q is Low) AND (col_rate is Medium) THEN p=$L/4$.
- Rule 3: IF (Q is Low) AND (col_rate is High) THEN p=$L/8$.
- Rule 4: IF (Q is Medium) AND (col_rate is Low) THEN p=$L/4$.
- Rule 5: IF (Q is Medium) AND (col_rate is Medium) THEN p=$L/4$.
- Rule 6: IF (Q is Medium) AND (col_rate is High) THEN p=$L/16$.
- Rule 7: IF (Q is High) AND (col_rate is Low) THEN p=$L/8$.
- Rule 8: IF (Q is High) AND (col_rate is Medium) THEN p=$L/16$.
- Rule 9: IF (Q is High) AND (col_rate is High) THEN p=$L/16$.

The rules were designed experimentally considering, on the one hand, the higher the Q, the smaller the p; and on the other hand, the higher the col_rate, the smaller the p. Regarding the first condition, the goal is to perform an early L examination when the collision rate is high, in order to rapidly update L and thus reduce the number of collisions. Regarding the second condition, the idea is to check L early when its value is high in order to avoid long and inappropriate frame sizes, which will slow down the identification process.

Finally, the proposed L *examination* strategy is applied to a typical DFSA protocol based on EPC C1G2, resulting in Fuzzy Frame Slotted Aloha (FFSA) anti-collision protocol. The complete frame update policy of FFSA is proposed with the aim of lowering the tags identification time of the Slot Counter protocol, and it is presented next.

- L *calculation*: $f(\hat{n})$. The first part of the policy for the frame size calculation sets the value of L minimizing the expected time to identify one tag in a frame $t_{IT}(n, L)$. A detailed analysis is performed in Appendix A, and it is concluded that in order to minimize the time required to identify one tag in a frame, L must be $1/\rho$ times the estimated tag set size $\hat{n}$, that is, L=$\hat{n}/\rho$. The reader needs to calculate the value of ρ just once at the beginning of the inventory round. The traditional Minimum Mean Square Error (MMSE) estimator [Vogt 02] is used to obtain $\hat{n}$.

- L *examination*: PbP. The previously presented FRBS is used to dynamically update the value of the pointer slot p.

- *Frame break condition*: Lower $t_{IT}(n, L)$. A new frame is started if the expected average time to identify one tag in the upcoming frame is lower than that in the current frame. Following this strategy, the reader guarantees that if a new frame is started at slot p, the expected average time required to identify one tag will be reduced.

The flow diagram is shown in Appendix A. The performance of FFSA is evaluated and compared with the Slot Counter protocol and with eight additional DFSA protocols. Simulated results are shown in Appendix A, and they demonstrate that FFSA significantly decreases the identification time per tag for a wide range of tag populations compared with earlier DFSA protocols. FFSA achieves a 10.71% improvement in the tag identification rate (tags/s) in relation to the Slot Counter protocol, employed in EPC C1G2.

3.2 Fuzzy logic for L calculation: FuzzyQ protocol

The Slot Counter protocol performs a smooth modification of L with the parameters Q and C, so that $Q{=}Q{\pm}C$. However, the exact selection of C is not specified. The standard only recommends using high C values if the previous Q value was low and vice versa, in the range of $[0.1; 0.5]$. Several papers can be found in the literature which deal with the parameter C to update Q and ultimately update L. Most of these protocols are based on a smooth increase in Q. Therefore, when the collision or idle rate is high, they must employ a relatively high number of slots, and reader and tag bits to find an appropriate L, leading to a relatively high identification time and low throughput (identified tags per second). To solve this problem, the related publication (see Appendix B) proposes a fast strategy which applies fuzzy logic to achieve a more abrupt step size of the Q parameter. This contribution has been patented [Arjona 17], and it is presented next.

The proposed strategy applies a FRBS for L *calculation* in DFSA anti-collision protocols based on EPC C1G2. For this purpose, a zeroth-order Takagi Sugeno-Kang fuzzy system with a complete AND-composed rule is proposed. The pro-

posed system has two inputs: SW which codifies the idle or collision response rate, and Q which codifies the current value of this parameter. The membership functions used to codify the input variables are trapezoidal and the t-norm minimum is used to implement the AND operator. As shown in Fig. 3.2, both input variables are codified with an initial number of trapezoids: two for SW and three for Q.

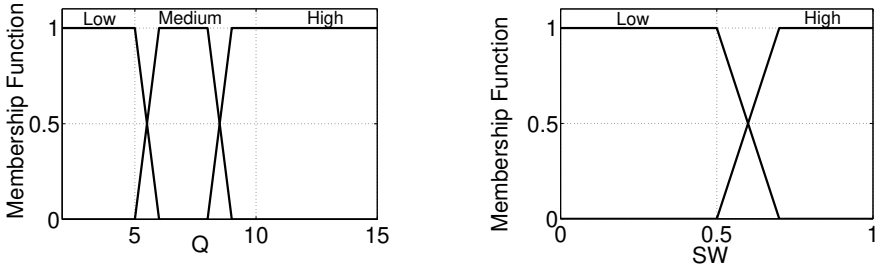

(a) (b)

Figure 3.2: Input membership functions: (a) Q, (b) SW.

The output ΔQ represents the variation of Q, and it is codified by three singletons with four possible values: Null = 0, Low = 1, Medium = 2, and High = 3. The rule set of the FRBS is composed by the following six rules:

- Rule 1: IF (Q is Low) AND (SW is Low) THEN ΔQ is Low.
- Rule 2: IF (Q is Low) AND (SW is High) THEN ΔQ is High.
- Rule 3: IF (Q is Medium) AND (SW is Low) THEN ΔQ is Null.
- Rule 4: IF (Q is Medium) AND (SW is High) THEN ΔQ is Medium.
- Rule 5: IF (Q is High) AND (SW is Low) THEN ΔQ is Null.
- Rule 6: IF (Q is High) AND (SW is High) THEN ΔQ is Low.

Rules were designed considering, on the one hand, the higher the frame size, the lower the increment of Q; and on the other hand, the higher the idle or collision rate, the higher the increment of Q.

Finally, the proposed fast L *calculation* strategy is applied to a typical DFSA protocol based on EPC C1G2, resulting in FuzzyQ anti-collision protocol. The

complete frame update policy of FuzzyQ is proposed with the aim of lowering the tags identification time of the Slot Counter protocol, and it is presented next.

- L *calculation*: $f(Q)$. The previously presented FRBS is used to update L.
- L *examination*: PbP. A strategic slot refereed as *check slot* is defined to check whether the current L is appropriate given the values of SW and Q. The value of this slot is updated once per frame. The *check slot* is defined as L/CP, where CP stands for check point and $CP \in \mathbb{N}$. The value CP=9 is selected in the related publication.
- *Frame break condition*: A new frame is started if the new L differs from the old one, or if the current slot is the last slot of the frame(EoF condition).

The flow diagram of FuzzyQ is shown in Appendix B. The performance of FuzzyQ is evaluated and compared with the Slot Counter protocol and with the protocol Chen[Chen 14]. Simulated results are shown in Appendix B, and they demonstrate that FuzzyQ achieves a 7% average improvement in terms of tags identification time with respect to the protocol used in the standard. The related publication presents the first application of fuzzy logic to model an RFID anti-collision protocol.

CHAPTER

4

Tag estimation in DFSA anti-collision protocols

THE estimation of the number of tags is needed in a wide array of important wireless applications, such as tag identification, privacy-sensitive RFID systems, and warehouse monitoring [Shahzad 15]. This chapter is concerned with tag identification applications. In this field, it is well known that the anti-collision protocol reaches its maximum efficiency when the transmission frame size equals the tag population. Therefore, by dynamically adjusting the frame size according to the estimated tag population present in the system at any time, the overall performance of the RFID system will be improved. The estimation algorithm employed must be dynamic, since the tag population varies (decreases as tags are identified by the reader), and scalable, maintaining a positive performance for a wide range of tag set sizes.

This chapter summarizes three of the publications that form this dissertation (see Appendix C, D, and E). The first one presents the accurate and scalable tag estimator sMMSE. The second publication configures sMMSE to perform a faster estimation for L calculation, and proposes the Timing-Aware Frame Slotted Aloha

(TAFSA) protocol. TAFSA calculates L as a function of $\hat{n}$ so that the tag identification rate is maximized. The third publication presents the Energy-Aware Slotted Aloha (EASA) protocol. EASA protocol calculates L as a function of $\hat{n}$ so that the energy per tag identified consumed by the reader is minimized.

The protocol FFSA (see Appendix A), presented in Chapter 3, also employs a tag estimation strategy for *L calculation*, using a traditional tag estimator. However, the main novelty of this protocol is the proposed *L examination* strategy with fuzzy logic. For this reason, FFSA is not included in this section.

4.1 sMMSE tag estimator

The knowledge of the number of tags is needed in many RFID applications. It is often desirable to simply estimate the number of tags without explicitly identifying individual tags, contributing to reduce the processing time, and preserve people's privacy. Furthermore, the number of passive tags can be very large due to their low cost, easy disposability, and powerless operation. In these scenarios, tag estimation schemes need to be scalable to large population sizes in order to provide an accurate estimate $\hat{n}$ maintaining a restrained estimation time. An scalable estimation scheme, called scalable Minimum Mean Square Error (sMMSE), is proposed in the related publication (see Appendix C) to provide an accurate tag estimate $\hat{n}$ under large-scaled tag environments.

The proposed scheme accurately estimates the number of tags by minimizing the distance between the observed reading results and their theoretical expected values. The flow-diagram is shown in the related publication (see Appendix C). The estimation mechanism is divided into two phases:

1. Dynamic increase of L to be adapted to $\hat{n}$.

2. Tag estimation with a minimum mean square error function.

The estimator sMMSE presents a flexible performance, because it can be tuned to improve two metrics: the estimation time ET and the estimation error ϵ. The performance of these two metrics is configured with two key parameters: T_{RR} determines the limits of the slots occupancy at which the frame size should be increased,

and Δ sets the frame size increase factor. The related publication obtains a value of T_{RR} and Δ that minimizes ϵ for a wide range of tags, named $\{T_{RR}, \Delta\}_{sMMSE}$. The analysis performed in the related publication sets $\{T_{RR}, \Delta\}_{sMMSE}$ = $\{0.4, 2.0\}$. Therefore, the proposed estimator doubles the frame size when at least 2/5 (40%) of the frame is with filled bit-collisions.

The performance of sMMSE is evaluated and compared with several current estimators [Kodialam 06, Kodialam 07, Li 10, Han 10, Shahzad 15], under different tag set sizes. Numerical results indicate that sMMSE significantly decreases the normalized estimation error and maintains a low estimation time compared to existing strategies. Simulated results prove the accuracy and scalability of sMMSE, being a suitable candidate where high accuracy and low estimation time are sought.

4.2 Tag estimation for L calculation: TAFSA protocol

Currently, there is a growing number of RFID tags sharing a reader interrogation area [Yang 14, Pradhan 17], which leads to higher tag collision rates. As a solution, fast anti-collision protocols are required to minimize the total tags identification time. An anti-collision protocol is considered fast when it provides a high Tag Identification Rate (TIR), defined as the number of tags identified by a unit of time.

The related publication (see Appendix D) shows that TIR mainly depends on the L *calculation* strategy of the frame update policy employed by a DFSA protocol. Then, an extensive study of the L *calculation* strategy which maximizes TIR is provided. According to this study, L should be set as $1/\rho$ times the estimated tag set size $\hat{n}$ (using a power-of-two value), that is, $L = 2^{round(log_2(\hat{n}/\rho)}$. Thus, the frame size which maximizes TIR depends on ρ and $\hat{n}$. The reader obtains the value of ρ just once at the beginning of the inventory round, according to the RFID system timing parameters, by solving

$$\begin{aligned} &\rho^2(T_{QA}e^{\rho} - T_{QR}e^{\rho}) + \rho(nT_k e^{\rho} + \\ &+ nT_{QR}e^{\rho}) - e^{\rho}(nT_k + nT_{QR}) - nT_i + nT_k = 0. \end{aligned} \tag{4.1}$$

In order to obtain $\hat{n}$, the estimator tMMSE is employed, presented next.

The parameters T_{RR} and Δ of sMMSE estimator (introduced in Section 4.1) are configured to minimize ET while providing an accurate tag estimate, resulting in the time-Minimum Mean Squared Error (tMMSE) tag estimator. The analysis presented in the related publication (see Appendix D) concludes that $\{T_{RR}, \Delta\}_{tMMSE}$ = $\{1, 2\}$.

In conclusion, the proposed strategy for L *calculation* obtains the value of L that maximizes the tag identification rate. The estimator tMMSE is applied to calculate $\hat{n}$ and the value of L is updated with the function $L = 2^{round(log_2(\hat{n}/\rho)}$. The value of ρ is obtained as a function of the timing parameters of the particular RFID system by solving (4.1).

Finally, the proposed L *calculation* strategy is applied to a typical DFSA protocol based on EPC C1G2, resulting in Timing-Aware Frame Slotted Aloha (TAFSA) anti-collision protocol. TAFSA presents a timing-aware frame, because L is calculated according to the timing parameters of a real RFID system based on the current standard. The complete frame update policy of TAFSA is presented next.

- L *calculation*: $f(\hat{n})$. The frame size is calculated as $L = 2^{round(log_2(n/\rho)}$, where tMMSE is used to obtain $\hat{n}$, and ρ is obtained by solving (4.1).
- L *examination*: The strategy FbF is used.
- *Frame break condition*: The strategy EoF is used.

The performance of TAFSA is evaluated and compared with several protocols of the state of the art in relation to TIR, and the number of normalized slots and transmitted bits. Considering a typical RFID scenario, simulated results (shown in Appendix D) show that TAFSA, with 56.7 tags identified per second on average, achieves a 10% average improvement in TIR in relation to the strategies of the comparison. Therefore, TAFSA is a suitable candidate where high TIR is sought in passive RFID systems.

4.3 Tag estimation for L calculation: EASA protocol

The growing interest in mobile devices is transforming wireless identification technologies. Mobile and battery-powered RFID readers, such as hand readers and

smart phones, are becoming increasingly attractive [Hessar 13, Agrawal 17]. These RFID readers require energy-efficient anti-collision protocols to minimize the tags collisions. Therefore, it is desired to expand the reader's battery life by using an energy-aware tag anti-collision protocol.

Energy-efficient protocols involve a low reader energy consumption per tag identified E/n. The related publication (see Appendix E) presents a thorough study of E/n and analyzes the main factor that affects this metric: the *L calculation* strategy of the frame update policy employed by a DFSA protocol. An energy consumption model is presented where E depends on the power required by the reader to transmit and receive information to and from the tags. During the identification process, the reader transmits a set of commands and a Continuous Wave (CW) to power up passive tags, with power P_{t_x}. To receive the data from the tags, the reader needs an extra power P_{r_x}.

The analysis presented in the related publication (see Appendix E) concludes that in order to minimize E/n, the frame size should be set as $1/\rho$ times the estimated tag set size $\hat{n}$ (using a power-of-two value), that is, $L = 2^{round(log_2(\hat{n}/\rho)}$. Thus, the frame size which minimizes E/n depends on $\hat{n}$ and ρ. The traditional Minimum Mean Square Error (MMSE) estimator [Vogt 02] is employed to obtain $\hat{n}$. The reader obtains the value of ρ just once at the beginning of the inventory round as:

$$\rho = 1 + W\left[\frac{P_{t_x}(T_i - T_k) - P_{r_x}T_{EPC}}{e(P_{t_x}T_k + P_{r_x}T_{EPC})}\right] \tag{4.2}$$

where $W(x)$ represents the Lambert W-function. From (4.2), it is clear that the value of ρ depends on the timing and power parameters of the RFID system.

In conclusion, the proposed strategy for L *calculation* minimizes the reader energy consumption per tag identified. This strategy first employs MMSE estimator to obtain $\hat{n}$, and then updates the frame size with the function $L = 2^{round(log_2(\hat{n}/\rho)}$. The value of ρ is obtained as a function of the transmitting and receiving power, and the timing parameters of the particular RFID system, according to (4.2).

Finally, the proposed L *calculation* strategy is applied to a typical DFSA protocol based on EPC C1G2, resulting in Energy-Aware Slotted Aloha (EASA) anti-collision protocol. EASA presents an energy-aware frame, because this protocol

sets the frame size so that E/n is minimized. The complete frame update policy of EASA is presented next.

- L *calculation*: $f(\hat{n})$. The frame size is calculated as $L = 2^{round(log_2(\hat{n}/\rho)}$, where MMSE is used to obtain $\hat{n}$, and ρ is obtained with (4.2).
- L *examination*: The strategy FbF is used.
- *Frame break condition*: The strategy EoF is used.

The performance of EASA is evaluated and compared with several recent anti-collision protocols of the state of the art regarding the energy per tag identified consumed by the reader in one inventory round E/n. Simulation results (see Appendix E) show that EASA clearly improves E/n for all n evaluated, with an average of 15 mJ consumed by the reader per tag identified. Overall, EASA presents a 6% average reduction in E/n compared to the protocol with the second lowest E/n. Therefore, EASA is a suitable candidate where energy-efficiency is sought in passive RFID systems.

CHAPTER

5

Experimental validation of DFSA protocols

COMMERCIAL RFID readers are generally black box systems which provide only limited configuration, and they do not give the option to observe or modify the MAC or Physical layer behaviour. Therefore, it is not possible to study the physical implementation of existing anti-collision protocols. To tackle this problem, a Software Defined Radio (SDR) Ultra High Frequency (UHF) RFID reader is presented to evaluate the performance of RFID anti-collision protocols. Because this reader is software-defined, anti-collision protocols can be implemented by writing user-level software in C++.

The proposed reader is capable of identifying not only commercial tags but also the well-known sensor tags called WISP [Sample 08]. Additionally, the reader is capable of reading sensor data from the WISP tags. This chapter summarizes two of the publications that form this dissertation (see Appendix F and G). The contributions of these chapters are expected to be useful for researchers to (i) validate the performance of different user-configurable anti-collision protocols based on EPC C1G2 standard and (ii) design and implement custom identification and sensing protocols to improve the communication with WISP tags.

5.1 SDR-UH-RFID reader

A SDR-UHF-RFID reader is proposed in the related publications (see Appendix F and G) to evaluate the performance of anti-collision protocols under different configurations. The reader is composed of an USRP N210, an SBX daughterboard, and a Linux PC. A Gigabit switch is used to communicate the USRP with a Linux PC. The transmit and receive ports of the daughterboard are connected to two circularly polarized patch antennas of 6dBi gain. The reader uses a set of software modules built on GNU radio 3.7.11 .

In order to differentiate between the three types of slots (idle, single, collision), the reader sets a threshold energy value E_{th} for the energy of the received signal E_r to detect an idle response. Thus, an idle slot occurs when the energy of the received signal is lower than this threshold, that is, when $E_r < E_{th}$. Additional details about the reader configuration can be found in the related publications (see Appendix F and G). Performance evaluation results are obtained experimentally and by simulation, as follows:

- Experimental: tags are identified with the proposed SDR-UHF-RFID reader, and two different approaches are used to evaluate the results.
  - Analytical: the reader counts the number of transmitted reader commands (Qc, QA, QR, ACK), and the received tags' responses (RN16, EPC). The duration of each reader command and tags' responses is known a priori by the reader.
  - Timer: a timer is started in the reader program when the reader transmits the first command Qc, and it is stopped when the reader correctly identifies the required n tags present inside its interrogation zone. With this approach, the experimental results also provide information about the reader processing time.
- Simulation: results are obtained with Matlab R2017a. Tags are assumed to be uniformly distributed and physical-layer effects are not considered.

The proposed reader provides a useful platform for evaluating the performance of DFSA protocols in a real scenario for different configuration parameters. First,

the reader is configured to identify (receive the EPC code) from commercial tags. Then, this reader is adapted with extended functionalities to identify WISP tags and to read data from their accelerometer sensor.

5.2 Commercial tags identification with Slot Counter

The related publication (see Appendix F) implements the Slot Counter protocol in the previously presented SDR-UHF-RFID reader. The main goal is to identify commercial tags with a user-configurable anti-collision protocol. In order to efficiently communicate with commercial tags, the reader is configured with the following parameters: $BLF = 40$kHz, $Tari = 24\mu s$, $P_t = 22$mWatts, $RTcal = 72\mu s$, and $TRcal = 200\mu s$.

The experimental set-up is shown in Figure 5.1. The performance of the Slot Counter protocol and an ideal DFSA protocol is evaluated in the proposed experimental scenario. The reader performs several inventory rounds for varying sets of Alien-9640 tags $n\in$[16,32,64].

From the experimental evaluation of the Slot Counter protocol, it is concluded that its performance is greatly influenced by the initial frame size and by the number of tags inside the interrogation zone. Also, the experimental results of the identification time obtained with the timer are higher than the analytical results, as expected, because the SDR reader requires some time for the processing and calculations tasks.

From the experimental analysis of the ideal DFSA anti-collision protocol performed, it is demonstrated that its performance is strongly influenced by the frame size. Also, performance improvements are observed in the experimental results in relation to the theoretical expected values. This occurs due to a lower probability of collision slots in the physical scenario evaluated.

Details about the experimental evaluation of the two protocols can be found in the related publication (see Appendix F).

Figure 5.1: The physical RFID system used in the experimental validation. The picture shows an Ettus Research N210 Software Defined Radio, a PC that controls the SDR, a switch to connect the SDR to the PC, two circularly polarized antennas. Alien-9640 tags are attached to foam panels, which are inserted into the black racks.

5.3 Sensor tags identification with FuzzyQ

The related publication (see Appendix G) implements FuzzyQ protocol (Appendix B) in the SDR-UHF-RFID reader presented in Section 5.1. The main goal is to identify WISP 5.1 tags with a user-configurable anti-collision protocol. The reader configuration presented in Section 5.2 is not appropriate for identifying WISP tags, because these tags have different timing requirements and restrictions to commercial tags. In order to efficiently communicate with WISP 5.1 tags, the reader is configured with the following parameters: $BLF = 160$kHz, $Tari = 12.5\mu s$, $P_t = 180$mWatts, $RTcal = 36.6\mu s$, and $TRcal = 50\mu s$. Furthermore, extended functionalities are added to this reader so that it can identify WISP 5.1 tags and read data from their accelerometer sensor.

FuzzyQ is implemented in the previously configured reader by re-writing user-level software in C++. This protocol presents a fast strategy to read RFID tags by not limiting the variation of Q to steps of one unit and considering instead a range of values, in order to achieve a more abrupt step size (0, $\pm$1, $\pm$2, or $\pm$3). In order to consider these 7 different step size values, the reader QA command, as defined in the EPC C1G2 standard, is modified, resulting in the modified QA command, mQA. The specification of mQA is shown in Table 5.1.

Table 5.1: Modified QueryAdjust (mQA) command.

	Command	**Session**	**UpDn**
# of bits	4	2	3
Description	1001	00: S0 01: S1 10: S2 11: S3	000: no change to Q 001: Q = Q-3 010: Q = Q-2 011: Q = Q-1 100: Q = Q+3 101: Q = Q+2 110: Q = Q+1

WISP tags are programmed to follow EPC C1G2 standard and to backscatter the information at 160kHz. Additionally, they are re-programmed to (i) transmit $RN16$ just at one slot per frame, and ii) stay idle until the reader starts a new inventory round once they are identified.

In order to evaluate the performance of FuzzyQ in a real scenario, the reader executes several inventory rounds for n=4 WISP 5.1 tags. The experimental set-up is shown in Figure 5.2. The performance of FuzzyQ is compared with that of the Slot Counter protocol in the proposed experimental scenario. Next, both protocols are compared by simulation for higher tag set sizes up to n=1024.

The performance of FuzzyQ and Slot Counter is validated and compared by measuring the Tags Identification Rate TIR metric, defined as the total number of tags identified per second. The related publication (see Appendix G) shows that

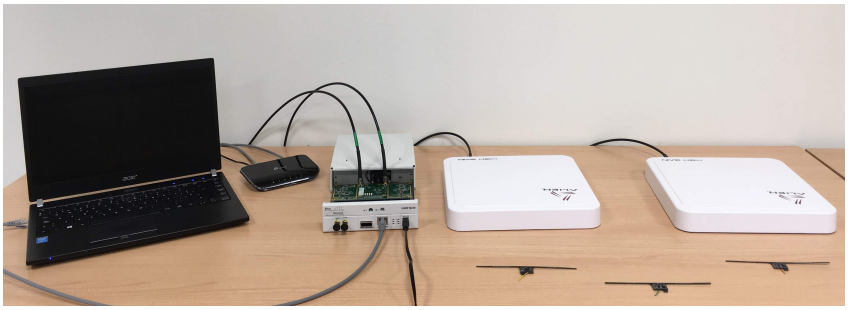

Figure 5.2: The physical RFID system used in the experimental validation. The photo shows an Ettus Research N210 Software Defined Radio, a laptop that controls the SDR, a switch to connect the SDR to the laptop, two circularly polarized antennas and three WISP tags on the front.

FuzzyQ improves TIR in relation to Slot Counter, both in the experimental and simulation scenario. These results demonstrate the ability of FuzzyQ to reduce the number of collision slots by using mQA command.

For both protocols, analytical TIR is higher than simulation TIR, because capture effect[1] contributes to a reduction in the number of collision slots. Additionally, experimental results obtained by calculating TIR with the timer are higher than the values calculated analytically, as expected, because the SDR system requires some time for the processing and calculations tasks.

Finally, the related publication demonstrates the significant role of anti-collision protocols in the process of reading data from RFID sensors, because the performed analysis concludes that the identification time represents more than 59% of the sensing time. Additional details about this section can be found in the related publication.

In conclusion, the proposed SDR-UHF-RFID reader is expected to be useful for researchers to validate the performance of user-configurable identification and sensing protocols with the aim of improving the communication with off-the-shelf and WISP tags.

[1]Physical layer effect which is very common in RFID systems. Tags response amplitudes can vary due to different distances from the reader antenna, or due to multi-path fading present in the channel [Solic 17]. As a result, the reader successfully resolves one tag reply in a collided slot.

CHAPTER

6

Conclusion and future work

THROUGHOUT this dissertation one main goal has been pursued: to improve the performance of existing DFSA tag anti-collision protocols based on the current RFID standard by lowering their tag identification time and also the energy consumed by the reader. To do so, a set of efficient protocols have been developed which employ two different scalable and dynamic strategies to update the frame size: fuzzy logic and tag estimation. This chapter summarizes the main conclusions that have been drawn. Then, an outlook is presented for potential applications and future research.

6.1 Conclusions

As described through this dissertation, DFSA protocols are currently the most popular strategies used to deal with tag collisions in RFID systems, because most RFID manufactures use a DFSA protocol which is part of the current standard in RFID technology (the Slot Counter protocol). This work focuses on the strategy employed by DFSA protocols to update the transmission frame size.

The first chapter of this dissertation introduced RFID technology and presented an up-to-date classification of RFID systems according to their form and functionality. Then, this chapter provided evidence for the necessity of using DFSA

anti-collision protocols to minimize the impact of tags collisions in the process of identifying a set of tags.

Chapter 2 presented an overview of DFSA protocols and analyzed their frame update policy. Then, an analysis and classification of the main DFSA protocols of the state-of-the-art according to their frame update policy was presented. From this analysis, it was concluded that the frame update policy represents a key component of a DFSA protocol, and thus the frame update policy greatly influences the performance of the anti-collision protocol.

Chapter 3 proposed two DFSA protocols which improve the performance of existing DFSA protocols. The two protocols apply a fuzzy logic strategy to update the frame size. Fuzzy Frame Slotted Aloha (FFSA), the first proposed protocol, proved an improvement of 10.7% in the tag identification rate (number of tags identified per second) in relation to the Slot Counter protocol. Then, the protocol FuzzyQ was proposed and it showed a 7% average improvement in the tags identification time (total time required to identify a set of tags) in relation to the Slot Counter protocol.

Chapter 4 introduced two DFSA protocols that improve the performance of existing DFSA protocols: Timing-Aware Slotted Aloha (TAFSA) and Energy-Aware Slotted Aloha (EASA). Both protocols employ a tag estimation strategy to set the value of the frame size according to the estimated number of tags. TAFSA revealed a 10% improvement in the tag identification rate (number of tags identified per second) in relation to several existing protocols. Then, EASA exhibited a 6% improvement in E/n (energy consumed by the reader per tag identified) in relation to several existing protocols.

Finally, Chapter 5 presented an SDR-UHF-RFID reader to evaluate the performance of user-configurable anti-collision protocols. This chapter demonstrated the feasibility of implementing DFSA protocols based on EPC C1G2 in a configurable physical system. Finally, it was concluded that tag anti-collision protocols constitute a very significant part of the process of reading RFID sensors, because the identification time represents more than 59% of the sensing time.

Through all of these contributions, it is my hope that this dissertation becomes a solid step towards more efficient DFSA anti-collision protocols, so that RFID

readers can perform a faster identification of a growing number of traditional and CRFID tags inside their interrogation area.

6.2 Future work

Nowadays, RFID technology constitutes a trending topic in different fields of research. For instance, this technology is replacing the traditional barcodes identification systems in the supply chain and inventory management fields.

Recent advances in modern technology have made it possible to attach a passive RFID tag to a large variety of items. Passive tags are becoming increasingly attractive due to their low cost ($\approx$10 cents), a small sticker form factor, and the operation range over 10 meters from the reader. This scenario involves a growing number of RFID tags sharing a reader interrogation area, which leads to higher tag collision rates. Furthermore, due to the current popularity in wireless systems, mobile and battery-powered RFID readers, such as hand readers and smart phones, are increasingly being used. Therefore, fast and energy-aware tag anti-collision protocols are required to minimize the total tags identification time and to expand the reader's battery life. The goal of this dissertation is to build towards that end.

This work introduced four different DFSA anti-collision protocols which improve the performance of existing DFSA protocols. This goal was achieved by applying fuzzy logic and tag estimation strategies to the frame update policy of DFSA protocols. The improvement capacity of the proposed solutions is clear.

A combination of the two presented strategies, fuzzy logic and tag estimation, for the frame update policy of DFSA protocols is proposed as future work. A frame update policy which combines fuzzy logic and the presented tMMSE tag estimator will be studied to further improve the performance of existing DFSA protocols in terms of the tags identification time and the energy efficiency.

As next steps, the protocols TAFSA, EASA, and FFSA will be implemented in the physical RFID system presented in this dissertation in order study the consequences of some typical physical layer effects in RFID communication (such as the capture effect) over the protocols performance. Then, the protocols will be analyzed an re-configured to correct these effects.

6. CONCLUSION AND FUTURE WORK

Currently, there is an increasing popularity in RFID sensor networks which use passive RFID tags with attached sensors (CRFID tags). In order to read data from these sensors, tags must be previously identified. Thus, the tags identification process is a previous step to read data from their attached sensor. Taking this into consideration, one of the protocols presented in this dissertation will be adapted and employed to design a more complex protocol which performs both the identification and sensing phase of a CRFID tag. The resulting protocol will efficiently identify the tag first and it will then read data from its sensor. The feasibility of this protocol will be validated using experimentation system presented in this dissertation and WISP tags.

Bibliography

[Agrawal 17] T. Agrawal, P.K. Biswas and R. Sharma. *A novel-Q DFSA algorithm for passive RFID system*. Pervasive and Mobile Computing, Vol. 40, No. Supplement C, pp. 89 – 103, September 2017. 1, 39

[Arjona 17] L. Arjona, H. Landaluce and A. Perallos. *Procedimiento de anticolision para identification de transpondedores en un sistema RFID. Spanish Patent 201531673*, February 2017. 32

[Capetanakis 79] J. Capetanakis. *Tree algorithms for packet broadcast channels*. IEEE Transactions on Information Theory, Vol. 25, No. 5, pp. 505–515, Sep 1979. 7

[Chen 14] W. T. Chen. *A fast anticollision Algorithm for the EPCglobal UHF class-1 generation-2 RFID standard*. IEEE Communications Letters, Vol. 18, No. 9, pp. 1519–1522, Sept 2014. 26, 34

[Chen 16] W. T. Chen. *Optimal Frame Length Analysis and an Efficient Anti-Collision Algorithm With Early Adjustment of Frame Length for RFID Systems*. IEEE Transactions on Vehicular Technology, Vol. 65, No. 5, pp. 3342–3348, May 2016. 26

[Chen 17] Y. Chen, J. Su and W. Yi. *An Efficient and Easy-to-implement Tag Identification Algorithm for UHF RFID Systems*. IEEE Communications Letters, Vol. 21, No. 7, pp. 1509–1512, January 2017. 26

[Duan 17] L. Duan, X. Zhang, Z. J. Wangng and F. Duan. *A Feasible Segment-by-Segment ALOHA Algorithm for RFID Systems*. Wireless Personal Communications, Vol. 96, No. 2, pp. 2633–2649, Sep 2017. 26

[Eom 10] J. B. Eom and T. J. Lee. *Accurate tag estimation for dynamic framed-slotted ALOHA in RFID systems*. IEEE Communications Letters, Vol. 14, No. 1, pp. 60–62, January 2010. 26

[EPCglobal 15] EPCglobal. *Radio Frequency Identity Protocols class-1 generation-2 UHF RFID protocol for communications at 860 MHz–960 MHz*, 2015. 3, 19, 26

[Farsens] Farsens. *Battery Free RFID Sensors*. http://www.farsens.com/en/products/battery-free-rfid-sensors/. Accessed July 2018. 4

[Finkenzeller 03] K. Finkenzeller. RFID handbook: Fundamentals and applications in contactless smart cards and identification. John Wiley & Sons, Inc., New York, NY, USA, 2 edition, 2003. 3

[Han 10] H. Han, B. Sheng, C. C. Tan, Q. Li, W. Mao and S. Lu. *Counting RFID Tags Efficiently and Anonymously*. In Proceedings IEEE INFOCOM, pp. 1–9, March 2010. 37

[Hessar 13] F. Hessar and S. Roy. *Energy Based Performance Evaluation of Passive EPC Gen 2 Class 1 RFID Systems*. IEEE Transactions on Communications, Vol. 61, No. 4, pp. 1337–1348, April 2013. 1, 39

[Klair 10] D.K. Klair, C. Kwan-Wu and R. Raad. *A Survey and Tutorial of RFID Anti-Collision Protocols*. Communications Surveys Tutorials, IEEE, Vol. 12, No. 3, pp. 400–421, Third 2010. 7

[Kodialam 06] M. Kodialam and T. Nandagopal. *Fast and Reliable Estimation Schemes in RFID Systems*. In Proceedings of the 12th Annual International Conference on Mobile Computing and Networking,

MobiCom '06, pp. 322–333, New York, NY, USA, 2006. ACM. 37

[Kodialam 07] M. Kodialam, T. Nandagopal and W. C. Lau. *Anonymous Tracking Using RFID Tags*. In IEEE INFOCOM - 26th IEEE International Conference on Computer Communications, pp. 1217–1225, May 2007. 37

[Li 10] T. Li, S. Wu, S. Chen and M. Yang. *Energy Efficient Algorithms for the RFID Estimation Problem*. In Proceedings IEEE INFOCOM, pp. 1–9, March 2010. 37

[Murofushi 17] R. H. Murofushi and J. J. P. Z. S. Tavares. *Towards fourth industrial revolution impact: smart product based on RFID technology*. IEEE Instrumentation Measurement Magazine, Vol. 20, No. 2, pp. 51–56, April 2017. 1

[Nikitin 06] P. V. Nikitin and K. V. S. Rao. *Performance limitations of passive UHF RFID systems*. In IEEE Antennas and Propagation Society International Symposium, pp. 1011–1014, July 2006. 2

[Plessky 10] V. P. Plessky and L. M. Reindl. *Review on SAW RFID tags*. IEEE Transactions on Ultrasonics, Ferroelectrics, and Frequency Control, Vol. 57, No. 3, pp. 654–668, March 2010. 3

[Pradhan 17] S. Pradhan, E. Chai, K. Sundaresan, L. Qiu, M. A. Khojastepour and S. Rangarajan. *RIO: A Pervasive RFID-based Touch Gesture Interface*. In Proceedings of the 23rd Annual International Conference on Mobile Computing and Networking, pp. 261–274, October 2017. 1, 37

[Sample 08] A. P. Sample, D. J. Yeager, P. S. Powledge, A. V. Mamishev and J. R. Smith. *Design of an RFID-Based Battery-Free Programmable Sensing Platform*. IEEE Transactions on Instrumentation and Measurement, Vol. 57, No. 11, pp. 2608–2615, Nov 2008. 2, 4, 41

[Shahzad 15] M. Shahzad and A.X. Liu. *Fast and Accurate Estimation of RFID Tags*. IEEE/ACM Transactions on Networking, Vol. 23, No. 1, pp. 241–254, Feb 2015. 35, 37

[Solic 14] P. Solic, J. Radic and N. Rozic. *Energy Efficient Tag Estimation Method for ALOHA-Based RFID Systems*. IEEE Sensors Journal, Vol. 14, No. 10, pp. 3637–3647, Oct 2014. 26

[Solic 16] P. Solic, J. Radic and N. Rozic. *Early Frame Break Policy for ALOHA-Based RFID Systems*. IEEE Transactions on Automation Science and Engineering, Vol. 13, No. 2, pp. 876–881, April 2016. 26

[Solic 17] P. Solic, J. Maras, J. Radic and Z. Blazevic. *Comparing Theoretical and Experimental Results in Gen2 RFID Throughput*. IEEE Transactions on Automation Science and Engineering, Vol. 14, No. 1, pp. 349–357, Jan 2017. 46

[Su 16] J. Su, Z. Sheng, D. Hong and G. Wen. *An Effective Frame Breaking Policy for Dynamic Framed Slotted Aloha in RFID*. IEEE Communications Letters, Vol. 20, No. 4, pp. 692–695, April 2016. 26

[Vogt 02] H. Vogt. *Efficient Object Identification with Passive RFID Tags*. In Friedemann Mattern and Mahmoud Naghshineh, editors, Pervasive Computing, volume 2414 of *Lecture Notes in Computer Science*, pp. 98–113. Springer Berlin Heidelberg, 2002. 31, 39

[Wu 13] H. Wu, Y. Zeng, J. Feng and Y. Gu. *Binary Tree Slotted ALOHA for Passive RFID Tag Anticollision*. IEEE Transactions on Parallel and Distributed Systems, Vol. 24, No. 1, pp. 19–31, Jan 2013. 21. 7

[Yang 14] L. Yang, Y. Chen, X. Y. Li, C. Xiao, M. Li and Y. Liu. *Tagoram: Real-time Tracking of Mobile RFID Tags to High Precision Using COTS Devices*. In Proceedings of the 20th Annual Interna-

tional Conference on Mobile Computing and Networking, pp. 237–248, September 2014. 1, 37

[Zhang 11] H. Zhang, J. Gummeson, B. Ransford and K. Fu. *Moo: A Batteryless Computational RFID and Sensing Platform*. Technical report, Department of Computer Science, University of Massachusetts, Amherst, 2011. 2, 4

[Zhao 15] Y. Zhao, J. R. Smith and A. Sample. *NFC-WISP: A sensing and computationally enhanced near-field RFID platform*. In IEEE International Conference on RFID, pp. 174–181, April 2015. 2, 4

APPENDIX

A

Paper I

A Novel Frame Update Policy for RFID DFSA Tag Anti-Collision Protocols

This paper is currently under second review in a JCR journal. The submitted version is appended here.

A Novel Frame Update Policy for RFID DFSA Tag Anti-Collision Protocols

Laura Arjona, Hugo Landaluce, Asier Perallos, and Enrique Onieva

***Abstract*—Asset identification with Radio Frequency Identification (RFID) technology is becoming increasingly popular. The negligible cost of commercial RFID tags compared to the item they are attached to makes it possible to tag almost any item. An RFID system consists of a reader and various numbers of tags. These tags obtain their power from the reader's signal and require fast and energy efficient anti-collision protocols to minimize the collisions with the other tags sharing the reader's interrogation zone. Therefore, RFID application developers must be mindful of anti-collision protocols. Dynamic Frame Slotted Aloha (DFSA) anti-collision protocols have been extensively analyzed, because EPCglobal Class 1 Generation 2 (EPC C1G2), the current standard in RFID, employs this strategy. They are distinguished by their policy for updating the transmission frame size. The present paper analyzes the frame size update policy of DFSA protocols in order to propose a novel policy to lower the tag identification time. This policy is then applied to Fuzzy Frame Slotted Aloha (FFSA) anti-collision protocol. Moreover, this paper surveys and classifies DFSA state-of-the-art protocols according to their frame size update policy. Simulation results show that FFSA significantly decreases the tag identification time and energy consumption per tag for a wide range of tag populations compared with earlier DFSA protocols. FFSA achieves a 10.71% improvement in the tag identification rate (tags/s) in relation to the Slot Counter protocol, employed in EPC C1G2.**

***Index Terms*—Radio Frequency Identification (RFID), EPCglobal standard, anticollision, tag estimation, frame update policy, energy aware.**

I. Introduction

THE growing interest in asset recognition makes Radio Frequency Identification (RFID) technology increasingly attractive. The RFID market was worth 9 billion in 2014, and the IDTechEx forecast is that it will rise to $\sim$30 billion in 2024 [1]. Most RFID applications require a fast, and in some cases energy efficient, tag identification rate, especially with increasing tag populations [2]. Tags are uniquely identified with an identification code (ID), which consists of a sequence of bits. The coexistence of several tags sharing the reader's interrogation zone provides RFID technology with great flexibility at the expense of suffering from the tag collision problem, which occurs when two or more tags respond simultaneously to a reader command, resulting in a waste of energy and an increase in the tag identification time. Therefore, RFID systems require an anti-collision protocol to deal with tag collisions and minimize their impact. The main existing anti-collision protocols in the literature can be classified into Aloha-based and tree-based protocols.

The authors are with the University of Deusto, Faculty of Engineering, Avda. Universidades, 24, 48007, Bilbao.
E-mail: laura.arjona@deusto.es

Tree-based protocols, in essence, split colliding tags into subsets, and further split the subsets repeatedly up to the successful response of all the tags that are within the interrogation zone. Aloha-based protocols divide the time into frames, so that tags randomly choose one slot per frame to respond. EPCglobal Class 1 Generation 2 (EPC C1G2), the current standard in RFID systems [3], adopts a Dynamic Frame Slotted Aloha (DFSA) anti-collision protocol. Most RFID manufacturers currently follow the EPC C1G2 standard, enhancing the research relevance of DFSA protocols. Consequently, many DFSA algorithms have recently appeared in the literature to solve the RFID tag collision problem. This type of protocol is characterized by the strategy it employs to update the transmission frame size along the identification process.

There are several papers comparing the performance of the most important Aloha algorithms [4]–[6]. However, they do not establish a clear classification, nor do they adopt EPC C1G2 constraints. The authors in [7] present a classification of the most important anti-collision protocols up to 2009. Although they provide an extensive analysis of several DFSA protocols, they do not study the frame break condition. Besides, a key limitation of that paper is that it only surveys protocols published before the year 2009. [8] presents a classification of DFSA protocols, without considering protocols based on tag estimation.

In the present paper, a classification of the main state-of-the-art DFSA anti-collision protocols according to their frame update policy is presented.

The main contributions made in this work are:

1) Analysis of the frame update policy in DFSA tag anti-collision protocols.
2) Study and classification of state-of-the-art DFSA tag anti-collision protocols according to their frame update policy.
3) Novel frame update policy for DFSA protocols, and novel anti-collision protocol, Fuzzy Frame Slotted Aloha (FFSA), which applies this new policy to lower the average time to identify one tag.
4) Tag identification time and Energy consumption evaluation of FFSA and comparison with several anti-collision protocols of the state-of-the-art.

The rest of this paper is organized as follows. Section II presents the transmission model and RFID standard EPC C1G2. Section III surveys and analyzes the frame update policy for DFSA protocols. This is followed by an analysis and classification of state-of-the-art DFSA anti-collision protocols in Section IV. A novel frame update policy is presented in Section V. After that, Section VI introduces the FFSA anti-

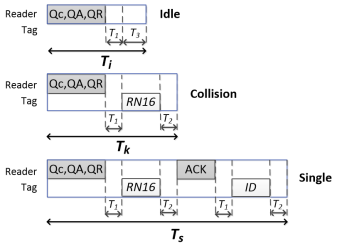

Fig. 1: Transmission model of EPC C1G2.

collision protocol. Section VII provides the results of the performance evaluation followed by some identified limitations. Finally, Section VIII concludes this paper.

II. Background

Some definitions are provided to properly set the background of this paper and to better understand its main contributions.

A. Transmission model

The strategies analyzed in this paper are based on the RFID transmission model between the reader and the tags defined in Fig. 1, meeting EPC C1G2 requirements. In this model, a *slot* is defined as a period of time that separates the tags' responses. Conventionally, three types of slots are considered, in terms of the tags' responses to the reader's commands: single (only one tag replies), collision (more than one tag replies in the same slot), and idle (none of the tags reply). The duration of each type of slot, single, collision, and idle, is referred to as T_s, T_k, and T_i, respectively. These slots are accurately specified in the standard, and their duration is determined by the link timing parameters T_1, T_2, and T_3. A sequence of L slots is referred to as a *frame*, where L represents its size. An identification process is composed of a set of frames and tags that can respond in only one slot per frame. Finally, a *command* is a bit-string transmitted by the reader to the tags.

B. RFID Standard EPCglobal Class 1 Generation 2

EPC C1G2 employs a DFSA protocol to arbitrate collisions: the Slot Counter protocol. The reader starts the identification process by transmitting a Query (Qc) command, and then alternates between QueryAdjust (QA) and QueryRep (QR) commands. QA starts a new frame with the updated size L and implies that tags must randomly select a slot in the frame (the initial value of their internal slot count SC), while QR tells the tags to decrement SC. Thus, when SC=0, the tag transmits a 16-bit random number $RN16$. The frame size is set as L=2^Q, and its value is dynamically updated with the parameters Q and C, where Q=round(Qfp). Regarding the time slot occupancy, there are three possible scenarios to update the value of Qfp, as shown in Fig. 1.

- Single slot: Q_{fp} remains unchanged. In this case, the reader replies to the tag with an ACK command followed by the same $RN16$ received by the tag, and the tag transmits its ID.
- Collision slot: $Q_{fp} = Q_{fp} + C$.
- Idle slot: $Q_{fp} = Q_{fp} - C$.

III. Analysis of Frame Update Policies for DFSA Protocols

A wide variety of DFSA protocols can be found in the literature which update L with the aim of improving different metrics regarding the process of tag identification. Establishing a clear classification of all DFSA protocols is not straightforward. A key feature which differentiates a DFSA protocol is the strategy it follows to update the frame size along the identification of a set of tags. To this end, this section establishes a classification of the main frame update policies employed by DFSA anti-collision protocols. The classification presented in this work considers three different perspectives to update L, which respond to the following three questions: how is L calculated? When is L examined? When a new frame must be started? A classification of the main up-to-date policies is summarized in Table I. Furthermore, the main anti-collision protocols found in the literature are classified in this section according to the policy they employ.

A. Frame size calculation

The reader adjusts L in each reading cycle according to the responses from the competing tags in each frame. The number of tags that enter into the coverage area usually varies randomly, thus the number of tags that compete in each cycle is unknown, and the frame size adjustment is not trivial. Two main strategies can be found in the literature to set a value for the frame size in DFSA protocols: the first calculates L as a function of the parameter Q, and the second sets L as a function of the estimated number of tags $\hat{n}$.

1) Parameter Q: f(Q)
   The frame size can be adjusted by controlling the number and states of the slots in each frame with parameter Q, so that Q increases when collisions are detected, and decreases with increasing number of idle slots. Several approaches in the literature update L by adjusting Q [3], [9]–[13].
2) Tag set size estimation
   Many works in the literature have addressed the tag estimation task in order to provide an optimal frame size according to the estimated number of tags. It is known that a DFSA protocol reaches its maximum slot efficiency, defined as the ratio between the number of tags and the total number of slots required to identify them, when the frame size is equal to the number of tags [2]. Therefore, in order to optimize this metric, the reader should set the frame size equal to the estimated number of tags. However this condition only applies when equal durations for each type of slot are assumed. EPC C1G2 considers unequal time intervals for each slot. For this reason, some approaches set the frame size according to $\hat{n}$ but assuming unequal processing durations for each type of slot (single, collision, idle) [14] [15].
   Once the tag set size has been estimated, assuming equal or unequal durations of the slots, the next step is to calculate L according to $\hat{n}$. Two main strategies to set

L as a function of $\hat{n}$ can be found in the literature, and they are presented next.

- Continuous function of $\hat{n}$: f($\hat{n}$)
  The first strategy is to set L as a continuous function of $\hat{n}$. The reader analyzes the information extracted from the tags' responses (c_s,c_k,c_i) and sets L as a function of these values. Several anti-collision protocols follow this strategy [15]–[24].
- Look-up table (LUT) according to $\hat{n}$: LUT($\hat{n}$)
  The second strategy is to set L according to an LUT based on $\hat{n}$. The idea is to define different ranges of $\hat{n}$ and assign a different value of L for each $\hat{n}$ range. Several approaches in the literature follow this strategy, including [25]–[27], [29]–[33].

B. Frame size examination

This section answers the question related to *when* (in which slot) L must be examined, considering that an examination refers to a new calculation of L. DFSA algorithms do not assign a fixed value to L for the complete identification process, rather, L is dynamically updated. Therefore, the reader must examine whether the current value is appropriate or not during the reading process and decide if a new frame is needed. For this purpose, a strategy is defined to establish in which slot or slots within a frame the value of L must be examined. Four main strategies can be found in the literature, presented next from lower to higher examination frequency.

1) Frame by Frame (FbF)
   The simplest strategy is to calculate L only at the last slot of each frame [18]–[24], [30], [31].
2) Pointer by Pointer (PbP)
   Some protocols have defined some particular slots within the frame, referred as the pointer p in the present paper ($p<L$), where L is examined to check its appropriateness [13], [15], [25], [32], [33]. These pointers are usually set as a fraction of the current frame size.
3) Slot by Slot (SbS)
   The third strategy is based on examining L at every slot of the frame [3], [9]–[12], [16], [17], [26], [28].
4) Hybrid
   The protocols [27], [29] present a two-phase tag identification process. To examine the frame size, they apply the strategy SbS in the first phase, and FbF in the second.

C. Frame break condition

The previous section presented the main strategies for establishing in which slot or slots within a frame must L be examined. This section will present the different policies followed by the reader to decide, after calculating L, whether a new frame must be started, or on the contrary, if the reader must proceed with the next slot. Five main strategies can be found in the literature.

1) Different L
   Several protocols start a new frame when the new value of L differs from the current one [3], [9], [10], [12], [13], [15], [16], [26], [32].

TABLE I: Classification of DFSA frame update policies.

	Operation
L calculation	f(Q)
	f($\hat{n}$)
	LUT($\hat{n}$)
L examination	FbF
	SbS
	PbP
	Hybrid
Frame break condition	Different L
	LUT($\hat{n}$)
	$c_{s2}>c_{s1}$
	Lower IT
	EoF

2) L fits n from an LUT: LUT($\hat{n}$)
   Some algorithms define an LUT based on $\hat{n}$ and L [25], [27], [29], [33] to check the appropriateness of L. First, the reader searches in the LUT for the corresponding value of L for the previously obtained $\hat{n}$. Then, if this new value differs from the current one, a new frame is started. Otherwise, the reader proceeds to the next slot of the current frame.
3) Higher expected number of successful slots: $c_s(n, L)$
   The authors in [17] define a policy to break the current frame and start a new one if the expected number of successful slots in the rest of the current frame $c_{s1}(n, L)$ is less than that expected in the new frame $c_{s2}(n, L)$. That is, a new frame is started if $c_{s2}(n, L)>c_{s1}(n, L)$.
4) Lower Identification Time: Lower IT
   The authors in [11] present a frame cancellation strategy to minimize the total expected time to identify a tag set. This work presents an strategy, where a new frame is started if the expected average time for one tag identification $t_{IT}(n, L)$ in the new frame is lower than the one in the current frame.
5) End of Frame: EoF
   In this case, a new frame is started when the current frame has finished. This strategy is intrinsic to a DFSA-based anti-collision protocol, and it is applied in all the protocols analyzed in the present paper.

IV. Analysis and Classification of DFSA Tag Anti-Collision Protocols

This section presents some of the most important DFSA protocols in the literature, and classifies them according to their frame update policy. In order to present these strategies, a system model with one reader and n tags is defined, and a DFSA frame of size L is defined. The classification is presented in Table II.

A. Slot-Counter

The Slot Counter protocol [3] was presented in Section II.B. This algorithm sets L as a function of the parameter Q, and its value is examined at every slot of the frame (SbS). Then the reader starts a new frame whenever L changes. Note that EPC C1G2 establishes that the frame length must be a power of two.

TABLE II: Classification of DFSA anti-collision protocols according to their frame update policy.

	L calculation	L examination	Frame break condition
Slot Counter [3]	f(Q)	SbS	different L at $slot$ or EoF
FuzzyQ [37]	f(Q)	PbP	different L at p or EoF
Chen14 [25]	LUT($\hat{n}$)	PbP	LUT($\hat{n}$) at p or EoF
ds-DFSA [27]	LUT($\hat{n}$)	PbP+FbF	LUT($\hat{n}$) at p or EoF
DS-MAP [29]	LUT($\hat{n}$)	PbP+FbF	LUT($\hat{n}$) at p or EoF
Eom [22]	f($\hat{n}$)	FbF	EoF
ILCM-FbF [18]	f($\hat{n}$)	FbF	EoF
ILCM-SbS [17]	f($\hat{n}$)	SbS	Higher expected $c_s(n, L)$ at $slot$ or EoF
Chen16 [15]	f($\hat{n}$)	PbP	different L at p or EoF
FFSA	f($\hat{n}$)	PbP	Lower expected $t_{IT(n,L)}$ at p or EoF

B. FuzzyQ

Arjona *et al.* [13] present FuzzyQ, a method which integrates fuzzy logic with a DFSA anti-collision protocol. A fuzzy rule based system (FRBS) is defined to model the current Q and the idle or collision response rate (SW) as fuzzy sets to adaptively calculate L. It follows a PbP to examine L at slot p=$L/9$, and a new frame is started if L is modified.

C. Chen14

Chen [25] presents an anti-collision protocol which calculates L as a function of $\hat{n}$ and according to an LUT, where

$$\hat{n} = (c_s + 2.39c_k)p. \tag{1}$$

Then L is examined at just one slot per frame, determined by p=$L/4$, claiming to significantly reduce the number of total update slots.

D. ds-DFSA

Su *et al.* [27] present a two-phase anti-collision protocol, called the detected sector based DFSA (ds-DFSA). In the first phase, $\hat{n}$ is calculated recursively based on the number of single and collision slots in the current frame up to Fds according to

$$\hat{n} = (c_s + 2.39c_k)L/Fds, \tag{2}$$

where Fds is determined according to an LUT. When L is considered appropriate, based on an LUT for $\hat{n}$, phase one ends and what is obtained is the average number of collided tags per slot: $n_{ave} = (\hat{n} - c_s)/c_k$. Then, the frame size for phase two is obtained as the closest power-of-two value to n_{ave}. In phase two, individual tag identification is performed for each collided slot of phase one. In this phase, the tag estimation is performed with (2) setting Fds=L, and an FbF strategy is applied to examine L.

E. DS-MAP

Chen *et al.* propose in [29] a two phase protocol, referred to as Dynamic Sub-frame MAP (DS-MAP). In both phases, L is calculated based on $\hat{n}$, which is obtained as the value of n maximizing the following maximum *a posteriori* probability function

$$P(n|c_i, c_s, c_k) = \frac{L!}{c_i!c_s!c_k!} p_i(c_i)p_s(c_s|c_i)p_k(c_k|c_s, c_i) \tag{3}$$

where $p_i(c_i)$ is the probability of having an empty slot, and $p_s(c_s|c_i), p_k(c_k|c_s, c_i)$ are the conditional probabilities of successful transmission and collision for the slot. In the first phase, L is calculated with an LUT for $\hat{n}$, and a PbP strategy is followed to examine L. The authors set p according to an LUT for L.

The second phase begins when the current frame size matches $\hat{n}$. In the second phase, DS-MAP calculates L with an LUT for $\hat{n}$, where $\hat{n}$ is obtained as the sum of each partial estimate of n at each p slot of the current frame. Then an FbF strategy is followed to examine L.

F. Eom

Eom *et al.* [22] introduce a DFSA anti-collision protocol which calculates L according to $\hat{n}$. The estimation mechanism is based on the number of collided tags per slot γ. Thus,

$$\hat{n} = \gamma c_k + c_s \tag{4}$$

where γ is found iteratively based on a threshold value. Then, it follows an FbF policy to examine L, starting a new frame when the current one ends.

G. ILCM-FbF

Solic *et al.* [18] present the Improved Linearized Combinational Model with Frame by Frame examination of L (ILCM-FbF). This protocol is based on the estimation of the tag population using the function

$$\hat{n} = kc_s + l \tag{5}$$

where k and l are both obtained as functions of c_k and L. Then, at the end of the frame, L is calculated by L=$2^{round(log_2(\hat{n}))}$.

H. ILCM-SbS

Solic *et al.* [28] present an improved version of ILCM-FbF [18], called the Improved Linearized Combinational Model with Slot by Slot examination of L (ILCM-SbS). At every slot, the tag set size is estimated with (5). It is important to note that for ILCM-SbS, the values of k and l in (5) are different from those obtained in [18], and in ILCM-SbS they depend on L and the number of collision slots up to the current slot. Similarly, c_s refers to the number of single slots up to the current slot. When $\hat{n}$ is calculated, a new frame is started if the expected number of successful slots in the rest of the current frame is less than the one expected in the new frame, that is, c_{s2}>c_{s1}.

I. Chen16

Chen proposes in [15], as an extension of [25], an anti-collision algorithm based on the early and optimal adjustment of the frame length with the aim of maximizing the normalized throughput U, defined as $U{=}(c_sT_s)/(c_sT_s + c_iT_i + c_kT_k)$. In this protocol, $\hat{n}$ is obtained with (1) in every frame at slot $p{=}L/5$. The value of this pointer is selected as the slot where the maximum U is obtained. Next, the author sets $L{=}y\hat{n}$ as the new frame size (using the closest power-of-two value), where y is expressed as a second-order polynomial

$$y = -0.0097(T_k/T_i)^2 + 0.273T_k/T_i + 0.7707. \quad (6)$$

Then, if L is modified, the reader terminates the current frame and starts a new one.

V. The Proposed Fuzzy Frame Update Policy

This section introduces a novel fuzzy frame update policy, designed to lower the average time required to identify one tag. The proposed policy meets EPC C1G2 requirements, considering a unique duration for each type of slot. The three parts of the proposed policy (frame size calculation, frame size examination, and frame break condition) are presented next.

A. Frame size calculation: f($\hat{n}$) to minimize $t_{IT}(n, L)$

The first part of the policy for the frame size calculation sets the value of L minimizing the expected time to identify one tag in a frame. For this purpose, $t_{IT}(n, L)$ is defined as the expected time to identify one tag among n in a frame of size L:

$$t_{IT}(n, L) = \frac{T_s c_s(n, L) + T_k c_k(n, L) + T_i\ c_i(n, L)}{c_s(n, L)} \quad (7)$$

where $c_s(n, L)$, $c_k(n, L)$, and $c_i(n, L)$ represent the expected value of the number of single, collision, and idle slots in a frame, respectively.

The durations of the slots, T_s, T_k, and T_i, are set according to the standard as shown in Fig. 1

$$T_s = T_{command} + 2T_1 + 2T_2 + T_{RN16} + T_{ACK} + T_{ID}, \quad (8)$$

$$T_k = T_{command} + T_1 + T_{RN16} + T_2, \quad (9)$$

and

$$T_i = T_{command} + T_1 + T_3. \quad (10)$$

where $T_{command}$ refers to the duration of the reader transmitted command Qc, QA, or QR, referred as T_{Qc}, T_{QA}, and T_{QR}, respectively.

In every frame, the reader will transmit just one QA or Qc in the first slot, and in the rest of slots it will transmit QR commands. Assuming a frame with sufficiently large L, $T_{command}{=}T_{QR}$ is applied in (8), (9), and (10) when one frame is analyzed.

The parameters T_{Qc}, T_{QA}, and T_{QR} are calculated as the Reader-to-Tag synchronization time $T_{FSync_{RT}}$ or $T_{Preamble_{RT}}$, defined in [3], plus the length of each of the parameter divided by the reader data rate DR_r, calculated as $DR_r{=}1/((T_{data_0} + T_{data_1})/2)$, where $T_{data_0}{=}Tari$, and $T_{data_1}{=}1.5{\cdot}Tari$. $Tari$ represents the reference time interval for a data-0 transmission. Thus, $T_{Qc}{=}T_{FSync_{RT}}$+22 bits/DR_r, $T_{QA}{=}T_{Preamble_{RT}}$+9 bits/$DR_r$, and $T_{QR}{=}T_{Preamble_{RT}}$+4 bits/$DR_r$.

The parameters T_{RN16} and T_{ID} refer to the time the tag employs to transmit RN16 and its ID, respectively. They are calculated as the Tag-to-Reader synchronization time $T_{Preamble_{TR}}$ plus the length of each of the parameter divided by the tag data rate DR_t, calculated as $DR_t{=}1/BLF$. The parameter BLF refers to the Backscatter-link frequency. Thus, $T_{RN16}{=}T_{Preamble_{TR}}$+17 bits/$DR_t$ and $T_{ID}{=}T_{Preamble_{TR}}$+129 bits/$DR_t$. The duration of the reader command ACK is referred as T_{ACK}, and it is obtained as $T_{ACK}{=}T_{Preamble_{RT}}$+18 bits/$DR_r$.

Next, the value of L minimizing $t_{IT}(n, L)$ is obtained. In order to perform the analysis, a system model with one reader and n tags is defined. The probability that r tags among n occupy a slot within a frame of size L can be approximated by a binomial distribution $P_r(n, L)$ [22]

$$P_r(n, L) = \binom{n}{r}\left(\frac{1}{L}\right)^r\left(1 - \frac{1}{L}\right)^{n-r}. \quad (11)$$

Additionally, $p_s(n, L)$, $p_k(n, L)$, and $p_i(n, L)$ correspond to the probabilities that only one tag, more than one tag, or no tag, respectively occupy a slot [13]. If L is sufficiently large, the distribution of the tags can be approximated by a Poisson distribution with mean $\rho{=}n/L$ [22].

When $r = 0$ in (11), $c_i(n, L)$ can be approximated by

$$c_i(n, L) = Lp_i(n, L) = L\left(1 - \frac{1}{L}\right)^n \approx Le^{-\rho}. \quad (12)$$

When $r = 1$ in (11), $c_s(n, L)$ can be approximated by

$$c_s(n, L) = Lp_s(n, L) = L\frac{n}{L}\left(1 - \frac{1}{L}\right)^{n-1} \approx L\rho\left(\frac{n/\rho}{n/\rho - 1}\right)e^{-\rho} \quad (13)$$

Then, $c_k(n, L)$ can be approximated by

$$c_k(n, L) = Lp_k(n, L) = L(1 - p_0 - p_1). \quad (14)$$

Substituting (12), (13), and (14) into (7), and applying $\frac{n/\rho}{n/\rho-1}{\approx}1$, the following expression is obtained

$$t_{IT}(\rho) \approx \frac{T_s\rho e^{-\rho} + T_i e^{-\rho} + T_k(1 - (1 + \rho)e^{-\rho})}{\rho e^{-\rho}}. \quad (15)$$

Computing the derivative of $t_{IT}(\rho)$ in (7) with respect to ρ yields

$$\frac{dt_{IT}(\rho)}{d\rho} = \frac{T_k(e^{\rho}(\rho - 1) + 1) - T_i}{\rho^2}. \quad (16)$$

Then posing $\frac{dt_{IT}(\rho)}{d\rho}{=}0$, one obtains the following equation

$$e^{\rho}(\rho - 1) + 1 = \frac{T_i}{T_k}. \quad (17)$$

Solving (17), the value of ρ which minimizes $t_{IT}(\rho)$ is obtained:

$$\rho = 1 + W\left((\frac{T_i}{T_k} - 1)e^{-1}\right) \quad (18)$$

where $W(x)$ represents the Lambert W-function. Finally, the optimal frame size which minimizes $t_{IT}(n, L)$ is

$$L = \frac{n}{\rho} \tag{19}$$

where ρ is obtained from (18).

The value of ρ in (18) is evaluated and presented in Fig. 2 as a function of T_i/T_k. Traditionally, $T_i \leq T_k$, and $T_i/T_k \in (0,1]$. It can be appreciated that ρ decreases when the difference between T_i and T_k grows, resulting in a increasing L. In conclusion, a higher difference in the values of T_i and T_k (with $T_i \leq T_k$) will result in a higher L. This result is coherent regarding the process of RFID tags identification. If the duration of collision slots is much higher than that of idle slots, it is required to increase L to reduce the number of collision slots. This occurs at the expense of an increase in the number of idle slots. However, because idle slots are much shorter than collision slots, this is an acceptable effect.

Analyzing (19), a timing-aware frame size calculation is obtained. The frame size is set according to the timing parameters of the RFID system (which determine the value of T_i and T_k) in addition to the tag set size n.

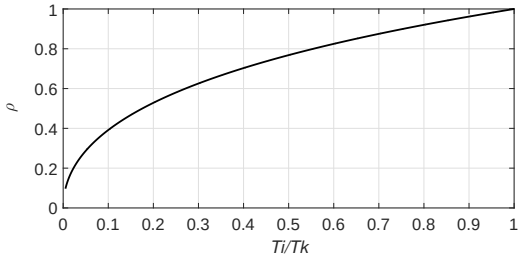

Fig. 2: Evaluation of ρ solution in (18) for T_i/T_k.

B. Frame size examination: PbP

The second part of a frame update policy refers to the slot where L is examined. According to Table I, three main strategies can be applied. The FbF strategy is not efficient in the case of large frames filled with many collisions, because the reader must wait until the frame has finished to update the frame size, increasing the identification time [18]. The SbS strategy might overload a reader that had only a limited capacity, because L is calculated at every slot. Finally, the PbP strategy provides the flexibility of breaking the current frame before it ends, maintaining a low computational complexity in the reader. To this end, the proposed policy will apply a PbP strategy where the value of the pointer slot is dynamically updated using fuzzy logic. Several strategies in the literature also apply a PbP strategy. However, most of them use a pointer with a fixed value and they do not adapt properly to varying sizes of tag population [13], [15], [25], [27]. Two recent papers [29], [33] present a varying pointer, but its value is updated as a function of the frame size exclusively.

The proposed policy applies a fuzzy rule based system (FRBS) to adjust the value of the pointer efficiently. For this purpose, the current L and the tag collision rate col_rate are modeled as fuzzy sets to adaptively update the value of the pointer. A zeroth-order Takagi–Sugeno–Kang fuzzy system with a complete AND-composed rule [34] is proposed. The membership functions used to codify the input variables are trapezoidal and the t-norm minimum is used to implement the AND operator. Trapezoidal membership functions have been selected due to their representation simplicity (the operations involved in the fuzzification of trapezoidal membership functions are subtraction and division), allowing faster calculations than with other types of membership functions [35]. The proposed system, shown in Fig. 3, has two inputs:

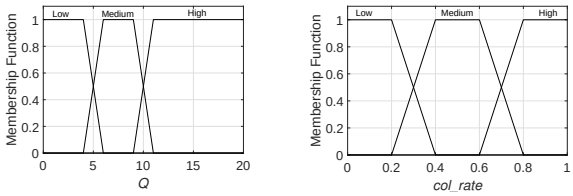

Fig. 3: Membership functions: (a) for Q, (b) col_rate.

- col_rate: codifies the tag collision rate up to the current slot. It is defined by $col\_rate = c_k/slot\_index$, and $0 \leq col\_rate \leq 1$.
- Q: codifies the current value of this parameter which determines L, where $Q \in \mathbb{N}$ and $0 \leq Q \leq 20$.

Additionally, the variable *slot_index* represents the reader's internal counter, which keeps track of the present slot in the current frame. As shown in Fig. 3, both input variables are codified with three trapezoids. Values outside the range are assumed to be equal to the corresponding limit, thereby offering the maximum coverage. The output p represents the slot where L must be examined. The rule set of the FRBS has nine rules, presented in Table III. For instance, the first rule is IF (col_rate is Low) AND (Q is Low) THEN p=$L/2$. The rules were designed experimentally considering, on the one hand, the higher the Q, the smaller the p; and on the other hand, the higher the col_rate, the smaller the p. Specific values for membership functions and consequents in the rule base have been adjusted experimentally.

TABLE III: Rule set to obtain pointer p.

		Q		
		Low	Medium	High
col_rate	Low	$L/2$	$L/4$	$L/8$
	Medium	$L/4$	$L/4$	$L/16$
	High	$L/8$	$L/16$	$L/16$

C. Frame break condition: Lower $t_{IT}(n, L)$

Finally, the last part of the policy determines the condition to break the current frame and start a new one. The expected average time to identify one tag among n in the current frame of size L_c is obtained as

$$t_{IT_c} = t_{IT}(n, L)|_{n=\hat{n}, L=L_c}, \tag{20}$$

and the expected average time to identify one tag among n in the newly calculated frame of size L_n is

$$t_{IT_n} = t_{IT}(n, L)|_{n=\hat{n}, L=L_n}. \tag{21}$$

In order to lower the tag identification time, a new frame will be started if the condition $t_{IT_n}<t_{IT_c}$ is satisfied. Thus, at slot p, the reader obtains t_{IT_n} and t_{IT_c} with (20) and (21), assuming $T_{command}=T_{QR}$, and then compares the values. Following this strategy, the reader guarantees that if a new frame is started at slot p, the expected average time required to identify one tag will be reduced.

VI. RFID Anti-Collision Protocol Fuzzy Frame Slotted Aloha (FFSA)

In this section, the frame update strategy presented in Section V is applied to a DFSA anti-collision protocol, resulting in the Fuzzy Frame Slotted Aloha (FFSA) protocol. The pseudocode of FFSA is presented in Fig. 4 Initially, the reader sets the value of ρ with (18) according to the RFID system timing parameters, and starts the identification procedure by broadcasting Qc.

Each tag selects a slot in the frame to transmit its $RN16$, and the reader updates the variables c_s, c_k, and c_i accordingly. When the reader reaches the last slot of the frame, the remaining tag population size is estimated with a traditional Mean Minimum Square Error (MMSE) estimator [30]

$$\hat{n} = \min_{n} \left| \begin{pmatrix} p_i(n,L)L \\ p_s(n,L)L \\ p_k(n,L)L \end{pmatrix} - \begin{pmatrix} c_i \\ c_s \\ c_k \end{pmatrix} \right|. \tag{22}$$

Then a new frame is started by broadcasting QA, specifying the new frame size as

$$Q_n = log_2((\hat{n} - c_s)/\rho), L_n = 2^{round(Q_n)}. \tag{23}$$

At every slot, col_rate is calculated and p is set as the current slot if col_rate=1. If the current slot is a pointer, the reader calculates $\hat{n}$ with (22) and sets L_n with (23). Then, it obtains t_{IT_c} and t_{IT_n} with (20) and (21). If the condition $t_{IT_n}<t_{IT_c}$ is satisfied, a new frame is started and p is updated with the FRBS. Otherwise, the reader broadcasts QR to proceed to the next slot. The identification process ends when there are no collision slots in the current frame and the frame is terminated.

FFSA presents a timing-aware frame, because its size is set according to the timing parameters of the RFID system in addition to the tag set size.

Reader Operation

```
Initialization: calculate ρ with (18), broadcast Qc
while 1 do
    read slot and update c_i, c_s, c_k
    if slot_index = L_c and c_k = 0 then
        break
    end if
    if slot_index = L_c then
        n̂ = MMSE(c_s, c_k, c_i)
        Q_n = log_2((n̂ − c_s)/ρ), L_n = 2^round(Q_n), L_c = L_n
        broadcast QA
    else
        col_rate = c_k/slot_index
        if col_rate = 1 then
            p = slot_index
        end if
        if slot_index = p then
            n̂ = MMSE(c_s, c_k, c_i)
            Q_n = log_2((n̂ − c_s)/ρ), L_n = 2^round(Q_n)
            if t_IT_n < t_IT_c then
                p = FRBS(col_rate, Q_n), L_c = L_n
                broadcast QA
            else
                slot_index = slot_index +1
                broadcast QR
            end if
        else
            slot_index = slot_index +1
            broadcast QR
        end if
    end if
end while
```

Tag Operation

```
while energized by the reader do
    receive reader's commands
    if QA or Qc then
        Generate SC ∈ [0, L − 1]
    else
        if QR then
            SC = SC − 1
        end if
    end if
    if SC = 0 then
        transmit RN16
        if ACK then
            transmit ID
        end if
    end if
end while
```

Fig. 4: Pseudocode of FFSA. First the operation of the reader is presented, then the operation of the tag.

A. Asymptotic overhead of the estimators

Table IV summarizes and compares the main anti-collision protocols which are evaluated in this work according to the asymptotic overhead of their tag estimator. The asymptotic overhead $O(\cdot)$ refers to the expected number of slots required for achieving $\hat{n}$ [36].

The Estimation Frequency per frame refers to how often the tag set size is estimated within a frame, and it is obtained as the maximum number of times that the protocol estimates the tag set size in one frame. The estimator of the proposed protocol presents $O(c_i+c_s+c_k)$ and an Estimation Frequency of 2 (estimation is performed at slot p and L). From this table, it is concluded that all the protocols of the comparison employ an estimator with a linear asymptotic overhead, and they estimate the tag set size once ore twice per frame. The protocol ILCM-SbS presents the highest Estimation Frequency per frame, because it estimates the tag set size at every slot of the frame. The Slot Counter and FuzzyQ protocols do not estimate the tag set size, but they calculate L based on Q (see Table II).

TABLE IV: Comparison of the estimators regarding their asymptotic overhead $O(\cdot)$ and the Estimation Frequency per frame

Protocol	Estimator $O(\cdot)$	Estimation Frequency per frame
Slot Counter [3]	–	0
FuzzyQ [37]	–	0
Chen14 [25]	$c_i + c_s + c_k$	2
ds-DFSA [27]	$c_i + c_s + c_k$	2
DS-MAP [29]	$c_i + c_s + c_k$	2
Eom [22]	$c_i + c_s + c_k$	1
ILCM-FbF [18]	$c_i + c_s + c_k$	1
ILCM-SbS [28]	$c_i + c_s + c_k$	L
Chen16 [15]	$c_i + c_s + c_k$	2
FFSA	$c_i + c_s + c_k$	2

VII. Performance Evaluation

This section evaluates the performance of FFSA and compares it with the anti-collision protocols of the state of the art presented in Section IV. A scenario with one reader and a varying number of tags has been evaluated with Matlab R2017a, where the tags are uniformly distributed. Physical-layer effects are not considered here, assuming a non-impaired channel and no capture effect. Note that these assumptions are widely used for the analysis of known anti-collision protocols whose analysis focuses on the media access control layer [15], [17], [18], [22], [25], [27], [29], [37].

Evaluation is performed for one inventory round, defined as the period of time that begins when the reader transmits the initial command Qc and it ends when the reader interrupts the identification process and the tags loose their state. This work assumes that an inventory round ends when all the tags in the reader interrogation zone have been identified.

The simulation responses have been averaged over 1000 iterations for accuracy in the results. In order to evaluate the protocols' performance, two different metrics are measured:

- Average time to identify one tag in one inventory round t_{IT}, obtained as the total identification time divided by n:
$$t_{IT} = \frac{T_s c_{s_T} + T_k c_{k_T} + T_i c_{i_T}}{n} \quad (24)$$
The variables c_{s_T}, c_{k_T}, and c_{i_T} represent the total number of single, collision, and idle slot, respectively, in one inventory round. The value of $T_{command}$ in (8), (9), and (10) will vary depending on the slot location within a frame:
  - First slot of the inventory round: $T_{command}$=T_{Qc}.
  - First slot of the frame: $T_{command}$=T_{QA}.
  - None of the two above: $T_{command}$=T_{QR}.
- Average energy consumption per tag E/tag.
Currently, mobile and battery powered readers, such as hand-readers and smart-phones, are increasingly being used and therefore, the study of the power consumption in passive RFID is becoming engaging. The energy consumed by the reader during the identification of a whole set of tags, defined as E, is modeled in [38]. During the identification process, the reader transmits a set of commands and a continuous wave to power up the tags, with power P_t. To receive the data from the tags, the reader needs an amount of extra power P_r. Defining E_t and E_r as the reader consumed energy during the transmitting and receiving states, one obtains

$$\begin{aligned} E &= E_t + E_r \\ &= P_t\ nt_{IT} \\ &\quad + P_r\ [c_{s_T}(T_{RN16} + T_{EPC}) + c_{k_T} T_{RN16}] \\ &= P_t(T_s c_{s_T} + T_k c_{k_T} + T_i c_{i_T}) \\ &\quad + P_r\ [c_{s_T}(T_{RN16} + T_{EPC}) + c_{k_T} T_{RN16}]. \end{aligned} \quad (25)$$

The protocols are compared in two different scenarios: S1 and S2. These represent practical scenarios, considering different slots duration and assuming $0 \leq Q \leq 15$, as specified by EPC C1G2 standard. For each scenario, t_{IT} and E/tag are evaluated as a function of the control variable indicated with *, n in S1 and BLF in S2. Table V shows the parameters employed. BLF is varied from the minimum to the maximum value specified in EPC C1G2. S2 represents a special case since BLF also influences $Tari$, which represents the reference time interval for a data-0 transmission, and affects $RTcal$, $TRcal$, T_1, and T_2. These parameters are also modified every time BLF changes during the simulation. In both scenarios, the initial L is set to 16, and P_t and P_r are fixed to 825 mW and 125 mW [38], respectively. In FFSA, the initial value for p is set to 8, and this value has been obtained experimentally.

TABLE V: Parameters used in simulations. * indicates the control variable.

Scenario	S1	S2
n	[32–4096] tags*	[32–4096] tags
BLF	40 kbps	[40–640] kbps*
$Tari$	6.25 μs	6.25 μs
$RTcal$	15.63 μs	[15.63–62.50] μs
$TRcal$	17.34 μs	[17.34–69.38] μs
T_1	24.50 μs	[16.06–24.50] μs
T_2	375.50 μs	[23.44–375.50] μs
T_3	15.63 μs	15.63 μs

A. Effect of the number of tags n (S1)

This section compares the selected protocols with n as the control variable in S1. Different sizes of the tag set, from 32 to 4096, have been evaluated. Additionally, c_{k_T} and c_{i_T} per tag are measured, assuming that t_{IT} and E are mostly influenced by them. The results are shown in Fig. 5. Most protocols show a quasi-constant t_{IT} and E/tag for n up to 1024 in Fig. 5.a and Fig. 5.b, respectively, with FFSA requiring the lowest average time and energy to identify one tag. The strategies ds-DFSA and Chen14 show an increasing t_{IT} and E/tag for n>1024, because they limit the frame size to 1024 when n is greater than 710. FuzzyQ also presents a peak at n=1024, because the value of the Q parameter is bounded from above. The improvement of FFSA comes from the reduction in c_{k_T} at the expense of an increase in c_{i_T}, as can be appreciated in Fig. 5.c and Fig. 5.d respectively. Because the duration of

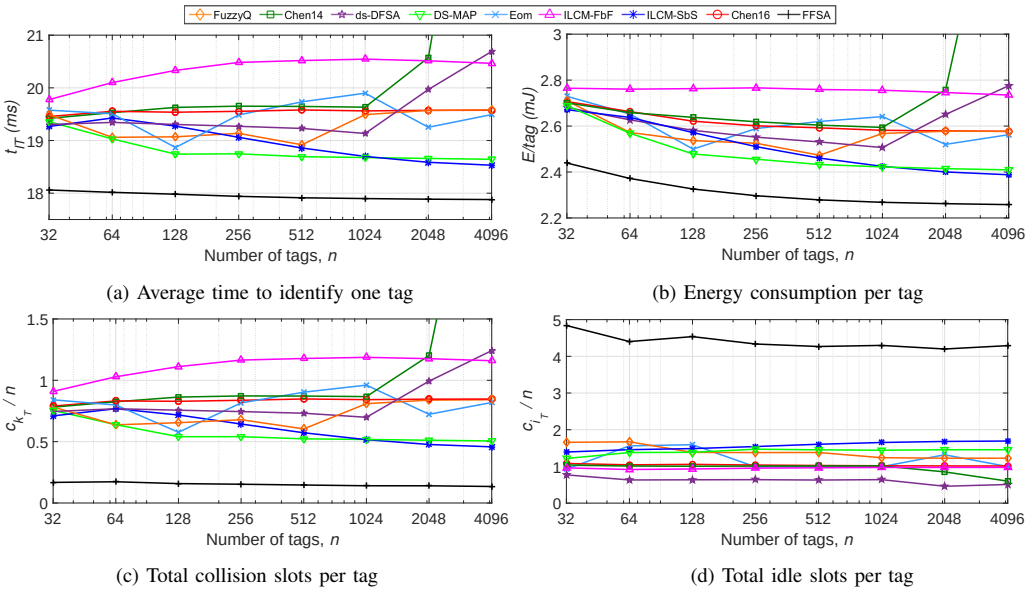

(a) Average time to identify one tag

(b) Energy consumption per tag

(c) Total collision slots per tag

(d) Total idle slots per tag

Fig. 5: Simulation results of the average time to identify one tag (a), the energy consumption per tag (b), c_{k_T} per tag (c), and c_{i_T} per tag (d) in S1.

an idle slot is much shorter than that of a collision slot, the reduction in c_{k_T} leads to a lower t_{IT} and E/tag for FFSA. The strategies ILCM-FbF and Chen14 present the highest c_{k_T}, leading to the highest t_{IT} and E/tag.

When designing an anti-collision protocol, a compromise between performance and complexity should be considered. Therefore, it is important to measure the number of slots dedicated to calculate L in relation to the total number of slots, referred to as the L update rate in the present paper. FbF strategies will have a varying rate, depending on the total number of frames employed in the identification process. PbP strategies will also have a varying rate, depending mainly on the value of their pointer. A protocol following a SbS policy will have a rate of 100%, because L will be calculated at every slot.

The value of the L update rate is measured for each protocol and averaged for all n in S1. It is important to note that a frame size update does not necessarily involve the start of a new frame, but it refers to a new calculation of L. Simulation results are shown in Table VI. For DS-MAP, sub-frame updates in the second phase are also included in this metric.

FFSA presents the lowest rate, since the value of the pointer is determined with an FRBS to effectively break the frame before the tag collision rate becomes notably high. It is followed by the two FbF strategies evaluated, Eom and ILCM-FbF, which calculate L once per frame. Then, the remaining PbP strategies present a varying rate. In Figs. 5.a and 5.b, it was shown that DS-MAP performed as the second best protocol in terms of t_{IT} and E/tag. However, Table VI shows that this occurred at the expense of a higher number of slots dedicated to calculate L, increasing the computational complexity for the reader. Finally, ILCM-SbS presents the highest rate, with a value of 100%, since L is calculated at every slot of the frame.

TABLE VI: Comparison of L update rate (%) in S1.

Protocol	L update rate
FuzzyQ	0.85
Chen14	0.90
ds-DFSA	24.34
DS-MAP	2.91
Eom	0.42
ILCM-FbF	0.48
ILCM-SbS	100.00
Chen16	1.10
FFSA	0.24

B. *Effect of tag Backscatter Link Frequency BLF (S2)*

The metrics t_{IT} and E are greatly dependent on the tag BLF. Additionally, the performance of FFSA and Chen16 is greatly influenced by this parameter, because they set L according to the slots duration, which is affected by BLF.

For this purpose, the previous protocols are evaluated for different timing configuration of the RFID system, by varying BLF from the minimum (40 kbps) to the maximum (640 kbps) value allowed by EPC C1G2, and setting $Tari$ to its minimum value (6.25 μs) and. The simulation results are averaged for n from 32 to 4096, and shown in Table VII. The value of ρ employed by FFSA is also presented, and it has been obtained with (18).

All the protocols present an decreasing t_{IT} and E/tag with increasing BLF. For the highest values of BLF, all the protocols present a similar behavior, and FFSA does not introduce a significant performance improvement. This occurs because the value of ρ (see Table VII) takes a significantly higher value, causing a larger number of collision slots. As BLF decreases, FFSA shows a significant reduction in t_{IT} and E/tag in relation to the prior protocols.

To analyze the previous results, c_{k_T} and c_{i_T} per tag are

TABLE VII: Effect of BLF and ρ on the protocols' performance in S2. Quantities in bold represent the best results among the protocols in the comparison. * Indicates the control variable.

	t_{IT} (ms)					E/tag (mJ)				
BLF* (kbps)	40	80	124	274	640	40	80	124	274	640
ρ	0.25	0.32	0.39	0.53	0.69	0.25	0.32	0.39	0.53	0.69
FuzzyQ	19.29	9.87	6.53	3.22	1.65	16.23	8.30	5.49	2.70	1.38
Eom	19.50	9.96	6.59	3.24	1.65	16.40	8.38	5.54	2.71	1.38
ILCM-FbF	20.32	10.38	6.86	3.36	1.70	17.19	8.78	5.80	2.83	1.43
ILCM-SbS	18.95	9.70	6.43	3.18	1.64	15.90	8.14	5.40	2.66	1.37
Chen16	19.56	9.36	6.23	3.12	**1.61**	16.46	7.80	5.20	2.60	1.35
ds-DFSA	19.54	9.26	6.59	3.22	1.63	16.46	8.39	5.54	2.71	1.36
Chen14	20.70	10.57	6.99	3.42	1.73	17.54	8.95	5.91	2.89	1.46
DS-MAP	18.82	9.61	6.37	3.14	**1.61**	15.79	8.06	5.34	2.62	**1.34**
FFSA	**17.94**	**9.30**	**6.21**	**3.01**	1.62	**14.94**	**7.74**	**5.17**	**2.58**	1.35

measured as functions of BLF and averaged for all the tag set sizes n in S2. The simulation results are shown in Fig. 6.

On the one hand, when BLF gets close to its upper limit, the increase in c_{i_T} of FFSA is not compensated for by the small reduction in c_{k_T} in relation to the prior protocols, limiting the performance improvement of the proposed protocol. On the other hand, while the prior protocols present a quasi-constant c_{k_T} with decreasing BLF, FFSA presents a notably decreasing c_{k_T}, and this is reflected in a reduction in t_{IT} and E/tag in relation to the prior protocols. For BLF>80 kbps, Chen16 behaves similarly to FFSA. However, when BLF gets closer to its lowest value, the low resulting value of y in (6) leads to an increasing c_{k_T} and decreasing c_{i_T}.

In conclusion, the savings in the tag identification time and energy consumption of FFSA are still substantial for most of the range of BLF, which confirms that the proposed protocol is a time and energy saving procedure in S1 and S2.

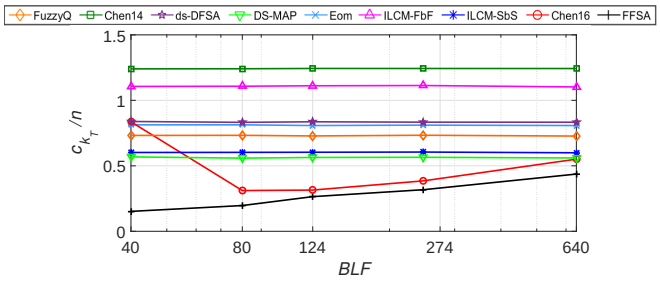

(a) Total collision slots per tag

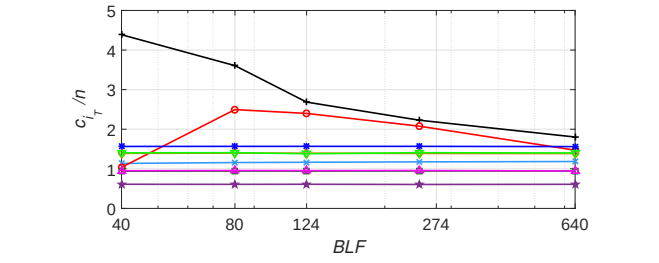

(b) Total idle slots per tag

Fig. 6: Simulation results of c_{k_T} per tag (a) and c_{i_T} per tag (b) in S2.

C. Comparison with Slot Counter Protocol (S1)

This section compares the performance of the previous anti-collision protocols with the Slot Counter protocol [3] with C=0.3 [11].

For this purpose, the average number of tags identified per second in S1 is obtained as $1/t_{IT}$ in (24), defined as the total number of tags divided by the total identification time in one inventory round.

The simulation results are shown in Fig. 7. The Slot Counter protocol presents, on average, a higher tag identification rate than ILCM-FbF and Chen14. The rest of the strategies improve the performance of Slot Counter in relation to this metric. FFSA presents the highest number of tags identified per second, with an average 10.71% improvement in relation to Slot Counter.

D. Identified limitations

In Table VII it was shown that if BLF gets close to its upper limit, FFSA does not present a significant improvement in t_{IT} and E, mainly due to the high value of ρ. To mitigate this effect, the value of ρ should be upper-bounded for high values of BLF.

Furthermore, an ideal communication channel has been considered in this research. However, the capture effect is very common in passive RFID systems [39]. This phenomenon occurs when the reader successfully resolves one tag reply in a collided slot. On the one hand, this effect could decrease t_{IT}, because fewer collided slots and more single slots would occur. On the other hand, the capture effect may hide some tags, providing erroneous information to the tag estimator and increasing the estimation error. Thus, the updated L value may not be appropriate, affecting t_{IT} negatively. The study of the capture effect on t_{IT} and an evaluation of FFSA taking this effect into account is proposed as future work.

VIII. Conclusion

A comprehensive survey and classification of the frame update policies for RFID DFSA anti-collision protocols has been presented. In general, such a policy can be divided into three parts: L update, L calculation, and frame break condition. Then, several state-of-the-art DFSA anti-collision

protocols have been analyzed and classified according to this policy. Lastly, a novel frame update policy has been proposed, resulting in Fuzzy Frame Slotted Aloha (FFSA), a fast and energy efficient DFSA anti-collision protocol. With a 10.71% improvement in the tag identification rate (tags/s) in relation to the protocol employed in the current RFID standard, FFSA is a suitable candidate where low tag identification time and low energy consumption are sought in RFID systems.

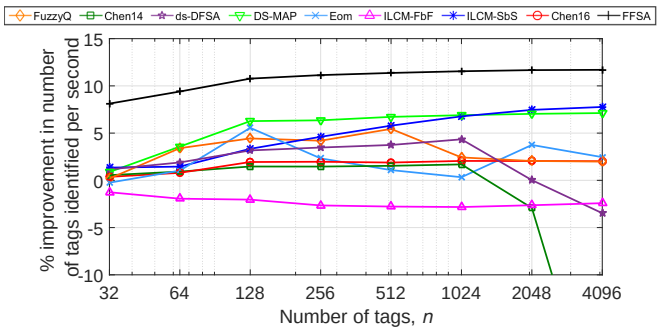

Fig. 7: Improvement (%) with Slot Counter protocol in terms of the number of tags identified per time unit (tag/s) in S1.

ACKNOWLEDGMENTS

This work has been supported by the Spanish Ministry of Economy and Competitiveness under the projects ESPHIA (TIN2014-56042-JIN) and iLogisTICs (TEC2013-45585-C2-2-R).

REFERENCES

[1] IDTechEx, "RFID Forecasts, Players and Opportunities 2014−2024," May 2014.

[2] D. Klair, C. Kwan-Wu, and R. Raad, "A survey and tutorial of RFID anti-collision protocols," *Communications Surveys Tutorials, IEEE*, vol. 12, pp. 400–421, Mar 2010.

[3] "Radio Frequency Identity Protocols class-1 generation-2 UHF RFID protocol for communications at 860 MHz–960 MHz," Nov 2013.

[4] L. Burdet, "RFID Multiple Access Methods," *Technical Report ETH Zurich*, 2004.

[5] C.-H. Quan, W.-K. Hong, and H.-C. Kim, *Performance Analysis of Tag Anti-collision Algorithms for RFID Systems*, Berlin: Springer-Verlag, 2006, pp. 382–391.

[6] Z. Tang and Y. He, "Research of multi-access and anti-collision protocols in RFID systems," in *International Workshop on Anti-Counterfeiting, Security and Identification, April 2007*, pp. 377–380.

[7] M. V. Bueno-Delgado, J. Vales-Alonso, and F. J. Gonzalez-Castao, "Analysis of DFSA anti-collision protocols in passive RFID environments," in *35th Annual Conference of IEEE Industrial Electronics, Nov. 2009*, pp. 2610–2617.

[8] L. Arjona, H. Landaluce, A. Perallos, P. Lopez-Garcia, and N. Cmiljanic, "Analysis of RFID anti-collision protocols based on the standard EPC-global Class-1 Generation-2," in *21st European Wireless Conference, May 2015*, pp. 1–6.

[9] K. K. Donghwan Lee and W. Lee, "Q+-algorithm: An enhanced RFID tag collision arbitration algorithm," *4th International Conference on Ubiquitous Intelligence and Computing, Hong Kong, China, July 11–13, 2007*.

[10] M. Daneshmand, C. Wang, and K. Sohraby, "A New Slot-Count Selection Algorithm for RFID Protocol," in *Second International Conference on Communications and Networking in China, Aug. 2007*, pp. 926–930.

[11] L. Zhu and T.-S. Yum, "The optimal reading strategy for EPC Gen-2 RFID anti-collision systems," *IEEE Transactions on Communications*, vol. 58, pp. 2725–2733, Sept 2010.

[12] J. Teng, X. Xuan, and Y. Bai, "A fast Q algorithm based on EPC Generation-2 RFID protocol," in *6th International Conference on Wireless Communications Networking and Mobile Computing, Sept. 2010*, pp. 1–4.

[13] L. Arjona, H. Landaluce, A. Perallos, and E. Onieva, "Fast fuzzy anti-collision protocol for the RFID standard EPC Gen-2," *IET Electronics Letters*, vol. 52, no. 8, pp. 663–665, 2016.

[14] T. F. L. Porta, G. Maselli, and C. Petrioli, "Anticollision protocols for single-reader RFID systems: Temporal analysis and optimization," *IEEE Transactions on Mobile Computing*, vol. 10, pp. 267–279, Feb 2011.

[15] W. T. Chen, "Optimal frame length analysis and an efficient anti-collision algorithm with early adjustment of frame length for RFID systems," *IEEE Transactions on Vehicular Technology*, vol. 65, pp. 3342–3348, May 2016.

[16] C. Floerkemeier and M. Wille, "Comparison of transmission schemes for framed ALOHA based RFID protocols," in *International Symposium on Applications and the Internet Workshops, Jan. 2006*, pp. 4–97.

[17] P. Solic, J. Radic, and N. Rozic, "Early frame break policy for ALOHA-based RFID systems," *IEEE Transactions on Automation Science and Engineering*, vol. 13, pp. 876–881, Apr 2016.

[18] P. Solic, J. Radic, and N. Rozic, "Energy efficient tag estimation method for ALOHA-based RFID systems," *IEEE Sensors Journal*, vol. 14, pp. 3637–3647, Oct 2014.

[19] F. Schoute, "Dynamic frame length ALOHA," *IEEE Transactions on Communications*, vol. 31, pp. 565–568, Apr 1983.

[20] J.-R. Cha and J.-H. Kim, "Dynamic framed slotted ALOHA algorithms using fast tag estimation method for RFID system," in *3rd IEEE Consumer Communications and Networking Conference, Jan. 2006*, vol. 2, pp. 768–772.

[21] W.-T. Chen and G. Lin, "An efficient anti-collision method for RFID System," *IEICE Transactions on Communications*, vol. E89, no. B, pp. 3386–3392, 2006.

[22] J.-B. Eom and T.-J. Lee, "Accurate tag estimation for dynamic framed-slotted ALOHA in RFID systems," *IEEE Communications Letters*, vol. 14, pp. 60–62, Jan 2010.

[23] W.-T. Chen, "An efficient scheme for multiple access in a RFID system." In *Proceedings of the 2006 International Conference on Wireless Networks, 2006*.

[24] W.-T. Chen, "An accurate tag estimate method for improving the performance of an RFID anticollision algorithm based on dynamic frame length ALOHA," *IEEE Transactions on Automation Science and Engineering*, vol. 6, pp. 9–15, Jan 2009.

[25] W.-T. Chen, "A fast anticollision algorithm for the EPCglobal UHF class-1 Generation-2 RFID standard," *IEEE Communications Letters*, vol. 18, pp. 1519–1522, Sept 2014.

[26] I. Joe and J. Lee, "A novel anti-collision algorithm with optimal frame size for RFID system," in *5th ACIS International Conference on Software Engineering Research, Management Applications, Aug. 2007*, pp. 424–428.

[27] J. Su, Z. Sheng, D. Hong, and G. Wen, "An effective frame breaking policy for dynamic framed slotted Aloha in RFID," *IEEE Communications Letters*, vol. 20, pp. 692–695, Apr 2016.

[28] P. Solic, J. Radic, and N. Rozic, "Early frame break policy for ALOHA-based RFID systems," *IEEE Transactions on Automation Science and Engineering*, vol. 13, pp. 876–881, Mar 2015.

[29] Y. Chen, J. Su, and W. Yi, "An efficient and easy-to-implement tag identification algorithm for UHF RFID systems," *IEEE Communications Letters*, vol. PP, no. 99, pp. 1–1, 2017.

[30] H. Vogt, "Efficient object identification with passive RFID tags," in *Pervasive Computing* (F. Mattern and M. Naghshineh, eds.), vol. 2414 of *Lecture Notes in Computer Science*, Berlin: Springer-Verlag, 2002, pp. 98–113.

[31] B. S. Wang, Q. S. Zhang, D. K. Yang, and J. S. Di, "Transmission control solutions using interval estimation method for EPC C1G2 RFID tag identification," in *International Conference on Wireless Communications, Networking and Mobile Computing, Sept. 2007*, pp. 2105–2108.

[32] B. Knerr, M. Holzer, and C. Angerer, "Slot-by-slot minimum squared error estimator for tags populations in FSA protocols," in *Proc. 2nd Int. EURASIP Workshop on RFID, 2008*, pp. 1–13.

[33] J. Su, Z. Sheng, D. Hong, and V. C. M. Leung, "An efficient sub-frame based tag identification algorithm for UHF RFID systems," in *IEEE International Conference on Communications, May 2016*, pp. 1–6.

[34] T. Takagi and M. Sugeno, "Fuzzy identification of systems and its applications to modeling and control," *IEEE Transactions on Systems, Man and Cybernetics*, vol. SMC-15, pp. 116–132, Jan 1985.

[35] T. J. Ross, "Fuzzy Logic with Engineering Applications, Third Edition," *Wiley Publishing*, Dec 2010.

[36] Z. Zhou, B. Chen, and H. Yu, "Understanding RFID Counting Protocols," *IEEE/ACM Transactions on Networking*, vol. 24, pp. 312–327, Feb 2016.

[37] L. Arjona, H. Landaluce, A. Perallos, and N. Cmiljanic, "Hardware based analysis of RFID anti-collision protocols based on the standard EPCglobal Class-1 Generation-2," in *International Wireless Communications and Mobile Computing Conference, Aug. 2015*, pp. 226–231.

[38] H. Landaluce, A. Perallos, E. Onieva, L. Arjona, and L. Bengtsson, "An energy and identification time decreasing procedure for memoryless RFID tag anticollision protocols," *IEEE Transactions on Wireless Communications*, vol. 15, pp. 4234–4247, June 2016.

[39] H. Wu and Y. Zeng, "Passive RFID tag anticollision algorithm for capture effect," *IEEE Sensors Journal*, vol. 15, pp. 218–226, Jan 2015.

APPENDIX

B

Paper II

Fast fuzzy anti-collision protocol for the RFID standard EPC Gen-2

This paper was published in the journal *"IET Electronic Letters"* on April 2016. Its DOI is: 10.1049/el.2015.3258. It is published as Open Access and can accessed online trough the IET Digital Library. The published version is appended here.

Fast fuzzy anti-collision protocol for the RFID standard EPC Gen-2

L. Arjona✉, H. Landaluce, A. Perallos and E. Onieva

A new methodology which integrates fuzzy logic with RFID anti-collision protocols is proposed. The resulting FuzzyQ protocol significantly decreases the identification time by updating the transmission frame size in a dynamic and adaptive way. Simulation results show the performance of FuzzyQ compared with earlier protocols based on the standard EPC Gen-2.

Introduction: RFID technology is becoming popular in asset identification, tracking, and localisation applications, greatly increasing the density of available tags in interrogation zones. The coexistence of tags sharing the same communication channel requires solutions to handle collisions. Anti-collision protocols are sought to mitigate the degradation of the reader's bandwidth, its power consumption, and the delay caused by collisions.

EPCglobal Class 1 Generation 2 (EPC C1G2) [1] is the current standard in RFID systems. EPC C1G2 employs the Slot Counter protocol to arbitrate collisions, commonly known as the Q-protocol. A key feature of the Q-protocol is the frame size (L), which is dynamically updated by means of the parameter named Q ($L = 2^Q$). To manage the identification process, the reader begins with transmitting a Query (Qc) command, and then alternates between QueryAdjust (QA) and QueryRep (QR) commands. QA starts a new frame with the updated size and arranges that the tags randomly select a slot in the frame [the initial value of their internal slot counter (SC)], whereas QR tells the tags to decrement SC. Thus, when SC = 0, the tag transmits a 16 bit random number (RN16); and once it is acknowledged, the tag transmits its IDentification code (ID).

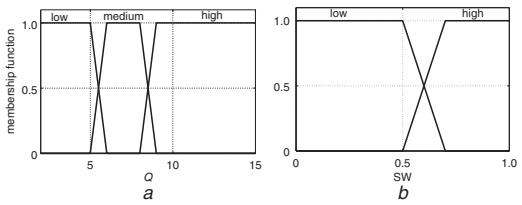

Fig. 1 *Input membership functions for FuzzyQ*
a Q
b SW

The lack of definition about the function to update Q has led to many different alternatives. Several papers can be found in the literature which deal with the parameter Q to update L [2, 3]. Most protocols are based on a smooth increase in L. Therefore, when the collision or idle rate is high, they must employ a relatively high number of slots and reader and tag bits to find an appropriate L. Moreover, the examination of L at every slot results in an increase in the protocol's identification time (IT). The solution presented in [3] suggests examining L at just one slot per frame, set at L/i, $i \in [4,\ 2,\ 4/3]$, claiming to significantly reduce the number of total examination points. However, this protocol is based on tag estimation, being restricted to a maximum tag population of 1420 tags. Moreover, the estimation behaves poorly at the early and final stages of the identification process, limiting the protocol's performance.

The aim of this Letter is to apply fuzzy logic to the Q-protocol in order to lower the IT by effectively updating L. Fuzzy logic has already been applied to RFID systems, in areas such as security and antennas design. Nevertheless, to the best of our knowledge, this is the first time that it has been employed to model an RFID anti-collision protocol.

To evaluate the proposed protocol, a novel performance metric is introduced, the stability factor (SF). The metric of the number of slots has been widely employed in the literature. However, it lacks relevant information, since different slots can have different durations. For the purpose of considering this effect, the parameter SF is defined and evaluated for the comparative protocols, providing information about the rate of introducing new frames.

Proposed FuzzyQ protocol: A fuzzy rule-based system (FRBS) is applied to the Q-protocol in order to adjust L, resulting in what we call the FuzzyQ protocol. This protocol models the current L and the slot waste (SW), which represents the idle or collision response rate, as fuzzy sets to adaptively update the value of Q. A zeroth-order Takagi–Sugeno–Kang fuzzy system with a complete AND-composed rule [4] is proposed. The membership functions used to codify the input variables are trapezoidal and the t-norm minimum is used to implement the AND operator. The proposed system (see Fig. 1) has two inputs:

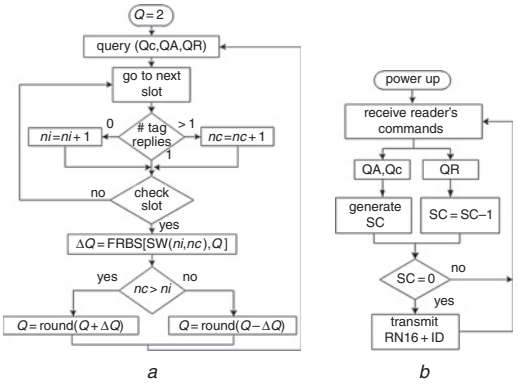

Fig. 2 *Flow diagram of FuzzyQ*
a For reader
b For tags

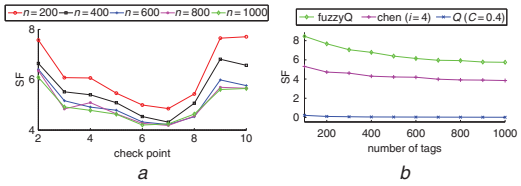

Fig. 3 *CP selection for FuzzyQ, and comparison with Chen(i = 4) and Q(C = 0.4) for CP = 9*
a Effect of *check point* over SF
b Evaluation of SF

- SW: codifies the idle or collision response rate and it is defined as follows: SW = max(ni, nc)/slot_pointer, where nc and ni represent the total number of collisions and idle responses in the current frame, respectively, up to and including the current slot.
- Q: codifies the current value of this parameter which determines L, where $Q \in \mathbb{N}$ and $2 \leq Q \leq 15$.

Examining SW, it represents the number of idle and collision slots in relation to the total number of slots, assuming that the tags' slot selection is uniformly distributed along the frame. Additionally, the variable *slot_pointer* represents the reader's internal counter, which keeps track of the present slot in the current frame. As shown in Fig. 1, both input variables are codified with an initial number of trapezoids: two for SW and three for Q. Values outside the range are assumed to be equal to the corresponding limit, thereby offering maximum coverage. The output ΔQ represents the variation of Q, and it is codified by three singletons with four possible values: Null = 0, Low = 1, Medium = 2, and High = 3. The rule set of the FRBS is composed by six rules:

- Rule 1: IF (Q is Low) AND (SW is Low) THEN ΔQ is Low.
- Rule 2: IF (Q is Low) AND (SW is High) THEN ΔQ is High.
- Rule 3: IF (Q is Medium) AND (SW is Low) THEN ΔQ is Null.
- Rule 4: IF (Q is Medium) AND (SW is High) THEN ΔQ is Medium.
- Rule 5: IF (Q is High) AND (SW is Low) THEN ΔQ is Null.
- Rule 6: IF (Q is High) AND (SW is High) THEN ΔQ is Low.

Rules were designed considering, on the one hand, the higher the frame size, the lower the increment of Q; and on the other hand, the higher the idle or collision rate, the higher the increment of Q.

Once designed, the FRBS is employed to determine the variation in the previous frame size (L) of the Q-protocol. FuzzyQ seeks to lower the IT of the Q-protocol employed in the standard EPCglobal by introducing the two following strategies: (i) to check whether the current L is appropriate given the values of SW and Q at strategic slots and not at every slot. These slots, called *check slots*, are distributed one per frame. The *check slot* is defined as L/CP, where CP stands for *check point* and CP $\in \mathbb{N}$. (ii) Not limiting the variation of Q to steps of one unit and to consider instead a range of values, in order to achieve a more abrupt step size (0, 1, 2, or 3). This

value, defined as ΔQ, corresponds to the output of the FRBS. A step size of 0 means that Q remains unchanged.

Identification procedure: The process of identification for the proposed FuzzyQ in the form of a flowchart is depicted in Fig. 2 and described subsequently. The value of Q is initialised to 2, which is the smallest value it can take, and therefore $L = 4$. Tags with SC = 0 transmit their ID while the rest of them wait for further commands from the reader. Next, the reader sends the corresponding query (Qc, QA, or QR) and updates the counters *nc* and *ni* according to the tags' responses. If the reader detects a collision, *nc* is increased by one; if no tag responds, *ni* is increased by one; and otherwise, both counters remain unchanged. At this point, if the current slot is a *check slot*, ΔQ is obtained from the FRBS. Next, Q is increased by ΔQ if $nc > ni$, and decreased by the same factor otherwise. Finally, the resulting Q is rounded. If the current slot is not a *check slot*, the identification process will continue with the following slot.

Table 1: Performance comparison of FuzzyQ in terms of SE and IT

		SE		IT	
		CP = 2	CP = 9	CP = 2	CP = 9
Tag population	64	0.289	0.297	0.450	0.465
	128	0.302	0.312	0.879	0.891
	512	0.305	0.328	3.555	3.535
	1024	0.306	0.335	7.087	6.972

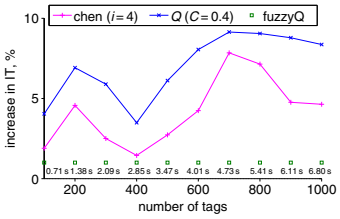

Fig. 4 *Improvement introduced by FuzzyQ in the IT*

Two extra considerations must be taken into account. When evaluating a *check slot*, a new frame is started only if the newly obtained Q differs from the current value. If this condition is not satisfied, the identification process will move to the next slot. Additionally, when the reader reaches the last slot of the frame, ΔQ is computed again in order to obtain the size of the next frame.

Simulation results: This section presents the results of the simulation experiments using MATLAB R2013a. The simulation uses a scenario with one reader and a varying number of tags, *n*, from 100 to 1000 tags, with a step size of 100. The tags are uniformly distributed and an ideal channel is assumed for the experiment [2]. The simulation responses are averaged over 1000 iterations for accuracy in the results. It is assumed that the identification procedure ends when all tags have been identified.

To analyse the performance of the proposed protocol, three main parameters are analysed in this section:

(i) *Slot efficiency (SE)*: The ratio between the number of tags and the number of time slots required to identify them.
(ii) *IT*: The total time employed by the reader to successfully identify all tags in a set.
(iii) *SF*: The fraction of QR commands in relation to the total number of commands and the number of examinations, defined by: $SF = [tQR/(tQR + tQA)]/texams$

where *t*QA and *t*QR are the total number of QA and QR, respectively, sent by the reader during a complete identification round; and *t*exams is the number of *check slots* examined in the same round.

For all the presented simulations, the reader's and tag's command length is set according to the standard [1], with an ID of 96 bits. Moreover, in order to compute IT, a reader data rate of 128 kbit/s and a tag data rate of 47.4 kbit/s were employed.

SF provides information about the rate of introducing new frames. The parameter *t*exams relativises this factor to the number of attempts made to begin a frame. It is also important to note here that the slot duration employed to start a new frame (equal to *t*QA) is higher than the duration applied to decrement the tag's counter SC (equal to *t*QR). Analysing more in depth SF, on the one hand, the numerator is desired to be a maximum, since the length of QA is higher than the length of QR, and a lower number of reader-transmitted bits will lower IT. On the other hand, *t*exams is desired to be a minimum, contributing to the decrease of IT. As a result, SF is desired to be a maximum.

First, the value of CP must be selected so that it maximises the protocol's performance. Thereupon, SF is computed for a range of CP varying from 2 to 10. The value CP = 1 has not been considered because it involves just one examination of the frame size, whereas the rest of the values of CP might require up to two examinations (the first at *check slot* and the second at the end of the frame to determine the size of the next frame). The results are shown in Fig. 3*a*.

Fig. 3*a* shows two relative maxima at CP = 2 and 9. Therefore, in order to establish which one FuzzyQ must employ, SE and IT are analysed for both of these values of CP, on five different tag sets. Table 1 shows the simulation results.

As can be appreciated in Table 1, SE is higher for CP = 9 for all evaluated tag populations. Regarding IT, CP = 2 produces a higher SE factor for populations of 64 and 128 tags. However, most applications deal with sets larger than 128 tags. Consequently, CP = 9 is selected.

Once CP is set, the performance of the proposed protocol is evaluated in comparison with the algorithm presented in [3] with $i = 4$, Chen($i = 4$), and the Q-protocol with $C = 0.4$, $Q(C = 0.4)$ [1]. Considering the protocol Chen($i = 4$), the value of $i = 4$ has been chosen due to the fact that it results in the highest SE in [3]. First, the three protocols are compared regarding SF, as shown in Fig. 3*b*. FuzzyQ achieves a considerably higher value of SF than the other protocols for all tag sets evaluated. This is because FuzzyQ adapts to the population oscillations more effectively, lowering the rate of introducing new frames.

Finally, IT is evaluated. The IT is a highly relevant performance indicator, since it greatly influences the performance of the global RFID system. Fig. 4 shows the percentage increase in IT of the comparative strategies in relation to FuzzyQ. It can be appreciated that FuzzyQ presents an average improvement of 4.2% with respect to Chen($i = 4$) and a 7% average improvement with respect to the $Q(C = 0.4)$ protocol. The outcomes show that FuzzyQ lowers the IT needed by the other strategies. First, FuzzyQ reduces the proportion of QA in relation to the total number of queries and *t*exams. Secondly, by limiting the *check point* to one per frame, the number of examinations is reduced and so is the total number of QAs. Finally, by setting ΔQ to a range of values of up to three units, the protocol employs fewer slots to reach an appropriate value of L. As a result, a lower IT is justified.

Conclusion: A novel protocol based on the standard EPC C1G2 has been presented for fast RFID tag identification. Simulated results suggest that FuzzyQ is a dextrous protocol, using an FRBS, and achieving a relatively low IT while providing competitive results in terms of SF. FuzzyQ achieves a 4.2% average improvement in IT in relation to the strategy Chen($i = 4$) and an average improvement of 7% with respect to the $Q(C = 0.4)$ protocol.

Acknowledgments: This work has been supported by the Spanish Ministry of Economy and Competitiveness under the iLogisTICs project (TEC2013-45585-C2-2-R) and the Basque Government under the UBITRACE project (PC2013-71A).

Submitted: *18 September 2015* E-first: *14 March 2016*
doi: 10.1049/el.2015.3258
One or more of the Figures in this Letter are available in colour online.

L. Arjona, H. Landaluce, A. Perallos and E. Onieva (*Deusto Institute of Technology (DeustoTech), University of Deusto, Bilbao, Spain*)

✉ E-mail: laura.arjona@deusto.es

References

1 'Radio frequency identity protocols class-1 generation-2 UHF RFID protocol for communications at 860 MHz–960 MHz', November 2013
2 Daneshmand, M., Wang, C., and Sohraby, K.: 'A new slot-count selection algorithm for RFID protocol'. Second Int. Conf. on Communications and Networking, Shanghai, China, August 2007, pp. 926–930
3 Chen, W.-T.: 'A fast anticollision algorithm for the EPCglobal UHF class-1 generation-2 RFID standard', *IEEE Commun. Lett.*, 2014, **18**, pp. 1519–1522
4 Takagi, T., and Sugeno, M.: 'Fuzzy identification of systems and its applications to modeling and control', *IEEE Trans. Syst. Man Cybern.*, 1985, **SMC-15**, pp. 116–132

APPENDIX

C

Paper III

Scalable RFID Tag Estimator with Enhanced Accuracy and Low Estimation Time

This paper was published in the journal *"IEEE Signal Processing Letters"* on July 2017. Its DOI is: 10.1109/LSP.2017.2692201. It can accessed online trough the IEEE Xplore Digital Library. The published version is appended here.

Scalable RFID Tag Estimator With Enhanced Accuracy and Low Estimation Time

Laura Arjona, Hugo Landaluce, Asier Perallos, and Enrique Onieva

***Abstract*—The knowledge of the number of tags is critical in many radio frequency identification (RFID) applications. This paper is concerned with the problem of estimating an RFID tag population size when the number of tags is much higher than the frame size. A novel estimation scheme called "Scalable Minimum Mean Square Error" (sMMSE) is proposed. The proposed estimator updates the frame size by considering two key parameters: One determines the limit of the slots occupancy at which the frame size should be increased, and the other one sets the frame size increase factor. A formal study is provided to adjust these parameters with the aim of lowering the estimation error while scaling to highly populated tag sets. Numerical results indicate that sMMSE significantly decreases the normalized estimation error and maintains a low estimation time compared to existing strategies.**

***Index Terms*—Anticollision, bit-collision, bit-tracking, EPC-global standard, estimation error, radio frequency identification (RFID), tag estimation.**

I. Introduction

RADIO frequency identification (RFID) technology is becoming increasingly popular to the point where almost anything can be tagged. A typical RFID system consists of two communication devices: tags and readers. Tags are uniquely differentiated with an identification code ID, which is read by the reader through a wireless channel [1]. The knowledge of the number of tags is needed in many RFID applications such as tag identification, privacy-sensitive RFID systems, and warehouse monitoring [2]. Often, in such scenarios, it is desirable to simply estimate the number of tags without explicitly identifying individual tags, helping to reduce the processing time, and preserve people's privacy [3]. Note that although estimation can help tags identification, in this letter the identification problem is not considered.

This letter treats the problem of estimating the size of a given tag population when the number of tags is much higher than the frame size. A slotted Aloha frame of size L is defined as a sequence of L time slots where tags can only respond to the reader's commands once in a frame. This type of frame is commonly employed in frame slotted Aloha (FSA) and dynamic FSA anticollision protocols for RFID [4], whose performance is highly affected by the update of L.

Several publications in the literature deal with the estimation problem by analyzing the tags' transmissions along a slotted Aloha frame [2], [5]–[8]. In order to present these strategies, a system model with one reader and n tags is defined. Conventionally, three type of slots are considered attending to the tags' responses to the reader's commands: idle (no tags respond), single (only one tag responds), and collision (more than one tag responds). The variables c_i, c_s, and c_k correspond to the number of idle, single, and collision slots in a frame, respectively.

In many applications, the number of passive tags can be very large due to their low cost, easy disposability, and powerless operation [9]. In those scenarios, tag estimation schemes need to be scalable to large population sizes in order to provide an accurate estimate $\hat{n}$ maintaining a restrained estimation time. Table I summarizes and compares the main scalable estimators that will be evaluated in this letter. The asymptotic overhead $O(\cdot)$ refers to the expected number of slots required for achieving $\hat{n}$ [3]. The total number of slots required in the proposed estimator N_s will be obtained in Section III, and ε refers to the normalized estimation error, defined as

$$\varepsilon = \frac{|\hat{n} - n|}{n}. \tag{1}$$

The first tag estimation scheme, called unified probabilistic estimator (UPE), was proposed by Kodialam and Nandagopal in 2006 [5]. UPE makes identification based on either the number of idle slots or that of collision slots in a frame. It requires the differentiation among idle, single, and collision slots, which

TABLE I
COMPARISON OF THE ESTIMATORS REGARDING THE INFORMATION NEEDED TO OBTAIN $\hat{n}$ AND THEIR ASYMPTOTIC OVERHEAD $O(\cdot)$

	Key information to obtain $\hat{n}$	$O(\cdot)$
UPE [5]	Proper randomization and c_i, c_k	–
EZB [6]	c_i	$O(1/\varepsilon^2 \log n)$
MLE [7]	c_i, c_s, c_k	$O(1/\varepsilon^2 \log n)$
FNEB [8]	Indices of the first non-idle slots	$O(1/\varepsilon^2 \log n)$
ART [2]	Average run length of non-idle slots	$O(1/\varepsilon^2 + \log n)$
sMMSE	Tag Response Rate, RR	N_s

Manuscript received February 21, 2017; accepted March 24, 2017. Date of publication April 7, 2017; date of current version May 18, 2017. This work was supported by the Spanish Ministry of Economy and Competitiveness under the projects ESPHIA (TIN2014-56042-JIN) and iLogisTICs (TEC2013-45585-C2-2-R). The associate editor coordinating the review of this manuscript and approving it for publication was Dr. Seung-Jun Kim. *(Corresponding author: Laura Arjona Aguilera.)*

The authors are with the DeustoTech, University of Deusto, Bilbao 48007, Spain (e-mail: laura.arjona@deusto.es; hlandaluce@deusto.es; perallos@deusto.es; enrique.onieva@deusto.es).

Color versions of one or more of the figures in this letter are available online at http://ieeexplore.ieee.org.

Digital Object Identifier 10.1109/LSP.2017.2692201

takes a significant amount of time. The asymptotic overhead has not been obtained due to its biased estimator [3].

Kodialam *et al.* [6] proposed the enhanced zero based estimator (EZB), which performs estimation based on the total number of idle slots in a frame.

Li *et al.* proposed the maximum likelihood estimator (MLE) [7] for active tags with the aim of minimizing the power consumption of active tags.

Han *et al.* [8] introduced a tag estimation scheme called first non empty based (FNEB) estimator, based on the size of the first run of "0"s in a frame. FNEB assumes that the frame size can be arbitrarily large, which is not practical.

Shahzad and Liu [2] presented the average run-based tag (ART) estimation based on the average run length of ones in the bit string received. Table I shows that ART presents the lowest asymptotic overhead of the prior estimators. The additive overhead comes from a conceptual separation of two phases in this algorithm.

This letter proposes a new scalable estimation scheme, called scalable minimum mean square error (sMMSE), which provides an accurate and fast tag estimate $\hat{n}$ under large-scaled tag environments. Using bit-tracking to identify the bit-collisions in one slot [10], sMMSE updates the frame size by considering two key parameters: T_{RR} determines the limit of the slots occupancy at which the frame size should be increased, and Δ sets the frame size increase factor. Note that bit-tracking is supported by the RFID standard ISO 18000-6 [11] for detecting bit-level collisions. Additionally, a formal study is provided to adjust these two key parameters with the aim of lowering the estimation error for a wide range of tag population sizes.

II. Proposed sMMSE Estimator

The proposed scheme accurately estimates the number of tags by minimizing the distance between the observed reading results and their theoretical expected values. The estimation mechanism is divided into two phases.

1) Dynamic increase of L to be adapted to n.

Phase 1 starts when the reader transmits the 4-bit length query estimation (QE) command, specifying L. Initially, $L = 1$. After receiving this command, each tag randomly selects a value v between 0 and $kL-1$, where k represents the tag's ID length.

Then each tag generates a sequence of length k bits, consisting of all "0"s and sets the (v mod k)th bit to "1", where mod represents the modulo operation. The generated sequence is transmitted in the $\lfloor v/k \rfloor$th slot of the frame, where $\lfloor \cdot \rfloor$ operation rounds the element to the nearest integer toward $-\infty$. Next, the reader orderly receives the tags' sequences from slot 0 to slot $L-1$ and then builds the sequence S of length kL, by concatenating the sequences received in each slot: $S = \{s_0, s_1, ..., s_{kL-1}\}$ where $s_i \in \{0, 1, X\}$. When $s_i = X$, a bit-collision is detected in position i using bit-tracking. Let sb_i represent a selected bit in position i, so that $\mathrm{sb}_i = 1$ when $s_i = 1$ or $s_i = X$, and $\mathrm{sb}_i = 0$ otherwise. The reader then computes the tag response rate RR, defined as $\mathrm{RR} = (\sum_{i=0}^{kL-1} \mathrm{sb}_i)/(kL)$. Then if $\mathrm{RR} \geq T_{\mathrm{RR}}$ (where T_{RR} is a threshold value for RR and it is fixed for a complete estimation round), L is increased by a factor of Δ, i.e., $L = L\Delta$. Phase 1 is repeated until $\mathrm{RR} < T_{\mathrm{RR}}$, meaning that L is adapted to n. In that case, phase 2 begins and the number of tags is estimated with the sMMSE function H_{sMMSE}, defined next.

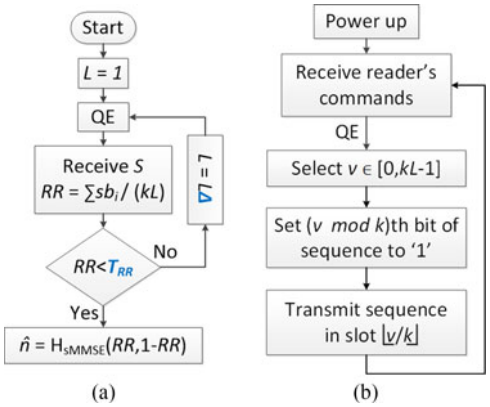

Fig. 1. Flow diagram of sMMSE tag estimator: (a) for reader, (b) for tags.

2) Tag estimation with a minimum mean square error (MMSE) function.

For the second phase, let $\mathbf{v_f} = [\mathrm{RR}, 1-\mathrm{RR}]$ denote the vector representing the observed tags' responses. Then, the expected value $E(\cdot)$ of $\mathbf{v_f}$ is defined as the vector $\mathbf{V_F} = [E(\mathrm{RR}), E(1-\mathrm{RR})]$. Thus $E(\mathrm{RR}) = 1-P_x(n, kL, 0)$ and $E(1-\mathrm{RR}) = P_x(n, kL, 0)$, where $P_x(n, L, x)$ refers to the probability that x out of n tags occupy a slot in a frame of size L, and can be approximated with a binomial distribution [12]

$$P_x(n, L, x) = \binom{n}{x}\left(\frac{1}{L}\right)^x\left(1-\frac{1}{L}\right)^{n-x}. \tag{2}$$

Then the proposed estimator is defined based on the Chebyshev's inequality

$$H_{\mathrm{sMMSE}}(\mathbf{v_f}) = \arg \min_{[n \in N]} P_n(\mathbf{v_f}) \tag{3}$$

where N represents the upper bound of the number of tags and

$$\begin{aligned} P_n(\mathbf{v_f}) &= \|\mathbf{v_f} - \mathbf{V_F}\|^2 \\ &= \left(\mathrm{RR} - 1 + \left(1-\frac{1}{kL}\right)^n\right)^2 \\ &\quad + \left(1 - \mathrm{RR} - \left(1-\frac{1}{kL}\right)^n\right)^2. \end{aligned} \tag{4}$$

sMMSE estimates the number of tags $\hat{n}$ as the value of n for which the distance between the observed vector $\mathbf{v_f}$ and its expected value $\mathbf{V_F}$ becomes minimal

$$\hat{n} = H_{\mathrm{sMMSE}}(\mathbf{v_f}). \tag{5}$$

Next, Fig. 1 shows the flow diagram of sMMSE for the reader and tag. The performance of the proposed estimator is greatly influenced by the key parameters Δ and T_{RR}, so they must be carefully configured. The next sections study the tuning of Δ and T_{RR} to maximize the accuracy of the estimation while scaling over a wide range of tag population sizes.

TABLE II
T_{RR} AND Δ VALUES WHICH MINIMIZE THE NORMALIZED ESTIMATION ERROR ε FOR A GIVEN TAG SET SIZE n IN SMMSE

n	100	200	300	400	500	600	700	800	900	1000
T_{RR}	0.65	1.00	0.65	0.80	0.80	0.60	0.35	0.55	0.45	0.45
Δ	2.4	2.4	3.0	3.0	3.0	2.0	3.0	3.0	2.0	2.0
$\overline{\varepsilon}10^{-3}$	91.7	163.0	1.9	5.1	5.1	1.9	1.3	4.9	2.8	2.8
$\sigma 10^{-3}$	114.6	182.2	4.7	9.4	9.4	2.3	3.0	7.2	3.7	3.7

A. Parameter Tuning

In this section, Δ and T_{RR} are adjusted in order to minimize ε defined in (1) for a given n. In order to study the effect of Δ and T_{RR} on ε, the error matrix $\text{EM}(n)$ is defined as a function of n

$$\text{EM}(n) = \begin{pmatrix} e_{11}(n) \ ... \ e_{1c}(n) \\ ... \qquad ... \\ e_{r1}(n) \ ... \ e_{rc}(n) \end{pmatrix} \tag{6}$$

where

$$e_{ij}(n) = \varepsilon|_{T_{\text{RR}}=T_{\text{RR}_i},\Delta=\Delta_j}. \tag{7}$$

To set $\text{EM}(n)$, the vectors $\mathbf{T_{RR_v}}$, $\mathbf{\Delta_v}$, and $\mathbf{n_v}$, with lengths r, c, and t, respectively, must be defined: $\mathbf{T_{RR_v}} = [T_{\text{RR}1}, T_{\text{RR}2}, ..., T_{\text{RR}r}]$, $\mathbf{\Delta_v} = [\Delta_1, \Delta_2, ..., \Delta_c]$, $\mathbf{n_v} = [n_1, n_2, ..., n_t]$. For instance, the element $e_{2,1}(n = 100)$ corresponds to the estimation error ε when $n = 100$, $T_{\text{RR}} = T_{\text{RR}2}$, and $\Delta = \Delta_1$. The last step is to generate one error matrix for each value of n using (7), specifying the previous vectors as follows: $\mathbf{T_{RR_v}} = [0.1, 0.2, 0.3, ..., 1]$ with $r = 10$, $\mathbf{\Delta_v} = [1, 1.1, 1.2, ..., 3]$ with $c = 21$, and $\mathbf{n_v} = [100, 200, 300, ..., 1000]$ with $t = 10$. These values have been set according to empirical results, derived from the analysis and experimentation of the proposed estimator. Furthermore, for each $n \in \mathbf{n_v}$, the values of T_{RR} and Δ which minimize ε in (1) are obtained. These values correspond to T_{RR_i} and Δ_j, which provide the lowest $e_{ij}(n)$ in $\text{EM}(n)$. Additionally, the average normalized estimation error $\overline{\varepsilon}$, defined as $\overline{\varepsilon} = (\sum_{i=1}^{t} \varepsilon|_{n=n_i})/t$, is evaluated with the tag vector $\mathbf{n_v}$ for each one of the previously obtained values of T_{RR} and Δ. A scenario with one reader and a varying number of tags has been evaluated with MATLAB R2015a, where the tags are uniformly distributed. Physical-layer effects are not considered here, assuming a nonimpaired channel and no capture effect [13]. Communication between the reader and tags is considered to be perfectly synchronized. Note that these assumptions are extensively used for the analysis of known algorithms whose analysis focuses on the media access control layer [1]–[3], [5]–[8][14]. The simulation responses have been averaged over 1000 iterations for accuracy in the results.

Results are obtained by executing sMMSE with $k = 128$ bits, and shown in Table II. The parameter σ refers to the standard deviation of $\overline{\varepsilon}$. It can be appreciated that there is a unique value of T_{RR} and Δ, which minimize ε for each n. These values show an un-normal fluctuate, with no conclusive relationship between them. In addition, it is clear that there is a considerable variation in $\overline{\varepsilon}$ depending on T_{RR} and Δ. A naive conclusion could be to select the values of T_{RR} and Δ that minimize ε for $n = 700$ as the fixed values for sMMSE, since they provide the lowest $\overline{\varepsilon}$ for $\mathbf{n_v}$. However, this would not be justified since these values have been obtained for a particular n, and their applicability for different tag set sizes has not been demonstrated. On the one hand, given that n is not known in advance, the parameters selection according to n cannot be made. On the other hand, in applications where the maximum possible number of tags is known, the two parameters could be set accordingly.

Considering that n is unknown for the reader, a unique value of T_{RR} and Δ must be defined independently of n. A unique and scalable value of T_{RR} and Δ, valid for different tag set sizes, is obtained in the next section.

B. Scalable Tuning

This section obtains a value of T_{RR} and Δ that minimizes ε for a wide range of tags, named $\{T_{\text{RR}}, \Delta\}_{\text{sMMSE}}$. To do so, the matrix $\overline{\text{EM}}$ is defined as the sum of all the matrices $\text{EM}(n)$ evaluated for the tag vector $\mathbf{n_v}$

$$\overline{\text{EM}} = \begin{pmatrix} \overline{e}_{11} \ ... \ \overline{e}_{1c} \\ ... \qquad ... \\ \overline{e}_{r1} \ ... \ \overline{e}_{rc} \end{pmatrix} = \sum_{y=1}^{t} \text{EM}(n_y) \tag{8}$$

where $\overline{e}_{ij} = \sum_{y=1}^{t} e_{ij}(n_y)$ and

$$\{T_{\text{RR}}, \Delta\}_{\text{sMMSE}} = \arg \min_{[T_{\text{RR}},\Delta]} \overline{e}_{ij}. \tag{9}$$

With the specific vectors $\mathbf{T_{RR_v}}$, $\mathbf{\Delta_v}$, and $\mathbf{n_v}$ employed in the previous analysis, the value obtained is $\{T_{\text{RR}}, \Delta\}_{\text{sMMSE}} = \{0.4, 2.0\}$, which is fixed for a complete estimation round. Therefore, the proposed estimator doubles the frame size when at least 2/5 (40%) of the frame is with filled bit-collisions.

III. PERFORMANCE ANALYSIS

This section presents the results of the simulation experiments using the scenario presented in Section II-A. The performance of the proposed scheme is evaluated and compared with the estimators presented in Section I: UPE [5], EZB [6], MLE [7], FNEB [8], and ART [2], using $\beta = 0.05$ and $\alpha = 0.95$ [2][15]; and with the estimator Zanella [16] to distinguish between the k-bit proposal and the traditional Aloha. For UPE, L is set to 128, the smallest evaluated n. For FNEB, a maximum frame size of 1024 is assumed. The upper bound of the number of tags N is set to $2n$ for sMMSE, FNEB, MLE, and EZB. Finally, the values $\{T_{\text{RR}}, \Delta L\}_{\text{sMMSE}}$ are employed for sMMSE.

A. Estimation Error

The metric ε is evaluated versus the number of tags and shown in Fig. 2. It can be observed that sMMSE presents the lowest ε of the compared strategies for all the tag population sizes evaluated except for $n = 128$, where it presents a similar behavior to that of EZB and Zanella. As n increases, sMMSE presents a decreasing ε while the rest of the strategies maintain a quasi-constant error except from FNEB and Zanella. Additionally, it is also important to note that although T_{RR} and Δ have been tuned for n up to

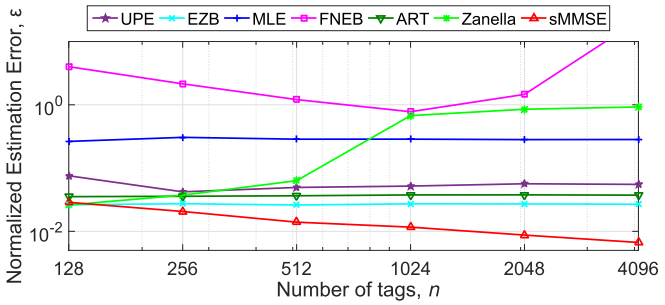

Fig. 2. Evaluation and comparison of the normalized estimation error ε for different RFID tag set sizes.

1000 tags in Section II-B, sMMSE scales to 4096 tags with the most accurate results. Therefore, there is evidence that sMMSE maintains its accuracy while scaling over a wide range of sizes of the tag population.

B. Estimation Time

This section evaluates the time required by the proposed estimator to find $\hat{n}$. For sMMSE, the estimation time ET is determined by the total number of frames required to estimate the tag population size. A minimum of one frame is required, and an additional one is necessary when the condition RR>T_{RR} is satisfied at the end of the current frame f. Thus, given a tag population size n and a frame of size L, the probability of starting a new frame $P_F(n, L)$ can be approximated with a logistic function

$$P_F(n, L) = \frac{1}{1 + \exp\left[-\gamma\left(1 - \left(1 - \frac{1}{kL}\right)^n\right) - T_{\text{RR}}\right]} \tag{10}$$

where γ represents the steepness of the logistic function. Then, the total number of frames $N_F(n, L)$ can be expressed as

$$N_F(n, L) = 1 + \sum_{f=1}^{f\max} P_F(n, L\Delta^{f-1}) \tag{11}$$

and the total number of slots N_s can be obtained as the sum of the first $N_F - 1$ terms of a finite geometric series

$$N_s(n, L) = L\frac{1 - \Delta^{N_F}}{1 - \Delta}. \tag{12}$$

The asymptotic overhead of the proposed estimator can be obtained then as Ns. With (10), (11), and (12), the estimation time ET of the proposed estimator can be expressed as

$$\text{ET}(n, L) = N_F(n, L)(T_{\text{QE}} + T_1 + T_2) + \frac{N_s(n, L)k}{t_{\text{DR}}} \tag{13}$$

where T_{QE} is the duration of QE, T_1 and T_2 correspond to the link timing parameters according to the RFID Standard EPC Global Class-1 Generation-2 (EPC C1G2) [17], and t_{DR} refers to the tag data rate. Next, (13) is evaluated for different n and $L = 1$, and compared with simulation results using the timing parameters of Table III, set in accordance with EPC C1G2. $Tari$ represents the reference time interval for a data-0 transmission, conditioning the configuration parameters $TR\text{cal}$ and $RT\text{cal}$, which affect T_1, T_2, and the durations of QueryRep and

TABLE III
SIMULATION PARAMETERS ACCORDING TO EPC C1G2 [17]

Parameter	Value	Parameter	Value
$Tari$	12.50 μs	t_{DR}	620 kb/s
$TRcal$	$3Tari$	T_{QR}	118.75 μs
$RTcal$	31.25 μs	T_{QA}	196.88 μs
T_1	30.13 μs	T_{QE}	118.75 μs
T_2	16.25 μs	T_{slot}	85.09 μs

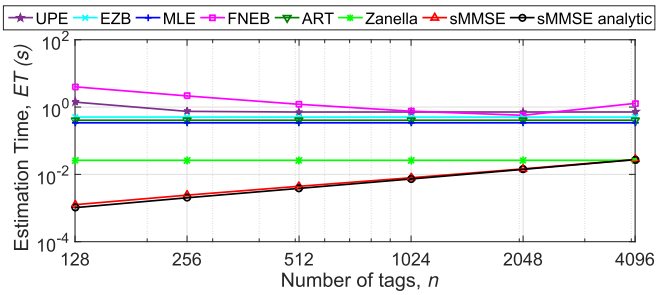

Fig. 3. Evaluation and comparison of the RFID tag estimation time ET for different tag set sizes.

QueryAdjust commands, referred as T_{QR} and T_{QA}, respectively. The value of $\gamma = 30$ in (10) is assumed and $f\max$ is set to 10. Results are compared with the estimators presented in Table I. The duration of a slot corresponds to that of a collision slot and it is referred as T_{slot} in Table III, since the identification process is not considered here. The average estimation time is evaluated and the simulation results are shown in Fig. 3. Analytic results for sMMSE according to (13) are also included in the comparison. As shown in the figure, sMMSE shows the lowest ET for $n < 4096$, because it requires the lowest number of slots to obtain the estimate. FNEB presents the highest ET, whilst the performance of UPE, EZB, MLE, ART, and Zanella is hardly affected by n. Although sMMSE shows an increasing ET with increasing n, it keeps lower than the rest of the estimators in the shown interval. Its increasing ET gradient occurs because sMMSE requires a higher L to estimate highly populated tag sets. It should be noticed that, under dense tag populations, sMMSE obtains a more accurate estimate than the prior estimation schemes at the expense of a slower behavior. However, sMMSE does not overcome the ET of Zanella until $n \geq 4096$, and that of MLE and ART until $n > 33408$, not shown in the graph for better clarity.

IV. CONCLUSION

A novel scalable scheme for accurate RFID tag estimation has been presented. The novel estimator, called sMMSE, applies two key parameters to update the frame size; and they are tuned to minimize the estimation error when the tag set size is much higher than the frame size. sMMSE scales to highly populated tag sets, with a low normalized estimation error while maintaining a low estimation time. Simulated results prove the accuracy of sMMSE, being a suitable candidate where high accuracy and low estimation time are sought.

REFERENCES

[1] J. Su, Z. Sheng, G. Wen, and V. C. M. Leung, "A time efficient tag identification algorithm using dual prefix probe scheme (DPPS)," *IEEE Signal Process. Lett.*, vol. 23, no. 3, pp. 386–389, Mar. 2016.

[2] M. Shahzad and A. Liu, "Fast and accurate estimation of RFID tags," *IEEE/ACM Trans. Netw.*, vol. 23, no. 1, pp. 241–254, Feb. 2015.

[3] Z. Zhou, B. Chen, and H. Yu, "Understanding RFID counting protocols," *IEEE/ACM Trans. Netw.*, vol. 24, no. 1, pp. 312–327, Feb. 2016.

[4] D. Klair, C. Kwan-Wu, and R. Raad, "A survey and tutorial of RFID anti-collision protocols," *IEEE Commun. Surveys Tut.*, vol. 12, no. 3, pp. 400–421, Jul–Sep. 2010.

[5] M. Kodialam and T. Nandagopal, "Fast and reliable estimation schemes in RFID systems," in *Proc. 12th Annu. Int. Conf. Mobile Comput. Netw.*, New York, NY, USA, 2006, pp. 322–333.

[6] M. Kodialam, T. Nandagopal, and W. C. Lau, "Anonymous tracking using RFID tags," in *Proc. 26th IEEE Int. Conf. Comput. Commun.*, May 2007, pp. 1217–1225.

[7] T. Li, S. Wu, S. Chen, and M. Yang, "Energy efficient algorithms for the RFID estimation problem," in *Proc. IEEE INFOCOM*, Mar. 2010, pp. 1–9.

[8] H. Han, B. Sheng, C. C. Tan, Q. Li, W. Mao, and S. Lu, "Counting RFID tags efficiently and anonymously," in *Proc. IEEE INFOCOM*, Mar. 2010, pp. 1–9.

[9] M. Shahzad and A. X. Liu, "Every bit Counts: Fast and scalable RFID estimation," in *Proc. 18th Annu. Int. Conf. Mobile Comput. Netw.*, New York, NY, USA, 2012, pp. 365–376.

[10] Y. Lai, L. Hsiao, and B. Lin, "Optimal slot assignment for binary tracking tree protocol in RFID tag identification," *IEEE/ACM Trans. Netw.*, vol. 23, no. 1, pp. 255–268, Feb. 2015.

[11] *Information Technology Automatic Identification and Data Capture Techniques—Radio Frequency Identification for Item Management Air Interface—Part 6: Parameters for Air Interface Communications at 860C960 MHz*, ISO/OEC Standard FDIS 18000-6, 2003.

[12] H. Vogt, "Efficient object identification with passive RFID tags," in *Pervasive Computing (Lecture Notes in Computer Science)*, F. Mattern and M. Naghshineh, Eds., vol. 2414. Berlin, Germany: Springer-Verlag, 2002, pp. 98–113.

[13] Y. Wang, H. Wu, and Y. Zeng, "Capture-aware estimation for large-scale RFID tags identification," *IEEE Signal Process. Lett.*, vol. 22, no. 9, pp. 1274–1277, Sep. 2015.

[14] H. Landaluce, A. Perallos, E. Onieva, L. Arjona, and L. Bengtsson, "An energy and identification time decreasing procedure for memoryless RFID tag anticollision protocols," *IEEE Trans. Wireless Commun.*, vol. 15, no. 6, pp. 4234–4247, Jun. 2016.

[15] X. Liu *et al.*, "Multi-category RFID estimation," *IEEE/ACM Trans. Netw.*, vol. 25, no. 1, pp. 264–277, Feb. 2017.

[16] A. Zanella, "Estimating collision set size in framed slotted aloha wireless networks and RFID systems," *IEEE Commun. Lett.*, vol. 16, no. 3, pp. 300–303, Mar. 2012.

[17] "EPC Radio-Frequency Identity Protocols Generation-2 UHF RIFD. Specification for RFID Air Interface," Version 2.0.1, 2015. Available online: http://www.gs1.org/epcrfid/epc-rfid-uhf-air-interface-protocol/2-0-1

APPENDIX

D

Paper IV

Timing-aware RFID anti-collision Protocol to increase the Tag Identification Rate

This paper has been published in the journal *"IEEE Access"* on June 2018. Its DOI is: 10.1109/ACCESS.2018.2849223. It is published as Open Access and can be accessed online trough the IEEE Xplore Digital Library. The published version is appended here.

IEEE Access
Multidisciplinary ⋮ Rapid Review ⋮ Open Access Journal

Received May 14, 2018, accepted June 12, 2018, date of publication June 20, 2018, date of current version July 6, 2018.

Digital Object Identifier 10.1109/ACCESS.2018.2849223

Timing-Aware RFID Anti-Collision Protocol to Increase the Tag Identification Rate

LAURA ARJONA, HUGO LANDALUCE, ASIER PERALLOS, AND ENRIQUE ONIEVA
Faculty of Engineering, University of Deusto, 48007 Bilbao, Spain
DeustoTech-Fundacion Deusto, Deusto Foundation, 48007 Bilbao, Spain
Corresponding author: Laura Arjona (laura.arjona@deusto.es)

ABSTRACT Radio frequency identification (RFID) technology is one of the most popular systems to uniquely identify items by attaching a tag to them. The growing number of tagged items that need to be identified in one reader interrogation area leads to high tag collision rates. Therefore, fast anti-collision protocols are required to minimize the total tags identification time. Fast protocols involve a high tag identification rate (*TIR*), defined as the number of tags identified per time unit. In this paper, a thorough study of *TIR* is provided, analyzing the main factor which affects it: the frame size update strategy. Applying the conclusion of this analysis, the anti-collision protocol Timing-Aware Frame Slotted Aloha (TAFSA), is presented to increase *TIR*. TAFSA presents a timing-aware frame, because its size is set according to the timing parameters of a real RFID system based on the current standard. The performance of the proposed protocol is evaluated and compared with several state of the art Aloha-based anti-collision protocols. Considering a typical RFID scenario, simulation results show that TAFSA, with an average of 56.7 tags identified per second, achieves a 10 % average improvement in *TIR* in relation to the strategies of the comparison.

INDEX TERMS Radio frequency identification (RFID), EPC-global standard, anticollision, tag estimation, *TIR*, timing-aware.

I. INTRODUCTION

Radio Frequency Identification (RFID) is currently the most popular technology for item identification and tracking, and thus the main enabler for the IoT vision. The huge improvement in Ultra High Frequency (UHF) RFID, is leading to a widespread diffusion of several kinds of passive RFID tags in products. Current examples of RFID expansion can be found in activity recognition, localization systems, and mobile sensing [1]–[4]. The RFID market was worth 9 billion in 2014, and the IDTechEx forecast is that it will rise to ∼30 billion in 2024 [5].

RFID technology uses a spectrum of radio frequency to transfer the identification information between two communication devices: reader and tags [6]. The coexistence of several tags provides RFID technology with a great flexibility at the expense of the tag collision problem. Tags share the same communication channel (the air) and may respond simultaneously to the same interrogation command, interfering and garbling their waveforms. The reader then is unable to interpret the information received from the tags, requiring a re-transmission, and extending the tag identification time. Anti-collision protocols are then proposed to arbitrate tags' responses and to increase the number of tags identified by a time unit.

In the literature, three main types of anti-collision protocols have been reported: Aloha-based, tree-based, and hybrid protocols. The three types of protocols can be applied to active (battery-operated tags), passive (tags backscatter information), or semi-passive (combination of active and passive) RFID systems. Tree based protocols [7]–[9], in essence, split colliding tags into subsets, and further split the subsets repeatedly up to the successful response of all the tags that are within the interrogation zone. Aloha-based protocols [10], [11] divide time into frames so that tags randomly choose one slot per frame to respond. While in Frame Slotted Aloha (FSA) the frame size L is fixed during the identification process, in Dynamic Frame Slotted Aloha (DFSA) it is variable, and the protocol's performance is greatly influenced by the update of L. The fact that the standard EPCglobal Class-1 Generation-2 (EPC C1G2) [12] currently uses a DFSA structure to arbitrate collisions highlights the research relevance of this scheme. Finally,

hybrid protocols combine the advantages of tree and Aloha protocols [13].

Currently, there is growing number of RFID tags sharing a reader interrogation area, which leads to higher tag collision rates. As a solution, fast anti-collision protocols are required to minimize the total tags identification time. An anti-collision protocol is considered fast when it provides a high Tag Identification Rate (*TIR*), defined as the number of tags identified by a unit of time. *TIR* mainly depends on the employed strategy to update the frame size. This work provides an extensive study of how the frame size update strategy affects the *TIR* of an anti-collision protocol. The conclusions extracted are applied to the design of the Timing-Aware Frame Slotted Aloha (TAFSA) anti-collision protocol. TAFSA presents a timing-aware frame, because its size is set according to the timing parameters of a real RFID system based on the current standard. The performance of TAFSA is evaluated and compared with several recent strategies in the literature. The results of the performance evaluation show that the proposed protocol increases *TIR* in relation to the strategies in the comparison. The following main contributions are made in this work:

1) Analytical study of the L which maximizes the *TIR* metric.
2) Presentation of a novel anti-collision protocol: TAFSA. The proposed protocol applies the results obtained in the previous contribution to increase the *TIR* in an RFID system based on EPC C1G2.
3) Configuration of sMMSE estimator [17] to lower the estimation time, resulting in tMMSE estimator.
4) Analysis of the tag estimation error of tMMSE when L is adjusted to power of 2 values and how this error affects *TIR*.
5) *TIR* evaluation of TAFSA and comparison with several anti-collision protocols of the state of the art.

The rest of the paper is organized as follows. Section II presents the RFID Standard EPC C1G2 and several related Aloha-based anti-collision protocols in the literature. Section III provides a thorough analysis of the main factor which affects *TIR* and obtains the value of L which maximizes it. The proposed TAFSA anti-collision protocol is presented in section IV. Section V provides the results of the performance evaluation followed by the study of the physical implementation feasibilities in Section VI. Finally, Section VII concludes this paper.

II. BACKGROUND

Some definitions are provided to properly set the background of this work and to better understand the main contributions:

- A ***slot*** is a period of time that separate tags' responses. Conventionally, three types of slots are considered attending to the tags' responses to the reader's commands: idle (none of the tags replies), single (only one tag replies), and collision (more than one tag replies in the same slot). The duration of each type of slot is referred as T_i, T_s, and T_k, respectively. These slots are accurately specified in the current standard [12], and their duration is determined by the link timing parameters (T_1, T_2, T_3).
- A ***frame*** is a sequence of slots. Tags can respond in only one slot per frame. An identification process is composed of a set of frames.
- A ***command*** is a bit-string transmitted by the reader to the tags.
- The ***identification time*** refers to the time required by the reader to identify a complete tag set of size n.
- The ***estimation time*** ET is defined as the time the reader employs to calculate an estimated tag set size, referred as $\hat{n}$. This parameter is presented in [17].
- An ***inventory round*** is the period of time that begins when the reader transmits the initial command (Qc) and it ends when the reader interrupts the identification process and the tags loose their state. Ideally, an inventory round ends when all the tags in the reader interrogation zone have been identified.

Now that the main concepts have been explained, the state of the art in DFSA protocols is presented.

A. DFSA ANTI-COLLISION PROTOCOLS

The current standard in RFID systems is EPC C1G2 [12], which defines a DFSA anti-collision protocol named Slot Counter. Following this protocol, the reader transmits Query (Qc), QueryAdjust (QA), and QueryRep (QR) commands to schedule tags' responses in time. Commercial tags contain an internal counter SC to keep track of the selected slot in each frame. A tag transmits a 16-bit random number ($RN16$) when SC=0. Once the reader acknowledges the $RN16$ with the ACK command, the tag transmits its IDentification code (ID) of length k.

Most RFID manufacturers currently follow the EPC C1G2 standard, enhancing the research relevance of DFSA-based protocols. Consequently, many DFSA protocols based on the standard have recently appeared with the aim of improving different metrics regarding the process of tag identification. A wide variety of DFSA protocols can be found in the literature which update L with the tag set size estimated by the reader, referred as $\hat{n}$. Most of them focus on a single-reader scenario, but there are also protocols with accurate estimators for the case of multiple-readers [18], [19]. This work focuses on single-reader systems.

In order to present the single-reader strategies, a system model with one reader and n tags is defined. A DFSA frame of size L is defined. The variables c_s, c_k, and c_i correspond to the number of single, collision, and idle slots in the frame, respectively, and up to the current slot. Additionally, p_s, p_k, and p_i correspond to the probability that only one tag, no tag, or more than one tag occupies a slot, respectively. Some of the most relevant DFSA-based protocols in the literature are introduced next. The examination slot refers to the particular slot within each frame where L is updated.

1) EOM

Eom and Lee [21] introduce a DFSA anti-collision protocol which updates L according to the estimated tag set size. The estimation mechanism is based on the number of collided tags per slot (γ). The authors show the positive performance of the protocol in terms of the estimation error and the total number of slots used for identification. However, the authors did not distinguish between the three types of slots to measure the total number of slots, making the comparative with the rest of the protocols unfair.

2) ILCM-FbF and ILCM-SbS

Solic *et al.* [10] present the Improved Linearized Combinational Model with Frame by Frame examination of L (ILCM-FbF) for the optimal frame size adaptation. They present a DFSA protocol based on the estimation of the tag population with a linear function which depends on c_k and L. Then, at the end of the frame, L is updated with $\hat{n}$. Simulation scenario is limited, because the results are only compared with the Slot Counter protocol.

The protocol Improved Linearized Combinational Model with Slot by Slot examination of L (ILCM-SbS) is presented in [22] as an improved version of [10]. Simulation results show that ILCM-SbS lowers the time required to identify a set of tags compared with some protocols of the state of the art. However, this strategy might overload a reader that has only a limited capacity, because L is calculated at every slot.

3) CHEN14 AND CHEN16

Chen [23] presents an anti-collision protocol (Chen14) which examines L at just one slot per frame, determined as L/i, claiming to significantly reduce the number of total examination slots. The presented protocol updates L as a function of $\hat{n}$, and then L is updated based on $\hat{n}$. Simulation results show an improved performance in terms of normalized throughput, defined as $Throughput = c_s/(c_s + c_k + c_i)$. However, this metric assumes equal duration for each type of slot, and contrasting the EPC C1G2 requirements, these slots have different durations.

As an extension of the study in [23], Chen proposes in [24] an anti-collision algorithm (Chen16) based on the early and optimal adjustment of the frame length. Chen16 is proposed with the aim of maximizing the normalized throughput (U), defined as $U = (c_s T_s)/(c_s T_s + c_i T_i + c_k T_k)$. In this protocol, the tag set size is estimated in every frame at the examination point $L/5$. The value of this slot has been selected as the slot where maximum U is obtained. Based on the previous $\hat{n}$, if a new frame is required, the author updates L with the variable y, where y is expressed as a second-order polynomial. Simulation results show competitive values regarding U, but the function defined to set y is not valid for all the range of T_k/T_i. Particularly, if $T_k >> T_i$, y takes negative values, leading to negative values for L. Additionally, the examination point $L/5$ has been set based on a particular scenario with specific timing parameters. Therefore, this value might not be appropriate for a scenario with different timing settings of the RFID system.

4) SSA AND DSSA

Duan *et al.* [25] propose the segment-by-segment Aloha protocol (SSA) to effectively decrease the frame adjustment times with satisfactory throughput. In this protocol, one frame is composed of a set of slot-segments, and each slot-segment is composed of s_L continuous time slots, where s_L=4.

In order to increase the protocol's throughput, the authors introduce dynamic SSA (DSSA) protocol, where s_L is dynamically varied by tracking, real-time, the number of single slots. Both protocols present a positive performance regarding the throughput and the number of tags identified per second. However, they are compared with just one additional protocol, and for one specific scenario, with a particular set of timing configuration.

III. TIMING-AWARE ALOHA FRAME ANALYSIS

Traditionally, the most common metric to evaluate the performance of an RFID anti-collision protocol has been the Slots Efficiency (SE) [15], defined as

$$SE = \frac{c_s}{c_i + c_s + c_k}. \tag{1}$$

Ideally, an anti-collision protocol is desired to reach SE=1, meaning that just one slot per tag is required for the complete tag set identification. However, this is not achievable in practical applications, where collision and idle slots are present. An anti-collision protocol reaches its maximum SE when the frame size equals the number of tags, that is, L=n [15]. However, this condition only applies when T_i=T_s=T_k. The EPC C1G2 standard specifies different durations for idle, single, and collision slots, referred as T_i, T_s, and T_k. Therefore, traditional SE is not a meaningful parameter to measure the performance of an RFID system. Moreover, this metric does not consider the time-overhead of each frame.

To mitigate the different slots duration effect, the metric $Time\_SE$ is introduced in [27]

$$Time\_SE = \frac{c_s}{c_{total} + (\beta - 1)c_i} \tag{2}$$

where c_{total}=c_i+c_s+c_k and β=T_i/T_k. This metric considers different duration for T_k and T_i, but it assumes T_s=T_k and it does not include the time-overhead information.

In order to provide an accurate evaluation of an RFID system, the metric TIR is defined as the number of tags identified per time unit in one inventory round. It is calculated as the total number of single slots c_{s_T} divided by the total identification time it:

$$TIR = \frac{c_{s_T}}{it}; \quad it = c_{s_T} T_s + c_{k_T} T_k + c_{i_T} T_i + T_{overhead}, \tag{3}$$

where $T_{overhead}$ refers to the time-overhead of one inventory round, and it is defined as

$$T_{overhead} = T_{Qc} + (N_F - 1)T_{QA} + (N_S - N_F)T_{QR}. \tag{4}$$

The variables c_{k_T} and c_{i_T} represent the total number of collision and idle slots, respectively, in one inventory round.

The variables N_S and N_F refer to the total number of slots and the total number of frames in one inventory round, respectively. The parameters T_{Qc}, T_{QA}, and T_{QR} refer to the duration of the reader commands Qc, QA, and QR, respectively. They are calculated as the Reader-to-Tag synchronization time $T_{FSync_{RT}}$ or $T_{Preamble_{RT}}$, defined in [12] plus the length of each parameter divided by the reader data rate DR_r, calculated as DR_r=$1/((T_{data_0} + T_{data_1})/2)$, where $T_{data_0} = Tari$, and T_{data_1}=$1.5{\cdot}Tari$. *Tari* represents the reference time interval for a *data*-0 transmission. Thus, T_{Qc}=$T_{FSync_{RT}} + 22$ bits/DR_r, T_{QA}=$T_{Preamble_{RT}} + 9$ bits/DR_r, and T_{QR}=$T_{Preamble_{RT}} + 4$ bits/DR_r.

The duration of each slot is obtained as

$$T_i = T_1 + T_3, \tag{5}$$

$$T_s = 2T_1 + T_{RN16} + 2T_2 + T_{ACK} + T_{ID}, \tag{6}$$

and

$$T_k = T_1 + T_{RN16} + T_2; \tag{7}$$

where T_{RN16} and T_{ID} refer to the time the tag employs to transmit RN16 and its ID, respectively. They are calculated as the Tag-to-Reader synchronization time $T_{Preamble_{TR}}$ plus the length of each parameter divided by the tag data rate DR_t, calculated as DR_t=BLF/M. The parameter *BLF* refers to the Backscatter-link frequency. Thus, T_{RN16}=$T_{Preamble_{TR}}$+17 bits/DR_t and T_{ID}=$T_{Preamble_{TR}} + 129$ bits/DR_t. Finally, T_{ACK} corresponds to the duration of the reader command ACK, and it is obtained as T_{ACK}=$T_{Preamble_{RT}} + 18$ bits/DR_r. Table 1 summarizes the calculation of the reader and tags messages duration.

TABLE 1. Main EPC C1G2 timing parameters calculation.

Parameter	Description	Calculation
T_{data_0}	Duration of a reader data-0	$Tari$
T_{data_1}	Duration of a reader data-1	$1.5{\cdot}Tari$
$T_{Preamble_{RT}}$	Duration of R-T Preamble	T_{del}+T_{data_0}+ +$RTcal$+$TRcal$
$T_{FSync_{RT}}$	Duration of Frame Sync.	T_{del}+T_{data_0}+$RTcal$
$T_{Preamble_{TR}}$	Duration of T-R Preamble	$7/DRt$
DRr	Reader data rate	$1/((T_{data_0} + T_{data_1})/2)$
DRt	Tag data rate	BLF/M
T_{Q_c}	Duration of a Qc	$T_{FSync_{RT}}$+$22/DR_r$
T_{QA}	Duration of a QA	$T_{Preamble_{RT}}$+$9/DR_r$
T_{QR}	Duration of a QR	$T_{Preamble_{RT}}$+$4/DR_r$
T_{ACK}	Duration of a ACK	$T_{FSync_{RT}}$+$24/DR_r$
T_{RN16}	Duration of tag $RN16$	$23/DRt$
T_{ID}	Duration of tag ID	$135/DRt$

From (3), it follows that *TIR* is mainly influenced by the total number of each type of slot and their duration. On the one hand, T_i, T_s, T_k, T_{Qc}, T_{QA}, and T_{QR} are fixed for a particular RFID system, and they remain constant for one inventory round. On the other hand, c_i, c_s, and c_k, strictly depend on the anti-collision protocol employed to identify the tags and particularly, on the strategy it uses to update L with $\hat{n}$.

The next section studies the parameter L, the main factor which affects c_i, c_s, c_k, and ultimately, *TIR*. Also, the optimal L is derived to maximize *TIR*. The main variables used in the analysis are summarized in Table 2.

TABLE 2. Main parameters to analyze an Aloha frame.

Parameter	Description
T_1, T_2, T_3	Link-timing parameters
T_i, T_s, T_k	Duration of idle, single, and collision slots
c_i, c_s, c_k	Number of idle, single, and collision slots in one frame
$c_{i_T}, c_{s_T}, c_{k_T}$	Number of idle, single, and collision slots in one inventory round
$P_r(n, L)$	Probability that r among n tags occupy a slot in a frame of size L
$p_i(n, L), p_s(n, L), p_k(n, L)$	Probability of idle, single, and collision slot in a frame of size L
$c_i(n, L), c_s(n, L), c_k(n, L)$	Expected value of the number of idle, single, and collision slots in one frame
$P_F(n, L)$	Probability of starting a new frame at the end of current frame of size L
N_S	Total number of slots in one inventory round
N_F	Total number of frames in one inventory round
n_f	Number of unidentified tags at the beginning of frame f
L_f	Size of the frame f

A. FRAME SIZE SETTING ANALYSIS

In RFID systems adopting the EPC C1G2 requirements, each slot has a different duration, and T_i<T_k<T_s. During T_s, in addition to the bits transmitted during T_k, the tag must transmit its complete ID and receive the ACK from the reader. In this section, the value of L which maximizes *TIR* is derived. Following the EPC C1G2 constraints, L value must be a power of 2.

In order to perform the analysis, a system model with one reader and n tags is defined, where $c_s(n, L)$, $c_k(n, L)$, and $c_i(n, L)$ represent the expected value of the number of single, collision, and idle slots in a frame, respectively. The probability that r tags among n occupy a slot within a frame of size L can be approximated by a binomial distribution $P_r(n, L)$ [29]

$$P_r(n, L) = \binom{n}{r}\left(\frac{1}{L}\right)^r\left(1 - \frac{1}{L}\right)^{n-r}. \tag{8}$$

If L is assumed sufficiently large, the tags distribution can be approximated by a Poisson distribution with mean ρ.

$$\rho = \frac{n}{L}. \tag{9}$$

When $r = 0$ in (8), $c_i(n, L)$ can be approximated by

$$c_i(n, L) = Lp_i(n, L) = L\left(1 - \frac{1}{L}\right)^n \approx Le^{-\rho}. \tag{10}$$

When $r = 1$ in (8), $c_s(n, L)$ can be approximated by

$$c_s(n, L) = Lp_s(n, L) = n\left(1 - \frac{1}{L}\right)^{n-1} \approx L\rho\left(\frac{n/\rho}{n/\rho - 1}\right)e^{-\rho}. \quad (11)$$

Then, $c_k(n, L)$ can be approximated by

$$c_k(n, L) = L \cdot p_k(n, L) = L(1 - p_0 - p_1). \quad (12)$$

1) *TIR* FOR ONE INVENTORY ROUND

First, *TIR* is evaluated for one complete inventory round. It is assumed that an inventory round ends when the probability of collision is lower than α, that is, $p_k < \alpha$. Thus, given a tag set size n and a frame of size L, the probability of starting a new frame $P_F(n, L)$ can be approximated with a logistic function

$$P_F(n, L) = \frac{1}{1 + e^{-\gamma[1-(1+\rho)e^{-\rho}-\alpha]}} \quad (13)$$

where γ represents the steepness of the logistic function. Then, the total number of frames N_F can be expressed as

$$N_F = 1 + \sum_{f=1}^{fmax} P_F(n_f, L_f) \quad (14)$$

where *fmax* represents the upper limit of the total number of frames, and n_f refers to the number of unidentified tags at the beginning of each frame

$$n_f = n_{f-1} - c_s(n_{f-1}, L_{f-1}), \quad (15)$$

and L_f corresponds to the size of each frame

$$L_f = 2^{Q_f}. \quad (16)$$

The value of Q_f which maximizes *TIR* is obtained in the next subsection. Next, the total number of slots N_S can be obtained as

$$N_S = \sum_{f=1}^{round(N_F)} L_f \quad (17)$$

where round is a mathematical function to obtain the nearest integer. Finally, in order to calculate *TIR* using (3), the total number of idle, single, and collision slots in one inventory round can be obtained as

$$c_{i_T} = \sum_{f=1}^{round(N_F)} c_i(n_f, L_f), \quad (18)$$

$$c_{s_T} = \sum_{f=1}^{round(N_F)} c_s(n_f, L_f), \quad (19)$$

and

$$c_{k_T} = \sum_{f=1}^{round(N_F)} c_k(n_f, L_f). \quad (20)$$

Finally, taking the initial value n_1, which corresponds to the initial tag set size, *TIR* can be evaluated for a complete inventory round with (3). In order to obtain the L value of each frame which maximizes *TIR* in one inventory round, the next subsection analyzes *TIR* for one frame.

2) *TIR* FOR ONE FRAME

In the case of one frame, N_F=1 and N_S=L. Thus, substituting (18), (19), and (20) into (3) with N_F=1 and N_S=L, and applying $\frac{n/\rho}{n/\rho-1} \approx 1$, the following expression is obtained

$$TIR \approx \frac{L\rho e^{-\rho}}{L[e^{-\rho}(\rho T_s + T_i - T_k - \rho T_k) + T_k + T_{QR}] - T_{QR} + T_{Qc}}. \quad (21)$$

The parameter T_{Qc} is applied in (21) only when the first frame of the inventory round is analyzed. For the rest of frames, it is substituted by T_{QA}.

Next, computing the derivative of *TIR* in (21) respect to ρ and posing $\frac{dTIR}{d\rho}$=0, it yields the following equation

$$\rho^2(T_{QA}e^{\rho} - T_{QR}e^{\rho}) + \rho(nT_k e^{\rho} + nT_{QR}e^{\rho}) - e^{\rho}(nT_k + nT_{QR}) - nT_i + nT_k = 0. \quad (22)$$

A quadratic equation is obtained, with two solutions for ρ that must be found numerically. Then, according to (9), the frame size which maximizes *TIR* is obtained as L=n/ρ. Thus, Q_f=$round(log_2(n/\rho))$ and

$$L_f = 2^{round(log_2(n/\rho))}. \quad (23)$$

From (22) and (23), it is clear that the L which maximizes *TIR* depends on n and on the timing parameters of the RFID system. To solve (22) for different n, the timing parameters of Table 3 are used. These parameters are set following the EPC C1G2 restrictions. *Tari* is set to the standard's minimum of 6.25 μs and *BLF* is set to 40 kbps, conditioning the values of T_{data_1}, $T_{Preamble_{RT}}$, $T_{FSync_{RT}}$, and $T_{FSync_{TR}}$.

The positive solutions of (22) for ρ are shown in Fig. 1 for $\alpha = 0.01$, γ=30, and f_{max}=10. From this figure, it is clear that the solution of ρ converges to the value 0.3155, applying the parameters of Table 3.

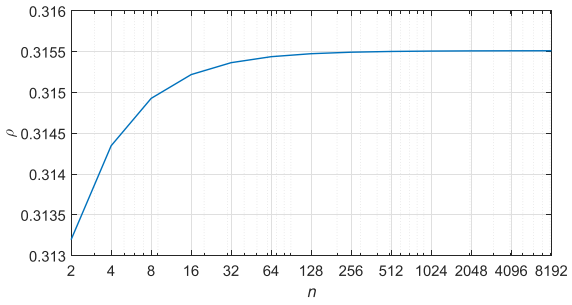

FIGURE 1. Solution of (22) for ρ, with $\alpha = 0.01$, γ=30, and f_{max}=10, varying n from 2 to 8192.

Next, the effect of ρ over *TIR* is analyzed for one inventory round. Analytical results are obtained by evaluating (3) for n from 2 to 8912 and averaging the results, and they are shown in Fig. 2.

TABLE 3. Simulation Parameters according to EPC C1G2 [12].

Parameter	Value	Parameter	Value
$Tari$	6.25 μs	BLF	40 kbps
$T_{Preamble_{RT}}$	234.38 μs	T_1	87.5 μs
$T_{Preamble_{TR}}$	700.00 μs	T_2	75 μs
$T_{FSync_{RT}}$	34.38 μs	T_3	8.75 μs
DR_r	128 kbps	DR_t	10 kbps
T_{QA}	104.69 μs	T_{QR}	65.63 μs
T_{Q_C}	406.25 μs	T_{QE}	65.63 μs

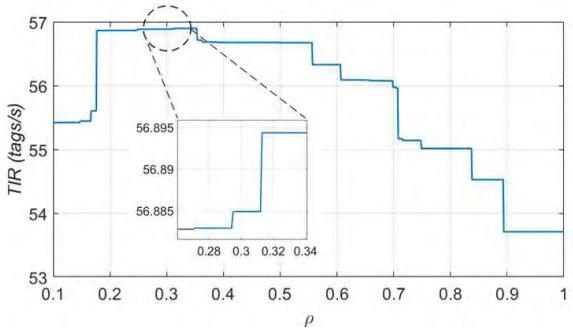

FIGURE 2. Solution of (22) for ρ, with $\alpha = 0.01$, γ=30, and f_{max}=10, varying n from 2 to 8192.

This Figure demonstrates that the solution of ρ obtained for one frame results in the highest *TIR* for one inventory round.

From this section, it can be concluded that, in order to maximize *TIR*, L must be selected considering the specific timing parameters of the RFID system. Once defined the strategy to set L, the next section presents the proposed anti-collision protocol.

IV. THE PROPOSED TAFSA ANTI-COLLISION PROTOCOL

This section applies the results obtained in the previous section to improve the *TIR* of DFSA anti-collision protocols. As a result, the novel TAFSA protocol, based on EPC C1G2, is presented to increase *TIR*. The proposed protocol sets L according to the timing parameters of the RFID system and the tag set size estimated with tMMSE estimator. TAFSA uses tMMSE because this estimator has been configured to lower the tag estimation time, contributing to achieve a faster identification.

Firstly, tMMSE is studied in this section. Next, the protocol description and its pseudo-code is provided.

A. TAG ESTIMATOR TMMSE

A portion of the identification time is employed in estimating the tag set size to set an appropriate L. Therefore, in order to increase *TIR*, it is desired to decrease the n tags identification time.

The estimator sMMSE [17] presents a flexible performance, because it can be tuned to improve two metrics: the estimation time *ET* and the estimation error ε_r. The performance of these two metrics can be configured with two key parameters: T_{RR} determines the limits of the slots occupancy at which the frame size should be increased, and Δ sets the frame size increase factor. This section presents and configures the time-Minimum Mean Squared Error (tMMSE) tag estimator, which minimizes *ET* in the estimator presented in [17] while providing an accurate tag estimate. For this purpose, the value of T_{RR} and Δ which minimize *ET* for a wide range of tag set sizes is calculated next.

1) DESCRIPTION OF tMMSE ESTIMATOR

The main novelty of the proposed estimator is the fast estimation performed while scaling to a wide range of tag set sizes. The estimation process starts when the reader transmits the 4-bit-length Query Estimation command QE of duration T_{QE}, specifying L. Initially, L=1. After receiving this command, each tag randomly selects a value v between 0 and $kL-1$, where k represents the tag's ID length. Then each tag generates a sequence of length k bits, consisting of all '0's and sets the (v *mod* k)th bit to '1', where *mod* represents the modulo operation. The generated sequence is transmitted in the $\lfloor v/k \rfloor$th slot of the frame, where $\lfloor \cdot \rfloor$ operation rounds the element to the nearest integer towards $-\infty$. Next, the reader orderly receives the tags' sequences from slot 0 to slot $L-1$ and then builds the sequence S of length kL bits, by concatenating the sequences received in each slot: $S=\{s_0, s_1, \ldots s_{kL-1}\}$ where $s_i \in \{0, 1, X\}$. When $s_i=X$, a bit-collision is detected in position i using bit-tracking. Let sb_i represent a selected bit in position i, so that $sb_i=1$ when $s_i=1$ or $s_i=X$, and $sb_i=0$ otherwise. The reader then computes the tag Response Rate *RR*, defined as $RR = \sum_{i=0}^{kL-1} sb_i/kL$. Then if $RR \geq T_{RR}$ (where T_{RR} is a threshold value for *RR* and it is fixed for a complete estimation round), L is increased by a factor of Δ, i.e., $L=L\Delta$. Then the reader transmits a QE and the previous process is repeated.

When $RR<T_{RR}$, meaning that L is adapted to n, the tag set size is estimated as the value of n minimizing the probability function P_n [17]

$$P_n = \left(RR - 1 + \left(1 - \frac{1}{kL}\right)^n\right)^2 + \left(1 - RR - \left(1 - \frac{1}{kL}\right)^n\right)^2. \quad (24)$$

If L is assumed sufficiently large, the tags distribution can be approximated by a Poisson distribution with mean $\mu = \frac{n}{kL}$. This yields

$$P_n \approx \left(RR - 1 + e^{-\mu}\right)^2 + \left(RR - 1 - e^{-\mu}\right)^2. \quad (25)$$

The proposed estimator obtains $\hat{n}$ by finding the minimum of the function P_n. Computing the derivative of P_n respect to μ in (25) and posing $\frac{dP_n}{d\mu}$=0, it yields the following equation

$$e^{-\mu} + RR - 1 = 0 \quad (26)$$

Thus, the number of estimated tags is found to be [17]

$$\hat{n} = kL\hat{\mu} \quad (27)$$

where $\hat{\mu}$ is the solution of (26) with a numerical method. It can be solved with a bisection search.

2) tMMSE CONFIGURATION

In this section, T_{RR} and Δ are adjusted in order to minimize ET for a wide range of tags, named $\{T_{RR}, \Delta\}_{tMMSE}$.

First, the matrix $\overline{TM}$ is defined as

$$\overline{TM} = \begin{pmatrix} \overline{et}_{11} & \dots & \overline{et}_{1c} \\ \dots & & \dots \\ \overline{et}_{r1} & \dots & \overline{et}_{rc} \end{pmatrix} \tag{28}$$

where

$$\overline{et}_{ij} = \sum_{t=1}^{k} et_{ij}(n_t) \tag{29}$$

and

$$et_{ij}(n) = ET|_{T_{RR}=T_{RR_i}, \Delta=\Delta_j}. \tag{30}$$

$\overline{TM}$ contains the values of ET provided by tMMSE for each possible value of the pair T_{RR} and Δ, averaged for a wide range of tag set sizes. To evaluate $\overline{TM}$, the vectors $\mathbf{T_{RR_v}}$, $\Delta_\mathbf{v}$ and $\mathbf{n_v}$, with lengths r, c, and t respectively, are defined [17]: $\mathbf{T_{RR_v}}$=[0.1, 0.2, . . . , 1] with r=10,$\Delta_\mathbf{v}$=[1, 1.1, . . . , 3] with c=21, and $\mathbf{n_v}$=[100, 200, . . . , 1000] with t=10. For instance, the element $et_{1,3}(n{=}100)$ corresponds to the estimation time calculated for n=100, T_{RR}=0.1, and Δ=1.2.

Finally, $\{T_{RR}, \Delta\}_{tMMSE}$ is calculated as the value of T_{RR} and Δ which minimize $\overline{et}_{ij}$ in (29)

$$\{T_{RR}, \Delta\}_{tMMSE} = arg \underset{[T_{RR}, \Delta]}{[}min\ \overline{et}_{ij}. \tag{31}$$

In order to evaluate (31), one full estimation process is completed for the tag sets $\mathbf{n_v}$, and the vectors $\mathbf{RR_v}$ and $\Delta_\mathbf{v}$, and ET are obtained with tMMSE. Finally, T_{RR} and Δ minimizing ET are calculated, configuring tMMSE estimator

$$\{T_{RR}, \Delta\}_{tMMSE} = \{1, 2\}. \tag{32}$$

Once tMMSE is configured, its pseudocode is shown in Fig. 3, and its performance is evaluated in the next section.

3) tMMSE PERFORMANCE EVALUATION

This section evaluates the performance of tMMSE regarding the estimation accuracy and time. To measure the accuracy of an estimation algorithm, the normalized estimation error is defined in [17] as

$$\varepsilon_r = \frac{|\hat{n} - n|}{n}. \tag{33}$$

Following the EPC C1G2 constraints, L value must be a power of 2. Consequently, different $\hat{n}$ may result in the same L_f (23). Defining n_U and n_L as the upper and lower bound of n, respectively, for which L_f remains invariable, the same L_f is obtained for any $\hat{n}$ satisfying $\hat{n}\in[n - n_L + 1, n + n_U - 1]$. If this condition is satisfied, the performance of the anti-collision protocol is not affected. Therefore, a variable estimation error is admissible while computing the tag population size without affecting *TIR*.

Next, $\hat{n}$ is evaluated for different tag set sizes to study if tMMSE satisfies the condition $\hat{n}\in[n - n_L + 1, n + n_U - 1]$. Simulation results are shown in Fig. 4. For a particular n, the allowed $\hat{n}$ can move inside the shaded area without affecting *TIR*. From this figure, it is appreciated that the previous condition is satisfied for most of the tag population sizes analyzed. There are two critical ranges, one from 720 to 770, and the other from 1450 to 1520, where the $\hat{n}$ provided by the estimator results in a L value out of the predefined boundaries. Because these two critical areas are narrow, it can be guaranteed that the estimation error of tMMSE does not affect *TIR* for most n analyzed.

tMMSE implementation for reader

```
L=1
while 1 do
    Transmit QE
    receive S
    calculate RR = Σ_{i=0}^{kL-1} sb_i/kL
    if RR<1 then
        break
    else
        L=2L
    end if
end while
obtain μ̂ by solving (26)
calculate n̂ with (27)
```

tMMSE implementation for tag

```
wait for QE command
select v∈ [0, kL − 1]
generate a k-bit sequence consisting of all '0's
set the (v mod k)th bit of the sequence to '1'
transmit sequence in slot ⌊v/k⌋
```

FIGURE 3. Pseudo-code of tMMSE estimator for reader and tags.

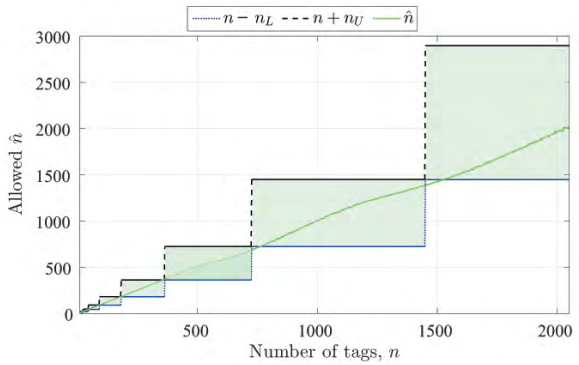

FIGURE 4. Analysis of $\hat{n}$ using tMMSE varying n from 10 to 2050, with ρ=0.315. Shaded area corresponds to $\hat{n}$ for which L_f (30) remains invariable given a tag population n.

Finally, ET and ε_r are evaluated for tMMSE and compared with those of sMMSE for different tag set sizes. Simulation results are shown in Fig. 5. From this figure, it can be appreciated that tMMSE lowers ET (solid line) while increasing ε_r (dashed line) compared to sMMSE. Additionally, while ε_r increases with n for tMMSE, it decreases with n for sMMSE.

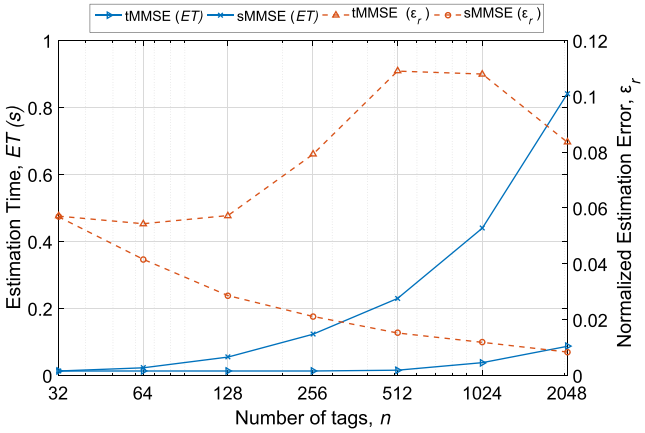

FIGURE 5. Evaluation and comparison of the estimation time *ET* (left, solid line) and normalized estimation error ε_r (right, dashed line) between sMMSE and tMMSE varying *n* from 32 to 2048.

It can be concluded that the accuracy of tMMSE can be compromised at the expense of obtaining a faster estimation in relation to the estimator presented in [17]. Thus, a faster tag estimator contributes to a faster tag identification process, which increases *TIR*.

B. TAFSA PROTOCOL DESCRIPTION

This section presents TAFSA anti-collision protocol, based on the current standard EPC C1G2. It has been designed to increase *TIR* in DFSA anti-collision protocols by considering the following three strategies.

- Initial tag set size estimation to set the initial L with tMMSE estimator, configured to lower *ET*.
- Timing-aware frame size, calculated as a function of parameter ρ, according to the RFID system timing configuration. As a result, TAFSA performance is adapted to the particular timing settings of the system.
- Tag set size re-estimation at the end of each frame to update L. Estimation is performed with tMMSE using the information of the selected slots (collision or success slot) in the current frame.

The pseudo-code for TAFSA to perform one full identification process of a set of tags is presented in Fig. 6, and the flow diagram is shown in Fig 7. Two phases are distinguished in the process of *n* tags identification:

Phase I: Initial *n* estimation.
The identification procedure starts by broadcasting the QE to estimate initial number of tags inside the interrogation zone of the reader. To estimate the initial *n*, the proposed protocol applies tMMSE. The initial frame size to perform the estimation is 1.

Phase II: Tag population identification.
First, the reader sets the value of ρ by solving (27). The value of ρ is obtained just once at the beginning of the inventory round, according to the RFID system timing parameters. Then, the initial L to begin the identification process is obtained with (23), and the reader starts the identification procedure by broadcasting Qc. Each tag selects a slot in the frame to transmit its ID. The reader continues the identification process analyzing each slot of the frame, updating the variables c_i, c_s, and c_k accordingly, and broadcasting QR to go from one slot to the next. When the reader reaches the last slot of the frame, the remaining tag set size is estimated with tMMSE. In this phase, to avoid the additional latency caused by the estimation frames of tMMSE, the reader estimates the number of tags based on the information of the selected slots in the last identification frame. Let ss_i represent a selected slot in position i, so that ss_i=1 under a collision or a success slot condition, and ss_i=0 otherwise. The reader then computes the Response Rate for slots as $RR_s = \sum_{i=0}^{L-1} ss_i/L$, and μ=n/L. Thus, $\hat{n}$=$L\hat{\mu}$, and $\hat{\mu}$ is obtained by solving (26). In the all-selected-slots scenario (RR_s=1), it is assumed $\hat{n}$=2.39c_k+c_s [31].

TAFSA implementation

Phase I

1: $T_{RR} = 1, \Delta = 2, L = 1$
2: $c_i = 0, c_s = 0, c_k = 0$, slot = 1
3: broadcast QE
4: $\hat{n} = kL\hat{\mu}$

Phase II

5: Calculate ρ by solving (27)
6: $Q = round(log_2(\hat{n}\rho^{-1})), L = 2^Q$
7: Broadcast Qc
8: **while** 1 **do**
9: read slot and update c_i, c_s, c_k
10: **if** idle **then**
11: $c_i = c_i + 1$
12: **else**
13: **if** single **then**
14: $c_s = c_s + 1$
15: **else**
16: $c_k = c_k + 1$
17: **end if**
18: **end if**
19: **if** slot = L **and** $c_k = 0$ **then**
20: break
21: **else**
22: **if** slot = L **then**
23: $RR_s = \sum_{i=0}^{L-1} ss_i/L$
24: $\hat{n} = L\hat{\mu}$
25: $Q = round(log_2((\hat{n} - c_s)\rho^{-1})), L = 2^Q$
26: $c_i = 0, c_s = 0, c_k = 0$, slot = 1
27: broadcast QA
28: **else**
29: broadcast QR
30: slot = slot +1
31: **end if**
32: **end if**
33: **end while**

FIGURE 6. Pseudo-code of TAFSA anti-collision protocol.

Then a new frame is started by broadcasting QA, specifying the new L according to (23).

It is important to note here that, unlike most DFSA protocols [10], [21]–[25], the initial L for TAFSA is not set to a fixed value, but it is set according to ρ and the initial n estimation with tMMSE. Besides, if the timing parameters of the RFID system vary, TAFSA adapts to these changes, obtaining a new solution for ρ and updating L accordingly. As a result, the positive performance of TAFSA in terms of *TIR* is hardly affected by applying a different RFID system with varying timing configuration. The next section evaluates the performance of the proposed anti-collision protocol.

V. EVALUATION OF THE TAG IDENTIFICATION RATE

This section evaluates the performance of TAFSA regarding *TIR*, and compares it with the anti-collision protocols of the state of the art presented in Section II.B: Eom [21], ILCM-FbF [10], ILCM-SbS [22], Chen14 [23], Chen16 [24], SSA [25], and DSSA [25]. Physical-layer effects are not considered here, assuming a non-impaired channel and no capture effect. Note that these assumptions are extensively used for the analysis of known anti-collision protocols whose analysis focuses on the media access control layer [7], [21], [24], [25]. Simulation results are obtained with Matlab R2017b. A scenario with one reader and a varying number of tags is evaluated, where the tags are uniformly distributed. The simulation responses have been averaged over 1000 iterations for accuracy in the results. Timing parameters are set according to Table 3. Some implementation details must be taken into consideration:

- The identification time of TAFSA includes the estimation time ET employed in Phase I. Thus, $it_{TAFSA}=c_{s_T}T_s+c_{k_T}T_k+c_{i_T}T_i+T_{overhead}+ET$. In Phase II $ET=0$.
- To evaluate the anti-collision protocols' performance with n, the tag set sizes considered are $N=[16, 32, 64, 128, 256, 512, 1024, 2048]$ and $n \in N$.
- L values are limited to power of 2, following EPC C1G2 specifications.
- Initial L is set to 16 ($Q=4$), following EPC C1G2 recommendation.
- The length of the ID is set to $k=128$.

Fig. 8 shows that TAFSA clearly improves *TIR* for all n evaluated, with an average of 56.7 tags identified per second. These result are in line with current physical RFID systems using commercial tags [30]. Buettner and Wetherall [30] evaluate a system for $n=8$ and $n=16$ using $BLF=40$kbps. Overall, TAFSA presents a 10% average improvement in *TIR* compared to ILCM-SbS, the protocol with the second highest *TIR*. Additionally, for all the protocols in the comparison, low variations of *TIR* with n are obtained, presenting a quasi-constant behavior for all the range of n evaluated. The strategies Chen14, SSA, and DSSA present a decreasing peak in *TIR* around $n = 1024$ and $n = 2048$, because they limit L to 1024 in both situations.

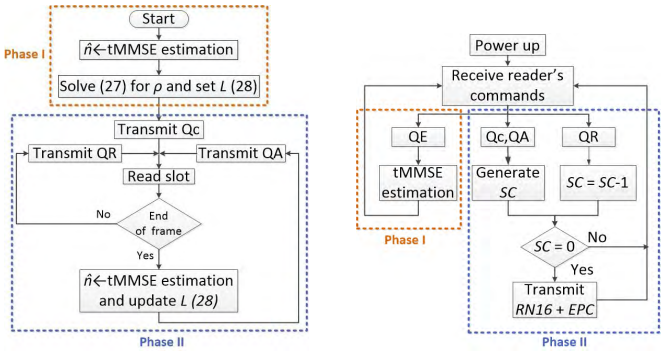

FIGURE 7. Flow diagram of TAFSA: (a) for reader, (b) for tags.

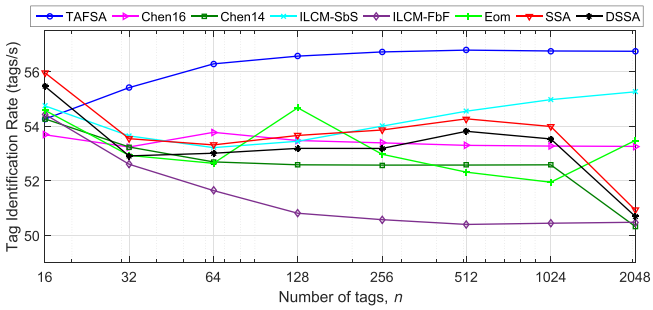

FIGURE 8. Comparison of *TIR* for all the presented strategies varying n from 16 to 2048.

The results shown in Fig. 8 correspond to a specific RFID system, with a particular set of timing parameters. Next, the protocols' performance is evaluated in terms of *TIR* under different RFID systems, with varying timing configuration. Assuming that each RFID system is characterized by a particular DR_r and DR_t, it is evaluated how the factor DR_r/DR_t affects the performance of all the protocols regarding *TIR*.

Firstly, *Tari*, which directly affects DR_r, is set to 25 μs while *BLF* is varied from 40 kbps to 640 kbps, according to the limits of EPC C1G2 [12]. Then, *BLF* is set to 40 kbps and *Tari* is varied from the minimum (6.25 μs) to the maximum (25 μs) value allowed by EPC C1G2. As a result, DR_r/DR_t varies from 0.2 to 3.2.

The values of T_1, T_2, and T_3 are also affected because they are set as a function of *Tari* and *BLF*. The resulting ρ value of TAFSA is also shown. Evaluated results are averaged for N and shown in Table 4.

Results show that TAFSA presents the highest *TIR* for all the range of DR_r/DR_t. Therefore, there is evidence that the TAFSA presents a timing-aware frame. Also, the smaller this ratio, the more notable the improvement in *TIR* of the proposed protocol in relation to the rest of the strategies.

When $DR_r/DR_t \leq 3.2$, the improvement in *TIR* of TAFSA becomes less significant in relation to the rest of the protocols. In this situation, *BLF* is fixed to 40kbps while *Tari* is decreased. Fixing *BLF* to its lowest allowed value has a negative impact over the total identification time, because TAFSA presents the highest number of bits per tag

TABLE 4. Study of the effect of DR_r/DR_t and ρ over *TIR*(*tags*/*s*), averaged for *N*, varying *Tari* and *BLF*. Quantities in bold represent the best results among the protocols in the comparison.

$Tari$ (μs)	25	25	25	25	25	25	25	16	11.43	8.89	7.27	6.25
BLF (kbps)	640	320	213.3	160	128	64	40	40	40	40	40	40
$1/\rho$	1.21	1.38	1.51	1.63	1.73	2.10	2.40	2.67	2.87	3.00	3.10	3.17
DR_r/DR_t	0.2	0.4	0.6	0.8	1	2	3.2	5	7	9	11	12.8
TAFSA	**404.38**	**277.69**	**211.91**	**171.94**	**144.65**	**80.90**	**52.95**	**54.42**	**55.20**	**55.73**	**56.10**	**56.32**
Chen16	395.10	271.82	206.86	167.30	140.36	77.78	50.66	51.88	52.57	52.95	53.09	53.31
Chen14	382.20	261.84	199.20	160.77	134.75	74.53	48.44	49.63	50.28	50.62	50.89	51.01
ILCM-SbS	387.74	269.64	206.95	167.75	141.18	78.63	51.39	52.72	53.50	53.85	54.20	54.30
ILCM-FbF	387.17	264.63	201.28	162.16	135.49	74.93	48.74	50.00	50.64	50.93	51.06	51.18
Eom	395.93	271.73	206.79	167.10	140.01	77.55	50.37	51.66	52.41	52.72	52.93	53.09
SSA	390.25	269.90	205.87	166.73	140.06	77.90	50.78	52.09	52.83	53.19	53.35	53.53
DSSA	391.40	269.96	205.71	166.60	139.79	77.64	50.54	51.77	52.51	52.87	53.16	53.25

(see Fig. 10.b). Thus, going back to Table 4, a decrease in BLF and DR_t makes more notable the impact of the bits per tag increase, slowing down the identification process.

Next, all the protocols are evaluated in terms of the normalized slots and the reader and tag bits, in order to provide a deeper insight of the *TIR* results.

A. NORMALIZED SLOTS

The metric *TIR* is tied to the number of slots employed and bits transmitted for the complete set identification. A new metric is presented in this section to fairly measure the total number of slots. This metric considers the different duration for each type of slot, since according to EPC C1G2, each type of slot has its own duration (5), (6), and (7). For this purpose, the three traditional slots (idle, single, collision) are normalized to the duration of the shortest one, that is, to T_i. Additionally, they are divided by the tag set size, providing information about the number of slots per tag. As a result, the normalized slots are presented next:

- Normalized idle slots per tag : $c_{iN} = \frac{c_{i_T}}{n}\frac{T_i}{T_i} = \frac{c_{i_T}}{n}$.
- Normalized single slots per tag: $c_{sN} = \frac{c_{s_T}}{n}\frac{T_s}{T_i}$.
- Normalized collision slots per tag: $c_{kN} = \frac{c_{k_T}}{n}\frac{T_k}{T_i}$.
- Total normalized slots per tag: $c_{tN} = c_{iN} + c_{sN} + c_{kN}$.

With these definitions, the algorithms presented in Section II.B are evaluated and the results are averaged for N. Simulation results are shown in Fig. 9.

The proposed protocol presents the highest c_{iN}, with around 4 normalized idle slots per tag. All protocols in the comparison update L with a power of 2 value close to n, except for TAFSA and Chen16. TAFSA updates L with (23), where ρ=0.3155, and Chen16 updates L with $L = y\hat{n}$, where y=1.2. Because TAFSA generates frames with a size around 3.2 times the estimated number of tags (scaled to a power of 2 value), it generates a higher number of slots than the alternative protocols, resulting in a higher number of idle slots. However, idle slots are the shortest of the three types, having a low impact over the total identification time. In particular, according to Table 3, an idle slot is around 27 times shorter than a collision slot. In relation to c_{kN}, the proposed protocol

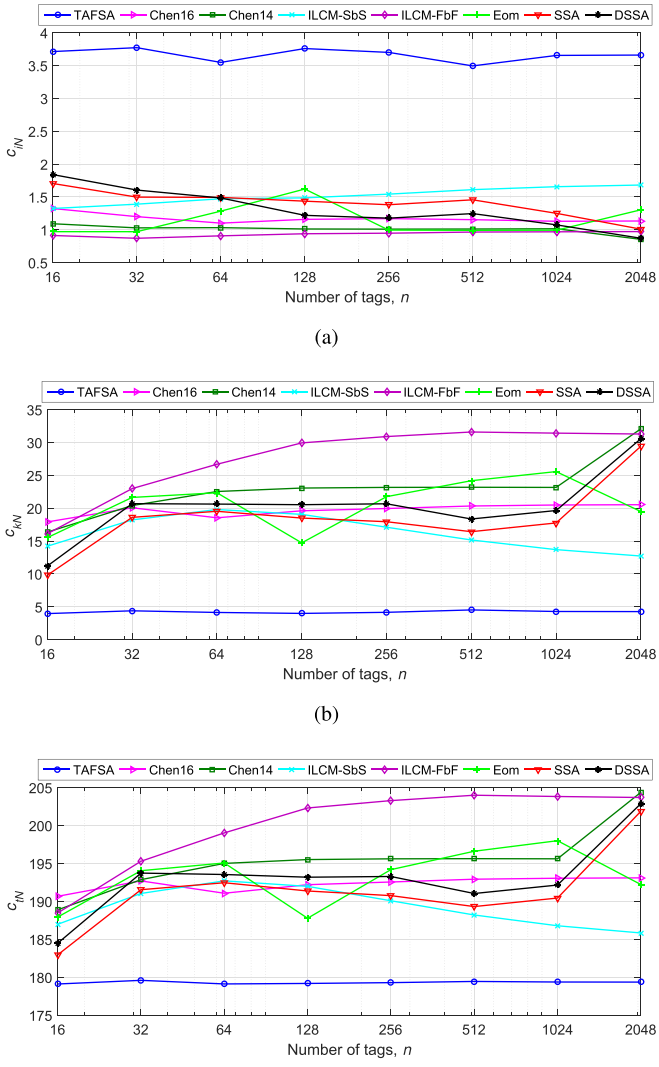

FIGURE 9. (a) normalized idle slots per tag c_{iN}, (b) normalized collision slots per tag c_{kN}, and (c) total normalized slots per tag c_{tN}, varying *n* from 16 to 2048.

achieves the lowest value of 5 slots. For all the protocols analyzed, c_{sN}=171.4 assuming c_{s_T}=n. Finally, TAFSA presents the lowest number of c_{tN}, because the reduction in c_{kN} is more

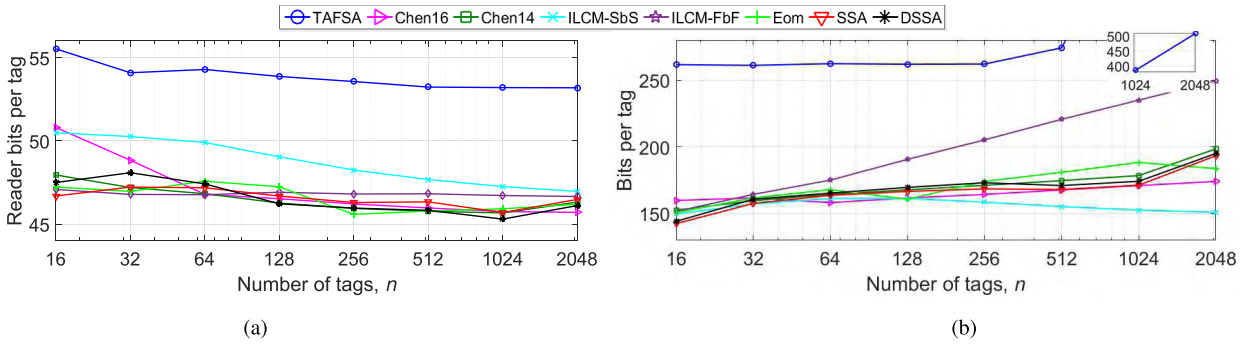

FIGURE 10. (a) reader bits per tag and (b) bits per tag to identify n tags, varying n from 16 to 2048.

notable than the increase in c_{iN}. On average, TAFSA requires 179 normalized total slots to identify one tag.

Recovering the results obtained in Fig. 8 and Table 4, it is noticed that the reduction in the total normalized slots of TAFSA results in a higher *TIR*. That is, the increase in the number of idle slots is compensated with a decrease in the number of collision slots.

B. READER AND TAGS TRANSMITTED BITS

In this section, the total number of reader transmitted bits per tag and the average number of bits transmitted by one tag are evaluated, because these metrics also influence *TIR*. Results are shown in Fig. 10.a and 10.b.

Regarding Fig. 10.a, TAFSA presents the highest number of total reader bits per tag because of the higher number of c_{iN} generated. The initial estimation with tMMSE hardly affects this metric.

Regarding Fig. 10.b, TAFSA presents a higher number of average bits per tag than the rest of the strategies. An increasing peak appears at n=512, because when $n>k$, additional frames are employed in the estimation. The initial tag estimation in phase I greatly affects the number of bits transmitted by one tag, since each tag must transmit k bits per frame. The estimation phase is inefficient in terms of bits. However, it does not have a noticeable negative impact over *TIR*, because the estimation process of TAFSA is a very short portion of the tag identification process.

Despite the higher values of the number of tag and reader bits of TAFSA, the proposed protocol achieves an improved performance in terms of *TIR*. This occurs because TAFSA greatly reduces the total number of collision slots by setting a timing-aware L, reducing the total reader and tags waiting periods. These waiting periods are represented by the link timing parameters T_1, T_2, and T_3, as defined in Section I. During these periods, the reader and the tags do not transmit any bit. The values used in this work are shown in Table 3. The total waiting time of a collision slot is defined by T_1+T_2=162.50μs, while the total waiting time of an idle slot is T_1+T_3=96.25μs. Therefore, the waiting time of a collision slot is about 1.7 times higher than that of an idle slot. Overall, it can be concluded that TAFSA results in time savings despite the higher number of reader and tag bits, because the waiting periods are reduced.

VI. PHYSICAL IMPLEMENTATION FEASIBILITIES

Commercial RFID readers employ the Slot Counter protocol (used in EPC C1G2), and they do not give the option to observe or modify the MAC or Physical (PHY) layer behavior. Therefore, it is not possible to physically implement the different existing anti-collision protocols with commercial readers. Several works in the literature present a real RFID system based on a Software-Defined-Radio (SDR) reader and commercial tags [30], [33], [34]. Because this reader is software-defined, different anti-collision protocols can be implemented by writing user-level software in C++.

As a conclusion, and considering that TAFSA is based on EPC C1G2, an SDR-RFID reader could use TAFSA to read commercial tags. In this context, the initial tag estimation of Phase I should be performed by simulation, because current commercial tags are not capable of interpreting and responding to the reader command QE. Although this implementation is out of the scope of this work, this section evaluates the performance of all the presented protocols in an scenario which is closer to a real RFID system.

For this purpose, the protocols are evaluated and compared under two common physical phenomena in RFID systems: capture effect and detection error. Capture effect is very common in passive RFID systems [35], and it occurs when the reader successfully resolves one tag reply in a collided slot. A different effect is the detection error [36], which means that a single tag response is detected as idle, due to fading or interference. As a result, re-transmissions are required in subsequent slots.

Next, the protocols evaluated in the previous section are evaluated in terms of the probability of capture effect P_c and the probability of a detection error P_d. Timing parameters are set according to Table 3. Simulation results are shown in Fig. 11. On the one hand, for a fixed P_d, *TIR* increases with increasing P_c for all the protocols in the comparative because fewer collided slots and more single slots occur. On the other hand, for a fixed P_c, *TIR* decreases with increasing P_d, because a higher number of total slots are required to complete one inventory round. In Fig. 11(a) and Fig. 11(b),

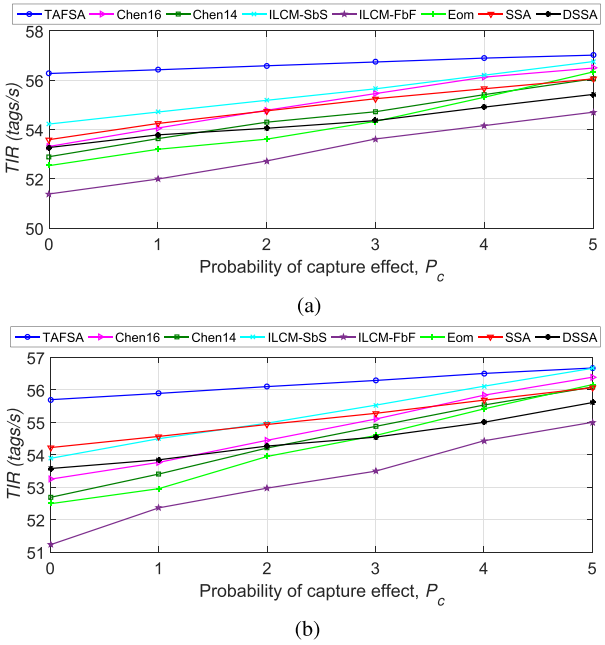

FIGURE 11. Evaluation of the capture effect over *TIR* for (a) P_d=0, (b) P_d=0.3. Results averaged for n from 16 to 2048.

the improvement in *TIR* of TAFSA in relation to rest of the protocols in the comparison becomes less significant with increasing P_c for the two P_d values evaluated, because it lowers the number of collision slots (see Fig. 9.b) which results in single slots due to the capture effect.

VII. CONCLUSION

A novel RFID anti-collision protocol based on the current standard EPCglobal Class-1 Generation-2 has been presented to increase the Tag Identification Rate (*TIR*). TAFSA presents a timing-aware frame, because its size is set according to the timing parameters of a real RFID system based on the current standard.

The metric *TIR* has been thoroughly studied, analyzing the main factor which affects it: the frame size L update strategy. From this study, it has been concluded that in order to increase *TIR*, L must be $1/\rho$ times the estimated number of tags, where ρ is set according to the timing parameters of the RFID system. Additionally, when selecting the tag estimator, it must be considered that *TIR* is unaffected for a variable range of the estimation error if L is restricted to power of 2 values. This means that the accuracy of the estimator can be relaxed in particular applications.

The proposed protocol was compared with several protocols of the state of the art in relation to *TIR*, and the number of normalized slots and transmitted bits. Considering a typical RFID scenario, simulation results showed that TAFSA, with 56.7 tags identified per second on average, achieves a 10 % average improvement in *TIR* in relation to the strategies of the comparison. Therefore, TAFSA is a suitable candidate where high *TIR* is sought in passive RFID.

REFERENCES

[1] L. Yang, Y. Chen, X. Y. Li, C. Xiao, M. Li, and Y. Liu, "Tagoram: Real-time tracking of mobile RFID tags to high precision using COTS devices," in *Proc. 20th Annu. Int. Conf. Mobile Comput. Netw.*, 2014, pp. 237–248.
[2] S. Pradhan, E. Chai, K. Sundaresan, L. Qiu, M. A. Khojastepour, and S. Rangarajan, "RIO: A pervasive RFID-based touch gesture interface," in *Proc. 23rd Annu. Int. Conf. Mobile Comput. Netw.*, 2017, pp. 261–274.
[3] F. Hessar and S. Roy, "Energy based performance evaluation of passive EPC Gen 2 Class 1 RFID systems," *IEEE Trans. Commun.*, vol. 61, no. 4, pp. 1337–1348, Apr. 2013.
[4] T. Agrawal, P. K. Biswas, and R. Sharma, "A novel-Q DFSA algorithm for passive RFID system," *Pervasive Mobile Comput.*, vol. 40, pp. 89–103, Sep. 2017.
[5] *RFID Forecasts, Players and Opportunities 2014–2024*, Cambridge, U.K., IDTechEx, May 2014.
[6] K. Finkenzeller, *RFID Handbook: Fundamentals and Applications in Contactless Smart Cards, Radio Frequency Identification and Near-Field Communication*. Hoboken, NJ, USA: Wiley, 2003.
[7] H. Landaluce, A. Perallos, E. Onieva, L. Arjona, and L. Bengtsson, "An energy and identification time decreasing procedure for memoryless RFID tag anticollision protocols," *IEEE Trans. Wireless Commun.*, vol. 15, no. 6, pp. 4234–4247, Jun. 2016.
[8] Y. Hou and Y. Zheng, "PHY assisted tree-based RFID identification," in *Proc. IEEE Conf. Comput. Commun.*, May 2017, pp. 1–9.
[9] Y. C. Lai, L.-Y. Hsiao, and B.-S. Lin, "Optimal slot assignment for binary tracking tree protocol in RFID tag identification," *IEEE/ACM Trans. Netw.*, vol. 23, no. 1, pp. 255–268, Feb. 2015.
[10] P. Šolić, J. Radić, and N. Rožić, "Energy efficient tag estimation method for ALOHA-based RFID systems," *IEEE Sensors J.*, vol. 14, no. 10, pp. 3637–3647, Oct. 2014.
[11] L. Barletta, F. Borgonovo, and M. Cesana, "0.469 PDFSA protocol for RFID arbitration," in *Proc. 19th Int. Conf. Softw., Telecommun. Comput. Netw.*, Sep. 2011, pp. 1–5.
[12] GS1 EPCglobal Inc., Brussels, Belgium. (Nov. 2013). *Radio-Frequency Identity Protocols Class-1 Generation-2 UHF RFID Protocol for Communications at 860 MHz–960 MHz, Version 2.0*. Accessed: Jun. 9, 2018 [Online]. Available: https://www.gs1.org/sites/default/files/docs/epc/Gen2_Protocol_Standard.pdf
[13] H. Wu, Y. Zeng, J. Feng, and Y. Gu, "Binary tree slotted ALOHA for passive RFID tag anticollision," *IEEE Trans. Parallel Distrib. Syst.*, vol. 24, no. 1, pp. 19–31, Jan. 2013.
[14] V. Pillai, H. Heinrich, D. Dieska, P. V. Nikitin, R. Martinez, and K. V. S. Rao, "An ultra-low-power long range battery/passive RFID tag for UHF and microwave bands with a current consumption of 700 nA at 1.5 V," *IEEE Trans. Circuits Syst. I, Reg. Papers*, vol. 54, no. 7, pp. 1500–1512, Jul. 2007.
[15] D. K. Klair, K.-W. Chin, and R. Raad, "A survey and tutorial of RFID anti-collision protocols," *IEEE Commun. Surveys Tuts.*, vol. 12, no. 3, pp. 400–421, 3rd Quart., 2010.
[16] S. Naderiparizi, A. N. Parks, Z. Kapetanovic, B. Ransford, and J. R. Smith, "WISPCam: A battery-free RFID camera," in *Proc. IEEE Int. Conf. RFID*, Apr. 2015, pp. 166–173.
[17] L. Arjona, H. Landaluce, A. Perallos, and E. Onieva, "Scalable RFID tag estimator with enhanced accuracy and low estimation time," *IEEE Signal Process. Lett.*, vol. 24, no. 7, pp. 982–986, Jul. 2017.
[18] C. Qian, H. Ngan, Y. Liu, and L. M. Ni, "Cardinality estimation for large-scale RFID systems," *IEEE Trans. Parallel Distrib. Syst.*, vol. 22, no. 9, pp. 1441–1454, Sep. 2011.
[19] S. Zhang, X. Liu, J. Wang, and J. Cao, "Tag size profiling in multiple reader RFID systems," in *Proc. IEEE Conf. Comput. Commun.*, May 2017, pp. 1–9.
[20] L. Arjona, H. Landaluce, A. Perallos, and E. Onieva, "Fast fuzzy anti-collision protocol for the RFID standard EPC Gen-2," *IET Electron. Lett.*, vol. 52, no. 8, pp. 663–665, 2016.
[21] J. B. Eom and T. J. Lee, "Accurate tag estimation for dynamic framed-slotted ALOHA in RFID systems," *IEEE Commun. Lett.*, vol. 14, no. 1, pp. 60–62, Jan. 2010.
[22] P. Šolić, J. Radić, and N. Rožić, "Early frame break policy for ALOHA-based RFID systems," *IEEE Trans. Autom. Sci. Eng.*, vol. 13, no. 2, pp. 876–881, Apr. 2015.
[23] W.-T. Chen, "A fast anticollision algorithm for the EPCglobal UHF Class-1 Generation-2 RFID standard," *IEEE Commun. Lett.*, vol. 18, no. 9, pp. 1519–1522, Sep. 2014.

[24] W.-T. Chen, "Optimal frame length analysis and an efficient anti-collision algorithm with early adjustment of frame length for RFID systems," *IEEE Trans. Veh. Technol.*, vol. 65, no. 5, pp. 3342–3348, May 2016.
[25] L. Duan, X. Zhang, Z. J. Wang, and F. Duan, "A feasible segment-by-segment ALOHA algorithm for RFID systems," *Wireless Pers. Commun.*, vol. 96, no. 2, pp. 2633–2649, Sep. 2017.
[26] Z. Zhou, B. Chen, and H. Yu, "Understanding RFID counting protocols," *IEEE/ACM Trans. Netw.*, vol. 24, no. 1, pp. 312–327, Feb. 2016.
[27] T. F. La Porta, G. Maselli, and C. Petrioli, "Anticollision protocols for single-reader RFID systems: Temporal analysis and optimization," *IEEE Trans. Mobile Comput.*, vol. 10, no. 2, pp. 267–279, Feb. 2011.
[28] H. Wu and Y. Zeng, "Bayesian tag estimate and optimal frame length for anti-collision ALOHA RFID system," *IEEE Trans. Autom. Sci. Eng.*, vol. 7, no. 4, pp. 963–969, Oct. 2010.
[29] H. Vogt, "Efficient object identification with passive RFID tags," in *Pervasive Computing* (Lecture Notes in Computer Science), vol. 2414, F. Mattern and M. Naghshineh, Eds. Berlin, Germany: Springer-Verlag, 2002, pp. 98–113. [Online]. Available: https://link.springer.com/chapter/10.1007%2F3-540-45866-2_9#citeas
[30] M. Buettner and D. Wetherall, "A software radio-based UHF RFID reader for PHY/MAC experimentation," in *Proc. IEEE Int. RFID Conf.*, Apr. 2011, pp. 134–141.
[31] G. Khandelwal, A. Yener, K. Lee, and S. Serbetli, "ASAP: A MAC protocol for dense and time constrained RFID systems," in *Proc. IEEE Int. Conf. Commun. (ICC)*, vol. 9, Jun. 2006, pp. 4028–4033.
[32] X. Liu *et al.*, "Multi-category RFID estimation," *IEEE/ACM Trans. Netw.*, vol. 25, no. 1, pp. 264–277, Feb. 2017.
[33] N. Kargas, F. Mavromatis, and A. Bletsas, "Fully-coherent reader with commodity SDR for Gen2 FM0 and computational RFID," *IEEE Wireless Commun. Lett.*, vol. 4, no. 6, pp. 617–620, Dec. 2015.
[34] P. Šolić, J. Maras, J. Radić, and Z. Blaževic, "Comparing theoretical and experimental results in Gen2 RFID throughput," *IEEE Trans. Autom. Sci. Eng.*, vol. 14, no. 1, pp. 349–357, Jan. 2017.
[35] H. Wu and Y. Zeng, "Passive RFID tag anticollision algorithm for capture effect," *IEEE Sensors J.*, vol. 15, no. 1, pp. 218–226, Jan. 2015.
[36] C. T. Nguyen, A. T. H. Bui, V.-D. Nguyen, and A. T. Pham, "Modified tree-based identification protocols for solving hidden-tag problem in RFID systems over fading channels," *IET Commun.*, vol. 11, no. 7, pp. 1132–1142, 2017.

LAURA ARJONA was born in Granada, Spain, in 1991. She received the B.S. degree in telecommunication engineering from the University of Granada, Granada, in 2014, and the M.S. degree in information and communication electronic systems from the National University of Distance Education, Madrid, Spain, in 2015. She is currently pursuing the Ph.D. degree with the DeustoTech Mobility Research Team, University of Deusto, Bilbao, Spain. In 2017, she visited the Sensor Systems Laboratory, Paul Allen Center for Computer Science and Engineering, University of Washington, where she was involved in research about SDR systems for passive sensors. She has authored several scientific articles, one national patent, one book chapter, and two intellectual properties. Her current research interests include RFID technology, anti-collision protocols, and wireless sensor networks. She was a recipient of the WRF Innovation Postdoctoral Fellowships in neuroengineering from the Institute of Neuroengineering, University of Washington, in 2018.

HUGO LANDALUCE received the M.Sc. degree in advanced electronics systems and the Ph.D. degree in informatics and telecommunications from the University of Deusto, Bilbao, Spain, in 2010 and 2014, respectively. He is currently a Post-Doctoral Researcher with the Mobility research Group, DeustoTech Institute of Technology. His main research interests include RFID technology, anti-collision protocols, and algorithm analysis and optimization.

ASIER PERALLOS received the B.Sc., M.Sc., and Ph.D. degrees in computer engineering from the University of Deusto. He has over 15 years of experience as a Lecturer with the Faculty of Engineering, University of Deusto. His teaching focuses on software design and distributed systems. He was an Associate Professor with the University of Deusto, where he currently serves as the Dean of the Faculty of Engineering. He is also a Principal Researcher of Deusto Smart Mobility with the Basque Government's Official Research Group that promotes the application of ICT to address smarter transport and mobility. In particular, his research background is focused on telematic systems, vehicular communication middleware, and intelligent transportation systems. Over a decade of experience in R&D Management, with tens of projects and technology transfer actions led.

ENRIQUE ONIEVA was born in Priego de Cordoba, Spain, in 1983. He received the B.E., M.E., and Ph.D. degrees in computer science with specialization in soft computing and intelligent systems from the University of Granada, Spain, in 2006, 2008, and 2011, respectively. From 2007 to 2012, he was with the AUTOPIA Program at the Centre for Automation and Robotics, Madrid. In 2012, he was with the Models of Decision and Optimization Group, University of Granada. Since 2013, he has been with the Mobility Unit, Deusto Institute of Technology (DeustoTech), where he carries out cutting-edge research in the application of soft computing techniques to the field of intelligent transportation systems. In addition, since 2015, he has been a Professor in artificial intelligence, machine learning, and big data with the University of Deusto. He has participated in over 20 research projects and authored over 90 scientific articles. His research interest is based on the application of soft computing techniques to intelligent transportation systems, including fuzzy-logic-based decision and control and evolutionary optimization.

APPENDIX

E

Paper V

Energy-aware RFID anti-collision Protocol

This paper has been published in the journal *"MDPI Sensors"* on June 2018. Its DOI is: 10.3390/s18061904. It is published as Open Access and can accessed online trough the MDPI Sensors journal website. The published version is appended here.

sensors

MDPI

Article

Energy-Aware RFID Anti-Collision Protocol

Laura Arjona *, Hugo Landaluce Simon and Asier Perallos Ruiz

Faculty of Engineering, University of Deusto and DeustoTech-Fundacion Deusto, Deusto Foundation, 48007 Bilbao, Spain; hlandaluce@deusto.es (H.L.S.); perallos@deusto.es (A.P.R.)

* Correspondence: laura.arjona@deusto.es

Received: 21 May 2018; Accepted: 7 June 2018; Published: 11 June 2018

Abstract: The growing interest in mobile devices is transforming wireless identification technologies. Mobile and battery-powered Radio Frequency Identification (RFID) readers, such as hand readers and smart phones, are are becoming increasingly attractive. These RFID readers require energy-efficient anti-collision protocols to minimize the tag collisions and to expand the reader's battery life. Furthermore, there is an increasing interest in RFID sensor networks with a growing number of RFID sensor tags. Thus, RFID application developers must be mindful of tag anti-collision protocols. Energy-efficient protocols involve a low reader energy consumption per tag. This work presents a thorough study of the reader energy consumption per tag and analyzes the main factor that affects this metric: the frame size update strategy. Using the conclusion of this analysis, the anti-collision protocol Energy-Aware Slotted Aloha (EASA) is presented to decrease the energy consumption per tag. The frame size update strategy of EASA is configured to minimize the energy consumption per tag. As a result, EASA presents an energy-aware frame. The performance of the proposed protocol is evaluated and compared with several state of the art Aloha-based anti-collision protocols based on the current RFID standard. Simulation results show that EASA, with an average of 15 mJ consumed per tag identified, achieves a 6% average improvement in the energy consumption per tag in relation to the strategies of the comparison.

Keywords: radio frequency identification; EPC-global standard; anti-collision; tag estimation; energy-aware

1. Introduction

Radio Frequency Identification (RFID) technology is becoming increasingly popular to the point where almost anything can be tagged. This is mainly because the cost of commercial RFID tags is negligible compared to the value of the products to which they are attached. Current examples of RFID expansion can be found in sensing, activity recognition and localization systems [1,2].

RFID technology uses a spectrum of radio frequency to transfer the identification information between two communication devices: reader and tags [3]. The coexistence of several tags provides RFID technology with a great flexibility at the expense of the tag collision problem. Tags share the same communication channel (the air) and may respond simultaneously to the same interrogation command, interfering and garbling their waveforms. The reader then is unable to interpret the information received from the tags, requiring a re-transmission and extending the tag identification time. Anti-collision protocols are then proposed to arbitrate tags' responses and to increase the number of tags identified by a time unit.

In the literature, three main types of anti-collision protocols have been reported: Aloha-based, tree-based and hybrid protocols. The three types of protocols can be applied to active (battery-operated tags), passive (tags backscatter information) or semi-passive (combination of active and passive) RFID systems. Tree-based protocols [4–6], in essence, split colliding tags into subsets and further split the subsets repeatedly up to the successful response of all the tags that are within the interrogation zone. Aloha-based

protocols [7] divide time into frames so that tags randomly choose one slot per frame to respond. While in Frame-Slotted Aloha (FSA), the frame size L is fixed during the identification process, in Dynamic Frame Slotted Aloha (DFSA), it is variable, and the protocol's performance is greatly influenced by the update of L. The fact that the standard EPC-global Class-1 Generation-2 (EPC C1G2) [8] currently uses a DFSA structure to arbitrate collisions highlights the research relevance of this scheme. For this reason, this work focuses on DFSA protocols. Finally, hybrid protocols combine the advantages of tree and Aloha protocols [9].

RFID systems, which have already been adopted in applications such as supply chains, are now considered a front-runner of the ubiquitous era with the emergence of mobile RFID [10]. Currently, mobile and battery-powered RFID readers, such as hand readers and smart phones, are increasingly being used [11,12]. Most popular applications focus on RFID-based indoor localization and identification systems with mobile readers [13–15]. Therefore, it is desired to expand the reader's battery life by using an energy-aware tag anti-collision protocol. This work presents the Energy-Aware Slotted Aloha (EASA) anti-collision protocol.

Defining n as the the total number of tags inside the reader interrogation zone and defining E as the total amount of energy consumed by the reader to identify the n tags, the metric E/n is defined as the energy per tag identified consumed by the reader, in one identification round. The ratio E/n provides information not only about the energy consumption of the RFID system using a particular anti-collision protocol, but it also provides information about the scalability of the system. Ideally, if the system is scalable to large population sizes, the ratio E/n should not vary considerably with increasing n, meaning that the reader energy consumption per tag is approximately constant and independent of n. In previous research, most energy saving protocols aim to reduce the energy cost of the reader and tags separately for active RFID systems [16–19]. They are not suitable for passive RFID systems. Other recent works focus on passive RFID systems, but they use tree-based anti-collision protocols [4,11,20].

The proposed protocol updates the frame size so that E/n is minimized. To do so, the frame size is set as a function of the estimated tag set size and the parameter ρ. The parameter ρ is defined as the ratio between the tag set size n and the frame size L, and its value is updated with the characteristics of the physical RFID system. The results of the performance evaluation show that the proposed protocol decreases E/n in relation to the strategies in the comparison. The following main contributions are made in this work:

1. Analytical study of the L that minimizes the E/n metric.
2. Presentation of a novel anti-collision protocol: EASA; the proposed protocol applies the results obtained in the previous contribution to decrease E/n in an RFID system based on EPC C1G2.
3. E/n evaluation of EASA and comparison with several anti-collision protocols of the state of the art.

The rest of the paper is organized as follows. Section 2 presents the RFID Standard EPC C1G2 and several related Aloha-based anti-collision protocols in the literature. Section 3 provides a thorough analysis of the main factor that affects E/n and obtains the value of L that minimizes it. The proposed EASA anti-collision protocol is presented in Section 4. Section 5 provides the results of the performance evaluation followed by the study of the physical identified limitations and future work in Section 6. Finally, Section 6 concludes this paper.

2. Background

Some definitions are provided to properly set the background of this work and to better understand the main contributions: Bulleted lists look like this:

- A command is a bit-string transmitted by the reader to the tags.
- An inventory round is the period of time that begins when the reader transmits the initial command (Qc), and it ends when the reader interrupts the identification process and the tags

loose their state. Ideally, an inventory round ends when all the tags in the reader interrogation zone have been identified.

- A slot is a period of time that separate tags' responses. Conventionally, three types of slots are considered attending to the tags' responses to the reader's commands: idle (none of the tags reply), single (only one tag replies) and collision (more than one tag replies in the same slot). The duration of each type of slot is referred as T_i, T_s and T_k, respectively. These slots are accurately specified in the current standard [8], and their duration is determined by the link timing parameters (T_1, T_2, T_3).
- A frame is a sequence of slots. Tags can respond in only one slot per frame. An identification process is composed of a set of frames.

The strategies analyzed in this work are based on the RFID transmission model between the reader and the tags defined in Figure 1, meeting EPC C1G2 requirements [8]. In this figure, three types of slots are represented: a single slot, with only one tag response (x), a collision slot, with three tags' simultaneous responses (xxx) and an idle slot, with no response. According to this figure, a single slot has a duration T_s, and this slot involves two reader commands and two tag's responses. A collision slot has a duration T_k, and it involves one reader command and one tags' response. Finally, an idle slot has a duration T_i, and it only involves one reader command. The parameter T_1 refers to the time needed for the tags to generate their responses after every reader command. The parameter T_2 refers to the time needed for the reader to receive all the tag transmissions. Finally, a slot will be considered idle when the reader waits for the tags' responses for a time T_3.

Now that the main concepts have been explained, the current standard in the RFID system is presented.

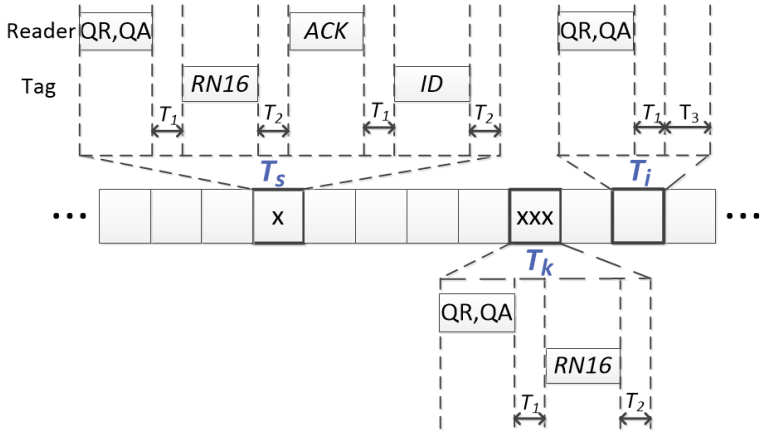

Figure 1. Link timing of EPC C1G2.

2.1. RFID Standard EPC C1G2

EPC C1G2 [8], the current standard in RFID systems, defines the requirements followed by the proposed protocol in this work. EPC C1G2 employs a DFSA protocol to arbitrate collisions, known as the Slot Counter protocol. The probability of collision is sensitive to the choice of L, which is dynamically updated by means of the parameter named Q ($L = 2^Q$). The optimum L setting depends on the unknown number of responding tags.

The slot counter protocol schedules tags' responses along time slots. In order to manage the identification process, the reader begins with transmitting Qc once and then alternates between the QueryAdjust(QA) and QueryRep(QR) commands. QA starts a new frame with the updated size and arranges that the tags randomly select a slot in the frame (the initial value of their internal slot counter SC), while QR tells the tags to decrement SC. Thus, when $SC = 0$, the tag transmits a 16-bit random number (RN16); and once it is acknowledged (ACK), the tag transmits its EPC code of length k.

2.2. Background of DFSA Anti-Collision Protocols

Currently, the EPC C1G2 standard is followed by most RFID manufacturers, enhancing the research relevance of DFSA-based protocols. Consequently, many DFSA protocols based on the standard have recently appeared with the main objective of improving a set of metrics regarding the process of tag identification. Several DFSA protocols can be found in the literature that update L using the tag set size estimated by the reader, referred to as $\hat{n}$.

Prior to presenting the most relevant single-reader strategies, a system model with one reader and n tags is defined. A DFSA frame of size L is defined. The variables c_s, c_k and c_i correspond to the number of single, collision and idle slots in the frame, respectively, and up to the current slot. Additionally, p_s, p_k and p_i correspond to the probability that only one tag, no tag or more than one tag occupies a slot, respectively. The examination slot refers to the particular slot within each frame where L is updated. Some of the most relevant DFSA-based protocols in the literature are introduced next.

2.2.1. Eom

Eom et al. [21] introduced a DFSA anti-collision protocol that updates L according to the estimated tag set size. The estimation algorithm is based on the number of collided tags per slot, referred to as γ. On the one hand, the protocol proposed by the authors in [21] shows a positive performance in terms of the estimation error and the total number of slots used for identification. On the other hand, the authors did not distinguish between the three types of slots to measure the total number of slots. Thus, the comparison with the rest of the protocols is unfair.

2.2.2. ILCM-FbF

The protocol Improved Linearized Combinational Model with Frame by Frame examination of L (ILCM-FbF) for the optimal frame size adaptation was introduced by Solic et al. in [7]. The authors presented a DFSA protocol based on the estimation of the tag population with a linear function that depends on c_k and L. Then, at the end of the frame, L is updated using the value of $\hat{n}$. The simulation scenario is limited, because the results are only compared with the slot counter protocol.

2.2.3. ILCM-SbS

The protocol Improved Linearized Combinational Model with Slot by Slot examination of L (ILCM-SbS) was presented by Solic et al. in [22] as an improved version of ILCM-FbF [7]. Simulation results showed that ILCM-SbS lowers the time required to identify a set of tags compared with some protocols of the state of the art. However, this strategy might overload a reader that has only a limited capacity, because L is calculated at every slot.

2.2.4. Chen14

Chen [23] presented an anti-collision protocol (Chen14) that examines L at just one slot per frame, determined as L/i, claiming to significantly reduce the number of total examination slots. The presented protocol updates L as a function of $\hat{n}$, and then, L is updated based on $\hat{n}$. Simulation results showed an improved performance in terms of normalized throughput, defined as $Throughput = c_s/(c_s + c_k + c_i)$. However, this metric assumes equal duration for each type of slot, and contrasting the EPC C1G2 requirements, these slots have different durations.

2.2.5. Chen16

Chen proposed in [24] an anti-collision algorithm (Chen16) based on the early and optimal adjustment of the frame length with the aim of maximizing the normalized throughput (U), defined as $U = (c_s T_s)/(c_s T_s + c_i T_i + c_k T_k)$. This protocol was presented as an extension of the study in [23]. In this Chen16 protocol, the tag set size is estimated in every frame at the examination point $L/5$. The value of this slot has been selected as the slot where maximum U is obtained. Based on the

previous $\hat{n}$, if a new frame is required, the author updates L with the variable y, where y is expressed as a second-order polynomial.

Simulation results show competitive values regarding U, but the function defined to set y is not valid for all the range of T_k/T_i. Particularly, if $T_k >> T_i$, y takes negative values, leading to negative values for L. Additionally, the examination point $L/5$ has been set based on a particular scenario with specific timing parameters. Therefore, this value might not be appropriate for a scenario with different timing settings of the RFID system.

2.2.6. SSA and DSSA

The Segment-by-Segment Aloha protocol (SSA) was proposed in [25] to effectively decrease the frame adjustment times with satisfactory throughput. In this protocol, one frame is composed of a set of slot-segments, and each slot-segment is composed of s_L continuous time slots, where $s_L = 4$. In order to increase the throughput of SSA, the authors introduced the Dynamic SSA (DSSA) protocol. DSSA varies s_L dynamically by tracking, in real time, the number of single slots. Both protocols present a positive performance regarding the throughput and the number of tags identified per second. However, the authors assume a simulation scenario where the protocols are compared with just one additional protocol, and for one specific scenario, with a particular set of timing configuration.

3. Energy-Aware Aloha Frame Analysis

Traditionally, the most common metric to evaluate the performance of an RFID anti-collision protocol has been the Slot Efficiency (SE) [26], defined as $SE = c_s/(c_i + c_s + c_k)$. Ideally, an anti-collision protocol is desired to reach $SE = 1$, meaning that just one slot per tag is required for the complete tag set identification. However, this is not achievable in practical applications, where collision and idle slots are present. An anti-collision protocol reaches the maximum SE when the frame size equals the number of tags, that is $L = n$ [26]. However, this condition only applies when $T_i = T_s = T_k$. The EPC C1G2 standard specifies different durations for idle, single and collision slots, referred to as T_i, T_s and T_k. Therefore, traditional SE is not a meaningful parameter to measure the performance of an RFID system. To mitigate the different slots' duration effect, the metric $Time\_SE$ is introduced in [27] $Time\_SE = c_s/[c_{total} + (\beta - 1)c_i]$, where $c_{total} = c_i + c_s + c_k$ and $\beta = T_i/T_k$. This metric considers different durations for T_k and T_i, but it assumes $T_s = T_k$ and does not include the time overhead information.

In order to provide an accurate evaluation of an RFID system, this work focuses on the metric E/n, defined as the energy per tag identified consumed by the reader in one inventory round. This metric considers different durations for T_i, T_s and T_k.

The energy consumed by the reader during the identification of a whole set of tags, defined as E, is modeled in [4]. The authors present an energy consumption model where E depends on the power required by the reader to transmit and receive information to and from the tags. During the identification process, the reader transmits a set of commands and a Continuous Wave (CW) to power up passive tags, with power P_{t_x}. To receive the data from the tags, the reader needs an extra power P_{r_x}. Defining E_t/n and E_r/n as the energy per tag identified consumed by the reader during the transmitting and receiving states in one inventory round, one obtains:

$$\frac{E}{n} = \frac{E_t}{n} + \frac{E_r}{n} \tag{1}$$

where:

$$E_t = P_{t_x}(c_s T_s + c_k T_k + c_i T_i) \tag{2}$$

and:

$$E_r = P_{r_x}\ [c_s(T_{RN16} + T_{EPC}) + c_k T_{RN16}] \tag{3}$$

The durations of the slots, T_i, T_s and T_k, are set according to the standard:

$$T_i = T_1 + T_3 + T_{command}, \tag{4}$$

$$T_s = 2T_1 + T_{RN16} + 2T_2 + T_{ACK} + T_{EPC} + T_{command}, \tag{5}$$

and:

$$T_k = T_1 + T_{RN16} + T_2 + T_{command} \tag{6}$$

where $T_{command}$ refers to the duration of the reader transmitted command Qc, QA or QR, referred to as T_{Qc}, T_{QA} and T_{QR}, respectively. In every frame, the reader will transmit just one QA or Qc in the first slot, and in the rest of slots, it will transmit QR commands. Assuming a frame with sufficiently large L, $T_{command} = T_{QR}$ is applied in (4)–(6) when one frame is analyzed.

The parameters T_{Qc}, T_{QA} and T_{QR} are calculated as the reader-to-tag synchronization time $T_{FSync_{RT}}$ or $T_{Preamble_{RT}}$, defined in [8] plus the length of each parameter divided by the reader data rate DR_r, calculated as $DR_r = 1/((T_{data_0} + T_{data_1})/2)$, where T_{data_0} = *Tari* and $T_{data_1} = 1.5{\cdot}Tari$. *Tari* represents the reference time interval for a *data*-0 transmission. Thus, $T_{Qc} = T_{FSync_{RT}} + 22\,\text{bits}/DR_r$, $T_{QA} = T_{Preamble_{RT}} + 9\,\text{bits}/DR_r$ and $T_{QR} = T_{Preamble_{RT}} + 4\,\text{bits}/DR_r$

The parameter T_{RN16} and T_{EPC} refer to the time the tag employs to transmit RN16 and its *EPC*, respectively. They are calculated as the tag-to-reader synchronization time $T_{Preamble_{TR}}$ plus the length of each parameter divided by the tag data rate DR_t, calculated as $DR_t = BLF/M$. The parameter BLF refers to the backscatter-link frequency. Thus, $T_{RN16} = T_{Preamble_{TR}} + 17\,\text{bits}/DR_t$ and $T_{EPC} = T_{Preamble_{TR}} + 129\,\text{bits}/DR_t$. Finally, T_{ACK} corresponds to the duration of the reader command ACK, and it is obtained as $T_{ACK} = T_{Preamble_{RT}} + 18\,\text{bits}/DR_r$. Table 1 summarizes the calculation of the reader and tag messages' durations.

Table 1. Main EPC C1G2 timing parameters' calculation.

Parameter	Description	Calculation
T_{data_0}	Duration of a reader data-0	$Tari$
T_{data_1}	Duration of a reader data-1	$1.5{\cdot}Tari$
$T_{Preamble_{RT}}$	Duration of R-T Preamble	$T_{del} + T_{data_0} + RTcal + TRcal$
$T_{FSync_{RT}}$	Duration of Frame Sync.	$T_{del} + T_{data_0} + RTcal$
$T_{Preamble_{TR}}$	Duration of T-R	$7/DRt$
DRr	Reader data rate	$1/((T_{data_0} + T_{data_1})/2)$
DRt	Tag data rate	BLF/M
T_{Q_c}	Duration of a Qc	$T_{FSync_{RT}} + 22/DR_r$
T_{QA}	Duration of a QA	$T_{Preamble_{RT}} + 9/DR_r$
T_{QR}	Duration of a QR	$T_{Preamble_{RT}} + 4/DR_r$
T_{ACK}	Duration of a ACK	$T_{FSync_{RT}} + 24/DR_r$
T_{RN16}	Duration of tag $RN16$	$23/DRt$
T_{EPC}	Duration of tag EPC	$135/DRt$

In the next section, the energy per tag identified consumed by the reader in one frame is analyzed, and the optimal L is derived to minimize the reader energy consumption in an RFID identification process.

Frame Size Calculation to Minimize the Reader Energy Consumption

Defining $E(n,L)/c_s(n,L)$ as the energy per tag identified consumed by the reader in one frame, one obtains:

$$\frac{E(n,L)}{c_s(n,L)} = \frac{E_t(n,L)}{c_s(n,L)} + \frac{E_r(n,L)}{c_s(n,L)} \tag{7}$$

where:

$$\frac{E_t(n,L)}{c_s(n,L)} = \frac{P_{t_x}\ [(c_s(n,L)T_s + c_k(n,L)T_k + c_i(n,L)T_i)]}{c_s(n,L)} \tag{8}$$

and:

$$\frac{E_r(n,L)}{c_s(n,L)} = \frac{P_{r_x}\ [c_s(n,L)(T_{RN16} + T_{EPC}) + c_k(n,L)T_{RN16}]}{c_s(n,L)} \tag{9}$$

where $c_s(n,L)$, $c_k(n,L)$ and $c_i(n,L)$ represent the expected value of the number of single, collision and idle slots in a frame, respectively. From (8) and (9), it follows that $E(n,L)/c_s(n,L)$ is mainly influenced by the number of each type of slot and their duration. On the one hand, T_i, T_s and T_k are fixed for a particular RFID system, and they remain constant for one frame. On the other hand, $c_i(n,L)$, $c_s(n,L)$ and $c_k(n,L)$ strictly depend on the anti-collision protocol employed to identify the tag set and, particularly, on the strategy it uses to update L.

In order to perform the analysis that derives the optimal L to minimize $E(n,L)/c_s(n,L)$, a system model with one reader and n tags is defined. The probability that b tags among n occupy a slot within a frame of size L can be approximated by a binomial distribution $P_b(n,L)$ [28]:

$$P_b(n,L) = \binom{n}{b}\left(\frac{1}{L}\right)^b\left(1-\frac{1}{L}\right)^{n-b}. \tag{10}$$

If L is assumed sufficiently large, the tags distribution can be approximated by a Poisson distribution with mean ρ.

$$\rho = \frac{n}{L}. \tag{11}$$

When $b = 0$ in (10), $c_i(n,L)$ can be approximated by:

$$c_i(n,L) = Lp_i(n,L) = L\left(1-\frac{1}{L}\right)^n \approx Le^{-\rho}. \tag{12}$$

When $b = 1$ in (10), $c_s(n,L)$ can be approximated by:

$$c_s(n,L) = Lp_s(n,L) = n\left(1-\frac{1}{L}\right)^{n-1} \approx L\rho\left(\frac{n/\rho}{n/\rho-1}\right)e^{-\rho}. \tag{13}$$

Then, $c_k(n,L)$ can be approximated by:

$$c_k(n,L) = L\cdot p_k(n,L) = L(1-p_0-p_1). \tag{14}$$

Substituting (12)–(14) into (8) and (9) and applying $\frac{n/\rho}{n/\rho-1} \approx 1$, the following expressions are obtained:

$$\frac{E_t(n,L)}{c_s} \approx \frac{P_{t_x}[T_s\rho e^{-\rho} + T_i e^{-\rho} + T_k(1-(1+\rho)e^{-\rho})]}{\rho e^{-\rho}} \tag{15}$$

and:

$$\frac{E_r(n,L)}{c_s} \approx P_{r_x}\frac{T_{RN16}\ \rho e^{-\rho} - T_{EPC}\ e^{-\rho} + T_{EPC}}{\rho e^{-\rho}}. \tag{16}$$

Next, computing the derivative of $E(n,L)/c_s(n,L)$ in (7) with respect to ρ yields:

$$\frac{d}{d\rho}\frac{E(n,L)}{c_s(n,L)} = \frac{d}{d\rho}\frac{E_t(n,L)}{c_s(n,L)} + \frac{d}{d\rho}\frac{E_r(n,L)}{c_s(n,L)} = P_{t_x}\frac{T_k[e^\rho(\rho-1)+1]-T_i}{\rho^2} + P_{r_X}\frac{T_{RN16}\ e^\rho(\rho-1)+T_{EPC}}{\rho^2} \tag{17}$$

and posing $\frac{d}{d\rho}\frac{E(n,L)}{c_s(n,L)} = 0$ yields the following equation:

$$\rho e^\rho - e^\rho + 1 = \frac{P_{r_x}T_i}{P_{t_x}T_k + P_{r_x}T_{EPC}}. \tag{18}$$

Solving (18), the value of ρ that minimizes $E(n,L)/c_s(\rho)$ is obtained:

$$\rho = 1 + W\left[\frac{P_{t_x}(T_i - T_k) - P_{r_x}T_{EPC}}{e(P_{t_x}T_k + P_{r_x}T_{EPC})}\right] \tag{19}$$

where $W(x)$ represents the Lambert W-function.

Then, according to (11), the frame size that minimizes $E(n,L)/c_s(n,L)$ is obtained as $L = n/\rho$. Following the EPC C1G2 constraints, the L value must be a power of two. Thus, $Q = round(log_2(n/\rho))$ and:

$$L = 2^{round[log_2(n/\rho)]}. \tag{20}$$

4. RFID Anti-Collision Protocol Energy-Aware Slotted Aloha

In this section, the analysis of the energy-aware Aloha frame presented in Section 3 is applied to a DFSA anti-collision protocol, resulting in the Energy-Aware Slotted Aloha (EASA) protocol. EASA is based on EPC C1G2, regarding the reader and the tag operation. The pseudocode of EASA is presented in Algorithm 1. First the operation of the reader is presented, then the operation of the tag. The variable *slot_index* represents the reader's internal counter, which keeps track of the present slot in the current frame.

Algorithm 1 Pseudocode of EASA. First, the operation of the reader is presented, then the operation of the tag.

Reader Operation

```
Initialization: slot_index = 1, L = 2^Q
calculate ρ by solving (19)
broadcast Qc
while 1 do
    read slot and update c_i, c_s, c_k
    if slot_index = L then
        n̂ = MMSE(c_i, c_s, c_k)
        Q = log2[(n̂ − c_s)/ρ], L = 2^round(Q)
        broadcast QA
    else
        slot_index = slot_index +1
        broadcast QR
    end if
end while
```

Tag Operation

```
while energized by the reader do
    receive reader's commands
    if QA or Qc then
        Generate SC∈[0, L − 1]
    else
        if QR then
            SC = SC − 1
        end if
    end if
    if SC = 0 then
        transmit RN16
        if ACK then
            transmit EPC
        end if
    end if
end while
```

First, the reader sets the value of ρ by solving (19). The value of ρ is obtained just once at the beginning of the inventory round, according to the RFID system parameters P_{t_x}, P_{r_x}, T_i, T_k and T_{EPC}.

These parameters define the particular RFID system used. Then, the initial L to begin the identification process is obtained with (20), and the reader starts the identification procedure by broadcasting Qc, specifying the initial Q value of the tags. Each tag selects a slot in the frame to transmit its EPC. The reader continues the identification process analyzing each slot of the frame, updating the variables c_i, c_s and c_k according to the tags' responses:

- Only one tag response is detected: $c_s = c_s + 1$.
- Two ore more tags response are detected: $c_k = c_k + 1$.
- No tag response is detected: $c_i = c_i + 1$.

Then, the reader broadcasts QR to go from one slot to the next. When the reader reaches the last slot of the frame, the remaining tag population size is estimated with a traditional Mean Minimum Square Error (MMSE) estimator [28]:

$$\hat{n} = \min_n \left\| \begin{pmatrix} c_i(n,L) \\ c_s(n,L) \\ c_k(n,L) \end{pmatrix} - \begin{pmatrix} c_i \\ c_s \\ c_k \end{pmatrix} \right\|^2 = \min_n \left\{ [c_i(n,L) - c_i]^2 + [c_s(n,L) - c_s]^2 + [c_k(n,L) - c_k]^2 \right\}. \quad (21)$$

This estimator compares the expected value of the number of idle, single and collision slots at the end of the frame ($c_i(n,L)$, $c_s(n,L)$ and $c_k(n,L)$, obtained with (12), (13) and (14)), with the observed numbers (c_i, c_s and c_k). Then, $\hat{n}$ is obtained as the value of n, which minimizes the mean square error of the expected and observed values. Finally, the frame size is updated with (20), and a new frame is started by broadcasting QA, specifying the new L. The tag operation follows the EPC C1G2 standard behavior (see Section 2.1). Therefore, EASA is compatible with commercial RFID tags.

EASA presents an energy-aware frame, because this protocol sets the frame size according to ρ and $\hat{n}$ so that E/n is minimized. Besides, if the timing parameters of the RFID system vary, EASA adapts to these changes, obtaining a new solution for ρ and updating L accordingly. Furthermore, EASA can be physically implemented in a real system and commercial tags, because EASA is based on EPC C1G2.

5. Energy Evaluation

This section evaluates the performance of EASA regarding the energy per tag identified consumed by the reader in one inventory round E/n and compares it with the anti-collision protocols of the state of the art presented in Section 2.2: Eom [21], ILCM-FbF [7], ILCM-SbS [22], Chen14 [23], Chen16 [24], SSA [25] and DSSA [25]. Physical-layer effects are not considered here, assuming a non-impaired channel and no capture effect. Note that these assumptions are extensively used for the analysis of known anti-collision protocols whose analysis focuses on the media access control layer [4,21,24,25]. Simulation results were obtained with MATLAB R2017b. A scenario with one reader and a varying number of tags is evaluated, where the tags are uniformly distributed. The simulation responses have been averaged over 1000 iterations for accuracy in the results. Timing parameters are set according to Table 2. Before proceeding with the performance evaluation, some implementation details must be taken into consideration:

- To evaluate the anti-collision protocols' performance with n, the tag set sizes considered are $N = [16, 32, 64, 128, 256, 512, 1024, 2048]$ and $n \in N$.
- L values are limited to a power of two, following the EPC C1G2 specifications.
- The initial L is set to 16 ($Q = 4$), following the EPC C1G2 recommendation.
- The length of the $EPC$is set to $k = 128$.

Table 2. Simulation parameters according to EPC C1G2 [8].

Parameter	Value	Parameter	Value
$Tari$	6.25 µs	BLF	40 kbps
$T_{Preamble_{RT}}$	234.38 µs	T_1	87.5 µs
$T_{Preamble_{TR}}$	700.00 µs	T_2	75 µs
$T_{FSync_{RT}}$	34.38 µs	T_3	8.75 µs
DR_r	128 kbps	DR_t	10 kbps
T_{QA}	104.69 µs	T_{QR}	65.63 µs
T_{Qc}	406.25 µs	T_{QE}	65.63 µs

Figure 2 shows that EASA clearly improves E/n for all n evaluated, with an average of 15 mJ consumed by the reader per tag identified. Overall, EASA presents a 6% average reduction in E/n compared to ILCM-SbS, the protocol with the second lowest E/n. Additionally, for all the protocols in the comparison, low variations of E/n with n are obtained, presenting a quasi-constant behavior for all the range of n evaluated. The strategies Chen14, SSA and DSSA present an increasing peak in E/n around n = 1024 and n = 2048, because they limit L to 1024 in both situations. From this figure, it can be concluded that the solution of ρ obtained for one frame results in the lowest energy consumed by the reader in one inventory round.

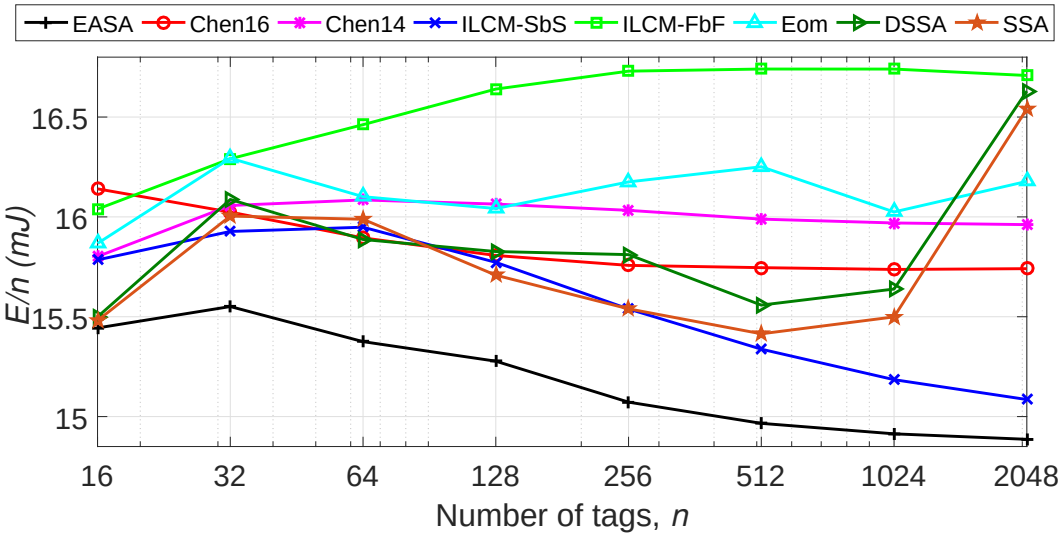

Figure 2. Evaluation of the energy consumption per tag in one inventory round, varying n from 16–2048, with P_{t_x} = 825 mW and P_{r_x} = 125 mW. EASA, Energy-Aware Slotted Aloha; ILCM-SbS, Improved Linearized Combinational Model with Slot by Slot; FbF, Frame by Frame; DSSA, Dynamic Segment-by-Segment Aloha.

Next, all the algorithms presented in Section 2.2 are evaluated in terms of the number of slots and the reader and tag bits, in order to provide a deeper insight into the E/n results. Results are averaged for N.

Figure 3 shows the evaluation results of the number of slots. The proposed protocol presents the highest c_i, with around 3–7 idle slots per tag, while the alternative protocols show around 1–2 idle slots per tag. All protocols in the comparison update L with a power of two value close to n, except for EASA and Chen16. EASA updates L with (20), where $\rho = 4.13$, and Chen16 updates L with $L = y\hat{n}$, where $y = 1.2$. Because EASA generates frames with a size around 4.13-times the estimated number of tags (scaled to a power of two value), it generates a higher number of slots than the alternative protocols, resulting in a higher number of idle slots. However, idle slots are the shortest of the three types, having a low impact on the total identification time. In particular, according to Table 2, an idle

slot is around 27-times shorter than a collision slot. In relation to c_k, the proposed protocol achieves the lowest value of 0.1–0.4 collision slots per tag.

Recovering the results obtained in Figure 2, it is noticed that the reduction in the number of collision slots per tag of EASA results in a lower E/n. That is, the increase in the number of idle slots is compensated with a decrease in the number of collision slots.

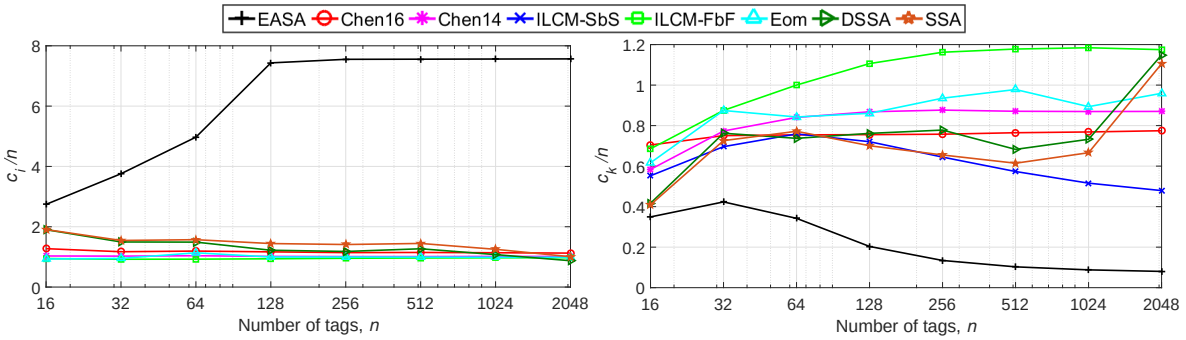

(**a**) (**b**)

Figure 3. (**a**) Total number of idle slots per tag c_i/n and (**b**) total number of collision slots per tag c_k/n, varying n from 16–2048.

Next, the total number of reader transmitted bits per tag and the average number of bits transmitted by one tag are evaluated, because these metrics also influence E/n. Results are shown in Figure 4a,b.

Regarding Figure 4a, EASA presents the highest number of total reader bits per tag because of the higher number of c_i/n generated. Despite the higher values of the number of reader bits of EASA, the proposed protocol achieves an improved performance in terms of E/n. This occurs because EASA greatly reduces the total number of collision slots, reducing the total reader and tag waiting periods. These waiting periods are represented by the link timing parameters T_1, T_2 and T_3, as defined in Section 2. During these periods, the reader and the tags do not transmit any bit, but the reader consumes energy from its battery by transmitting the *CW*. Using the values of Table 2, the total waiting time of a collision slot is defined by $T_1 + T_2 = 162.50$ µs, while the total waiting time of an idle slot is $T_1 + T_3 = 96.25$ µs. Therefore, the waiting time of a collision slot is about 1.7-times higher than that of an idle slot. Overall, it can be concluded that EASA results in energy savings despite the higher number of reader bits per tag, because it highly reduces the number of collision slots and the waiting time periods.

Regarding Figure 4b, EASA presents the lowest number of bits per tag compared the rest of the strategies, with an average of 146 bits. Because EASA generates fewer c_k/n (see Figure 3b), tags suffer fewer collisions, and therefore, they transmit fewer bits.

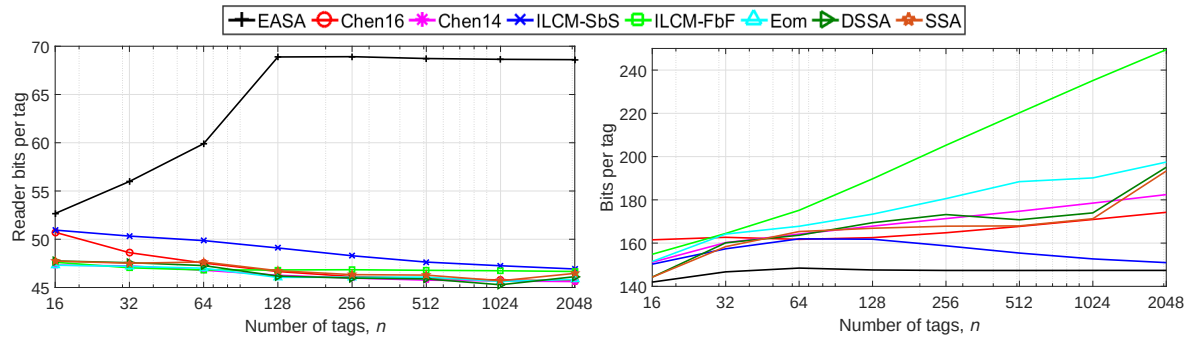

(**a**) (**b**)

Figure 4. (**a**) Reader bits per tag and (**b**) bits per tag to identify n tags, varying n from 16–2048.

5.1. Effect of P_{t_x} and P_{r_x} on E/n

Next, the total energy consumption for n tags' identification is evaluated when P_{t_x} and P_{r_x} are varied for two different tag set sizes (n = 64 and 1024). Firstly, E/n is evaluated when P_{r_x} is fixed to 125 mW, and P_{t_x} takes two values, 125 and 825 mW. Next, E/n is evaluated when P_{t_x} is fixed to 825 mW, and P_{r_x} takes the values 25 and 800 mW. These values of P_{t_x} and P_{r_x} have been selected considering that a typical commercial RFID reader, by regulation, provides a maximum output power of 1 W. The rest of the parameters are set according to Table 2. Simulation results are shown in Table 3. When P_{r_x} is set to 125 mW, all the protocols in the comparison show a similar behavior, presenting an increasing E/n with increasing n and increasing P_{t_x}. When P_{t_x} is set to 825 mW, E/n increases with increasing n, but it hardly varies for the two P_{r_x} values analyzed. In conclusion, for all the protocols analyzed, the reader transmitting power P_{t_x} greatly affects the energy per tag identified consumed by the reader in one inventory round, and the higher P_{t_x} for a particular P_{r_x}, the higher E/n. Furthermore, it can be seen that the protocols with the lowest number of slots (see Figure 3) and bits per tag (see Figure 4) present the lowest energy consumption (see Figure 2). Therefore, these two parameters are key regarding the energy efficiency of an anti-collision protocol.

EASA presents the lowest E/n for all the combinations of P_{t_x} and P_{r_x} evaluated. This occurs because the value of ρ is calculated as a function of these parameters (see (19)). Therefore, EASA presents an energy-aware behavior, because this protocol adapts to different values of P_{t_x} and P_{r_x}, lowering the overall E/n in relation to the alternative protocols.

Table 3. Energy consumption per tag E/n (mJ) evaluation varying P_{t_x} and P_{r_x} for $n = 64$ and $n = 1024$. Each combination of P_{t_x} and P_{r_x} results in a different ρ value for EASA. Quantities in bold represent the best results among the strategies in the comparison.

	P_{r_x} = 125 mW				P_{r_x} = 25 mW		P_{r_x} = 800 mW	
	P_{t_x} = 125 mW		P_{t_x} = 825 mW		P_{t_x} = 825 mW			
1/ρ	**7.41**		**4.13**		**3.39**		**7.32**	
Protocol	***n* = 64**	***n* = 1024**	***n* = 64**	***n* = 1024**	***n* = 64**	***n* = 1024**	***n* = 64**	***n* = 1024**
EASA	**2.63**	**2.44**	**15.32**	**14.91**	**15.10**	**238.04**	**17.20**	**257.10**
Chen16	2.76	2.60	15.86	15.73	15.56	248.63	18.12	273.58
Chen14	2.81	2.66	16.10	15.98	15.75	279.68	18.51	279.68
ILCM-SbS	2.77	**2.44**	15.84	15.19	15.60	240.69	18.17	257.88
ILCM-FbF	2.92	2.85	16.46	16.74	16.10	262.95	19.09	300.00
Eom	2.83	2.67	16.19	16.03	15.80	252.84	18.52	281.47
DSSA	2.77	2.57	16.00	15.64	15.66	247.32	18.16	271.18
SSA	2.76	2.53	15.88	15.50	15.63	245.10	18.12	266.85

5.2. Effect of Tari and BLF on E/n

The results shown in Figure 2 correspond to a specific RFID system, with a particular set of timing parameters, defined in Table 2. This work assumes that the two key parameters that define an RFID system are *Tari* and *BLF*, because most of the configuration parameters are obtained as a function of these two. Next, the protocols' performance is evaluated in terms of E/n for different RFID systems with varying *Tari* and *BLF*. The two parameters are varied from the whole range of values allowed by EPC C1G2 [8]. The values of P_{t_x} and P_{r_x} used are set according to Table 2.

The different values of *Tari* and *BLF* greatly affect the performance of EASA, because they result in different values of ρ to update the frame size L. As was shown in Section 3, the value of ρ is obtained as a function of T_i, T_k and T_{EPC} (see (19), which ultimately depends on *Tari* and *BLF*. Therefore, the value of ρ also depends on *Tari* and *BLF*

Firstly, *Tari* is set to 25 µs, while *BLF* is varied from 40–640 kbps. Then, *BLF* is set to 40 kbps, and *Tari* is varied from the minimum (6.25 µs) to the maximum (25 µs) value allowed by EPC C1G2.

As a result, $1/\rho$ varies from 1.36–4.13. The values of T_1, T_2 and T_3 are also affected because they are set as a function of *Tari* and *BLF*. The evaluated results are averaged for N and shown in Table 4.

Table 4. Study of the effect of *Tari* and *BLF* on E/n (mJ). Results are averaged for N. *Tari* and *BLF* are varied from the maximum to the minimum values allowed by EPC C1G, resulting in different ρ values for EASA. P_{t_x} and P_{r_x} are set to 825 mW and 125 mW, respectively. Quantities in bold represent the best results among the protocols in the comparison.

***Tari* (μs)**	25	**25**	**25**	**25**	**25**	**25**	**16**	**11.43**	**8.89**	**7.27**	**6.25**
***BLF* (kbps)**	**640**	**320**	**213.3**	**160**	**64**	**40**	**40**	**40**	**40**	**40**	**40**
$1/\rho$	**1.36**	**1.61**	**1.81**	**1.98**	**2.66**	**3.07**	**3.44**	**3.71**	**3.90**	**4.03**	**4.13**
EASA	2.13	3.10	4.12	5.04	**10.53**	**16.40**	**15.87**	**15.56**	**15.37**	**15.24**	**15.17**
Chen16	2.12	**3.09**	**4.06**	**5.03**	10.85	16.67	16.28	16.07	15.94	15.88	15.84
Chen14	**2.06**	3.10	4.07	5.05	10.93	16.81	16.42	16.23	16.11	16.05	16.00
ILCM-SbS	2.16	3.12	4.08	**5.03**	10.73	16.43	16.02	15.84	15.72	15.63	15.56
ILCM-FbF	2.17	3.18	4.19	5.20	11.28	17.37	16.98	16.77	16.67	16.58	16.54
Eom	2.11	3.11	4.09	5.08	11.02	16.94	16.55	16.35	16.23	16.15	16.12
DSSA	2.13	3.10	4.08	5.05	10.88	16.73	16.31	16.12	15.98	15.92	15.87
SSA	2.15	3.10	4.08	5.04	10.83	16.62	16.23	16.01	15.90	15.80	15.75

Overall, E/n decreases with increasing *BLF* for a particular *Tari* for all the protocols evaluated. It is important to note that a higher *BLF* involves a faster tag (higher data rate DR_t). Therefore, if DR_t increases, the reader consumes a lower amount of receiving power E_r, reducing the overall E/n.

EASA presents the lowest E/n when $1/\rho \geq 2.66$. Therefore, there is evidence that EASA presents an energy-aware frame. Furthermore, the higher the value of $1/\rho$, the more notable the improvement in E/n of the proposed protocol in relation to the rest of the strategies. This occurs because the frame size of EASA increases with increasing $1/\rho$ (see (20)), decreasing the probability of collisions. As $1/\rho$ decreases, the performance of EASA deteriorates. In this situation, the probability of collision in EASA is higher than in the previous situation (L is smaller for the same n). As a result, the reader consumes a higher amount of transmitting and receiving power E_r and E_t, increasing the overall E/n of EASA.

5.3. Analysis of Communication Channel Effects on the Battery Lifetime

An ideal communication channel has been considered in the previous analysis, where there are no communication errors between the reader and the tags, and tags are uniformly distributed inside the reader interrogation zone. However, the capture effect is very common in passive RFID systems [29]. This phenomenon occurs when the reader successfully resolves one tag reply in a collided slot. A different effect is the detection error [30], which means that a single tag response is detected as idle, due to fading or interference. As a result, re-transmissions are required in subsequent slots.

These two effects will influence the protocols' performance in terms of the metric E/n. As a result, the reader battery lifetime will be also affected. This section evaluates the protocol's performance in terms of the reader's battery duration under the capture effect and the detection error. For this purpose, an RFID system with n passive tags and one battery-operated reader is considered. The reader operates from a lithium rechargeable battery, which has 0.48 kJ of energy [31]. The reader is assumed to transmit until all n tags are read and is not affected by its orientation to the tags.

Next, the percentage of the reader energy consumed from the battery to identify $n = 1024$ tags with respect to the total battery capacity is measured when the capture effect P_c and the probability of a detection error P_d are present in the communication channel. First, E (J) is evaluated for $n = 1024$ for all the protocols. Then, the percentage is obtained considering that 0.48 kJ represents 100% of the battery capacity. The timing parameters of Section 5.1 are used. Simulation results are shown in Table 5.

Table 5. Percentage (%) of the reader battery consumed to identify $n = 1024$ tags. The reader uses a lithium battery, which has 0.48 kJ of energy [31]. The protocols are evaluated in terms of the probability of the capture effect P_c and the probability of a detection error P_d. The timing parameters of Section 5.1 are used. Quantities in bold represent the best results among the protocols in the comparison.

P_d	0	0	0	0.2	0.2	0.2
P_c	0	0.1	0.2	0	0.1	0.2
EASA	**3.18**	**3.18**	**3.17**	**3.22**	**3.21**	**3.20**
Chen16	3.36	3.30	3.25	3.33	3.28	3.25
Chen14	3.41	3.35	3.30	3.44	3.39	3.35
ILCM-SbS	3.24	3.22	3.19	3.25	3.22	**3.20**
ILCM-FbF	3.57	3.51	3.46	3.61	3.50	3.44
Eom	3.42	3.39	3.40	3.43	3.44	3.37
DSSA	3.31	3.26	3.24	3.24	3.24	3.23
SSA	3.34	3.31	3.33	3.32	3.33	3.33

On the one hand, for a fixed P_d, the reader battery consumption decreases with increasing P_c for all the protocols in the comparison because fewer collided slots and more single slots occur. On the other hand, for a fixed P_c, the battery consumption increases with increasing P_d, because a higher number of total slots is required to complete one inventory round.

Table 5 shows that the improvement of EASA in relation to the rest of the protocols in the comparison becomes less significant with increasing P_c. The capture effect leads to collision slots becoming single slots. Therefore, a high P_c will be favorable to protocols with a high number of collision slots. Because EASA achieves the lowest number of collision slots (see Figure 3b), P_c has a smaller impact on EASA performance compared to the alternative protocols. This behavior is more notable for $P_d = P_c = 0.2$, where EASA and ILCM show the same percentage.

Assuming a reader with a lithium rechargeable battery of 0.48 kJ of energy, the reader will be capable of reading up to 32,201 tags with the EASA protocol (performing 31.45 identification cycles of 1024 tags) before the battery is empty (in the scenario with $P_d = P_c = 0$). In contrast, if the reader uses ILCM-FbF (the protocol with the highest E), the number of tags read is reduced to 28,683 tags, which represents 3517.8 fewer tags than in the case of using EASA.

The results of this section show that the battery consumption of a mobile RFID reader that is working in an communication channel with the capture effect and detection error will be minimized if the reader employs EASA. Therefore, EASA provides a longer battery lifetime for the reader than the alternative protocols.

6. Conclusions and Future Work

A novel RFID anti-collision protocol based on the current standard EPC-global Class-1 Generation-2 has been presented to decrease the energy per tag consumed by the reader E/n. EASA presents an energy-aware frame, because this protocol sets the frame size according to the parameters ρ and $\hat{n}$ so that E/n is minimized.

The metric E/n has been thoroughly studied, analyzing the main factor that affects it: the frame size L update strategy. From this study, it has been concluded that in order to decrease E/n, L must be $1/\rho$-times the estimated number of tags, where ρ is set according to the timing and power parameters of the RFID system T_i, T_k, T_{EPC}, P_{t_x} and P_{r_x}.

The proposed protocol was compared with several protocols of the state of the art in relation to E/n and the number of slots and transmitted bits. Simulation results showed that EASA, with an average 15 mJ per tag consumed by the reader, achieves a 6% average improvement in E/n in relation to the strategies of the comparison. Therefore, EASA is a suitable candidate where energy-efficiency is sought in passive RFID.

Several works in the literature present an SDR-RFID system [32–34] to evaluate the performance of the slot counter protocol (used in EPC C1G2) in a real scenario. In these systems, it would be possible to analyze the capture effect and the detection error in a real scenario. Because EASA is based on EPC C1G2, it can be physically implemented with an SDR-RFID system and commercial tags. Although this implementation is out of the scope of this work, it is proposed as future work.

Author Contributions: Methodology, L.A.; Formal Analysis, L.A.; Writing-Original Draft Preparation, L.A. and H.L.S.; Writing-Review & Editing, L.A., H.L.S. and A.P.R.; Supervision, H.L.S. and A.P.R.

Conflicts of Interest: The authors declare no conflict of interest.

References

1. Yang, L.; Chen, Y.; Li, X.Y.; Xiao, C.; Li, M.; Liu, Y. Tagoram: Real-time Tracking of Mobile RFID Tags to High Precision Using COTS Devices. In Proceedings of the 20th MobiCom '14 Annual International Conference on Mobile Computing and Networking, Maui, HI, USA, 7–11 September 2014; pp. 237–248, doi:10.1145/2639108.2639111. [CrossRef]
2. Pradhan, S.; Chai, E.; Sundaresan, K.; Qiu, L.; Khojastepour, M.A.; Rangarajan, S. RIO: A Pervasive RFID-based Touch Gesture Interface. In Proceedings of the 23rd MobiCom '17 Annual International Conference on Mobile Computing and Networking, Snowbird, UT, USA, 16–20 October 2017; pp. 261–274, doi:10.1145/3117811.3117818. [CrossRef]
3. Finkenzeller, K. *RFID Handbook: Fundamentals and Applications in Contactless Smart Cards and Identification*, 2nd ed.; John Wiley & Sons, Inc.: New York, NY, USA, 2003.
4. Landaluce, H.; Perallos, A.; Onieva, E.; Arjona, L.; Bengtsson, L. An Energy and Identification Time Decreasing Procedure for Memoryless RFID Tag Anticollision Protocols. *IEEE Trans. Wirel. Commun.* **2016**, *15*, 4234–4247, doi:10.1109/TWC.2016.2537800. [CrossRef]
5. Hou, Y.; Zheng, Y. PHY assisted tree-based RFID identification. In Proceedings of the IEEE INFOCOM 2017—IEEE Conference on Computer Communications, Atlanta, GA, USA, 1–4 May 2017; pp. 1–9, doi:10.1109/INFOCOM.2017.8056984. [CrossRef]
6. Lai, Y.; Hsiao, L.; Lin, B. Optimal Slot Assignment for Binary Tracking Tree Protocol in RFID Tag Identification. *IEEE/ACM Trans. Netw.* **2015**, *23*, 255–268, doi:10.1109/TNET.2013.2295839. [CrossRef]
7. Solic, P.; Radic, J.; Rozic, N. Energy Efficient Tag Estimation Method for ALOHA-Based RFID Systems. *IEEE Sens. J.* **2014**, *14*, 3637–3647, doi:10.1109/JSEN.2014.2330418. [CrossRef]
8. GS1 EPCglobal Inc. Radio-Frequency Identity Protocols Class-1 Generation-2 UHF RFID Protocol for Communications at 860 MHz—960 MHz. Brussels, Belgium. November 2013, Version 2.0. Available online: https://www.gs1.org/sites/default/files/docs/epc/Gen2_Protocol_Standard.pdf (accessed on 9 June 2018).
9. Wu, H.; Zeng, Y.; Feng, J.; Gu, Y. Binary Tree Slotted ALOHA for Passive RFID Tag Anticollision. *IEEE Trans. Parallel Distrib. Syst.* **2013**, *24*, 19–31, doi:10.1109/TPDS.2012.120. [CrossRef]
10. Seidler, C. RFID Opportunities for Mobile Telecommunication Services. In *ITU-T Lighthouse Technical Paper*; ITU-T Technology Watch: Addis Ababa, Ethiopia, 2005.
11. Hessar, F.; Roy, S. Energy Based Performance Evaluation of Passive EPC Gen 2 Class 1 RFID Systems. *IEEE Trans. Commun.* **2013**, *61*, 1337–1348, doi:10.1109/TCOMM.2013.13.110603. [CrossRef]
12. Agrawal, T.; Biswas, P.; Sharma, R. A novel-Q DFSA algorithm for passive RFID system. *Pervasive Mob. Comput.* **2017**, *40*, 89–103, doi:10.1016/j.pmcj.2017.05.004. [CrossRef]
13. Yu, J.; Lee, W.; Du, D.Z. Reducing reader collision for mobile RFID. *IEEE Trans. Consum. Electron.* **2011**, *57*, 574–582, doi:10.1109/TCE.2011.5955194. [CrossRef]
14. Luo, J.; Zhou, S.; Cheng, H.; Liao, Y.; Bu, K. A Range-Free Localization of Passive RFID Tags Using Mobile Readers. In Proceedings of the IEEE 12th International Conference on Mobile Ad Hoc and Sensor Systems, Dallas, TX, USA, 19–22 October 2015; pp. 445–446, doi:10.1109/MASS.2015.34. [CrossRef]
15. Zanaj, E.; Ranxha, G.; Kaso, A.; Zanaj, B. 3D localization method for RFID tags by using mobile readers and virtual reference tags. In Proceedings of the 22nd International Conference on Software, Telecommunications and Computer Networks (SoftCOM), Split, Croatia, 17–19 September 2014; pp. 51–55, doi:10.1109/SOFTCOM.2014.7039059. [CrossRef]

16. Namboodiri, V.; Gao, L. Energy-Aware Tag Anticollision Protocols for RFID Systems. *IEEE Trans. Mob. Comput.* **2010**, *9*, 44–59, doi:10.1109/TMC.2009.96. [CrossRef]
17. Zhu, Y.; Jiang, W.; Zhang, Q.; Guan, H. Energy-Efficient Identification in Large-Scale RFID Systems with Handheld Reader. *IEEE Trans. Parallel Distrib. Syst.* **2014**, *25*, 1211–1222, doi:10.1109/TPDS.2013.175. [CrossRef]
18. Jia, X.; Feng, Q.; Ma, C. An Efficient Anti-Collision Protocol for RFID Tag Identification. *Commun. Lett. IEEE* **2010**, *14*, 1014–1016, doi:10.1109/LCOMM.2010.091710.100793. [CrossRef]
19. Zhang, L.; Xiang, W. An energy- and time-efficient M-ary detecting tree RFID MAC protocol. In Proceedings of the IEEE International Conference on Communications (ICC), London, UK, 8–12 June 2015; pp. 2882–2887, doi:10.1109/ICC.2015.7248764. [CrossRef]
20. Zhang, L.; Xiang, W.; Tang, X.; Li, Q.; Yan, Q. A Time- and Energy-Aware Collision Tree Protocol for Efficient Large-Scale RFID Tag Identification. *IEEE Trans. Ind. Inform.* **2018**, *14*, 2406–2417, doi:10.1109/TII.2017.2771772. [CrossRef]
21. Eom, J.B.; Lee, T.J. Accurate tag estimation for dynamic framed-slotted ALOHA in RFID systems. *IEEE Commun. Lett.* **2010**, *14*, 60–62, doi:10.1109/LCOMM.2010.01.091378. [CrossRef]
22. Solic, P.; Radic, J.; Rozic, N. Early Frame Break Policy for ALOHA-Based RFID Systems. *IEEE Trans. Autom. Sci. Eng.* **2015**, *13*, 876–881, doi:10.1109/TASE.2015.2408372. [CrossRef]
23. Chen, W.T. A fast anti-collision Algorithm for the EPCglobal UHF class-1 generation-2 RFID standard. *IEEE Commun. Lett.* **2014**, *18*, 1519–1522, doi:10.1109/LCOMM.2014.2334317. [CrossRef]
24. Chen, W.T. Optimal Frame Length Analysis and an Efficient Anti-Collision Algorithm With Early Adjustment of Frame Length for RFID Systems. *IEEE Trans. Veh. Technol.* **2016**, *65*, 3342–3348, doi:10.1109/TVT.2015.2441052. [CrossRef]
25. Duan, L.; Zhang, X.; Wang, Z.J.; Duan, F. A Feasible Segment-by-Segment ALOHA Algorithm for RFID Systems. *Wirel. Pers. Commun.* **2017**, *96*, 2633–2649, doi:10.1007/s11277-017-4316-y. [CrossRef]
26. Klair, D.; Kwan-Wu, C.; Raad, R. A Survey and Tutorial of RFID Anti-Collision Protocols. *IEEE Commun. Surv. Tutor.* **2010**, *12*, 400–421, doi:10.1109/SURV.2010.031810.00037. [CrossRef]
27. Porta, T.F.L.; Maselli, G.; Petrioli, C. Anticollision Protocols for Single-Reader RFID Systems: Temporal Analysis and Optimization. *IEEE Trans. Mob. Comput.* **2011**, *10*, 267–279, doi:10.1109/TMC.2010.58. [CrossRef]
28. Vogt, H. Efficient Object Identification with Passive RFID Tags. In *Pervasive Computing*; Mattern, F., Naghshineh, M., Eds.; Lecture Notes in Computer Science; Springer: Berlin/Heidelberg, Germany, 2002; Volume 2414, pp. 98–113, doi:10.1007/3-540-45866-2_9. [CrossRef]
29. Wu, H.; Zeng, Y. Passive RFID Tag Anticollision Algorithm for Capture Effect. *IEEE Sens. J.* **2015**, *15*, 218–226, doi:10.1109/JSEN.2014.2339653. [CrossRef]
30. Nguyen, C.T.; Bui, A.T.H.; Nguyen, V.D.; Pham, A.T. Modified tree-based identification protocols for solving hidden-tag problem in RFID systems over fading channels. *IET Commun.* **2017**, *11*, 1132–1142, doi:10.1049/iet-com.2016.1289. [CrossRef]
31. Klair, D.K.; Chin, K.W.; Raad, R. An Investigation into thie Energy Eficiency of Pure and Slotted Aloha Based REID Anti-Collision Protocols. In Proceedings of the IEEE International Symposium on a World of Wireless, Mobile and Multimedia Networks, Espoo, Finland, 18–21 June 2007; pp. 1–4, doi:10.1109/WOWMOM.2007.4351749. [CrossRef]
32. Kargas, N.; Mavromatis, F.; Bletsas, A. Fully-Coherent Reader With Commodity SDR for Gen2 FM0 and Computational RFID. *IEEE Wirel. Commun. Lett.* **2015**, *4*, 617–620, doi:10.1109/LWC.2015.2475749. [CrossRef]
33. Buettner, M.; Wetherall, D. A software radio-based UHF RFID reader for PHY/MAC experimentation. In Proceedings of the IEEE International Conference on RFID, Orlando, FL, USA, 12–14 April 2011; pp. 134–141, doi:10.1109/RFID.2011.5764613. [CrossRef]
34. Solic, P.; Maras, J.; Radic, J.; Blazevicevic, Z. Comparing Theoretical and Experimental Results in Gen2 RFID Throughput. *IEEE Trans. Autom. Sci. Eng.* **2017**, *14*, 349–357, doi:10.1109/TASE.2016.2532959. [CrossRef]

APPENDIX

F

Paper VI

Survey and Analysis of RFID DFSA Anti-Collision Protocols and their physical implementation capabilities

This paper was published as a book chapter in the book: *"RFID Technology: Design Principles, Applications and Controversies"*. The book was published by Nova Science Publishers, Ed. New York, on March 2018. Its ISBN is 978-1-53613-250-2. The full book can be purchased from the Nova Science Publishers online catalog. The author submitted version is appender here.

Chapter 1

SURVEY AND ANALYSIS OF RFID DFSA ANTI-COLLISION PROTOCOLS AND THEIR PHYSICAL IMPLEMENTATION CAPABILITIES

Laura Arjona,**[*] **Hugo Landaluce, Asier Perallos
University of Deusto, Faculty of Engineering. Bilbao
DeustoTech/Fundacion Deusto, Mobility. Bilbao
Aaron Parks[†]
University of Washington, Electrical Engineering Department. Seattle

Abstract

The growing interest in asset recognition is making Radio Frequency Identification (RFID) technology increasingly attractive, to the point where almost anything can be tagged. The coexistence of several tags sharing the reader interrogation zone provides RFID technology with a great flexibility at the expense of the tag collision problem. Considering that most RFID applications require fast and energy efficient tag identification rate, many Dynamic Frame Slotted Aloha (DFSA) anti-collision protocols have been recently proposed, based on EPCglobal Class 1 Generation 2, the current standard in RFID. Addressing the current interest in DFSA protocols which aim to improve the performance of the current standard, this chapter analyzes, evaluates, and classifies the most significant DFSA protocols. Furthermore, the physical implementation feasibility in a real scenario of these protocols is discussed.

Key Words: Radio Frequency Identification (RFID), EPCglobal standard, anticollision, tag estimation, frame update policy, energy aware.

[*]E-mail address: laura.arjona@deusto.es
[†]E-mail address: anparks@uw.edu

1. Introduction

The fourth industrial revolution is coming, promising to bring together the worlds of production and network connectivity in an Internet of Things (IoT) [1]. One capable and feasible technology to build in intelligence to a product is Radio Frequency Identification (RFID) technology [2]. This technology is currently the most popular technology for item identification and tracking, and thus the main enabler for the IoT vision. The huge improvement in Ultra High Frequency (UHF) RFID, is leading to a widespread diffusion of several kinds of passive RFID tags in products.

The coexistence of several tags in the same interrogation zone provides RFID technology with a great flexibility at the expense of the tag collision problem. Tags share the same communication channel (the air) and may respond simultaneously to the same interrogation command, interfering and garbling their waveforms. The reader then is unable to interpret the information received from the tags, requiring a retransmission, and extending the tag identification time. Anti-collision protocols are then proposed to arbitrate the tags responses and to increase the number of tags identified by a time unit, while keeping low the energy consumed during the process.

There are several papers comparing the performance of the most important Dynamic Frame Slotted Aloha (DFSA) anti-collision protocols for RFID [3–6]. However, they do not study their physical implementation feasibilities. Besides, a key limitation of these papers is that they only survey protocols published before the year 2010. The paper [7] presents a more recent classification of DFSA protocols, but their physical implementation is not covered, and protocols based on tag estimation are not included in the classification. Related to the physical implementation of an RFID anti-collision protocol, there are three main works in the literature presenting a Software Defined Radio (SDR) system to implement one. The authors in [8] study the performance of two protocols, but the analysis is limited to 16 tags. The authors in [9, 10] also evaluated the performance of an anti-collision protocol in an SDR system, but fixed-size frames are used within an inventory round. Also, the experimentation in [9] is limited to 16 tags.

Overall, the authors believe that this is the first work in the literature covering both the study and classification of up-to-date DFSA protocols, and a discussion of their potential physical implementation. This chapter focuses on the most significant up-to-date DFSA anti-collision protocols for RFID, covering their functionality as well as their physical implementation in a real RFID system.

The rest of this chapter is organized as follows. Section 2 provides a general overview of RFID technology. Section 3 introduces the tag collision problem. This is followed by a survey of the main state-of-the-art DFSA anti-collision protocols and a discussion about their physical implementation capabilities. After that, Section 5 provides the experimental results of the performance evaluation in a real scenario of two different DFSA anti-collision protocols. Finally, Section 6 concludes this chapter.

2. Overview of RFID technology

RFID is an automatic wireless data collection technology with a long history. First functional passive UHF RFID systems with a range of several meters appeared in early 1970s [11]. Since then, RFID has experienced a tremendous growth. At first glance, the concept of RFID and its application seems simple and straightforward. But in reality, RFID is a technology that spans systems engineering, software development, circuit theory, antenna theory, radio propagation, microwave techniques, receiver de-

sign, integrated circuit design, encryption, materials technology, mechanical design, and network engineering, to mention a few. This chapter focuses on the network stack development, in particular, on the Medium Access Control (MAC) layer.

2.1. Operation principles

A typical RFID system consists of a reader, antennas, tags, and a control unit (often a computer). The reader uses connected antennas to wirelessly communicate with the tags inside the interrogation zone using radio waves. The typical application of RFID technology is to read the identification code ID stored inside tags, which uniquely identifies them. Tags can be then attached to a wide variety of objects to uniquely identify them. RFID is often applied to inventory and asset management, as well as to electronic identification and tracking.

2.2. Classification

RFID originated from RADAR technology, and it has greatly evolved since then. Traditionally, the main purpose of RFID tags was to track and identify objects. Currently, there are tags which are also capable of performing sensing and computational tasks [12]. RFID systems can be classified into three groups according to their form and functionality.

1. Active RFID.
   Includes tags with a battery which emit radio signals, acting as a classical transceiver. These can have a very long range and they do not require a complex or expensive interrogator. They can be based on protocols such as ZigBee, Bluetooth / BLE, or LoRa. These are still considered RFID tags even though they do not use backscatter[1].
2. Semi-Passive RFID.
   Includes tags which communicate with the reader using backscatter and which use a battery to power digital logic in the tag.
3. Passive RFID.
   Includes tags without batteries which use backscatter to communicate with the reader. Passive RFID tags can be classified into four main groups.
   (a) Chip-based ID tags.
   Tags with an integrated circuit containing digital logic. These tags are designed to operate in one of the three following frequency ranges:
      i. Low Frequency (LF) - NFC 125 kHz.
      ii. High Frequency (HF) - NFC 13.56 MHz.
      iii. Ultra High Frequency (UHF) - EPC C1G2 [13] 900 MHz.
   (b) Chipless ID tags.
   Tags without an integrated circuit which still can backscatter their ID in some way. There are two main types of chipless ID tags.
      i. UHF Surface Acoustic Wave (SAW) tags. Their operation is based on micro-acoustics of piezoelectric crystals instead of semiconductor physics [14].

[1] Form of communication used by most commercial RFID tags. It consists of the variation of the amplitude of the incoming electromagnetic waves, which are reflected back in the tag antenna according to the digital data which is required to transmit.

ii. Other chipless UHF/microwave band tags. Currently, these types of tags are only seen in research.

(c) Computational RFID (CRFID) and RFID sensor tags.
Currently there is a growing class of battery-free computational and sensing tags which go beyond simple barcodes replacement functionality. Two main groups of CRFIDs have been reported in the literature.

i. UHF WISP, NFC-WISP, UMass Moo.
These are re-programmable and open source tags for rapid implementation of battery-free sensing or other applications [12].

ii. Digital UHF sensor and actuator tags such as Farsens products.

(d) Chipless UHF sensor tags.
These tags are shown only in research, and they can do sensing tasks using chipless methods.

3. The tag collision problem

Typically, an RFID communication system needs at least one reader and one or more tags. All the participants must share a unique communication channel: the air. Given the boom in the use of HF, UHF, and microwaves frequency ranges for communications, the readers' detection range has been greatly increased. As a consequence, it is very common to find several tags active in the same frequency, transmitting signals simultaneously.

Due to the shared nature of the communication channel, signals coming from different tags often collide, producing interferences and cancellations. The interferences produced between the messages transmitted by the tags are known as message collisions, and they cause illegible and lost data. In the field of RFID, this problem is known as the tag collision problem and it represents a focus of interest in current research. Collisions oblige the reader to retransmit commands asking for the tag's ID, wasting bandwidth, increasing the identification time and the power consumption of the global system.

Due to the restrictions in RFID, traditional multiple-access methods can not be applied to this technology to avoid the tags collisions. While classic multiple-access protocols chase a performance and stability improvement, as well as a reduction in the packets delay; collision-resolution protocols in RFID seek for a reduction in the total time required to identify a set of tags and in the energy consumed during the identification process. Due to their particular characteristics in addition to the different goals they chase, collision-resolution protocols in RFID are called anti-collision protocols.

In RFID, a collision occurs when two or more tags transmit their message simultaneously, as showed in Figure 1.

The two main characteristics desired for an anti-collision protocol are:

- Fast identification: the time employed for identifying the tags located in the reader interrogation zone must be as low as possible, so that it results imperceptible.
- Minimum energy consumption: both active and passive tags must strive to achieve a low power consumption. Thus, the hardware complexity must be minimized and the amount of information exchanged between the elements in the system must be reduced.

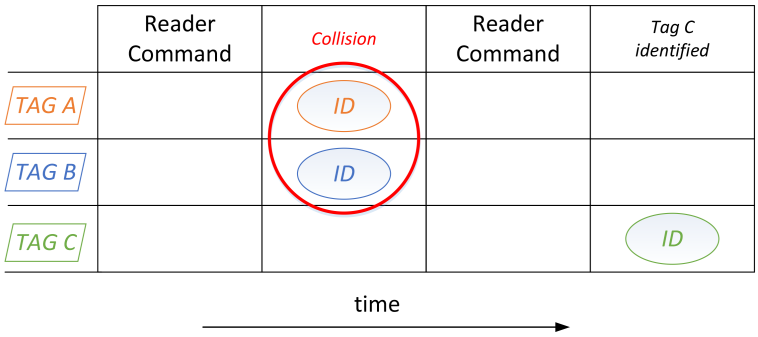

Figure 1. The tag collision problem in RFID

3.1. Anti-collision protocols

Some definitions are provided next to properly set the background of anti-collision protocols.

- *slot*: period of time that separates the tags' responses. Conventionally, three types of slots are considered, in terms of the tags' responses to the reader's commands: single (only one tag replies), collision (more than one tag replies in the same slot), and idle (none of the tags reply). In this context, the variables c_s, c_k, and c_i correspond to the number of single, collision, and idle slots in a frame, respectively.
- *frame*: sequence of L slots, where L represents the frame size. Tags can only transmit their response in one slot per frame.
- *query*: bit-string command transmitted by the reader to the tags.
- *inventory round*: period of time that begins when the reader transmits the initial query Qc and it ends when the reader interrupts the identification process and the tags loose their state. Ideally, an inventory round ends when all the tags in the reader interrogation zone have been identified.

The main existing anti-collision protocols in the literature can be classified into Aloha-based and tree-based protocols [15].

Tree-based protocols [16], in essence, split colliding tags into subsets, and further split the subsets repeatedly up to the successful response of all the tags that are within the interrogation zone.

Aloha based protocols divide time into slots and tags randomly choose one slot to respond. These protocols present four main variants. In Pure Aloha (PA), a tag will respond to the reader command randomly after being energized. Slotted Aloha (SA) divides time into slots and schedules tags to respond only at the boundary of the time slots. Frame Slotted Aloha (FSA) and Dynamic Frame Slotted Aloha (DFSA) divide time into frames and frames into slots and mandate each tag to respond in only one slot per frame. While in FSA the frame size is fixed during the identification process, in DFSA it is variable. The fact that EPCglobal Class-1 Generation-2 (EPC C1G2), the current standard in RFID, uses a DFSA structure to arbitrate collisions, highlights the relevance of this scheme. This chapter focuses on DFSA protocols.

3.2. Slot Counter anti-collision protocol

EPC C1G2 [13] employs a DFSA protocol to arbitrate collisions: the Slot Counter protocol. It specifies the transmission frame size L as a power of two, taking the value $L = 2^Q$, where $Q \in \mathbb{N}$ and $0 \leq Q \leq 15$. It also defines the parameter Q_{fp} to update the frame size, with $Q = round(Q_{fp})$. Figure 2 shows a flow chart of Slot Counter protocol.

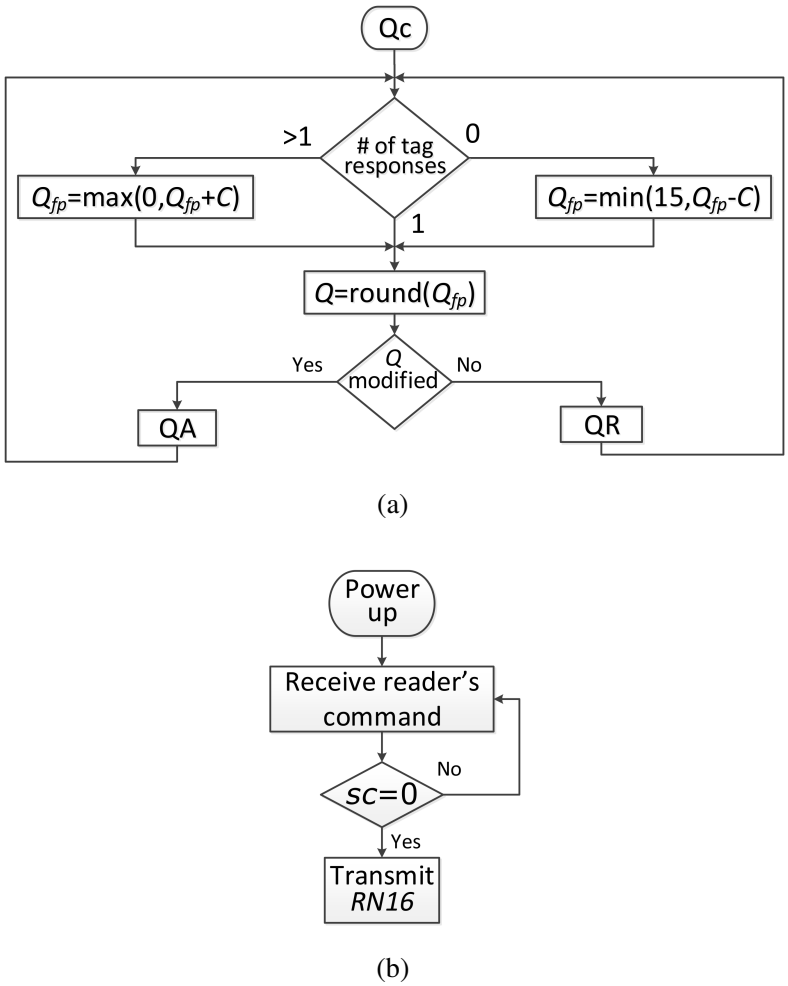

Figure 2. Flow diagram of Slot Counter anti-collision protocol: (a) for reader, (b) for tags

The reader starts the inventory round by transmitting Qc, and then alternates between QueryAdjust (QA) and QueryRep (QR) queries. QA starts a new frame with the updated L value and implies that tags must randomly select a slot in the frame (the initial value of their internal slot counter SC), while QR tells the tags to decrement SC. Thus, when SC=0, the tag transmits a 16-bit random number $RN16$. The frame size is set as L=2^Q, and its value is dynamically updated with the parameters Q and C, where Q=round(Q_{fp}). Regarding the time slot occupancy, there are three possible scenarios to update the value of Q_{fp}, as shown in Figure 2.

- Single slot: Q_{fp} remains unchanged. In this case, the reader replies to the tag with an ACK command followed by the same $RN16$ received by the tag, and the tag transmits its ID.
- Collision slot: Q_{fp}=Q_{fp}+C
- Idle slot: Q_{fp}=Q_{fp}−C

Next, the reader readjusts the frame size to $L = 2^Q$ where $Q = round(Q_{fp})$.

The next section introduces the main DFSA protocols of the state-of-the-art and classifies then according to their L update algorithm.

4. Dynamic Frame Slotted Aloha anti-collision protocols

Most RFID manufacturers currently follow the EPC C1G2 standard, enhancing the research relevance of DFSA protocols. Consequently, many DFSA algorithms have recently appeared in the literature to solve the RFID tag collision problem. They all share the dynamic nature of the frame size update along one inventory round. However, each of them applies a different strategy to give a particular value to the frame size.

A wide variety of DFSA protocols can be found in the literature which update L with the aim of improving different metrics regarding the process of tag identification. They all share the fact that the reader adjusts L within an inventory round according to the responses from the competing tags in each slot. In each frame of an inventory round, the frame size is adjusted at some specific slots, referred as *update slot* in this chapter. There are three main strategies which a DFSA protocol can follow to select the *update slot*:

- every slot of the frame is an update slot.
- only the last slot of the frame is an update slot.
- a particular slot within a frame is an update slot, referred as pointer slot in this work. The pointer slot is usually set as a fraction of the frame size.

Some protocols present a two-phase tag identification process [17, 18], and they use a combination of the previous strategies. A frame update strategy in DFSA involves two main steps:

1. Calculation of L at the *update slot*.
2. Decision whether to break the current frame and start a new one, or to proceed with the next slot of the current frame.

The generic procedure of a DFSA protocol following EPC C1G2 requirements is presented in Figure 3. Firstly, the reader transmits a query (Qc,QA,QR) and waits for the tags' responses. At the end of each time slot, the reader updates the parameters c_s, c_k, and c_i accordingly. Next, if the current slot is an *update slot*, the algorithm to update L is executed. Otherwise, the reader proceeds with the next slot of the frame. Finally, when the reader reaches the last slot of the frame, it starts a new frame.

4.1. Survey and classification

Establishing a clear classification of all DFSA protocols is not straightforward. A key feature which characterizes a DFSA protocol is the procedure it follows to update the frame size along the identification of a set of tags. The optimization of a

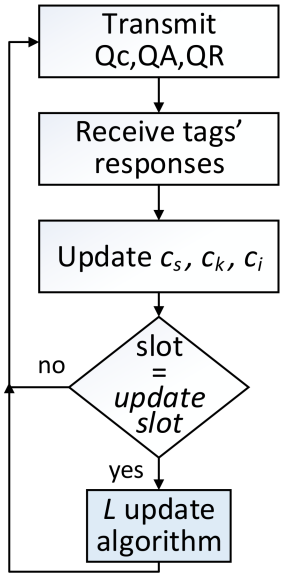

Figure 3. Flow chart of a generic DFSA anti-collision protocol.

DFSA protocol in the sense of the proper frame size selection has direct impact on energy consumption [10]. Therefore, this optimization is of great interest for designing RFID applications. To this end, this section establishes a classification of the main anti-collision protocols in the current state-of-the-art according to their frame update strategy. The classification is showed in Table 1. It is also showed the strategy which each protocol uses to set the *update slot*.

The number of tags that enter into the coverage area usually varies randomly, thus the number of tags that compete in each frame is unknown to the reader, and the frame size adjustment is not trivial. Two main strategies can be found in the literature to update the value for the frame size in DFSA protocols: the first calculates L as a function of the parameter Q, and the second sets L as a function of the estimated number of tags $\hat{n}$.

- Parameter Q: f(Q)

  The frame size can be adjusted by controlling the number and states of the slots in each frame with parameter Q, so that Q increases when collisions are detected, and decreases with increasing number of idle slots. Several approaches in the literature update L by adjusting Q: Q+ [19], Enhanced Slot Count algorithm [20], Improved Q [21], Fast Q [22], Slot Counter [13], and FuzzyQ [23].

- Tag set size estimation

  Many works in the literature have addressed the tag estimation task in order to provide an optimal frame size according to the estimated number of tags. It is known that a DFSA protocol reaches its maximum throughput, defined as the ratio between the number of tags and the total number of slots required to identify them, when the frame size is equal to the number of tags [15]. Therefore, in order to optimize this metric, the reader should set the frame size equal to the estimated number of tags.

  Once the tag set size has been estimated, the next step is to calculate L according

to $\hat{n}$. Two main strategies to set L as a function of $\hat{n}$ can be found in the literature, and they are presented next (see Table 1).

- Continuous function of $\hat{n}$: f($\hat{n}$)
  The first strategy sets L as a continuous function of $\hat{n}$. The reader analyzes the information extracted form the tags' responses (c_s,c_k,c_i) and sets L as a function of these values. Several anti-collision protocols follow this strategy: DFSA with Tag Enhanced Estimation (TEM) [24], Chen and Lin [25], Bayesian slot [26], Chen [27], Eom [28], Linearized Combinational Model (LCM) SbS [29], Improved Linearized Combinational Model (ILCM) [30], Early adjustment algorithm [31], and Improved Linearized Combinational Model (ILCM) SbS [32].
- Look-up table (LUT) according to $\hat{n}$: LUT($\hat{n}$)
  The second strategy is to set L according to an LUT based on $\hat{n}$. The idea is to define different ranges of $\hat{n}$ and assign a different value of L for each range of $\hat{n}$. Several approaches in the literature follow this strategy, including Vogt [33], FSA Type C-J [34], Optimal Interval Transmission Control Solution (OITCS) [35], MSE based FSA [36], Fast in-frame adjustment [37], ds-DFSA [38], and DS-MAP [18].

4.2. Physical implementation capabilities

Commercial RFID readers are generally black box systems which provide only limited configuration, and they do not give the option to observe or modify the MAC or Physical (PHY) layer behavior. Therefore, it is not possible to study the physical implementation of existing anti-collision protocols. There are some high-end RFID test equipment available in the market to evaluate the tag performance [39]. However, they are closed source, expensive, and generally do not allow complete control over the PHY and MAC layers.

To give the users control of the PHY and MAC layers of an RFID system, a Software Defined Radio (SDR) platform for low-level UHF RFID experimentation was presented in [9]. SDR is an innovative technology in which all the physical parameters of a radio front-end are completely software defined. The reader is implemented with an Universal Software Radio Peripheral (USRP) that implements EPC C1G2, and it is capable of identifying off the shelf Gen2 tags. All the signal processing is performed in a standard Linux PC, and the software is built on top of GNU radio. Given the importance of the frame size value on the performance of an RFID system, this SDR platform is very attractive to test the implementation feasibility and the real performance of anti-collision protocols.

To manage the tag collisions, this reader implements an FSA protocol. Thus, the frame size is not updated, but L is set to a constant value for a complete inventory round. This protocol only considers two types of slots, of equal duration: success slots and non-success slots. Idle and collision slots are assumed as non-success slots. Also, the reader transmits an ACK in every slot, resulting in a waste of energy when no tag actually responded.

Since this reader is software-defined, the implemented FSA protocol can be transformed into a DFSA protocol by re-writing user-level software. The anti-collision protocol should be implemented in C++. In order to implement a DFSA anti-collision protocol in the SDR reader presented in [9], the following modifications should be made.

- The reader should differentiate between the three types of slots (collision, idle, single) in order to update c_k, c_i, and c_s, and to execute the frame update algorithm.
- The reader should not transmit ACK if an idle slot is detected.
- At the end of each frame, the reader should transmit a QA query to start the next frame instead of transmitting Qc.

All the protocols presented in Table 1 can be implemented in an SDR system if the three suggested modifications are made, and they must restrict their frame size to a power of 2 values to follow the EPC C1G2 requirements.

Furthermore, it is important to note that EPC C1G2 considers a variation of Q from the current frame to the next in zero or one unit (new value is set as $Q-1$, Q, $Q+1$). While Qc specifies the Q value, QA only indicates the variation of current Q in one or zero unit. For this purpose, the reader must transmit Qc to start the initial frame, and QA to start the rest of the frames in one inventory round. Therefore, if a DFSA protocol needs to update L with a new Q value which differs from the current one in more than one unit, transmitting just one QA query is not appropriate. In this case, three main solutions are proposed:

- transmit Qc with the new Q value,
- transmit more than one consecutive QA,
- modify the query QA. The last 3 bits of this query indicate the variation of Q, so there are 8 different possible values. As a result, Q could vary in up to 3 units: $Q+0$, $Q+1$,$Q-1$, $Q+2$, $Q-2$, $Q+3$, $Q-3$. This QA modification can be easily implemented in the SDR reader. However, commercial tags will not be able to interpret this new functionality.

Considering the evaluation of the SDR RFID system with commercial tags, the third proposed solution is discarded. In relation to the first and second solutions, the query Qc contains 22 bits, while QA requires 9 bits. Although QA requires fewer bits than Qc, transmitting more than one consecutive QA takes longer time, because the reader must wait for the tag to decode the query before transmitting an additional one.

4.2.1. Protocols not following EPC C1G2

The previous section discussed the implementation of DFSA protocols following EPC C1G2. This section discusses the physical implementation feasibility of protocols which do not follow EPC C1G2 constrains. A clear example of this group are tree-based protocols [40].

There are some anti-collision protocols which require reader queries which are not part of EPC C1G2. Using the presented SDR, this would not be a problem in terms of the reader side of the protocol, since the reader behavior is defined by software. However, commercial tags will not be able to interpret and respond to these additional commands. Recently, the authors in [12] developed a software-defined tag, referred as WISP, whose responses to the reader's commands can be defined by software. Therefore, protocols which are no compliant with EPC C1G2 completely, could be implemented with an SDR reader and WISP tags.

5. Physical implementation of a DFSA protocol

In the previous section it was mentioned that in order to implement a DFSA anti-collision protocol in the SDR system presented in [9], three main modifications must

be made. This section presents the feasibility of those modifications. Besides, two different DFSA protocols are evaluated in a real scenario using an SDR reader.

Next, the following three main modifications are made to the SDR reader in order to be able to implement a DFSA protocol.

- A threshold energy value E_{th} is set for the energy of the received signal E_r to detect an idle response. Thus, an idle slot occurs when the energy of the received signal is lower than this threshold; that is, when $E_r < E_{th}$.
- If an idle slot is detected, the reader does not transmit ACK. As a result, idle slots duration is shortened and the identification process is accelerated.
- The query Qc will be transmitted when the variation in Q is greater than one unit at the end of each frame. The query QA will be transmitted otherwise.

In order to differentiate between idle, single, and collision slots, the reader follows the algorithm presented in Figure 4. First, the reader measures the energy of the received signal E_r. If $E_r < E_{th}$, then the slot is considered idle. If $E_r \geq E_{th}$, the reader then transmits ACK and waits for the EPC message. After its reception, it checks the CRC contained in the EPC message. If the CRC is correct, then the slot is a single slot. Otherwise, a collision slot is assumed.

As it can be seen from Figure 4, a slot is considered as a collision when $E_r > E_{th}$ and the received CRC from the tag is not correct. In the experimental real scenario evaluated, there are two main situations which are assumed as a collision slot by the reader:

1. collision type 1: there is a real tag collision, that is, two or more tags transmit their $RN16$ in the same time slot.
2. collision type 2: only one tag transmits the $RN16$, but the reader receives and decodes an erroneous CRC. In some scenarios, a single tag in a slot is not always successfully detected, since its amplitude is of lower level than required for a successful detection. This may be caused either by multipath effects or if during the interrogation the tag loses its power and cannot backscatter the full response.

On the contrary, there are two main situations which are assumed as a single slot by the reader:

1. single type 1: only one tag backscatters the $RN16$ and the reader correctly decodes the CRC.
2. single type 2: more than one tag backscatter the $RN16$ in the same slot, but the reader successfully resolves one tag reply. It can occur because tags response amplitudes can vary due to different distances from the reader antenna, or due to multipath fading present in the channel. This is known as the capture effect [41].

The presented tags' behavior will affect the performance of the anti-collision protocol, and it should be studied for the particular protocol implemented in the SDR reader and the particular real scenario.

The transmission model for the proposed SDR system, meeting EPC C1G2 [13] requirements, is showed in Figure 5. The duration of each type of slot, single, collision, and idle, is referred to as T_s, T_k, and T_i, respectively. T_1 refers to the time interval between a reader query and a tag response, while T_2 refers to the time interval between a tag transmission and a reader query. T_{QA}, T_{QR}, T_{Qc}, and T_{ACK} refer to the time the reader needs to transmit QA, QR, Qc, and ACK, respectively. Finally, T_{RN16} and T_{EPC} refer to the time required by a tag to transmit $RN16$ and EPC, respectively. It

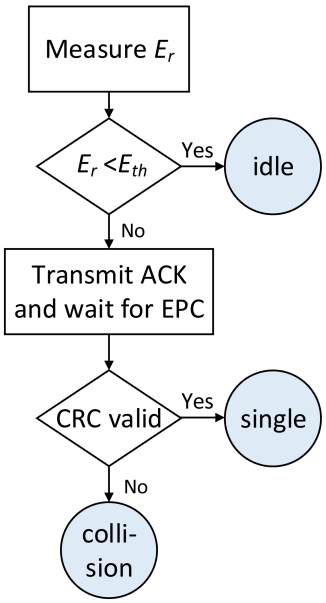

Figure 4. Slot type differentiation in the proposed SDR reader.

is appreciated that a single and collision slot have the same duration. The duration of each type of slot is obtained as:

$$T_k = T_s = T_1 + T_{RN16} + T_2 + T_{ack} + T_{EPC} + T_2, \quad (1)$$

$$T_i = T_1 + T_{RN16} + T_2, \quad (2)$$

5.1. Experimental set up

In this section, the proposed SDR RFID system is implemented in a real scenario to evaluate its performance. The block diagram of the system is showed in Figure 6, and the real implementation is presented in Figure 7. A commodity USRP FLEX900 is utilized, with a single SBX daughterboard, a Gigabit switch, and a PC. The transmit and receive ports of the daughterboard are connected with two circularly polarized patch antennas of 6dBi gain. Figure 8 shows a closer look into the switch and the USRP used.

Several off-the-shelf Alien-9640 tags [42] were used to evaluate the inventory process. They were attached to foam boards (30.5 cm $\times$ 91.5 cm), each board containing 16 tags. On board tags were vertically separated 1.5cm from each other. Figure 9 shows one of the boards employed. These boards were inserted into a 3D-designed plastic rack, facing the antennas, as showed in Figure 7. The rack was placed 1m above the floor. The separation between panels is 4 cm to avoid interference between tags. The distance between the first panel inserted into the rack and the antennas was about 50cm. The reader was configured to follow the parameters presented in Table 2, following the EPC C1G2 requirements. The transmission power of the reader was set to 13.37 dBm, measured with a mixed-signal oscilloscope. Next, one inventory round with a duration of one frame of 16 slots (L=16) was executed to ensure that the reader

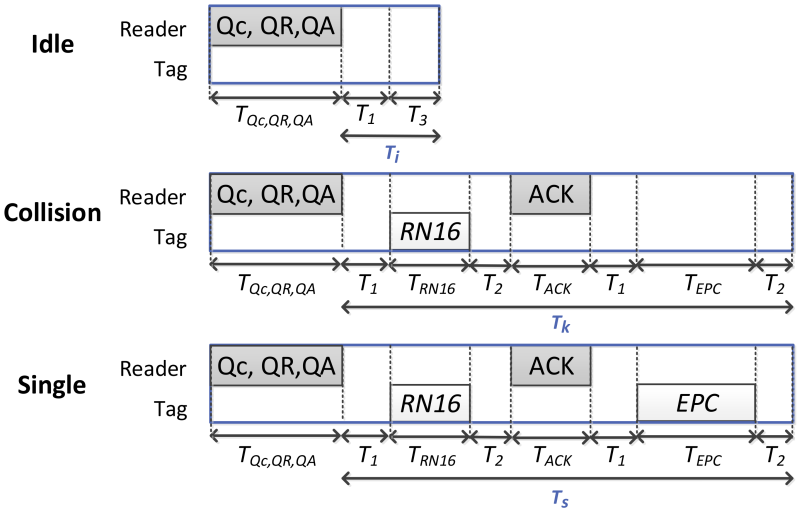

Figure 5. Transmission model of the proposed SDR system

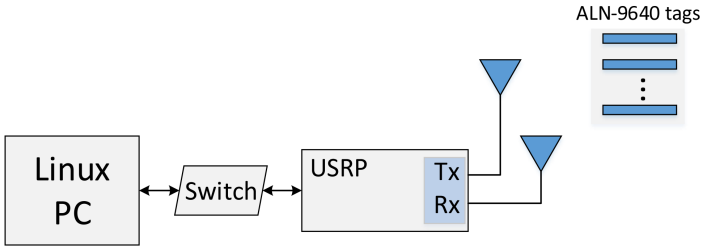

Figure 6. Block diagram of the proposed SDR RFID system.

can differentiate between the three types of slots. For this purpose, 16 tags (n=16) were placed in the reader interrogation zone. At the end of the frame, the signal received at the USRP source was saved and then plotted with MATLAB R2017a. Figure 10 shows slots 2, 3, and 4 (collision, single, and idle, respectively). This figure shows the equal duration for single and collision slots.

The next section validates the operation of the proposed SDR system by evaluating the performance of an ideal DFSA protocol and the Slot Counter protocol. For this purpose, three different tag set sizes are evaluated, n=16, 32, and 64, by inserting 1, 2, and 4 foam boards into the rack.

It is important to note that during RFID inventories, transmission losses due to fading may cause power outage events to the tags, which loose their state and abandon the ongoing identification round [43]. Therefore, the reader might miss some tags present in the interrogation area, and all the n tags are not identified in every single inventory round. Lost tags enter the identification process again when the next frame starts. Because this work focuses on the experimental performance of anti-collision protocols, an inventory round is assumed valid when at least 93.75 % of the n tags were identified (60 tags for n=64, 30 tags for n=32, and 15 tags for n=16) and the current frame was terminated. Furthermore, the reader must always end the current

Figure 7. Experimental setup.

frame before terminating the inventory round.

5.2. Ideal DFSA protocol

As mentioned in Section 4.2, a DFSA protocol reaches its maximum $throughput$, defined as

$$throughput = \frac{c_s}{c_s + c_i + c_k}, \tag{3}$$

when $L{=}n$ for a particular frame. This section evaluates the performance of an ideal DFSA protocol implemented in the SDR RFID system presented in the previous section. It is called ideal because the reader knows the number of tags inside the interrogation zone at the beginning of an inventory round. Thus, the reader can easily obtain the number of the remaining unidentified tags at the start of each frame, referred as n_u in this work, by subtracting the number of single slots from the initial number of tags. Thus, $n_u{=}n$ initially, and $n_u{=}n{-}c_s$ at the start of each frame. Consequently, the reader can set the new frame size as $L{=}n_u$.

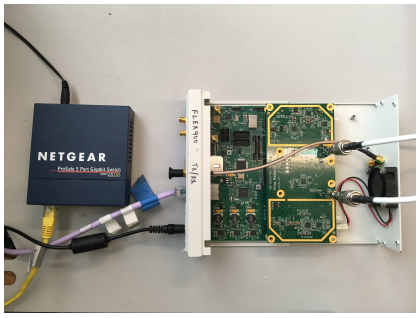

Figure 8. Switch and USRP for the experimental setup.

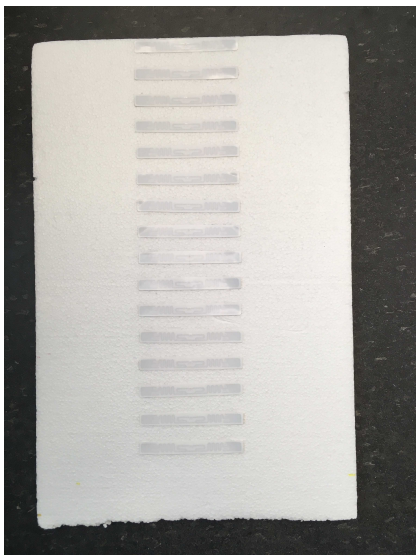

Figure 9. One of the foam boards employed in the setup.

5.2.1. Evaluation and comparison of the throughput in an ideal DFSA protocol

Firstly, the experimental $throughput$ is evaluated and compared with the analytic values. In order to perform an analysis of the $throughput$ in (3), a system model with one reader and n tags is defined. The probability that r tags among n occupy a slot can be approximated by a binomial distribution P_r [33]

$$P_r = \binom{n}{r}\left(\frac{1}{L}\right)^r\left(1-\frac{1}{L}\right)^{n-r}. \tag{4}$$

When $r = 0$ in (4), the probability of an idle slot p_i is obtained as

$$p_i = \left(1-\frac{1}{L}\right)^n. \tag{5}$$

Then, the expected number of idle is

$$c_i = Lp_i = L\left(1-\frac{1}{L}\right)^n. \tag{6}$$

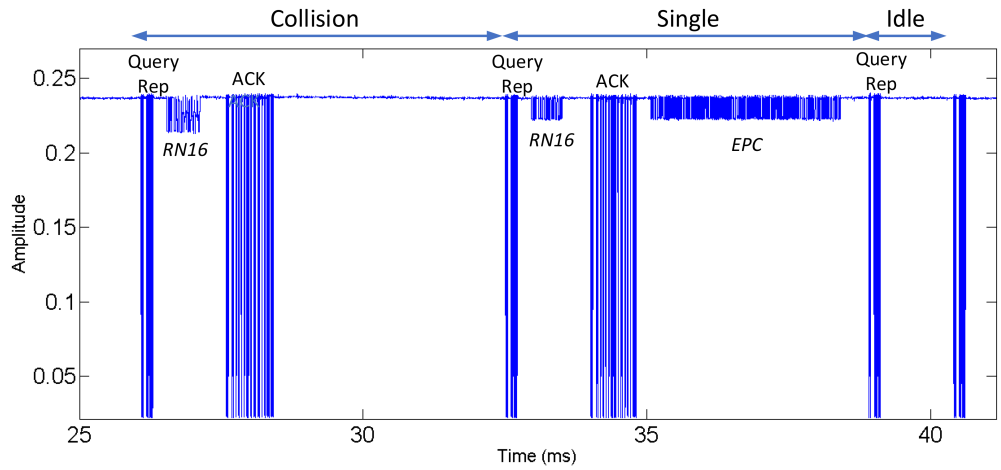

Figure 10. Capture of 3 slots in one FSA frame, with L=n=16.

When $r = 1$ in (4), the probability of a single slot p_s is obtained as

$$p_s = \frac{n}{L}\left(1 - \frac{1}{L}\right)^{n-1}. \tag{7}$$

Then, the expected number of single slots is

$$c_s = Lp_s = L\frac{n}{L}\left(1 - \frac{1}{L}\right)^{n-1}. \tag{8}$$

Finally, the probability of collision a slot p_k is obtained as

$$p_k = 1 - p_i - p_s. \tag{9}$$

Then, the expected number of collision slots is

$$c_k = L \cdot p_k = L(1 - p_i - p_s). \tag{10}$$

Finally, the analytical throughput for an ideal DFSA, with L=n, can be obtained as

$$throughput_{ideal} = \frac{n\left(1-\frac{1}{n}\right)^{n-1}}{n\left(1-\frac{1}{n}\right)^{n-1} + n\left(1-\frac{1}{n}\right)^{n} + n\left(1-\left(1-\frac{1}{n}\right)^{n} - \left(1-\frac{1}{n}\right)^{n-1}\right)}. \tag{11}$$

Next, the experimental $throughput$ is evaluated for an ideal DFSA. For each n, 100 valid inventory rounds are evaluated for an ideal DFSA protocol, where the reader sets Q=$log_2(n)$ at the beginning of the inventory round, and then sets Q=$log_2(n_u)$ at the start of the rest of the frame. Experimental results are compared with the analytical values for one frame obtained with (11). Results are averaged and showed in Figure 11.

Results shows that the highest experimental $throughput$ is obtained for n=64, the highest n evaluated. Also, it is appreciated that experimental results exceed the theoretical values for all the scenarios evaluated. To better understand these results,

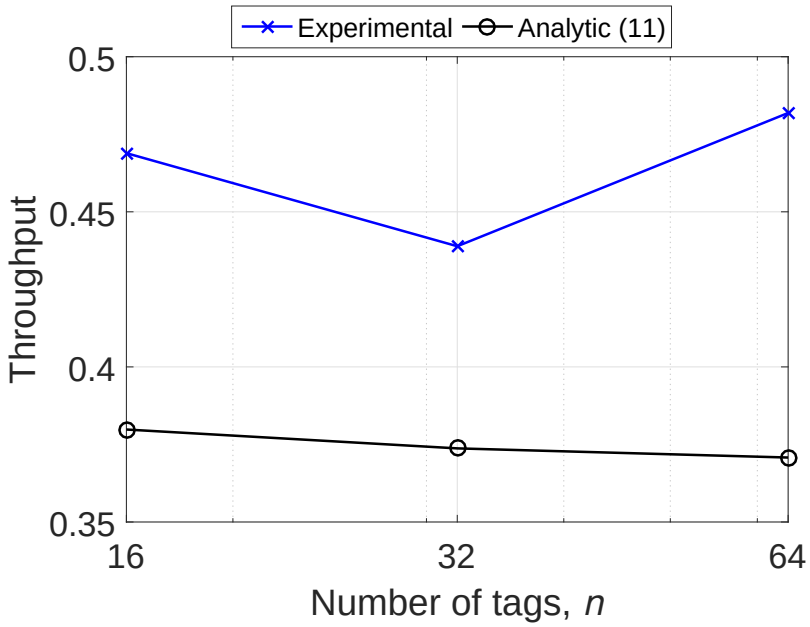

Figure 11. Comparison of experimental and analytic $throughput$ for an ideal DFSA (L=n) varying n from 16 to 64.

it is also evaluated the experimental probability of idle, single, and collision slots, by dividing the number of idle, single, and collision slots by the total number of slots. Experimental results are compared with the analytic values (5), (7), and (9), and they are showed in Figure 12.a, 12.b, and 12.c, respectively.

From this figure, it can be justified that the higher experimental $throughput$ in relation to the analytic values, comes from a lower probability of collision and a higher probability of single slots. This is due mainly to the capture effect, where a stronger tag response can be decoded if it collides with a weaker one. The probability of idle slots increases in the experimental results, but its negative effect over the $throughput$ is compensated by the considerable reduction in the probability of collision.

5.2.2. Evaluation of the tag identification time in an ideal DFSA protocol

This section evaluates the average time required to identify one tag, calculated as the number of uniquely identified tags divided by the total identification time it. At the end of an inventory round, the reader can obtain it in two different forms.

1. The reader keeps track of the number of single, collision, and idle slots, and the number of queries QA, QR, and Qc, and obtains it as

$$it = c_i \times T_i + c_s \times T_s + c_k \times T_k + tQA \times T_{QA} + tQR \times T_{QR} + tQc \times T_{Qc}, \quad (12)$$

   where tQA, tQR, and tQc refer the the total number of transmitted QA, QR, and Qc queries, respectively.

2. In order to include in the experimental it metric the processing time employed by the PC, a timer is started in the reader program when the reader starts the inventory round, and it is stopped when the current valid round is terminated. Then, it is calculated by reading the value from the timer.

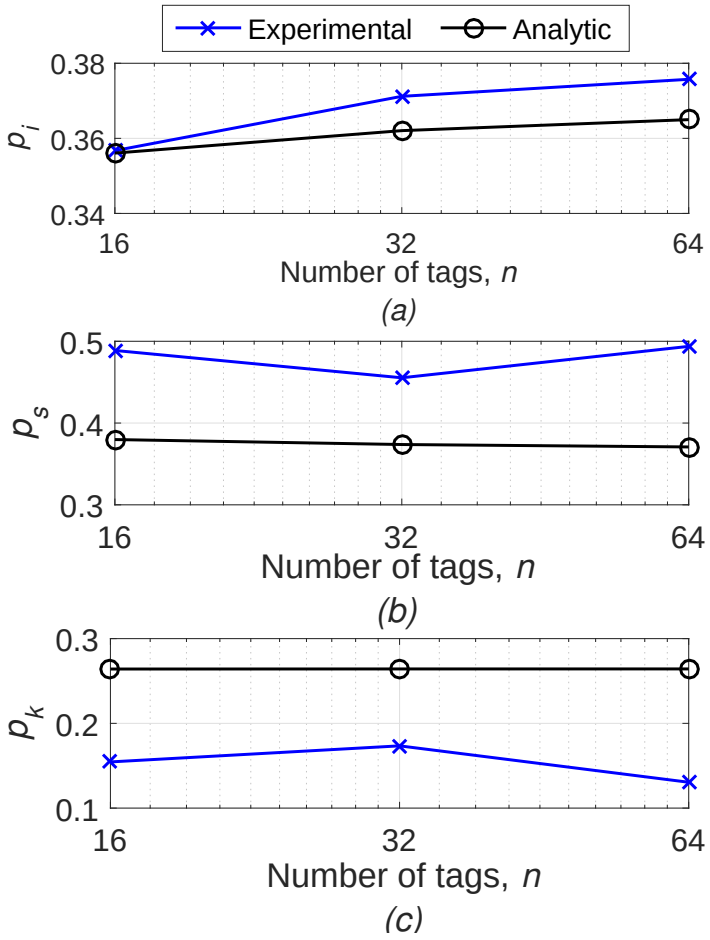

Figure 12. Comparison of the experimental and analytic performance evaluation of an ideal DFSA (L=n) as a function of n. (a) probability of idle slot, (b) probability of single slot, and (c) probability of collision slot. Analytic results are obtained with (5), (7), and (9).

Experimental results for the average time to identify one tag, obtaining it with (12) and with the timer, are averaged and showed in Figure 13.

It is appreciated that the lowest experimental and analytic time to identify one tag is obtained for the highest n=64, the highest tag set size evaluated. Also, the results obtained by calculating it with the timer are higher than the values calculated with (12), because the reader spends some extra time doing computation tasks.

In conclusion, the experimental results of the ideal DFSA show an improvement in the $throughput$ and the tag identification time in relation to the analytic values. This occurs due to a lower probability of collision slots in the physical scenario evaluated.

5.3. Slot Counter Protocol

In most real RFID applications, the ideal DFSA is not feasible, because the reader does not know the number of tags inside the interrogation zone at any time during an inventory round. Therefore, the value of n_u is unknown. In this case, a non-ideal

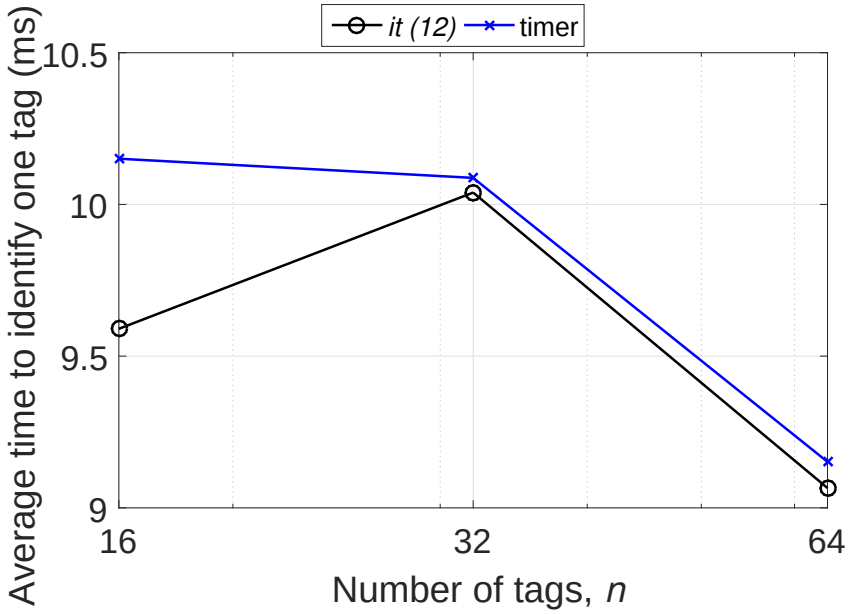

Figure 13. Comparison of the experimental and analytic time to identify one tag for an ideal DFSA (L=n) varying n from 16 to 64.

DFSA anti-collision protocol is applied to adjust the frame size according to the tags' responses within a frame. To evaluate a practical application, this section evaluates the performance of the Slot Counter protocol [13] using C=0.3.

Three different initial frame sizes L_o are evaluated for each group of tags by selecting three different values for the initial Q, named Q_o (L_o=$2^{round(Q_o)}$). The values used are Q_o=$log_2(n)-1$, Q_o=$log_2(n)$, and Q_o=$log_2(n)+1$. First, the $throughput$ and the average time to identify one tag are evaluated for 100 valid inventory rounds. Results are averaged and showed in Figure 14 and Figure 15, respectively.

Figure 14 shows that the experimental $throughput$ greatly varies with n. On the one hand, the value Q_o=$log_2(n)-1$ results in the highest $throughput$ for a smaller n. On the other hand, the value Q_o=$log_2(n)+1$ results in the highest $throughput$ for a bigger n.

Figure 15 shows that the lowest time to identify one tag is reached when Q_o=$log_2(n)+1$, that is, when the initial frame size is greater than the initial tag population size. Also, the value of the identification time obtained by calculating it with the timer is higher than that obtained with (12), as expected, because the PC requires some time for the processing and calculations tasks. Next, in the same scenario, it is also evaluated the number of idle and collision slots. Results are showed in Figure 16.a and 16.b, respectively.

From this figure, it can be justified that the improvement in the time to identify one tag for the Slot Counter protocol when Q_o=$log_2(n)+1$ comes from the reduction in the number of collision slots. For this Q_o value, it is obtained the highest number of idle slots. However, the duration of an idle slot is shorter than that of a collision slot, and thus its impact over the identification time is lower than that of a collision slot. The Slot Counter protocol presents, on average, the highest number of collision slots when Q_o=$log_2(n)-1$ because tags have a fewer number of initial slots to select

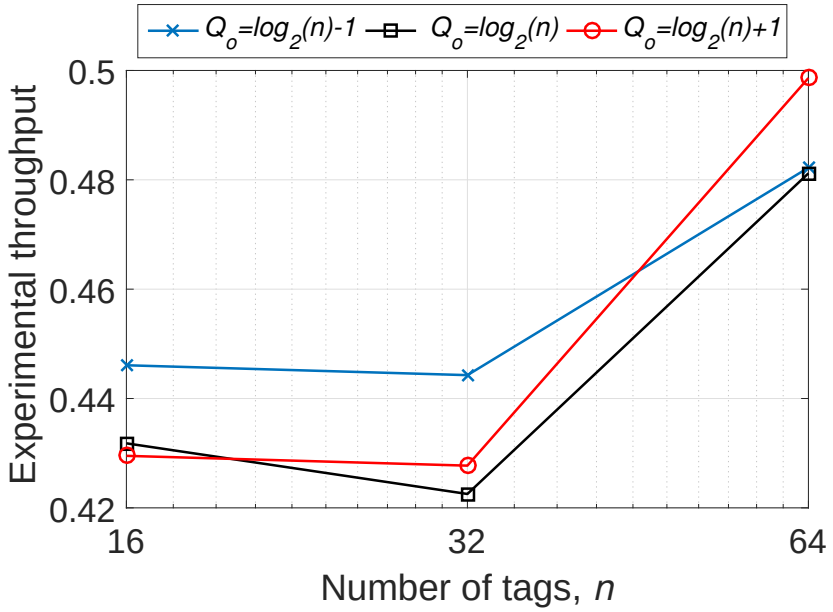

Figure 14. Experimental $throughput$ for Slot Counter protocol for three initial frame sizes, varying n from 16 to 64, with C=0.3.

to transmit their response and thus initial collisions are more likely to occur.

In most RFID applications, the number of tags is unknown for the reader, and n might vary with time. For this reason, the proposed SDR system provides a useful platform for evaluating the performance of DFSA protocols, such as the Slot Counter protocol, in a real scenario for different configuration parameters.

6. Conclusion

After providing a brief introduction of RFID technology, this chapter has analyzed and classified the most significant Dynamic Frame Slotted Aloha (DFSA) anti-collision protocols according to their frame size update strategy followed by a discussion of their physical implementation capabilities in a real scenario. From the presented analysis of anti-collision protocols, it is clear that researchers have studied DFSA protocols extensively. Current research on this type of protocols is focusing on obtaining faster and more accurate tag estimators to update L accordingly, and in developing protocols which consider some physical layer effects.

Next, an SDR RFID system has been presented to evaluate the performance of DFSA protocols following EPC C1G2 requirements in a real scenario. The proposed SDR system has been validated with an experimental implementation and evaluation of two DFSA anti-collision protocols using off-the-shelf RFID tags.

From the experimental analysis of the ideal DFSA anti-collision protocol performed in this chapter, it has been demonstrated that its performance is strongly influenced by the frame size. Also, performance improvements have been observed in relation to the analytical values. From the experimental evaluation of the Slot Counter protocol, it can be concluded that its performance is greatly influenced by the initial

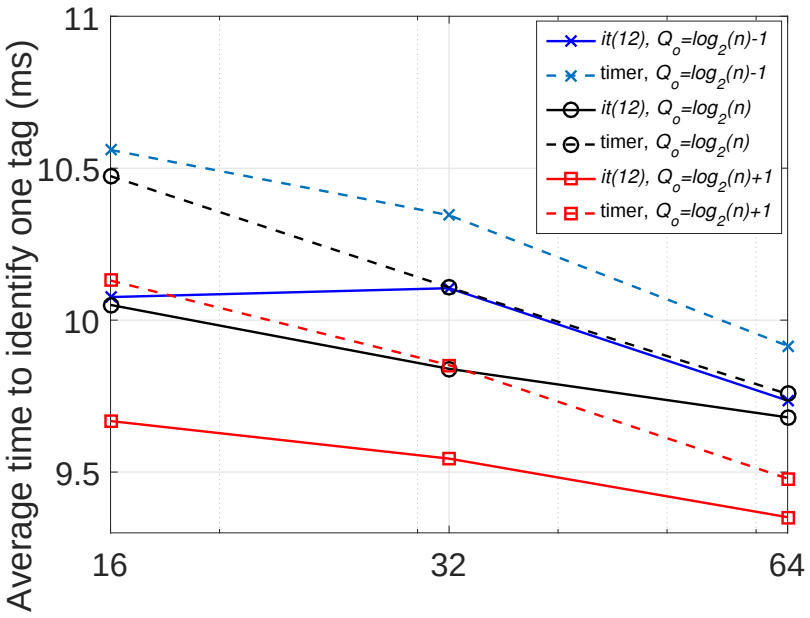

Figure 15. Average experimental time to identify one tag for Slot Counter protocol for three initial frame sizes, varying n from 16 to 64, with C=0.3.

frame size and by the number of tags inside the interrogation zone.

The improvement capacity of the proposed SDR RFID system is clear. Additional signal processing could be added to effectively differentiate between single and collision slots by analyzing the received $RN16$ response. As a result, the reader will not need to transmit an ACK if a collision is detected, decreasing the duration of collision slots. Also, new functionalities could be implemented in the proposed SDR RFID system by re-configuring the reader and programing an SDR tag, such as WISP tags, to interpret the additional reader commands. The resulting system could open a promising research area, providing a tool for interesting new RFID applications.

References

[1] GTAI - German and Trade Investment, "Industrie 4.0 - Smart Manufacturing for the Future," November 2016.

[2] R. H. Murofushi and J. J. P. Z. S. Tavares, "Towards fourth industrial revolution impact: smart product based on RFID technology," *IEEE Instrumentation Measurement Magazine*, vol. 20, pp. 51–56, April 2017.

[3] L. Burdet, "RFID Multiple Access Methods," *Technical Report ETH Zurich*, 2004.

[4] C.-H. Quan, W.-K. Hong, and H.-C. Kim, *Performance Analysis of Tag Anticollision Algorithms for RFID Systems*, pp. 382–391. Berlin, Heidelberg: Springer Berlin Heidelberg, 2006.

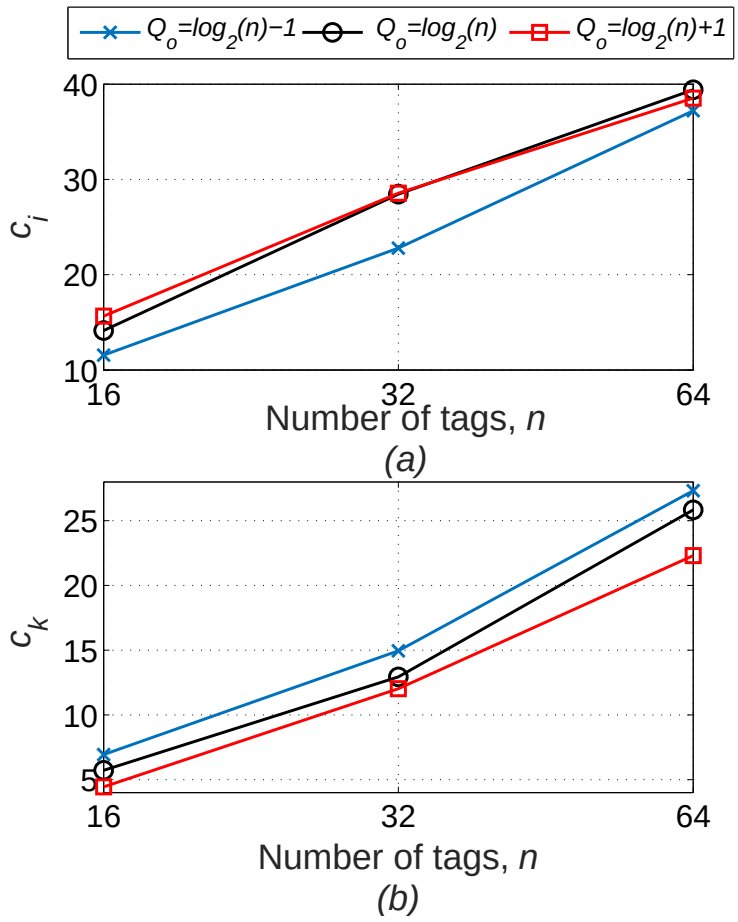

Figure 16. Experimental performance evaluation of Slot Counter as a function of n for three initial frame sizes, with C=0.3. (a) number of idle slots, (b) number of collision slots.

[5] Z. Tang and Y. He, "Research of Multi-access and Anti-collision Protocols in RFID Systems," in *International Workshop on Anti-Counterfeiting, Security and Identification (ASID)*, pp. 377–380, April 2007.

[6] M. V. Bueno-Delgado, J. Vales-Alonso, and F. J. Gonzalez-Castao, "Analysis of DFSA anti-collision protocols in passive RFID environments," in *35th Annual Conference of IEEE Industrial Electronics*, pp. 2610–2617, Nov 2009.

[7] L. Arjona, H. Landaluce, A. Perallos, P. Lopez-Garcia, and N. Cmiljanic, "Analysis of RFID anti-collision protocols based on the standard EPCglobal Class-1 Generation-2," in *21th European Wireless Conference*, pp. 1–6, May 2015.

[8] M. Buettner and D. Wetherall, "A software radio-based uhf rfid reader for phy/mac experimentation," in *2011 IEEE International Conference on RFID*, pp. 134–141, April 2011.

[9] N. Kargas, F. Mavromatis, and A. Bletsas, "Fully-coherent reader with commodity sdr for gen2 fm0 and computational rfid," *IEEE Wireless Communications Letters*, vol. 4, pp. 617–620, Dec 2015.

[10] P. Solic, Z. Blazevic, M. Skiljo, L. Patrono, R. Colella, and a. J. J. P. C. Rodrigues, "Gen2 RFID as IoT Enabler: Characterization and Performance Improvement," *IEEE Wireless Communications*, vol. 24, no. 3, pp. 33–39, 2017.

[11] P. V. Nikitin and K. V. S. Rao, "Performance limitations of passive UHF RFID systems," in *IEEE Antennas and Propagation Society International Symposium*, pp. 1011–1014, July 2006.

[12] A. P. Sample, D. J. Yeager, P. S. Powledge, A. V. Mamishev, and J. R. Smith, "Design of an rfid-based battery-free programmable sensing platform," *IEEE Transactions on Instrumentation and Measurement*, vol. 57, pp. 2608–2615, Nov 2008.

[13] "Radio Frequency Identity Protocols class-1 generation-2 UHF RFID protocol for communications at 860 MHz–960 MHz," April 2015. Version 2.0.1.

[14] V. P. Plessky and L. M. Reindl, "Review on SAW RFID tags," *IEEE Transactions on Ultrasonics, Ferroelectrics, and Frequency Control*, vol. 57, pp. 654–668, March 2010.

[15] D. Klair, C. Kwan-Wu, and R. Raad, "A survey and tutorial of RFID anti-collision protocols," *Communications Surveys Tutorials, IEEE*, vol. 12, pp. 400–421, Third 2010.

[16] J. Capetanakis, "Tree algorithms for packet broadcast channels," *IEEE Transactions on Information Theory*, vol. 25, pp. 505–515, Sep 1979.

[17] J. Su, Z. Sheng, D. Hong, and G. Wen, "An Effective Frame Breaking Policy for Dynamic Framed Slotted Aloha in RFID," *IEEE Communications Letters*, vol. 20, pp. 692–695, April 2016.

[18] Y. Chen, J. Su, and W. Yi, "An Efficient and Easy-to-implement Tag Identification Algorithm for UHF RFID Systems," *IEEE Communications Letters*, vol. PP, no. 99, pp. 1–1, 2017.

[19] K. K. Donghwan Lee and W. Lee, "Q+-algorithm: An enhanced RFID tag collision arbitration algorithm," *4th International Conference on Ubiquitous Intelligence and Computing, Hong Kong, China*, 2007.

[20] M. Daneshmand, C. Wang, and K. Sohraby, "A New Slot-Count Selection Algorithm for RFID Protocol," in *Second International Conference on Communications and Networking in China.*, pp. 926–930, Aug 2007.

[21] L. Zhu and T.-S. Yum, "The Optimal Reading Strategy for EPC Gen-2 RFID Anti-Collision Systems," *IEEE Transactions on Communications*, vol. 58, pp. 2725–2733, September 2010.

[22] J. Teng, X. Xuan, and Y. Bai, "A Fast Q Algorithm Based on EPC Generation-2 RFID Protocol," in *6th International Conference on Wireless Communications Networking and Mobile Computing (WiCOM)*, pp. 1–4, Sept 2010.

[23] L. Arjona, H. Landaluce, A. Perallos, and E. Onieva, "Fast fuzzy anti-collision protocol for the RFID standard EPC Gen-2," *IET Electronics Letters*, vol. 52, no. 8, pp. 663–665, 2016.

[24] J.-R. Cha and J.-H. Kim, "Dynamic framed slotted ALOHA algorithms using fast tag estimation method for RFID system," in *3rd IEEE Consumer Communications and Networking Conference*, vol. 2, pp. 768–772, Jan 2006.

[25] W. Chen and G. Lin, "An efficient anti-collision memethod for RFID System," *IEICE Transactions on Communications*, vol. E89, no. B, pp. 3386–3392, 2006.

[26] C. Floerkemeier and M. Wille, "Comparison of transmission schemes for framed ALOHA based RFID protocols," in *International Symposium on Applications and the Internet Workshops*, pp. 4 pp.–97, Jan 2006.

[27] W. Chen, "An Accurate Tag Estimate Method for Improving the Performance of an RFID Anticollision Algorithm Based on Dynamic Frame Length ALOHA," *IEEE Transactions on Automation Science and Engineering*, vol. 6, pp. 9–15, Jan 2009.

[28] J.-B. Eom and T.-J. Lee, "Accurate tag estimation for dynamic framed-slotted ALOHA in RFID systems," *IEEE Communications Letters*, vol. 14, pp. 60–62, January 2010.

[29] P. Solic, J. Radic, and N. Rozic, "Linearized combinatorial model for optimal frame selection in Gen2 RFID system," in *IEEE International Conference on RFID*, pp. 89–94, April 2012.

[30] P. Solic, J. Radic, and N. Rozic, "Energy Efficient Tag Estimation Method for ALOHA-Based RFID Systems," *IEEE Sensors Journal*, vol. 14, pp. 3637–3647, Oct 2014.

[31] W. T. Chen, "Optimal Frame Length Analysis and an Efficient Anti-Collision Algorithm With Early Adjustment of Frame Length for RFID Systems," *IEEE Transactions on Vehicular Technology*, vol. 65, pp. 3342–3348, May 2016.

[32] P. Solic, J. Radic, and N. Rozic, "Early Frame Break Policy for ALOHA-Based RFID Systems," *IEEE Transactions on Automation Science and Engineering*, vol. 13, pp. 876–881, April 2016.

[33] H. Vogt, "Efficient Object Identification with Passive RFID Tags," in *Pervasive Computing* (F. Mattern and M. Naghshineh, eds.), vol. 2414 of *Lecture Notes in Computer Science*, pp. 98–113, Springer Berlin Heidelberg, 2002.

[34] I. Joe and J. Lee, "A novel anti-collision algorithm with optimal frame size for RFID system," in *5th ACIS International Conference on Software Engineering Research, Management Applications*, pp. 424–428, Aug 2007.

[35] B. S. Wang, Q. S. Zhang, D. K. Yang, and J. S. Di, "Transmission Control Solutions Using Interval Estimation Method for EPC C1G2 RFID Tag Identification," in *International Conference on Wireless Communications, Networking and Mobile Computing*, pp. 2105–2108, Sept 2007.

[36] B. Knerr, M. Holzer, and C. Angerer, "Slot-by-slot minimum squared error estimator for tags populations in FSA protocols," in *in Proc. 2nd Int. EURASIP Workshop on RFID*, pp. 1–13, 2008.

[37] W.-T. Chen, "A fast anticollision Algorithm for the EPCglobal UHF class-1 generation-2 RFID standard," *IEEE Communications Letters*, vol. 18, pp. 1519–1522, Sept 2014.

[38] J. Su, Z. Sheng, D. Hong, and V. C. M. Leung, "An efficient sub-frame based tag identification algorithm for UHF RFID systems," in *IEEE International Conference on Communications (ICC)*, pp. 1–6, May 2016.

[39] P. V. Nikitin and K. V. S. Rao, "LabVIEW-Based UHF RFID Tag Test and Measurement System," *IEEE Transactions on Industrial Electronics*, vol. 56, pp. 2374–2381, July 2009.

[40] H. Landaluce, A. Perallos, E. Onieva, L. Arjona, and L. Bengtsson, "An Energy and Identification Time Decreasing Procedure for Memoryless RFID Tag Anticollision Protocols," *IEEE Transactions on Wireless Communications*, vol. 15, pp. 4234–4247, June 2016.

[41] P. Solic, J. Maras, J. Radic, and Z. Blazevic, "Comparing theoretical and experimental results in gen2 rfid throughput," *IEEE Transactions on Automation Science and Engineering*, vol. 14, pp. 349–357, Jan 2017.

[42] "A. technology ALN-9640 squiggle inlay," *Datasheet*. Accessed date April 1, 2017 [online]. Available: http://www.alientechnology.com/wp-content/uploads/Alien-Technology-Higgs-3-ALN-9640-Squiggle.pdf.

[43] J. Vales-Alonso, J. P. Muoz-Gea, J. J. Alcaraz, and F. J. Gonzlez-Castao, "Analysis of the power outage effects in rfid," *IEEE Communications Letters*, vol. 21, pp. 306–309, Feb 2017.

Table 1. Classification of state-of-the-art DFSA anti collision protocols

DFSA Protocol	**Operation**	**Update slot**	**Year**
Q+ [19]	f(Q)	every slot	2007
Enhanced Slot Count algorithm [20]	f(Q)	every slot	2007
Improved Q (IQ) [21]	f(Q)	every slot	2010
Fast Q [22]	f(Q)	every slot	2010
Slot Counter [13]	f(Q)	every slot	2007
FuzzyQ [23]	f(Q)	pointer slot	2016
DFSA with Tag Estimation Method (TEM) [24]	f($\hat{n}$)	last slot	2006
Chen and Lin [25]	f($\hat{n}$)	last slot	2006
Bayesian slot [26]	f($\hat{n}$)	every slot	2006
Chen [27]	f($\hat{n}$)	last slot	2009
Eom [28]	f($\hat{n}$)	last slot	2010
Linearized Combinational Model (LCM) [29]	f($\hat{n}$)	last slot	2012
Improved Linearized Combinational Model (ILCM) [30]	f($\hat{n}$)	last slot	2014
Early adjustment algorithm [31]	f($\hat{n}$)	pointer slot	2016
Improved Linearized Combinational Model (ILCM) SbS [32]	f($\hat{n}$)	every slot	2016
Vogt [33]	LUT(n)	last slot	2002
FSA Type C-J [34]	LUT(n)	every slot	2007
Optimal Interval Transmission Control Solution (OITCS) [35]	LUT(n)	last slot	2007
MSE based FSA [36]	LUT(n)	pointer slot	2008
Fast in-frame adjustment (FEIA) [37]	LUT(n)	pointer slot	2014
ds-DFSA [17]	LUT(n)	pointer + last slot	2016
SUBF-DFSA [38]	LUT(n)	pointer slot	2016
DS-MAP [18]	LUT(n)	pointer + last slot	2017

Table 2. SDR reader configuration parameters according to EPC C1G2 [13]

Parameter	**Value**	**Description**
$Tari$	$24\,\mu s$	Reference time interval for a data-0 symbol in reader-to-tag signaling
BLF	40 kHz	Backscatter Link Frequency
$RTcal$	$72\,\mu s$	Duration of a data-0 symbol plus a data-1 symbol
$TRcal$	$200\,\mu s$	Duration of a tag-to-reader calibration symbol
t_{DR}	$40\,kbps$	Tag data rate
R_{DR}	$27.78\,kbps$	Reader data rate
T_1	$240\,\mu s$	Time interval between a reader query and a tag response
T_2	$480\,\mu s$	Time interval between a tag transmission and a reader query
EPC length	135 bits	Number of bits of the electronic product code

APPENDIX

G

Paper VII

Experimental Validation of Anti-Collision Protocols for RFID Sensor Networks

This paper has been accepted for presentation at the workshop *"EURASIP RFID 2018"*, happening in Brno, Czech Republic, from September 11^{th} to September 12^{th} 2018. It will be published in the conference proceedings at end of the conference. The accepted version is appended here.

Experimental Validation of Anti-Collision Protocols for RFID Sensor Networks

Laura Arjona, Hugo Landaluce, Asier Perallos
Faculty of Engineering
University of Deusto
Bilbao, Spain
laura.arjona@deusto.es

Joshua R. Smith
Department of Computer Science and Engineering
University of Washington
Seattle, USA
jrs@cs.washington.edu

***Abstract*—Currently, there is an increasing interest in the use of RFID systems with passive or battery-less tags with sensors incorporated, also known as computational RFID (CRFID) systems. These passive tags use the reader signal to power up their microcontroller and an attached sensor. Following the current standard EPC C1G2, the reader must identify the tag (receive the tag's identification code) prior to receive data from its sensor. In a typical RFID scenario, several sensor tags share the reader interrogation zone, and during their identification process, their responses often collide, increasing their identification time. Therefore, RFID application developers must be mindful of tag anti-collision protocols when dealing with CRFID tags in dense RFID sensor networks. So far, significant effort has been invested in simulation-based analysis of the performance of anti-collision protocols regarding the tags identification time. However, no one has explored the experimental performance of anti-collision protocols in an RFID sensor network using CRFID. This paper: (i) demonstrates that the impact of one tag identification time over the total time required to read one sensor data from that same tag is very significant, and (ii) presents an UHF-SDR RFID system which validates the improvement of FuzzyQ, a fast anti-collision protocol, in relation to the protocol used in the current RFID standard.**

***Index Terms*—RFID, anticollision, DFSA, passive sensors, CRFID, SDR.**

I. Introduction

During the last few years Radio Frequency Identification (RFID) systems have been popularized due to their improved features over other auto identification techniques such as barcodes, or biometrics [1]. Recently, computational RFID (CRFID) systems have gained protagonism thanks to the use of sensors without the need of batteries [2], [3]. CRFID use passive or battery-less tags with sensors incorporated and are powered using the reader RF signal. A wireless sensor network using these passive sensors inherits all the benefits of RFID: passive operation, low cost, a small sticker form factor, and an operation range of over 10 meters from the reader [4].

An RFID sensor network is composed of at least one reader and several CRFID tags that include at least one sensor. The tag collision problem acquires the main focus when interrogating these tags. The communication channel is shared among them and, therefore, their responses need to be arbitrated in order to avoid simultaneous responses that will lead to collisions. This problem is one of the main cause of energy wastage and tag identification time increase. The solution to the tag collision problem is the use of an anti-collision protocol that minimizes the impact of these collisions. The existing anti-collision protocols in the literature can be classified into two main groups: tree-based and aloha-based protocols [5].

Tree-based protocols [6], in essence, split colliding tags into subsets, and further split the subsets repeatedly up to the successful response of all the tags that are within the interrogation zone.

Aloha-based protocols present four main variants [5]. In Pure Aloha (PA), a tag responds to the reader command randomly after being energized. Slotted Aloha (SA) divides time into slots and schedules tags to respond only at the boundary of the time slots. Frame Slotted Aloha (FSA) and Dynamic Frame Slotted Aloha (DFSA) divide time into frames and frames into slots and mandate each tag to respond in only one slot per frame. The most popular aloha variant is DFSA, which focuses on adjusting the frame size L so that L is adapted to the set of tags to be identified. EPCglobal Class 1 Generation 2 (EPC C1G2), the current standard in RFID systems [7], adopts a DFSA strategy. This standard, also included in ISO 18000-6C, is used in every commercial reader.

A significant amount of literature can be found on simulation-based analysis of the performance of tree-based and aloha-based anti-collision protocols [6], [8]–[11]. However, to the best of our knowledge, no experimental performance of anti-collision protocols in RFID sensor networks can be found. The particularities of an RFID sensor network involves not only the identification of all the sensors in the network, but also the time needed to read all those sensors. The presented work analyzes the relevance of these two processes and the time involved, and presents the experimental performance of an RFID sensor network with CRFID tags using two different aloha-based anti-collision protocols from the literature: Slot Counter [7] and FuzzyQ [10]. The Slot Counter is the reference protocol in RFID technology, because it is used in the standard EPC C1G2. The FuzzyQ protocol is also evaluated because it achieves a more abrupt variation of the frame size than Slot Counter, adapting faster to a dynamic tag population. Thus, FuzzyQ is a suitable candidate for RFID sensor networks, where fast and dynamic tags identification is sought. Thus, this paper contains the following two contributions:

- An analysis of the time needed to identify a tag (receive its Electronic Product Code (EPC)) with respect to the time needed to read its sensor.
- A comparative of the performance evaluation of two anti-collision protocols physically implemented with an UHF-SDR RFID experimentation hardware. The evaluation is made in terms of their tag identification rate.

The rest of the paper is organized as follows. Section II describes the background for the presented analysis and experimentation. Section III analyses the relation between the time required to identify one tag and the time to read its sensor. Section IV presents the implementation of Slot Counter and FuzzyQ protocols. The performance evaluation of the implementation of both protocols is given in Section V. And finally Section VI concludes this paper.

II. Background

First, some definitions are provided to properly set the background of this paper and to better understand its main contributions. After this, the two anti-collision protocols implemented in this work are presented: Slot Counter and FuzzyQ.

- *Sensor tag*: it refers to an RFID tag with an integrated sensor, such as an accelerometer.
- *Tag identification*: it refers to the whole needed process to read the tag identifier or EPC.
- *Slot*: period of time that separates the tags' responses. Conventionally, three types of slots are considered, in terms of the tags' responses to the reader's commands: single (only one tag replies), collision (more than one tag replies in the same slot), and idle (none of the tags reply).
- *Frame*: sequence of L slots, where L represents the frame size. An identification process is composed of a set of frames and tags can respond in only one slot per frame.
- *Inventory round*: the period of time that begins when the reader transmits the initial command, and ends when the reader interrupts the identification process and the tags loose their state. This work assumes that an inventory round ends when all the tags in the reader interrogation zone have been identified.

A. Slot Counter from EPC C1G2

EPC C1G2 specifies a DFSA protocol to arbitrate collisions: the Slot Counter protocol. The reader starts the identification process by transmitting a Query (Qc) command. After the first tags' response, the reader alternates between QueryAdjust (QA) and QueryRep (QR) commands. QA starts a new frame with the updated size L and implies that tags must randomly select a slot in the frame (the initial value of their internal slot counter SC), while QR tells the tags to decrement SC. Thus, when SC=0, the tag transmits a 16-bit random number $RN16$.

The frame size is set as L=2^Q, and its value is dynamically updated with the parameters Q and C, where Q=round(Qfp), and Qfp is updated according to the time slot occupancy with the value of C:

- Single slot: Q_{fp} remains unchanged. In this case, the reader replies to the tag with an acknowledge (ACK) command followed by the same $RN16$ received by the tag; and the tag transmits its EPC.
- Collision slot: $Q_{fp} = Q_{fp} + C$.
- Idle slot: $Q_{fp} = Q_{fp} - C$.

The standard does not specify the selection of C. It only recommends using high C values if the previous Q value was low and vice versa, in the range of $[0.1, 0.5]$.

B. FuzzyQ protocol

The protocol FuzzyQ was introduced in [10] for fast RFID tag identification. This protocol follows a similar procedure to the standard EPC C1G2 but integrates a fuzzy logic controller to update L considering the current Q and the collision or idle rate of the current frame. As a result, FuzzyQ significantly decreases the tag identification time by efficiently updating L in a dynamic and adaptive way.

A fuzzy rule based system (FRBS) is defined to model the current Q and the idle or collision rate as fuzzy sets to adaptively calculate L. At slot p=$L/9$ of every frame, L is updated with the FRBS. The value of p is analyzed and set in [10]. Then, a new frame is started if L is modified. Otherwise, the reader continues the identification process in the following slot. Fig. 1 shows a flowchart of FuzzyQ protocol. It achieves an average improvement of 7% in the tag identification time with respect to Slot Counter protocol [10].

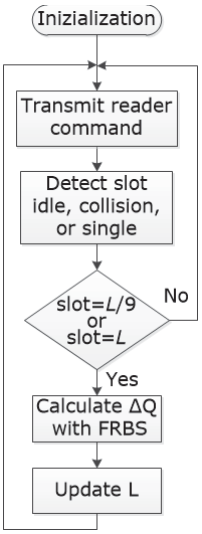

Fig. 1. Flowchart of FuzzyQ protocol

III. Tags identification in RFID sensor Networks

Following EPC C1G2 standard, the reader must identify a tag (receive the tag's EPC) prior to read data from its sensor. The time associated to these two processes is shown in Fig. 2. This section studies the effect of the time needed to identify all the tags inside the reader interrogation area (identification time) over the time needed to read all the tags' sensor (sensing time), in the single and multiple-tag environment.

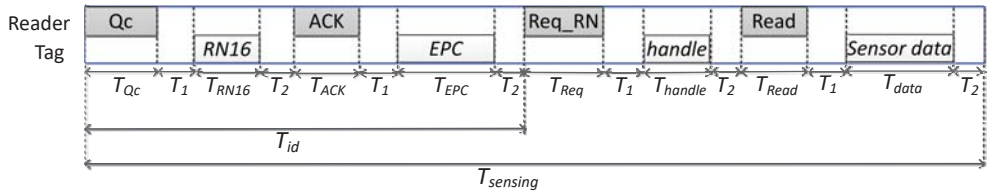

Fig. 2. Definition of tag sensor identification time and sensing time

First, a scenario with a single reader and a single tag inside the reader's interrogation zone is assumed. According to Fig. 2, the time required to identify one tag T_{id} is calculated as:

$$T_{id} = T_{Qc}+T_1+T_{RN16}+T_2+T_{ACK}+T_1+T_{EPC}+T_2, \quad (1)$$

and the time required to read one sensor data from a tag $T_{sensing}$ is calculated as

$$T_{sensing} = T_{id}+T_{Req}+T_1+T_{handle}+T_2+T_{Read}+T_1+T_{data}+T_2, \quad (2)$$

The parameters T_{Qc}, T_{ACK}, T_{Req}, and T_{Read} refer to duration of the reader's transmitted commands Qc, ACK, Req_RN, or Read, respectively, specified by the EPC C1G2 standard [7]. The parameters T_{RN16}, T_{EPC}, T_{handle}, and T_{data} refer to the duration of the tags' responses $RN16$, EPC, $handle$, and *sensor data*, respectively. Finally, T_1 refers to the time interval between a reader command and a tag response, while T_2 refers to the time interval between a tag transmission and a reader command. Table I summarizes the calculation of the reader and tags messages duration.

The duration of the reader's commands is calculated as the Reader-to-Tag synchronization time $T_{FSync_{RT}}$ or $T_{Preamb_{RT}}$, also defined in [7], plus the length in bits of each parameter divided by the reader data rate DR_r, calculated as DR_r=$1/((T_{data_0} + T_{data_1})/2)$, where T_{data_0}=$Tari$, and T_{data_1}=1.5·$Tari$. $Tari$ represents the reference time interval for a data-0 transmission. Thus, T_{Qc}=$T_{FSync_{RT}}$+$22/DR_r$, T_{ACK}=$T_{FSync_{RT}}$+$24/DR_r$, T_{Req}=$T_{Preamb_{RT}}$+$40/DR_r$, and T_{Read} =$T_{Preamb_{RT}}$+$58/DR_r$.

The duration of the tags' responses is calculated as the length in bits of each message (which includes the 6 bits of the Tag-to-Reader Preamble) divided by the tag data rate DR_t, calculated as DR_t=BLF/M, where BLF refers to the Backscatter-Link-Frequency, and M refers the number of subcarrier cycles per symbol. This work assumes that tags encode the backscattered data as FM0 baseband (M=1). Thus, DR_t=BLF, T_{RN16}=$23/BLF$, T_{EPC}=$135/BLF$, and T_{handle}=$38/BLF$. To calculate T_{data}, a WISP 5.1 tag [2] with an incorporated accelerometer sensor is considered. For this tag, a sensor read corresponds to 32 bits, and T_{data}=$71/BLF$.

From Fig. 2, it is clear that the time required to identify one tag plays a significant role in the total time required to read one sensor data. To evaluate the effect of T_{id} over $T_{sensing}$, it is defined the factor F as the fraction of a sensor tag identification time over the total time required to receive one sensor data

$$F = \frac{T_{id}}{T_{sensing}}. \quad (3)$$

TABLE I
EPC C1G2 TIMING PARAMETERS TO READ ACCELEROMETER SENSOR DATA FROM A WISP 5.1

Parameter	Description	Calculation
T_{data_0}	Reader data-0 duration	$Tari$
T_{data_1}	Reader data-1 duration	1.5·$Tari$
$T_{FSync_{RT}}$	Frame Sync. duration	T_{del}+T_{data_0}+$RTcal$
$T_{Preamb_{RT}}$	Reader Preamble duration	T_{del}+T_{data_0}+$RTcal$+$TRcal$
DRr	Reader data rate	$1/((T_{data_0} + T_{data_1})/2)$
DRt	Tag data rate	BLF/M
T_{Q_c}	Qc command duration	$T_{FSync_{RT}}$+$22/DR_r$
T_{QA}	QA command duration	$T_{Preamb_{RT}}$+$9/DR_r$
T_{QR}	QR command duration	$T_{Preamb_{RT}}$+$4/DR_r$
T_{ACK}	ACK command duration	$T_{FSync_{RT}}$+$24/DR_r$
T_{Req}	Req_RN command duration	$T_{Preamb_{RT}}$+$40/DR_r$
T_{Read}	Read command duration	$T_{Preamb_{RT}}$+$58/DR_r$
T_{RN16}	Tag $RN16$ duration	$23/BLF$
T_{EPC}	Tag EPC duration	$135/BLF$
T_{handle}	Tag $handle$ duration	$38/BLF$
T_{data}	Tag sensor $data$ duration	$71/BLF$

Next, F is evaluated and its upper and lower bound are calculated. For this purpose, it is considered a reader with an application-specific configuration following EPC C1G2 standard, and a WISP 5.1 tag. Evaluating (3) with (1) and (2), and grouping some terms, it is obtained

$$\begin{aligned} F &= \frac{T_{R_1} + b_1/BLF + t}{T_{R_1} + T_{R_2} + (b_1 + b_2)/BLF + 2t} \\ &= \frac{BLF(T_{R1} + t) + 1.45b_2}{BLF(T_{R_1} + T_{R_2} + 2t) + 2.45b_2)} \end{aligned} \quad (4)$$

where b_1=158 bits, b_2=109, bits, b_1=$1.45b_2$, t=$2(T_1$+$T_2)$, T_{R_1}=T_{Qc}+T_{ACK}, and T_{R_2}=T_{Read}+ T_{Req}.

The upper and lower bound of F are obtained by considering the slowest (lowest BLF) and fastest tag (highest BLF) configuration, respectively. The upper bound of F as BLF approaches 0 is

$$\lim_{BLF \to 0} F = \frac{1.45k_2}{2.45k_2} = 0.59. \quad (5)$$

And the lower bound of F as BLF approaches infinity is

$$\lim_{BLF \to \infty} F = \frac{T_{R_1} + t}{T_{R_1} + T_{R_2} + 2t}. \quad (6)$$

The results obtained in (5) and (6) show that F is upper bounded to 59%, and the lower bound depends on the link-timing-parameters (T_1 and T_2), and on the reader application-specific configuration.

Next, (6) is evaluated for BLF=640kHz, the highest value allowed by EPC C1G2, considering two scenarios: i) slow reader, with $Tari$=25μs, T_1=77μs, and T_2=32μs; and ii) fast reader, with $Tari$=6.25μs, T_1=16.8μs, and T_2=4.69μs. For scenario i), the value obtained is $\lim_{BLF\to\infty} F = 32.4\%$, and for ii), it is obtained $\lim_{BLF\to\infty} F = 33.7\%$.

In summary, it can be concluded that the vale of F is upper-limited to 59%, and its lower bound varies between 32.4% and 33.7%, depending on the reader configuration. It can be appreciated that the impact of one tag identification time over the total time required to read one sensor data from that same tag is very significant.

In an RFID scenario, there is typically more than one sensor tag inside the reader interrogation zone, and tags' $RN16$ messages often collide when responding to the reader commands. As a result, tags must re-transmit their $RN16$ in the same inventory round. In order to receive the data from a particular tag sensor, there is a very high probability that the reader will receive several $RN16$ messages from that tag. This will increase not only T_{id} but also $T_{sensing}$ and F.

In conclusion, the impact of the tags identification time over the total time required to read their sensor data is very significant. Therefore, anti-collision protocols are a key component of RFID sensor networks. The next section presents the physical implementation feasibility of the protocol used in the current standard, the Slot Counter, and a faster protocol, the FuzzyQ, in a real RFID scenario.

IV. Implementation of Slot Counter and FuzzyQ for RFID sensor networks

The Slot Counter and FuzzyQ anti-collision protocols have been implemented in a Software Defined Radio-Ultra High Frequency RFID (SDR-UHF RFID) system, consisting of an SDR reader, and WISP 5.1 tags. The reader uses the software modules of the system presented in [12] (source, matched filter, gate, decoder, and reader), modified to communicate with WISP 5.1 tags. These software modules are built on GNU radio 3.7.11, and extended functionalities have been added to them, highlighting the differentiation of idle and collision/success tags responses, anti-collision capabilities, and the implementation of additional reader commands. Because this reader is software-defined, FuzzyQ and Slot Counter (and many other DFSA protocols based on EPC C1G2) can be implemented by writing user-level software in C++.

A. Slot Counter implementation

This work presents an SDR RFID reader capable of communicating with accelerometer sensors included in WISP tags (version 5.1), and it is composed of an USRP N210, an SBX daughterboard, and a Linux PC. A Gigabit switch is used to communicate the USRP with the Linux PC. The transmit and receive ports of the daughterboard are connected to two circularly polarized patch antennas of 6dBi gain. The system is presented in Fig. 3.

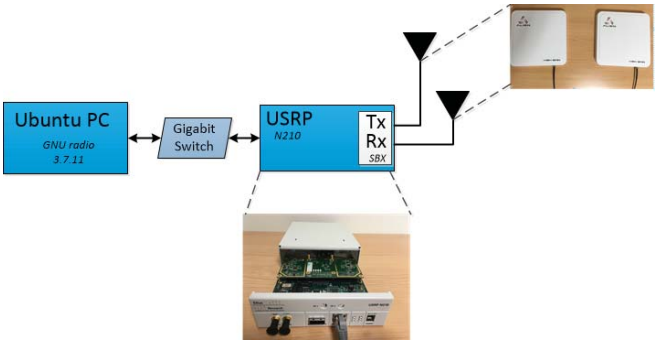

Fig. 3. A system description of the SDR-RFID reader

In order to differentiate between the three types of slots, a threshold energy value E_{th} is set for the energy of the received signal E_r to detect an idle response. Thus, an idle slot occurs when the energy of the received signal is lower than this threshold, that is, when E_r<E_{th}. This is shown in Fig. 4

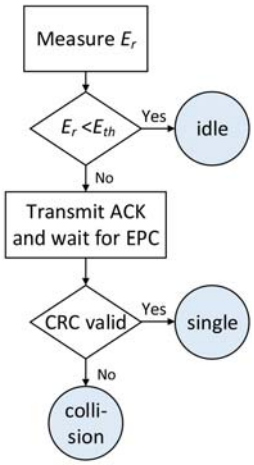

Fig. 4. Slot type differentiation in the proposed SDR-reader.

The Slot Counter protocol has been implemented using the value C=0.2. Regarding the tag-side implementation, WISP 5.1 tags have been used. They have been programmed to follow EPC C1G2 standard and to backscatter the information at 160kHz. Additionally, they have been re-programmed to i) transmit $RN16$ just at one slot per frame, and ii) stay idle until the reader starts a new inventory round once they are identified (transmitted their EPC).

B. FuzzyQ Implementation

FuzzyQ has been implemented in the reader presented in Fig. 3. This protocol presents a fast strategy to read RFID tags by not limiting the variation of Q to steps of one unit and considering instead a range of values, in order to achieve a more abrupt step size (0, $\pm$1, $\pm$2, or $\pm$3). In order to consider

these 7 different step size values, the reader QA command, as defined in the EPC C1G2 standard, needs to be modified.

According to EPC C1G2, the field $UpDn$ of QA command consists of 3 bits and it determines whether and how the tag adjusts Q, as shown in Table II. From this table, it is clear that Q can only be modified in steps of one unit.

TABLE II
QUERYADJUST COMMAND [7]

	Command	Session	UpDn
# of bits	4	2	3
Description	1001	00: S0 01: S1 10: S2 11: S3	110: Q=Q+1 000: no change to Q 011: Q=Q-1

The protocol FuzzyQ introduces the parameter ΔQ which represents the variation of Q. This protocol takes advantage of the 3-bits-length of the field $UpDn$, and considers 7 different variations in Q: Q=Q, Q=$Q\pm1$, Q=$Q\pm2$, and Q=$Q\pm3$. In order to consider all the possibilities, the modified QueryAdjust command is defined as mQA, by extending the values of the field $UpDn$. The specification of mQA is shown in Table III.

TABLE III
MODIFIED QUERYADJUST COMMAND

	Command	Session	UpDn
# of bits	4	2	3
Description	1001	00: S0 01: S1 10: S2 11: S3	000: no change to Q 001: Q = Q-3 010: Q = Q-2 011: Q = Q-1 100: Q = Q+3 101: Q = Q+2 110: Q = Q+1

Regarding the tag-side, WISP 5.1 tags have been used to validate FuzzyQ in a real scenario under EPC C1G2 requirements. They have been programmed to backscatter the information at 160kHz, and their firmware has been updated to interpret mQA. Additionally, they have been re-programmed to i) transmit $RN16$ just at one slot per frame, and ii) stay idle until the reader starts a new inventory round once they are identified.

V. EXPERIMENTAL RESULTS

This section evaluates and compares the performance of Slot Counter and FuzzyQ anti-collision protocols running in the proposed SDR-UHF RFID system. This system consists of the reader shown in Fig. 3, and 4 WISP tags placed 1m away from the reader's antennas. The transmission model for the proposed RFID hardware, meeting EPC C1G2 requirements, is shown in Fig. 5. The duration of each type of slot, single, collision, and idle, is referred to as T_s, T_k, and T_i, respectively.

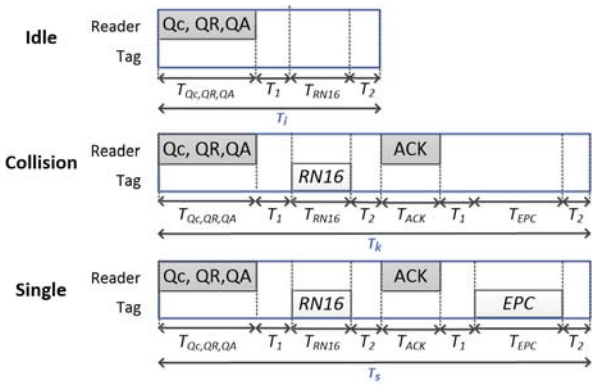

Fig. 5. Transmission model of the proposed SDR system

It is appreciated that a single and collision slot have the same duration. The duration of each type of slot is obtained as:

$$T_k = T_s = T_{Qc,QR,QA}+T_1+T_{RN16}+T_2+T_{ACK}+T_{EPC}+T_2, \quad (7)$$

and

$$T_i = T_{Qc,QR,QA} + T_1 + T_{RN16} + T_2. \quad (8)$$

The parameters of the implemented RFID system are presented in Table IV. First, the tag identification rate TIR is evaluated, and the experimental results are compared with simulated results for denser tag sets. Then, the parameter F is evaluated for both anti-collision protocols via simulation under different sizes of tag sets, from 4 to 1024 tags.

TABLE IV
PARAMETERS OF THE IMPLEMENTED RFID SYSTEM

Parameter	Value
BLF	160 kHz
$Tari$	12.5 μs
$T_{delimeter}$	12.5 μs
$RTcal$	36.6 μs
$TRcal$	50 μs
T_1	56 μs
$T_{2_{RN16}}$	253 μs
$T_{2_{epc}}$	352 μs
Divide Ratio (DR)	8
Num. of subcarrier cycles per symbol (M)	1
Initial Q	1
Transmission frequency	915 MHz
Transmission power	180 $mWatts$

A. Analysis of T_2

Considering BLF=160kHz, the maximum value of T_2 allowed by EPC C1G2 is $T_{2_{max}}$=120μs. After $T_{2_{max}}$, a commercial tag ignores the next reader command. In the presented system, the reader needs an average of $T_{2_{RN16}}$ after the reception of $RN16$ to process the tag's response and to transmit ACK. Also, the reader needs an average $T_{2_{epc}}$ after the reception of EPC to process the tag's response and to

transmit the next command. The experiments performed in this work showed that $T_{2_{EPC}} > T_{2_{max}}$, and $T_{2_{RN16}} > T_{2_{max}}$. This occurs because the USRP and GNU radio require a higher processing time than a commercial reader. However, a WISP tag will ignore this $T_{2_{max}}$ requirement imposed by EPC C1G2, and it will keep waiting for the next reader command after $T_{2_{max}}$. In conclusion, the values $T_{2_{RN16}}$ and $T_{2_{epc}}$ will be used in the protocols evaluation metrics.

B. Evaluation of the Tag Identification Rate

The performance of FuzzyQ is validated and compared with Slot Counter by measuring the Tag Identification Rate TIR metric, defined as the total number of tags identified per second. Experimental results have been obtained using 4 WISPs, following two different approaches:

- *analytical*: TIR is measured as the total number of tags identified divided by the total identification time. This time is calculated by measuring the number of transmitted reader commands (*Qc*, *QA*, *QR*, *ACK*, *Req_RN*, and *Read*), and the received tags' responses (RN16, EPC), and multiplying them by their corresponding duration, which the reader knows a priori.
- *timer*: TIR is measured as the total number of tags identified divided by the total identification time obtained with a software timer. For this purpose, a timer is started in the reader program when the reader transmits the first command Qc, and it is stopped when the reader correctly identifies the four tags present inside its interrogation zone. With this approach, the experimental results also provide information about the reader processing time.

Experimental results are shown in Fig. 6 and compared with simulation results for n=4. Clearly, FuzzyQ improves TIR in relation to Slot Counter. Additionally, experimental results obtained by calculating TIR with the timer are higher than the values calculated analytically, as expected, because the SDR system requires some time for the processing and calculations tasks. Analytical TIR is higher than simulation TIR for both protocols, because capture effect [1]contributes to a reduction in the number of collision slots c_k.

Next, both protocols have been compared by simulation for higher tag set sizes up to n=1024. Simulation results have been obtained with Matlab R2017a. In the simulation scenario, tags are assumed to be uniformly distributed and physical-layer effects are not considered. In order to get a fair comparison between the experimental and simulation results, the transmission model for the proposed SDR reader, shown in Fig. 5, has been used for the simulation scenario. The simulation responses have been averaged over 1000 iterations for accuracy in the results. The results are shown in Fig. 7, where it is appreciated a small increase in TIR with increasing n for the two protocols evaluated. Also, the improvement of

[1]Physical layer effect which is very common in RFID systems. Tags response amplitudes can vary due to different distances from the reader antenna, or due to multi-path fading present in the channel [13]. As a result, the reader successfully resolves one tag reply in a collided slot.

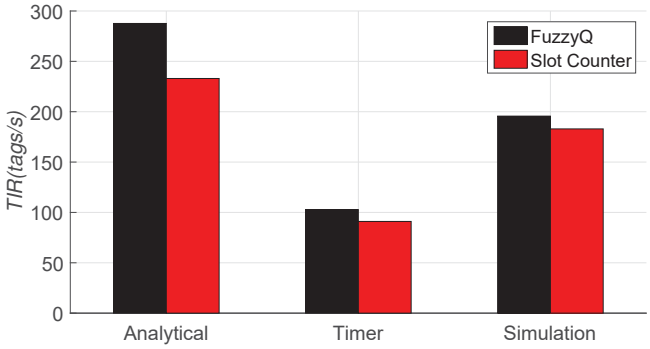

Fig. 6. Comparison of simulated and experimental (analytical and timer) TIR of FuzzyQ and Slot Counter for n=4.

FuzzyQ with respect to Slot Counter in maintained for n from 4 to 1024.

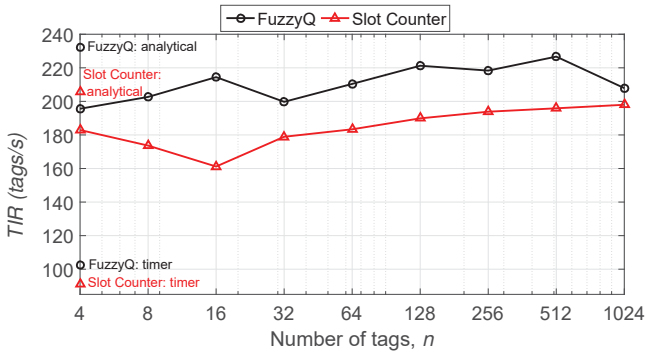

Fig. 7. Comparison of simulated TIR as a function of n for FuzzyQ and Slot Counter. Experimental results are included for n=4.

Next, the total number of collision and idle slots are evaluated for n=4. Experimental and simulation results are compared in Fig. 8. This figure shows the ability of FuzzyQ to reduce the number of collision slots by using mQA, at the expense of a higher number of idle slots. Additionally, this figure shows that the capture effect contributes to a reduction in experimental c_k with respect to the simulation c_k, for the two protocols evaluated.

Finally, this section compares and evaluates the total number of reader commands QA (mQA for FuzzyQ) and QR in one inventory round, referred to as tQA and tQR, respectively. Experimental and simulation results for n=4 are shown in Fig. 9. Clearly, FuzzyQ reduces the number of QR commands, at the expense of a higher number of mQA commands.

C. Evaluation of F

This section evaluates the parameter F (3) considering the RFID system presented in Section IV, using the parameters of Table IV.

1) Single tag environment: First, F is evaluated for the single tag environment, considering one WISP 5.1 tag with an accelerometer sensor incorporated. Evaluating (3), it is obtained F=43.89%. This result shows that about half of

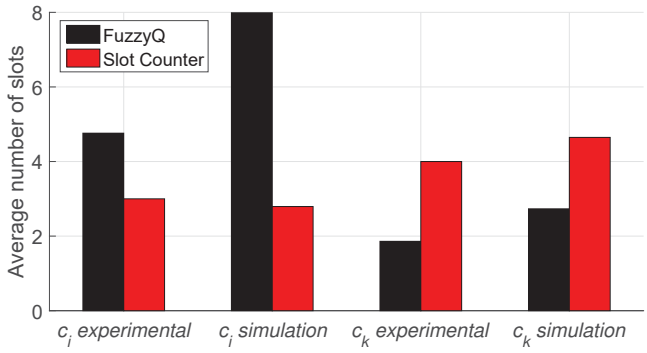

Fig. 8. Comparison of experimental and simulated c_i and c_k of FuzzyQ and Slot Counter for n=4.

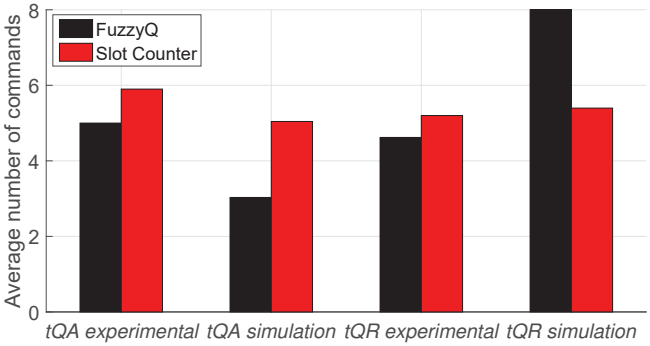

Fig. 9. Comparison of experimental and simulated tQA and tQR of FuzzyQ and Slot Counter for n=4.

the time required to read one accelerometer sensor data is employed in identifying the tag (receiving the EPC). Furthermore, this value falls between the lower bounds and upper bound of F obtained in Section III.

2) Multiple-tag-environment: Next, F is evaluated for the multiple tag environment. For this purpose, it is defined the factor F_n as total time required to identify n sensor tags (T_{id_n}) divided by the total time to read one sensor data from each one of the n sensors ($nT_{sensing}$)

$$F_n = \frac{T_{id_n}}{nT_{sensing}}. \tag{9}$$

The parameter T_{id_n} is obtained by simulation, by measuring the total time required by the protocol to identify n tags. The parameter $T_{sensing}$ is also obtained by simulation. Evaluation results are obtained with Matlab R2017a, defining a scenario where tags are assumed to be uniformly distributed. Simulation results are obtained for n from 4 to 1024 tags. The simulation responses have been averaged over 1000 iterations for accuracy in the results. Results are shown in Fig. 10.

This figure shows that FuzzyQ presents a lower F_n than Slot Counter, due to the ability of FuzzyQ to reduce the number of collision slots per tag with mQA command, as shown in Fig. 8. Finally, it is appreciated that most of the values of F_n in Fig. 10 overpass the upper limit of F (59%) because tags

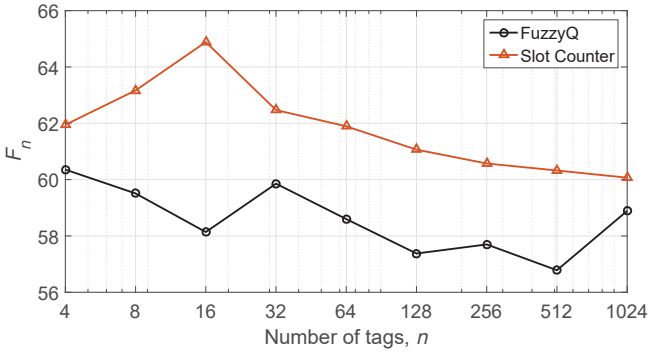

Fig. 10. Comparison of simulated F_n as a function of n for FuzzyQ and Slot Counter.

experience collisions in a multiple tag identification scenario, increasing the tags identification time.

D. Identified limitations and Future work

Given the capabilities of the hardware used, several problems have been found to fluently identify more than 4 WISP tags in the reader interrogation range. As a result, it was not possible to obtain a strong set of data streamed from bigger sets of WISP tags. The main reason for this behaviour was the low transmission power of the reader, which provided a weak transmission channel prone to detection errors and reading transmission errors. A possible solution to strengthen the communication among the reader and the WISP tags is to include a power amplifier before the transmission antenna in order to increase the antenna range. This modification will increase the power transmitted allowing the reader to interrogate a higher number of tags at a higher distance and it is proposed as future work.

VI. Conclusion

The experimentation of two anti-collision protocols, the Slot Counter and the FuzzyQ, has been performed and analyzed using an SDR-UHF RFID system. The aim of the experimentation was to compare two anti-collision protocols from a physical implementation perspective and to show the relevance of the identification phase of an RFID sensor network with respect to the sensing phase. For this last step, several simulations have been provided showing that in a multiple tag scenario of an RFID sensor network, the identification time represents more than 59% of the sensing time. In other words, the time required to identify one tag represents more than half of the total time to read one sensor data. To conclude, anti-collision protocols constitute an important and relevant part of the process of reading RFID sensors.

References

[1] K. Finkenzeller, *RFID Handbook: Fundamentals and Applications in Contactless Smart Cards and Identification*. New York, NY, USA: John Wiley & Sons, Inc., 2 ed., 2003.

[2] A. P. Sample, D. J. Yeager, P. S. Powledge, A. V. Mamishev, and J. R. Smith, "Design of an RFID-Based Battery-Free Programmable Sensing Platform," *IEEE Transactions on Instrumentation and Measurement*, vol. 57, pp. 2608–2615, Nov 2008.

[3] (2016) UMich Moo. [Online]. Available: http://spqr.cs.umass.edu/moo.
[4] H. Aantjes, A. Y. Majid, P. Pawe?czak, J. Tan, A. Parks, and J. R. Smith, "Fast downstream to many (computational) RFIDs," in *IEEE INFOCOM 2017 - IEEE Conference on Computer Communications*, pp. 1–9, May 2017.
[5] D. Klair, C. Kwan-Wu, and R. Raad, "A survey and tutorial of RFID anti-collision protocols," *Communications Surveys Tutorials, IEEE*, vol. 12, pp. 400–421, Third 2010.
[6] H. Landaluce, A. Perallos, E. Onieva, L. Arjona, and L. Bengtsson, "An Energy and Identification Time Decreasing Procedure for Memoryless RFID Tag Anticollision Protocols," *IEEE Transactions on Wireless Communications*, vol. 15, pp. 4234–4247, June 2016.
[7] "Radio Frequency Identity Protocols class-1 generation-2 UHF RFID protocol for communications at 860 MHz–960 MHz," April 2015. Version 2.0.1.
[8] C. Angerer, R. Langwieser, and M. Rupp, "RFID Reader Receivers for Physical Layer Collision Recovery," *IEEE Transactions on Communications*, vol. 58, pp. 3526–3537, December 2010.
[9] Y. Chen and F. h. Zhang, "Study on Anti-collision Q Algorithm for UHF RFID," in *2010 International Conference on Communications and Mobile Computing*, vol. 3, pp. 168–170, April 2010.
[10] L. Arjona, H. Landaluce, A. Perallos, and E. Onieva, "Fast fuzzy anti-collision protocol for the RFID standard EPC Gen-2," *IET Electronics Letters*, vol. 52, no. 8, pp. 663–665, 2016.
[11] J. V. Sobral, J. J. Rodrigues, R. A. Rabelo, J. C. L. Filho, N. Sousa, H. S. Araujo, and R. H. Filho, "A framework for enhancing the performance of Internet of Things applications based on RFID and WSNs," *Journal of Network and Computer Applications*, vol. 107, pp. 56 – 68, 2018.
[12] N. Kargas, F. Mavromatis, and A. Bletsas, "Fully-Coherent Reader With Commodity SDR for Gen2 FM0 and Computational RFID," *IEEE Wireless Communications Letters*, vol. 4, pp. 617–620, Dec 2015.
[13] P. Solic, J. Maras, J. Radic, and Z. Blazevic, "Comparing Theoretical and Experimental Results in Gen2 RFID Throughput," *IEEE Transactions on Automation Science and Engineering*, vol. 14, pp. 349–357, Jan 2017.

Declaration

This work has been made thanks to the grant offered by the Basque Government, under the predoctoral formation program

(ref: PRE_2017_2_0154).

I herewith declare that I have produced this work without the prohibited assistance of third parties and without making use of aids other than those specified; notions taken over directly or indirectly from other sources have been identified as such. This work has not previously been presented in identical or similar form to any examination board.

The dissertation work was conducted from 2015 to 2018 under the supervision of Asier Perallos and Hugo Landaluce at the University of Deusto.

Bilbao, September 2018.

This dissertation was finished writing in Bilbao on September 2018

This page is intentionally left blank